ATMOSPHERIC PARTICLES AND NUCLEI

G. Götz
E. Mészáros
G. Vali

Akadémiai Kiadó, Budapest

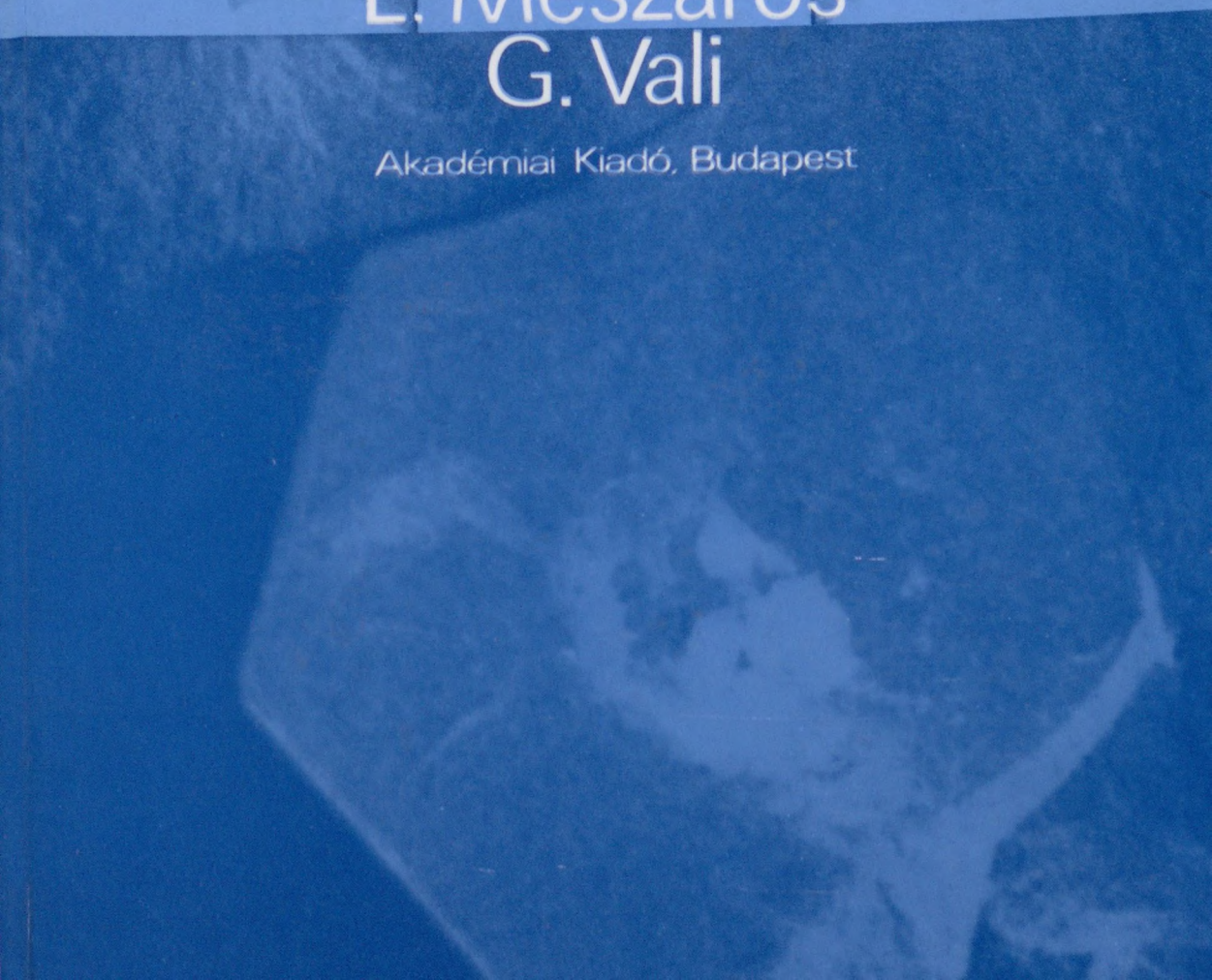

Atmospheric Particles and Nuclei

Atmospheric Particles and Nuclei

G. Götz, E. Mészáros
Institute for Atmospheric Physics
Budapest, Hungary

G. Vali
Department of Atmospheric Science, University of Wyoming
Laramie, WY., USA

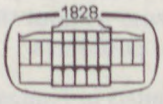

Akadémiai Kiadó, Budapest 1991

Cover
Electron micrograph of an aerosol particle identified as mica (photo A. Mészáros)

ISBN 963 05 5682 0

Printed in Hungary
by Akadémiai Kiadó és Nyomda Vállalat,
Budapest

To the memory of Agnes

Contents

1. Introduction *(E. Mészáros and G. Vali)* 13

2. The atmospheric aerosol *(E. Mészáros)*
2.1 Introduction 17
2.1.1 Definition of the aerosol 17
2.1.2 Characterization and measurement of atmospheric aerosol particles .. 19
2.2 Origin of atmospheric aerosol particles 23
2.2.1 Dispersal of particles of surface origin 23
2.2.2 Formation of atmospheric aerosol particles by chemical reaction and condensation 25
2.2.3 Other sources 29
2.2.4 Comparison of the strength of different aerosol sources 31
2.3 Concentration and size distribution of atmospheric aerosol particles 32
2.3.1 Concentration and vertical distribution of Aitken particles 32
2.3.2 The size distribution 35
2.3.3 Concentration and vertical profile of large and giant particles 42
2.4 Chemical composition of atmospheric aerosol particles 44
2.4.1 The main methods of identification 44
2.4.2 Chemical composition of tropospheric aerosols 45
2.4.3 Stratospheric particles 60
2.5 Variation of the size of aerosol particles as a function of the relative humidity 64
2.5.1 Theoretical considerations 64
2.5.2 Results of measurements 66
2.6. Removal of aerosol particles from the atmosphere 68
2.6.1 Dry deposition of aerosol particles 68
2.6.2 Wet deposition 71
2.6.3 Residence time of aerosol particles in the atmosphere 74
2.7 Mathematical modeling of atmospheric aerosols 75
References 77

3. Cloud condensation nuclei *(E. Mészáros)*
3.1 Statement of the problem 85
3.2 Theory of condensation 86
3.2.1 Condensation on water-soluble nuclei 86
3.2.2 Condensation on insoluble particles 91
3.3 Concentration and supersaturation spectra of cloud condensation nuclei .. 93
3.3.1 Principle of diffusion chambers 93
3.3.2 Results of CCN measurements 95

3.3.3 Aircraft observations 99
3.3.4 Production of cloud condensation nuclei 102
3.4 Size and nature of CCN 103
3.4.1 Estimation of the size and nature of CCN on the basis of the measurements of aerosol characteristics 103
3.4.2 Combination of diffusion chamber observations with other experiments 105
3.4.3 Conclusion 108
3.5 CCN and cloud and precipitation formation 109
3.5.1 Theoretical considerations on droplet growth by condensation 109
3.5.2 Relationship between CCN and droplet characteristics 111
3.5.3 CCN and precipitation formation 116
3.5.4 Modification of clouds by artificial CCN 120
References 125

4. Nucleation of ice *(G. Vali)*
4.1 Introduction 131
4.2 Basic description of ice nucleation 132
4.3 Homogeneous nucleation of ice 133
4.4 Heterogeneous nucleation 145
4.4.1 General comments 145
4.4.2 Basic theory 146
4.4.3 Characteristics of ice nuclei 148
4.4.4 Some macroscopic factors 160
4.5 Ice nucleation in the atmosphere 162
4.5.1 Modes of atmospheric ice nucleation 162
4.5.2 Measurements of atmospheric ice nuclei 165
4.5.3 Concentrations of atmospheric ice nuclei 171
4.5.4 Sources of atmospheric ice nuclei 175
4.6 Artificial ice nuclei–cloud seeding 178
4.6.1 Historical note 178
4.6.2 Cloud seeding with coolants 179
4.6.3 Cloud seeding aerosols 181
References 186

5. Aerosols and climate *(G. Götz)*
5.1 Statement of the problem 193
5.2 Modifications of the radiation budget due to aerosol particles 195
5.2.1 Stratospheric aerosols 195
5.2.2 Tropospheric aerosols 200
5.3 Modeling the climatic effects of aerosol 203
5.3.1 Effects of naturally occurring aerosol and its anthropogenic increase . 205
5.3.2 Effects of volcanic eruptions 216
5.3.3 Effects of a large-scale nuclear exchange 222
5.4 The role of clouds in the radiation balance 229
5.4.1 The net radiative effect of clouds 229
5.4.2 Climatic impacts of anthropogenically altered cloud characteristics .. 232
5.4.3 Climatic impacts of biologically altered cloud characteristics 235
References 237

Appendix I.
Basic concepts of nucleation (Thermodynamic/kinetic approach) *(G. Vali)* ... 243
References ... 249

Appendix II.
Growth of cloud droplets *(E. Mészáros)*
Part A: Droplet growth by condensation ... 251
Part B: Drop growth by coalescence ... 253
References ... 254

Appendix III.
Radiative transfer calculations *(G. Götz)* ... 255
References ... 263

Appendix IV.
Terminology used ... 265

Index ... 269

Preface

In the Earth's atmosphere many tiny solid and liquid particles can be found. These so-called aerosol particles influence continuously our everyday life. They control the visibility in the air, the intensity of solar radiation reaching the surface of our planet, as well as the electric and radioactive properties of the atmospheric environment. These particles also play an essential role in the regulation of water cycle in nature, since water droplets and ice crystals in clouds form on aerosol particles called cloud condensation and ice nuclei. The structure of clouds, depending on the availability of nuclei, determines the formation of precipitation, and the transfer of solar and terrestrial radiation through the clouds. These questions have become particularly important in the last decades, because of attempts to stimulate precipitation artificially by introducing suitable nuclei in clouds. On the other hand, by emitting different pollutants into the atmosphere, human activities inadvertently modify the microphysical characteristics of clouds, and consequently the weather and climate processes.

The aim of this book is to present, in one volume, the physical and chemical properties of atmospheric aerosol particles and nuclei, as well as to describe in a coherent way their role in cloud and precipitation formation, and climate regulation. The authors wanted to give a relatively short description of the subject, to result in a book which is not too voluminous and sophisticated for students and beginners in the field. However, it is hoped that the detailed, although not complete, literature survey makes this volume useful also to researchers working in any field related to atmospheric sciences.

It should be mentioned that Chapter 2 of this volume is a revised and updated version of the aerosol chapter of a former book written by one of the authors (E. Mészáros: Atmospheric Chemistry. Fundamental Aspects. Elsevier Scientific Publishing Company, Amsterdam, 1981) and is published with the permission of Elsevier. This chapter was reviewed by Dr. J.P. Lodge (Boulder, Colorado, U.S.A.), while Chapter 5 was commented by Dr. R.E. Livezey (National Oceanic and Atmospheric Administration, Washington, D.C., USA). Their kind help is gratefully acknowledged. The authors are also indebted to their secretaries who carefully prepared the manuscript, and to Mrs. I. Kas, Mrs. J. Kerek and Mr. A. Marton (Publishing House of the Hungarian Academy of Sciences, Budapest, Hungary) for their valuable editorial assistance.

September 1989

The authors

1. Introduction

The Earth's atmosphere—a thin covering of gases, aerosol particles and clouds —provides the temperature control on which life depends, and is the medium through which oxygen, nitrogen, carbon dioxide, water, organic compounds and many other trace constituents are continually cycled. The composition of the atmosphere and the climate of the Earth have undergone radical changes over the 5-billion year history of this planet. And even now, changes are taking place due to natural evolution and due to man's activities. In fact the two causes cannot be separated any longer. By now, the changes brought about by human activity are probably comparable in magnitude to the changes that would take place anyway. In some specific aspects, like CO_2 and CH_4 concentrations, the anthropogenic influences seem to dominate. In many others the different causes cannot be isolated, and the overall results of atmospheric changes, together with the coupled changes in the oceans, in the biosphere and in the lithosphere, cannot be clearly evaluated yet. The formulation of such scientific predictions is one of the most important tasks facing science today.

This book focuses on atmospheric aerosol particles, which constitute a minor but very important component of the atmosphere, and which make special contributions to the maintenance and the evolution of the Earth's atmosphere. They influence the radiation budget and the global chemical cycles, and their effects in those processes can get strongly multiplied by the role they play in determining the microphysical properties of clouds. Because of their roles in cloud and precipitation processes, aerosols also are key parts of the global hydrological cycle. In spite of their ubiquity and importance, atmospheric aerosols are less well known than the gaseous components, and they are often neglected in considerations of global processes like climate studies. It therefore seemed appropriate to assemble a book which treats the nature and impacts of aerosol particles in relatively simple, physical terms; the book will, hopefully, be useful in putting many aspects of this diverse topic in an approachable perspective and will stimulate further interest in the study of the subject.

The Earth's atmosphere is a mixture of many different gases and of a wide variety of aerosol particles. Gases constitute the overwhelming majority of the mass of the atmosphere. Aerosol particles contribute only about 1 part in 10^9 (1 ppb) by mass. They are classified as a trace component of the atmosphere,

but a very complex one because of the large range of sizes of particles and their diversity of shapes and chemical composition.

Both the gases and the aerosols of the atmosphere participate in the global flow of chemical compounds in nature. In these biogeochemical cycles substances are continuously exchanged among the different media of the Earth: hydrosphere, lithosphere, biosphere etc. Being the most mobile/dynamic system among Earth's media the atmosphere provides some of the most important pathways for the biogeochemical cycles.

Atmospheric constituents interact with both solar and terrestrial radiation transfer. Solar UV radiation, lethal to living species, is absorbed by some atmospheric constituents, principally ozone, and, generally speaking, the intensity of solar radiation of different wavelengths reaching the surface is determined by atmospheric composition. Further, the infrared radiation emitted by the Earth is partly absorbed by certain components (carbon dioxide, water vapor etc.) which increases considerably the temperature of the air. In this way the climate of the Earth depends on the composition of the atmosphere.

As a function of their physical and chemical nature, specific fractions of the atmospheric aerosol can initiate cloud droplet and ice crystal formation. These groups of particles are called "cloud condensation nuclei" and "ice nuclei", respectively. The microphysical characteristics of clouds, as well as the amount of cloudiness, are altered by the abundance and activity of these nuclei. Through these connections, aerosols not only absorb and scatter solar radiation,[1] but they have an important indirect effect on climate since cloud droplets and crystals formed on nuclei influence the transfer of short-wave radiation in a significant way. Thus, 20–25% of the incoming solar radiation is reflected by clouds. Moreover, clouds are nearly perfect absorbers in the band of long-wave radiations emitted by the surface. This absorption reduces the heat loss of the lower layers of the atmosphere.

Precipitation initiation in clouds depends on the availability of water or ice embryos; without such embryos clouds would remain quite stable, that is, not produce precipitation over long periods of time, until dispersed by air motions. The formation of precipitation proceeds by the coalescence of smaller cloud droplets whose sizes, in turn, depend on the cloud condensation nuclei. In supercooled clouds (colder that 0 °C), the possibility exists for ice crystals to form on available ice nuclei and to grow rapidly into precipitation embryos. If natural ice nuclei are not numerous enough for efficient precipitation initiation, clouds can be seeded by man using suitable ice nuclei to stimulate precipitation artificially. For such manipulation, knowledge of crystal formation on natural ice nuclei is of crucial importance.

It follows from the above discussion that the presence of nuclei is vital for the process of continuous redistribution of water within the Earth–atmosphere system, including the grand cycle of returning water from the oceans as fresh

[1] The extinction of visible light by the aerosol particles is very essential not only for climate regulation but also for the control of visibility in the air.

water for terrestrial life. Since, under natural conditions, the majority of cloud condensation nuclei consist of sulfate particles formed in the air from gaseous precursors emitted by the biosphere, we can say that the biosphere to some extent regulates the precipitation which is essential for its existence.

Aerosol particles are also important from the point of view of atmospheric electricity and radioactivity. This means that gaseous ions formed in the air under the effect of ionizing radiation can coagulate with aerosol particles which reduces considerably their electrical mobility owing to the greater mass of aerosol particles. For this reason there is an inverse relation between the aerosol concentration and the electrical mobility of the air. On the other hand, radio active isotopes in the air are also attached to existing aerosol particles. In this way their behavior in the atmosphere and their different effects strongly depend on the characteristics of the particle bearing the isotope.

Atmospheric particles form, principally, by one of two processes: by chemical transformations of atmospheric trace gases (gas-to-particle conversion), and by dispersion from the Earth's surface. On the other hand, aerosol particles are removed from the air by dry and wet deposition. Dry deposition is controlled by sedimentation and turbulent motions in the air while wet deposition is due to the capture of the particles by cloud and precipitation elements. This means that the atmospheric cycles of water and aerosols are strongly interrelated. The interaction of sources and sinks determines the residence time and concentration of aerosol particles in the atmosphere.

Presentation of the various topics in this book proceeds from the general properties of aerosols to their role in cloud and precipitation formation and finally to their impact on climate. In Chapter 2 the relevant physical and chemical characteristics of aerosol particles are presented. The role of aerosol particles in cloud droplet and ice formation are discussed in Chapter 3 and 4, respectively. Finally, Chapter 5 treats the impact of aerosol particles on climate, including the indirect influence of aerosol particles on radiation through cloud processes. Some topics are separated into appendices; these are simple mathematical formulations for illustrating the discussion in the main body of the text, or summaries of general concepts. A brief terminology, which should be helpful in maintaining clarity of definitions, is also included, as Appendix IV.

2. The atmospheric aerosol

2.1 Introduction

2.1.1 Definition of the aerosol

An aerosol is defined as a dispersed system containing solid or liquid particles suspended in a gas. In the present case the gaseous medium is the air in which aerosol particles of different composition and size are suspended.

In more rigorous terms the principal characteristics of an aerosol or aerocolloidal system, are (HIDY and BROCK, 1970):

a) the sedimentation velocity of the particles is small;
b) inertial effects during particle motions can be neglected (the ratio of inertial forces to viscous forces is small);
c) the Brownian motion of the particles, due to the thermal agitation of gas molecules, is significant and
d) the surface of the particles is large compared to their volume.

The physical meaning of the above criteria will be defined in the following paragraphs. The principal force acting on an aerosol is generally gravitation. This means that the lifetime of a particle in the system is determined by its sedimentation velocity. If the particle radius is greater than the mean free path of gas molecules, the falling velocity v_s is given by the well-known Stokes equation:

$$v_s = \frac{2}{9} \frac{r^2 \varrho_p g}{\mu} \tag{2.1}$$

where r and ϱ_p are the radius and density of the particle, assumed spherical, μ is the dynamic gas viscosity (equal to 1.815×10^{-5} N s m^{-2} at a temperature of 20 °C) while g is the gravitational constant. In the atmosphere, v_s in Eq. (2.1) depends on altitude above the sea level. Furthermore, the updraft motions in the troposphere make the meaning of the sedimentation velocity rather complicated. If, for example, in the surface air a value of 10 cm s^{-1} is accepted as an upper limit, the radius of a spherical particle will be 30 μm if the density is taken to be unity. It must be emphasized, however, that due to the presence of updrafts, larger particles can also be found in the atmosphere at significant distances from their sources.

The ratio of inertial forces to viscous forces is *per definitionem* the Reynolds number (Re) of particles. In this way the second criterion after reduction can

be written in the form:

$$\frac{\varrho v r}{\mu} = \mathrm{Re} < 1 \tag{2.2}$$

where ϱ is the air density, while v is the speed of the particle motion caused by some external force. Physically Eq. (2.2) means that in a stable system the product of the particle speed and particle size cannot exceed a given value. Thus, under normal atmospheric conditions the speed of motion of a particle of 10 μm radius could not exceed 30 cm s^{-1}. In the case of $r = 30$ μm the critical velocity is 10 cm s^{-1}. If the external force arises from the gravitational field, this condition is obviously equivalent to the first criterion.

A very characteristic property of aerosol particles is their Brownian motion. This random motion is a result of the fluctuations in the impact of gas molecules on the particles. It goes without saying that the speed of this motion increases with decreasing size. Generally, Brownian motion is considered significant if the particle radius is smaller than 0.5 μm.

Finally, the fourth criterion is satisfied if the particle surface (in cm^2) exceeds the particle volume (in cm^3) at least a thousand times. For this reason, surface phenomena play an important role in the behavior of aerocolloidal systems.

The foregoing conditions determine the upper limit of the particle size. The lower limit can be specified in a very simple way. A system is considered an aerosol when the radius of the particles is greater than that of gas molecules. At the same time $m_a \gg m_g$, where m_a and m_g are the mass of aerosol particles and gas molecules, respectively. Bearing in mind the size of molecules in the air we might define the lower limit to be around 10^{-7} cm ($= 10^{-3}$ μm).

An important consequence of the Brownian motion of aerosol particles is their collision and subsequent coalescence. This so-called coagulation process for a monodisperse aerosol can be characterized by the particle loss per unit time (Hidy and Brock, 1970):

$$-\frac{\mathrm{d}N}{\mathrm{d}t} = 8\pi D r N^2 \tag{2.3}$$

where N is the number of particles per unit volume, t is the time and D is the diffusion coefficient of particles:

$$D = \frac{kT}{6\pi\mu r}\left(1 + \frac{A\lambda}{r}\right) \tag{2.4}$$

In Eq. (2.4) k is the Boltzmann constant (1.31×10^{-23} J/K × molecule), T is the absolute temperature, A is the Stokes-Cunningham correction[1], while λ is the mean free path of gas molecules[2]. Thus, the coagulation equation may be

[1] $A \cong 1.257 + 0.400 \times \exp(-1.10\, r/\lambda)$

[2] $\lambda = 6.53 \times 10^{-6}$ cm, at a temperature of 20 °C and a pressure of 1013 hPa.

written in the following form:

$$-\frac{dN}{dt} = \frac{4}{3}\frac{kT}{\mu}\left(1+\frac{A\lambda}{r}\right)N^2 \tag{2.5}$$

It is concluded on the basis of Eq. (2.5) that the intensity of the particle loss due to thermal coagulation is directly proportional to the square of the particle concentration, while the coagulation efficiency increases with decreasing particle radius. This means that the coagulation of small particles at a high concentration is a very rapid process. Equation (2.5) is valid only for monodisperse aerosols, i.e. aerosols composed of particles of uniform size. However, the same qualitative conclusion can also be drawn in the case of polydisperse systems.

It should be emphasized that the dynamics of aerocolloidal systems is not to be discussed here. For further details the reader is referred to textbooks specialized in the field (e.g. HIDY and BROCK, 1970; TWOMEY, 1977).

2.1.2 Characterization and measurement of atmospheric aerosol particles

As we have emphasized in the introduction of this book the atmospheric aerosol plays an important part in the control of many atmospheric processes: cloud formation, radiation transfer, etc. For the study of the role of atmospheric particles the measurement of their physical and chemical characteristics is of crucial importance.

An essential physical characteristic of the particles is their concentration. We can characterize the particle concentration in two different ways. Firstly, the number concentration can be employed which is the number of the particles in unit gas volume. Secondly, the particle mass in unit gas volume (mass concentration) or in unit mass of air (mixing ratio) can be given. Since, as we have seen previously, the size of the particles varies by several orders of magnitude, for particle characterization the determination of the size distribution is also necessary (see Subsection 2.3.2).

The effects of the particles in the air also depend on their composition. Thus the study of the chemical nature of individual particles or a particle ensemble is also of interest.

In this subsection the physical detection and collection of aerosol particles for further studies will be presented, while the main methods of chemical identification are discussed in a separate subsection (2.4.1).

From the point of view of particle characterization and measurements the aerosol classification of JUNGE (1963) is very convenient. JUNGE divided aerosol particles in three groups:

Aitken[1] particles:	$r < 0.1\ \mu m$;
large particles:	$0.1 \leq r < 1.0\ \mu m$;
giant particles:	$r = 1.0\ \mu m$.

[1] The concentration of these particles is generally measured by means of expansion chambers, the first versions of which were constructed by AITKEN.

In the range of Aitken particles, diffusion effects are significant and particle coagulation is rapid. However, in case of giant particles, these phenomena can be neglected, and the behavior of aerosol particles is mostly determined by their sedimentation due to gravitation. The large particles constitute a transition between the two characteristic ranges mentioned. Since their size is comparable to the wavelength of visible light, these particles play a great role in the optical properties of air. Large and giant particles have a significant inertia which can be utilized for their measurement (see below). Moreover, the giant particles and a significant portion of the large particles can be studied with an optical microscope.

Because of their small radius, the size and size distribution (see Subsection 2.3.2) of Aitken particles may be determined with a diffusion battery. This device is composed by an ensemble of capillary tubes, through which the air is drawn at low velocity. As a result of their Brownian diffusion, the smaller aerosol particles are deposited on the walls of the tubes during the aspiration. This particle loss is a function of the diffusion coefficient and consequently of the size of the particles (see Eq. (2.4)).

The total number concentration of aerosol particles can be measured with expansion chambers. In these devices the air sampled is humidified and suddenly expanded to produce a significant water vapor supersaturation. In the supersaturated environment, water condenses on the aerosol particles[1]. The number of droplets formed in this way is equal to the particle concentration. The droplets are generally counted by allowing them to settle on a microscope slide or, after calibration, by the extinction of a light beam through the chamber. This type of measurement actually determines the total number concentration of particles. However, since the concentration of Aitken particles is much larger than that of large and giant particles (see later), the result essentially gives the number of particles with radius smaller than 0.1 μm.

The smaller aerosol particles can be captured from the air for subsequent counting and size measurement by means of so-called thermal precipitators. In these instruments, metal wires are heated to produce a temperature gradient. Aerosol particles move away from the wire in the direction of a cold surface, since the impact of more energetic gas molecules from the heated side gives them a net motion in that direction. The particles captured are studied with an electron microscope. Another way to measure Aitken particles is by charging them electrically under well-defined conditions. The charged particles are passed through an electric field and are captured as a result of their electrical mobility. Since size and electrical mobility are related, the size distribution of particles can be deduced. These devices are called electrical mobility analyzers.

There are several methods to detect large particles. Thus, particles can be studied *in situ* in the gaseous medium. In single particle optical counters, the particles are illuminated and the light scattered individually by each particle is

[1] Supersaturation is designed in such a way that water does not condense on different ions in the air.

measured photoelectrically at a given angle. The number of such scattering signals is a measure of the particle number while the amplitude of each signal gives, after suitable calibration, the particle size. In another type of optical device, the light scattered by a cloud of particles in a fixed solid angle is measured. In this case the device is called an integrating nephelometer.

Generally, the large and giant particles are collected from a given air sample by inertial deposition. Inertial sampling is carried out by placing an obstacle or collector in the air stream as shown in Fig. 2.1*a*. As can be seen the air goes around the obstacle, while the trajectory of particles with an inertia higher than that of the air molecules deviates from the trajectory of the latter and the particles strike the collector. With increasing gas stream velocity, and with decreasing collector size, the radius of the particles collected decreases. In other words this means that the efficiency of the collection (impaction) increases. The impaction efficiency "is defined as the ratio of the volume of gas cleared of particles by the collection element to the total volume swept out by the collector" (FRIEDLANDER, 1977). During aircraft sampling the collector (e.g. a microscopic slide) is exposed directly in the moving air. If the aircraft has a velocity of 200 km hr^{-1}, large particles can be captured with an acceptable efficiency on slides 0.1 mm wide. For giant particles this characteristic size is 1 mm.

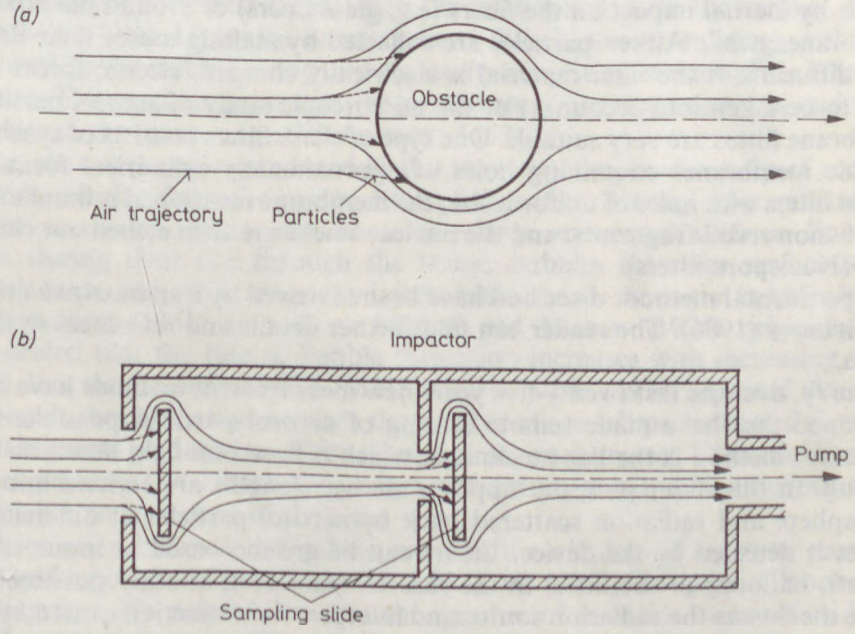

Fig. 2.1
Inertial collection of aerosol particles by an obstacle and by a two-stage impactor

In the surface air the wind speed is generally not high enough for the direct collection of large particles. However, a suitable relative velocity can be achieved by attaching the collecting slide to the end of a rotating arm. Alternatively, the air can be accelerated by pumping it into or through a tube. In this latter case the stream velocity can be further increased by passing the air through narrow slits or jets. Such a device is called an impactor; its collection efficiency is an inverse function of the slit size. A great advantage of this sampling procedure is that particles with different dimensions can be separated by means of an impactor containing slits (jets) with different sizes, Fig. 2.1*b* represents in a schematic way such an instrument of two stages, termed a cascade impactor. As we see the air is sucked gradually through progressively narrower slits. This allows the capture of smaller and smaller particles by the slides placed at an appropriate distance behind the jets. The particles collected are counted and their size is measured by an optical or electron microscope or they may be analyzed chemically (see Subsection 2.4.1).

The different collection procedures are combined by suitable filters consisting of fine fibers or membranes. These filters remove large and giant particles from the air by inertial impact on the fibers (e.g. glass fibers) or around the holes of membranes, while Aitken particles are collected by making use of their Brownian diffusion. It the filter material is electrically charged, electric forces also have to be taken into account. For the microscopic study of aerosol particles, membrane filters are very suitable. One type of these filters consists of synthetic organic membranes containing holes of approximately cylindrical form. To obtain filters with holes of uniform size, the membrane mentioned is bombarded with fission recoil fragments, and the nuclear tracks are then etched out chemically (Nuclepore filters).

Experimental methods discussed have been reviewed by FRIEDLANDER (1977) and SPURNY (1986). The reader can find further details and references in these books.

Finally, over the last twenty-five years new measurement methods have been developed that have made remote sensing of aerosol particles possible. One important method is the lidar technique which is based on *li*ght *d*etection *a*nd *r*anging. In this, laser pulses at appropriate wavelengths are emitted into the atmosphere and radiation scattered back by aerosol particles at different altitudes is detected by the device. Lidars can be ground-based or mounted on aircraft, balloons or satellites. In the case of spacecraft, another possibility is to use the Sun as the radiation source and interpret the extinction caused by the presence of the aerosol as particle concentration. These methods have been successful in particular in the study of the aerosol particles in the upper troposphere and lower stratosphere, as discussed by INN *et al.* (1982).

2.2 Origin of atmospheric aerosol particles

2.2.1 Dispersal of particles of surface origin

Apart from a very minor contribution from meteorites and pollens, atmospheric particles arise from two basic processes[1]:

a) dispersal of materials from the Earth's surface;
b) chemical reaction and condensation of atmospheric gases and vapors.

The dispersal of surface materials produces particles in two major categories: sea salt, and soil or mineral particles.

Sea salt particles can be formed by direct dispersal of ocean water from the foam of the waves. However, these particles are generally too large to remain airborne, even after evaporation of water. A much greater number of particles is produced by the bursting of gas bubbles reaching the water surface. According to the laboratory work of MOORE and MASON (1954) this process takes place in two stages. In the first stage, when the bubble arrives to the surface, small particles are ejected from the bursting water film. In the second stage, a thin jet is formed by the water flowing into the cavity remaining in the surface after the rupture. The particles formed in the second stage are less numerous and their sizes are in the giant range (WOODCOCK, 1953)

The sea salt particles produced in this way are composed mostly of sodium chloride, which reflects the composition of sea water. Among other substances, marine particulate matter also contains a large amount of sulfates. Furthermore, during their rise through the water, bubbles scavenge surface-active organic materials which are partly injected into the air when the bubbles burst.

WOODCOCK (1953) as well as MOORE and MASON (1954) originally demonstrated that the rate of bubble formation increases with increasing wind speed. In a more recent work A. MÉSZÁROS and VISSY (1974) reported that over the oceans the correlation between the number of sea salt particles and the wind speed becomes gradually weaker as the particle size decreases. Thus, the smallest sea salt particles ($r < 0.3$ μm) may originate from a type of bubbles the formation of which is independent of the wind speed.

The relation between the bubble size and the number of airborne particles produced upon bursting was studied by DAY (1963) during his laboratory investigation. He pointed out that the number of particles increases with increasing bubble size. A bubble with a size of several millimeters forms some hundreds of particles when it bursts. The results of simultaneous observations of size spectra of bubbles in foam patches and giant sea salt particles in the air over a surf zone in Texas show that both spectra follow the gamma distribution function (PODZIMEK, 1984). On the basis of his atmospheric observations made

[1] Such processes as particle coagulation may also produce new large particles, but not new particulate matter.

in Hawaii, BLANCHARD (1969) assumed that the intensity of sea salt particle formation is between 25–100 cm^{-2} s^{-1} at the surface of the ocean. This range is in a good agreement with the laboratory results of MOORE and MASON (1954).

Airborne sea salt particles are transported to higher levels and over the continents by atmospheric motions. Thus, such particles were observed over Australia (TWOMEY, 1955), North America (BYERS *et al.*, 1957) and Europe (MÉSZÁROS, 1964). Due to removal processes near the surface level as well as to convective motions, the concentration of sea salt particles increases with increasing height in the lower troposphere over the continents in contrast to the situation over the ocean where their number decreases with increasing altitude (WOODCOCK, 1953; LODGE, 1955; BLANCHARD *et al.*, 1984). Because of the relationship between relative humidity and particle size (see Section 2.5), low relative humidity promotes the transport of sea salt particles.

The other category of particles originates from the solid surface of the Earth. This dispersal is obviously due to the effect of wind on rocks and soils. A well-known and highly visible example of this process is the formation of dust clouds and storms. However, the quantitative explanation of this particle production mechanism is not easy, except when some external mechanical force agitates the surface (vehicles, animals, people, etc.). The main reason for the difficulties in the explanation is the decrease of the wind speed with decreasing height above surface, usually extrapolating to zero wind speed at the surface. It is believed that turbulent flow is necessary (see TWOMEY, 1977) for the detachment of grains. According to the most acceptable estimates the global strength of this source is 100–500 Tg yr^{-1} (SMIC, 1971[1]; PROSPERO, 1984).

An important proportion of mineral particles produced by wind erosion is insoluble in water. Their composition can be characterized by determining the so-called aerosol–crust enrichment factor on the basis of the analyses of atmospheric aerosol samples and rocks or soils. The enrichment factor (EF) defined by RAHN (1976) is given by the following expression[2]

$$\mathrm{EF} = \frac{(X/\mathrm{Ref})_{\mathrm{aerosol}}}{(X/\mathrm{Ref})_{\mathrm{crust}}} \tag{2.6}$$

where X is the concentration of the element considered in the aerosol or in the crust, while "Ref" is the concentration of a crustal reference element (generally Al, Ti or Fe). It follows from this definition that a certain element is considered of mineral origin if its enrichment factor is near unity. By using this approach and Ti as reference element A. MÉSZÁROS *et al.* (1984) demonstrated that, in agreement with the results of many other workers, under continental conditions Al and Si are the most important elements of soil origin, these elements almost certainly occur in silicate compounds.

Some particles of crustal origin are removed from the air in the vicinity of

[1] SMIC: Study of Man's Impact on Climate.

[2] EF can also be defined to characterize particles of oceanic origin. In this case in the denominator the oceanic ratio should be used (the reference element is generally Na).

sources, while another fraction is transported to great distances. Thus, particulate matter collected over the Atlantic Ocean contains a significant quantity of Saharan dust under some conditions (JUNGE and JAENICKE, 1971); in fact, such dust particles were collected and identified even over the West Indies (PROSPERO, 1968; BLIFFORD, 1970). Furthermore, dust particles from Asian desert were identified by several workers (see BRAATEN and CAHILL, 1986) at the Mauna Loa Observatory in Hawaii. Elements of soil origin like Al and Fe were even found in relatively high concentrations at the South Pole, Antarctica (ZOLLER *et al.*, 1979). It was also shown (ANDREAE *et al.*, 1986) that, during their transport over the oceans, silicate species can be mixed with sea salt components.

2.2.2 Formation of atmospheric aerosol particles by chemical reaction and condensation

Particles formed by the dispersal of surface materials generally have radii larger than about 0.1 μm. This means that Aitken particles must be produced by another mechanism, namely by condensation of vapors, preceded in many cases by gaseous chemical reactions. These reactions are generally initiated by photochemical processes.

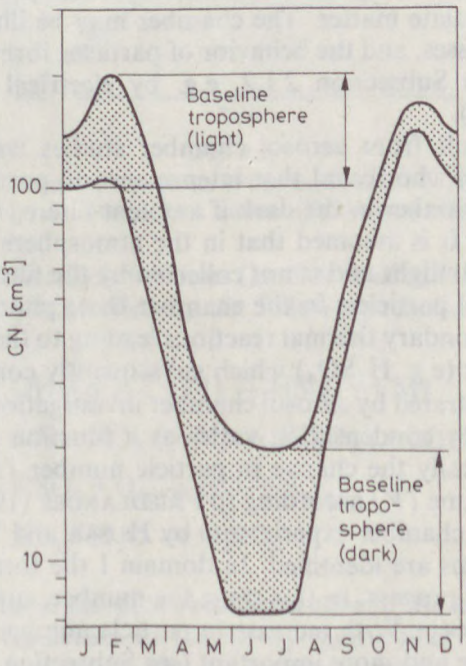

Fig. 2.2

Annual variation of the number concentration of aerosol particles (CN) over Antarctica according to HEITZENBERG (1985). The dotted area represents the concentration fluctuation. (By courtesy of Kluwer Academic Press)

Thus, a large set of data obtained by McWilliams (1969) in clear air (W. Ireland) by means of expansion chambers showed that the concentration of Aitken particles is lower in the winter than in the summertime. Furthermore, McWilliams' observations also demonstrated that more aerosol particles can be detected during daylight than at night. This finding was confirmed by the investigations of Vohra *et al.* (1970) and A. Mészáros and Vissy (1974) according to which, in a clean maritime environment, the number of Aitken particles is at a maximum during the afternoon. It was also shown by atmospheric measurements (e.g. Lopez *et al.*, 1973) that after sunrise the aerosol concentration increases, which also points in the direction that particles with radii smaller than 0.1 μm are produced by photochemical reactions. Further, Hogan and Bernard (1978) have reported that over Antarctica there is a steady increase in concentration after astronomical sunrise. Moreover, in Antarctic winter very small concentrations can be measured. This finding was recently confirmed by numerous data published by Bigg *et al.* (1984), Heitzenberg (1985) and Bodhaine *et al.* (1986). The annual variation presented in Fig. 2.2 is taken from the work of Heitzenberg (1985).

The formation of aerosol particles from gaseous components can be investigated under laboratory conditions. In so-called aerosol chambers an artificial atmosphere is created to which small quantities of appropriate trace gases (e.g. SO_2, NO_2, H_2O, NH_3 and organics) are added. It is also possible to use ambient air purified of particulate matter. The chamber may be illuminated to initiate photochemical processes, and the behavior of particles formed is studied by the methods outlined in Subsection 2.1.2, e.g. by electrical mobility analyzers (Whitby *et al.*, 1972).

An important result from aerosol chamber studies was the discovery of Bricard *et al.* (1968) who found that intense aerosol particle production can be observed in the chamber in the dark if ambient filtered air is sampled from a sunlit atmosphere. It is assumed that in the atmosphere some gaseous substance is excited by sunlight and is not collected by the filter used to obtain air that is free of aerosol particles. In the chamber these photochemically excited molecules initiate secondary thermal reactions leading to the formation of some supersaturated vapor (e.g. H_2SO_4) which subsequently condenses.

It was also demonstrated by aerosol chamber investigations that the behavior of particles formed by condensation varies as a function of time. Figure 2.3 reproduces schematically the change in particle number *(N)*, particle surface *(A)* and particle volume *(V)* according to Friedlander (1978). The curves are based on irradiation chamber experiments by Husar and Whitby (1973) and three separate domains are identified. In domain I the formation of new particles is the dominant process. In this stage the number, surface and volume of particles steadily increase. With increase in particle number (domain II), coagulation becomes more and more important (see Subsection 2.1.2). When the *N* curve has a maximum the coagulation loss just balances the particle formation rate. In domain III coagulation and condensation of the vapor on existing particles are the dominant processes. The number concentration decreases in

this time interval, while particle volume further increases. The value of the surface area remains approximately constant.

In the atmosphere, a good example of the above particle formation is the production of sulfate and nitrate particles from gaseous precursors. In continental air sulfate and nitrate particles come into being from sulfur dioxide and nitrogen oxides emitted into the atmosphere mostly by different pollution sources (e.g. combustion of fossil fuels). The oxidation of SO_2 and NO_x is due to the presence of hydroxyl radicals (OH) formed by photochemical processes

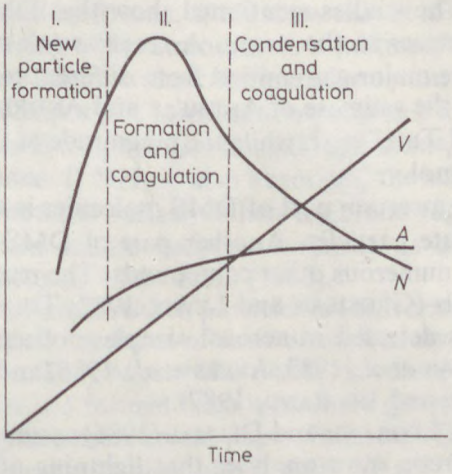

Fig. 2,3

Aerosol formation in an irradiated chamber (FRIEDLANDER, 1978). *N:* particle number; *V:* volume of particles; *A:* total particle surface. (By courtesy of Pergamon Press)

followed by thermal chemical reactions (LOGAN *et al.*, 1981). The oxidation of the gases mentioned is controlled by the following reaction steps (CALVERT *et al.*, 1985):

$$OH + SO_2\ (+M) \rightarrow HSO_3\ (+M)$$

$$OH + NO_2\ (+M) \rightarrow HNO_3\ (+M)$$

$$HSO_3 + O_2 \rightarrow HO_2 + SO_3$$

$$SO_3 + H_2O \rightarrow H_2SO_4$$

The end products of these gas-phase reactions are sulfuric and nitric acid vapor. Sulfuric acid vapor condenses in the air by bimolecular condensation (H_2O molecules also take part in the phase transition), while an important part of HNO_3 remains in vapor phase owing to its high saturation pressure (MIRABEL and JAECKER-VOIROL, 1988). In the case of HNO_3, condensation is promoted by existing aerosol particles which serve as nuclei for the phase transition (for

further details see e.g. KIANG *et al.*, 1973 and COX, 1974). The acidic solution droplets formed in this way are neutralized by biogenic NH_3 if this gas is available in the atmosphere.

Concerning the sources and nature of precursor gases under clean tropospheric conditions it was first believed that hydrogen sulfide is the only biogenic sulfur gas of any significance. However, results of more recent research indicate that H_2S is oxidized very rapidly in the ocean water (ANDREAE, 1986), and consequently cannot be released into the air. Many papers suggest (NGUYEN *et al.*, 1983; BIGG *et al.*, 1984; ANDREAE, 1986; ANDREAE and ANDREAE, 1988) that dimethyl sulfide (DMS) of oceanic origin plays an important role in sulfate particle formation. The studies mentioned show that DMS emission is due to microbiological processes in the ocean. A recent work of FALL *et al.*, (1988) demonstrates that the major gas emitted from different terrestrial plants is also DMS. According to the estimate of ANDREAE and ANDREAE (1988) the oceanic emission of DMS is 1 Tmol yr^{-1}, while the magnitude of the biogenic continental emission is 0.1 Tmol yr^{-1}.

In the atmosphere a certain part of DMS molecules is converted to SO_2 and consequently to sulfate particles. Another part of DMS produces first methanesulfonic acid and numerous other compounds. The reactions are initiated by OH and NO_3 radicals (GROSJEAN and LEWIS, 1982; TOON *et al.*, 1987). Methanesulfonic acid was detected in aerosol samples collected in clean maritime atmosphere (SALTZMAN *et al.*, 1983, AYERS *et al.*, 1986) and also in samples from Antarctic ice (SAIGNE and LEGRAND, 1987).

On the other hand, LEGRAND and DELMAS (1986) assumed on the basis of the results of their Antarctic snow analyses that lightning at tropical and/or mid latitudes is the most probable source of Antarctic nitrate. In other words this means that the combination of atmospheric O_2 and N_2 at high temperatures produced by lightning strokes constitutes the main global source of nitrogen-containing precursor gases.

It is further assumed that the sulfate aerosol layer in the stratosphere (see later) is due to sulfur-bearing gases like carbon disulfide and carbonyl sulfide (TURCO, 1982) mostly of biogenic origin. However, during volcanic eruptions a large amount of SO_2 is injected into the stratosphere (BERRESHEIM and JAESCHKE, 1983) which is converted into aerosol (KEESER and CASTLEMAN, 1982).

There is a considerable body of evidence suggesting that small organic particles are also formed by gas-to-particle conversion (DUCE, 1978). Under unpolluted conditions this particle formation is due to the release of natural hydrocarbons from vegetation. In agreement with the original idea of WENT (1966), LOPEZ *et al.*, (1984) assumed that different pinenes, emitted by pine forests, play an important part in the process. Further, natural forest, brush and grass fires also provide an important atmospheric aerosol particle source (see CADLE, 1973). In urban and industrial environments the cooling of vapors with low saturation pressure, released during combustion, produces a large quantity of aerosol particles composed mainly of carbonaceous materials. These processes are essential in particular since on the surface of elemental carbon (soot)

particles formed by condensation, adsorbed SO_2 molecules can be converted to sulfuric acid as discussed by NOVAKOV (1984).

A special case of the production of particulate matter by gas-to-particle conversion is provided by the irreversible transformation of trace gases in cloud and fog droplets. A good example of this process is the formation of sulfate from gaseous sulfur dioxide absorbed by cloud/fog elements. It is well documented (PENKETT *et al.*, 1979b) that the oxidation of SO_2 to form sulfate ions proceeds through the action of oxidizing agents like ozone and hydrogen peroxide formed by chemical reactions in the atmosphere (see LOGAN *et al.*, 1981). Laboratory experiments (summarized by BEILKE, 1985) show that at low pH values of cloud water ($pH < 5.5$), occurring under atmospheric conditions, the oxidation of SO_2 by H_2O_2 is much more effective than the transformation due to ozone molecules. O_2 may also be important in oxidation processes if catalyzed by active sites on soot or by transition metals (JACOB and HOFFMANN, 1983), at least under more polluted conditions. If NH_3 is also absorbed, the sulfuric acid present is transformed into ammonium sulfate. When the cloud/fog partially or totally evaporates[1], ammonium sulfate becomes airborne as demonstrated by the atmospheric observations of HEGG *et al.* (1980).

The formation rate of small Aitken particles in the troposphere was estimated by LOPEZ *et al.* (1974) on the basis of their aircraft measurements carried out over Southwest France. They argued that in an air column with a base area of 1 cm^2, 3×10^4 particles are formed each second. A quarter of this quantity is due to human activity. In a more recent paper, BIGG and TURVEY (1978) assume that the natural particle production rate is only 170 $cm^{-2}\ s^{-1}$, by two orders of magnitude smaller than the above estimate. BIGG and TURVEY establish this rate by using the results of their observations, carried out over Australia, together with an acceptable residence time of 3×10^5 s. It follows from this figure that the total Australian source strength is about $10^{19}\ s^{-1}$. This may be compared with the total particle flux of $4 \times 10^{19}\ s^{-1}$ produced by only one industrial area (Perth) which exceeds the global natural emission of the continent! The present author feels that the natural production rate proposed by LOPEZ *et al.* (1974) is too high, while BIGG and TURVEY'S value is too low, at least for the European continent. Thus, according to SELEZNEVA (1966), who made a large number of aircraft measurements over the European part of Soviet Union, the particle number is $6 \times 10^8\ cm^{-2}$ in a tropospheric air column. Using a residence time of 3×10^5 s, an acceptable production rate of $2 \times 10^3\ cm^{-2}\ s^{-1}$ is calculated.

2.2.3 Other sources

Beside the major aerosol formation mechanisms discussed in the previous section other sources also produce atmospheric particles. The strength of these sources can be neglected on the global scale. However, the effect of particles

[1] In the case of precipitation from the cloud, ammonium sulfate is removed from the air (see Section 2.6).

formed in these ways may be important under special conditions. For this reason these sources are briefly enumerated in this subsection.

First of all volcanic activity must be mentioned; it introduces both gases and particles into the atmosphere. The particles play an important temporary role in the control of atmospheric optical properties (MENDONCA *et al.*, 1978) and radiation balance (see Chapter 5). The particle production by volcanic activity was studied in detail after eruptions of Mt. St. Helens (Washington, USA) in 1980 and El Chichón (Southern Mexico) in 1982. These studies demonstrate that two sorts of volcanic particles can be identified. Ash constitutes the first category, while the second class comprises the population of sulfate particles formed, mostly in the stratosphere[1], by gas-to-particle conversion discussed in the last subsection. HOBBS *et al.* (1981) found that the ash emissions from Mt. St. Helens were more than 1000 times greater than those in the ambient air. FARLOW *et al.* (1981) reported that ash grains were composed mostly of different glasses. On the other hand, the observations of HOFMANN and ROSEN (1983) showed that after the eruptions of El Chichón 10^7 t of sulfuric acid entered the stratosphere, which is 40 times more than the quantity observed after the eruptions of Mt. St. Helens. While ash particles larger than about 0.1 μm fall relatively quickly out of the atmosphere, small sulfate particles remain in the stratosphere for at least one year.

Another special class of particles is meteoritic dust of cosmic origin. Smaller meteoritic particles ($r < 1$ μm) can reach the lower layers of the atmosphere without significant modifications. However, larger meteorites falling through the atmosphere partly or totally evaporate as a result of frictional heating. It is also possible that meteoric smoke is generated in meteor trails as proposed by HUNTEN *et al.* (1980). In spite of the fact that spherical droplets from condensation of the vapor formed by the evaporation of meteors can be identified in the troposphere (e.g. WIRTH and PRODI, 1972), meteoritic particles can be found generally above 20 km (see INN *et al.*, 1982). PETTERSON estimates (see CADLE, 1973) that 14 Tg of meteoritic material are collected annually by the atmosphere of our planet. The meteorological role of these particles is not too important. However, they play a part in the formation of noctilucent clouds in the mesosphere. Moreover, BOWEN assumed (see FLETCHER, 1962) that meteoritic dust particles may serve as ice-forming nuclei in clouds, but this theory is far from being generally accepted by cloud physicists.

Finally, many viruses, bacteria, pollens and spores can be found in the lower atmosphere. The size of viruses and bacteria is small, while the pollens and spores are in the giant size range. According to A. MÉSZÁROS (1977), on an average 20% of the giant particles in clean continental air are composed of pollen and spores during the appropriate seasons. The biological importance of these airborne materials is obvious.

[1] Volcanic clouds can reach high altitudes. Thus, the cloud of El Chichón spread to about 32 km.

2.2.4 Comparison of the strength of different aerosol sources

The strength of various natural and anthropogenic aerosol sources is tabulated in Table 2.1 (SMIC, 1971; PROSPERO, 1984). The precision of the estimates is represented by the intervals given. For further details, the interested reader is referred to the original works.

Table 2.1

Formation rate of atmospheric aerosol particles in Tg yr^{-1} units. (By courtesy of MIT Press)

Reference	SMIC (1971) <20 μm	Prospero (1984)
Natural aerosol sources		
Soil and rock debris*	100–500	60–360
Forest fires and slash-burning*	3–150	–
Sea salt	(300)	1000–2000
Volcanic debris	25–150	4–90
Particles formed from gases		
Sulfate	130–200	40–400
Ammonium salts from NH_3	80–270	–
Nitrate from NO_x	60–430	60–620
Hydrocarbons from plants	75–200	75–1100
Subtotal	773–2200	1239–4570
Man-made aerosol sources		
Particles (direct emission)	10–90	6–100
Particles formed from gases		
Sulfate from SO_2	130–200	100–200
Nitrate from NO_x	30–35	23–35
Hydrocarbons	15–90	15–27
Subtotal	185–415	144–362
Total	958–2615	1383–4932

Note: Asterisk denotes unknown amounts of indirect man-made contributions. The parenthesis in the case of sea salt (SMIC) means that only particles transported over long distances are taken into account.

The most important fact emerging from the data given is the ratio of the intensity of anthropogenic sources to the strength of natural production mechanisms. It can be seen that on a mass basis emission by natural sources exceeds anthropogenic production by a factor of 5–14. The other essential thing shown by the table is the importance of gas-to-particle conversion in the formation of aerosol particles. The fraction of particles formed by gaseous reactions is particularly significant in the case of man-made emissions.

2.3 Concentration and size distribution of atmospheric aerosol particles

2.3.1 Concentration and vertical distribution of Aitken particles

In this subsection we will discuss the number concentration of all particles, which is partically equivalent to the number of Aitken particles (see Subsection 2.1.2). All values discussed in the following were obtained using expansion chambers.

The early results of particle concentration measurements carried out under different conditions were compiled by LANDSBERG (see JUNGE, 1963). Some of his data are reproduced in Table 2.2. The figures tabulated make it evident that the majority of particles are of continental origin. It is also obvious that man's activity plays an important role in particle production. Furthermore, one can see from Table 2.2 that the number concentration of atmospheric aerosol particles decreases with increasing height.

Observations carried out during the last decades demonstrated that in remote oceanic and continental areas smaller concentrations can be measured than

Table 2.2

Average concentration of Aitken particles under various conditions according to LANDSBERG (see JUNGE, 1963). (By courtesy of Academic Press)

Location	Number of observations	Average concentration cm^{-3}
Cities	2500	147 000
Towns	4700	34 300
Country	3500	9 500
Sea shore	7700	9 500
Mountains		
500–1000 m	870	6 000
1000–2000 m	1000	2 130
above 2000 m	190	950
Islands	480	9 200
Oceans	600	940

those listed in the table. Thus, according to JUNGE and JAENICKE (1971), over the northern Atlantic Ocean the concentration is 600 cm^{-3} on an average. HOGAN *et al.* (1973) suggest that lowest concentrations in the surface air over the North Atlantic can be measured between 20°–25° N and 30°–50° W. Over this area the mean value is only about 300 cm^{-3}. In clean oceanic air of the Southern Hemisphere a lower average concentration ($\sim$400 cm^{-3}) can be detected (A. MÉSZÁROS and VISSY, 1974) than the value reported by JUNGE and

JAENICKE (1971). Moreover, according to information published by Japanese workers (OHTA and ITO, 1974), concentrations are generally between 150–200 cm^{-3} over the Pacific Ocean. The long-term mean of Aitken particle concentration at American Samoa (also in the Pacific ocean) is 274 cm^{-3} (BODHAINE and DELUISI, 1985) which is in a good agreement with the average value (300 cm^{-3}) measured in extremely clean air at Cape Grim (Tasmania, Australia) (HEITZENBERG, 1984). The results obtained by HOGAN and BERNARD (1978) over Antarctica demonstrate that the concentration is less than 50 cm^{-3} in wintertime. This finding was recently confirmed by BODHAINE *et al.* (1986) who report monthly average values of about 10 cm^{-3} in Antarctic winter. Further, GRAS and ADRIAANSEN (1985) found in Antarctic air during wintertime weekly median concentrations of a few tens of particles per cm^3. According to several authors (HOGAN and BERNARD, 1978; ITO, 1985; BODHAINE *et al.*, 1986) during Antarctic summer the number of aerosol particles is around 200 cm^{-3}, while others (GRAS and ADRIAANSEN, 1985) publish somewhat higher concentrations (300–400 cm^{-3}).

It follows from the data presented that in remote air of the Southern Hemisphere the concentration of Aitken particles is rather homogeneous. Except in austral winter over Antarctica, the particle number is around 200–300 cm^{-3}. However, in the Northern Hemisphere the situation is much more complicated owing to anthropogenic pollution sources. Even under Arctic conditions during late winter and early spring a haze layer (called Arctic haze, discovered by chemical measurements, see 2.4.2) of anthropogenic origin can be observed. Within this layer the Aitken particle concentration is typically 800–1000 cm^{-3}, while in clean air without pollution effects it varies between 50 and 100 cm^{-3} (SCHNELL, 1984). In summer the concentrations measured in Arctic regions (JAENICKE and SCHÜTZ, 1982) are rather similar to those observed in Antarctic areas.

It is questionable whether the higher values reported for the Northern Atlantic Ocean are also caused by anthropogenic pollutant emissions. Unfortunately, it is very difficult to answer this important question, since we have no suitable homogeneous data sets to estimate possible secular concentration trends. However, some information is available concerning variations in the electrical mobility of the air over different oceans. These data show (COBB and WELLS, 1970) that electrical mobility of the surface air over the northern part of the Atlantic Ocean decreased by a factor of 2 during the first 70 years of this century. In contrast this electrical parameter remained constant over the southern regions of the Pacific Ocean. Taking into account the relation between electrical mobility and aerosol particle concentration this finding suggests that the particle number concentration doubled during this century in remote areas of the Northern Hemisphere.

The vertical profile of aerosol particle concentration in the troposphere was widely studied by Soviet research workers. A great number of data obtained by aircraft flights is reviewed by SELEZNEVA (1966). Her compilation indicates that on the average the concentration drops to one-fourth of its ground level value

at an altitude of 900 m on an average, and that above 3000–4000 m the particle number becomes constant. SELEZNEVA assumes that this vertical distribution is mostly controlled by atmospheric exchange and particle coagulation (flights were made generally under weather situations without precipitation). In Fig. 2.4 the average results at 3000 m altitude are plotted. One can see that concentrations increase with increasing continental source density. It can also be seen that the concentrations measured at this altitude agree well with those reported for remote oceanic surface air (see above). This means that, except the first few kilometers above the continents, the troposphere is filled with aerosol particles at the same concentration. Disregarding sea salt particles of small number concentration, the composition of this aerosol, termed the tropospheric background aerosol (JUNGE, 1963), is also independent of place and time (see Section 2.4).

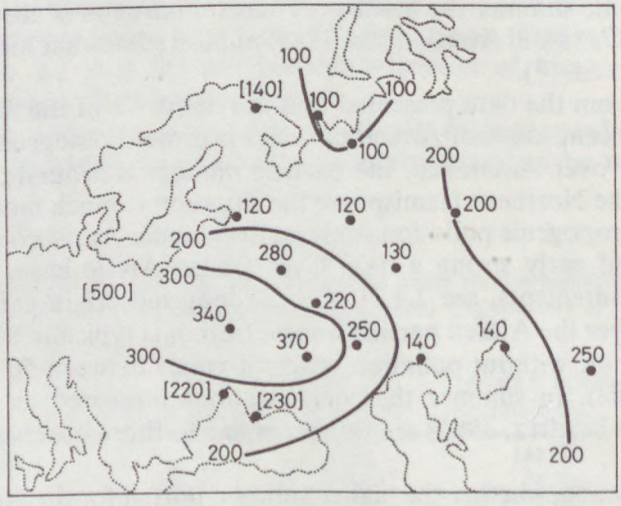

Fig. 2.4

Spatial distribution of the concentration of the Aitken particles at 3000 m over the European part of the USSR (SELEZNEVA, 1966). (By courtesy of *Tellus*)

The concentration of aerosol particles in the stratosphere was firstly measured by JUNGE (1963) by balloon flights over the central part of the USA. He found (see Fig. 2.5) that the number of aerosol particles, in agreement with the Soviet data discussed above, does not change with altitude in the upper troposphere. This constant concentration is around 300 cm^{-3}. Above the tropopause the concentration rapidly decreases with increasing height. Since the character of the vertical profile plotted in Fig. 2.5 was confirmed by several workers (e.g. KÄSELAU *et al.*, 1974; PODZIMEK *et al.*, 1977), it can be considered acceptable for use in further studies. On the basis of the stratospheric concentration distribution, it is believed that particles in this atmospheric domain may be of tropospheric origin. However, it is also possible that stratospheric Aitken

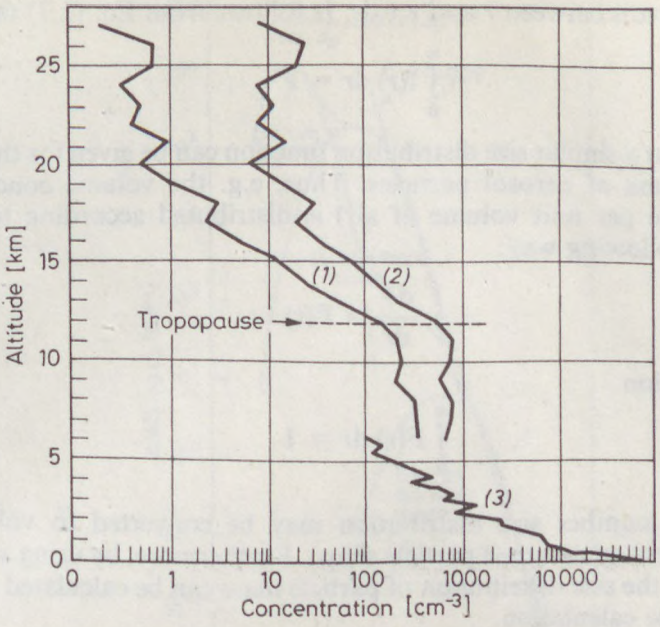

Fig. 2.5

Vertical profile of Aitken particles in the upper troposphere and stratosphere (1) under ambient conditions; (2) at standard temperature and pressure; both according to JUNGE, (1963); and (3) in the lower troposphere according to WEICKMANN (1957). (By courtesy of Academic Press)

particles, formed *in situ* by gaseous reactions, coagulate to create the stratospheric aerosol layer consisting of large particles.

The vertical profile of the concentration of Aitken particles in the lower troposphere over Antarctica was recently studied by HOGAN (1986) and ITO *et al.* (1986). HOGAN's observations indicate an aerosol decrease of 25 particles cm^{-3} km^{-1}. In contrast to this finding the vertical profile in Arctic haze was found to be more complicated as a function of the haze structure (SCHNELL, 1984).

2.3.2 The size distribution

Since the size of atmospheric particles covers several orders of magnitude (see Subsection 2.1.1) the concentration alone is not sufficient to characterize atmospheric particles. For more complete aerosol characterization the size distribution function must be used, which is defined as follows (FUCHS, 1964):

$$\frac{1}{N}\frac{dN}{dr} = f(r) \qquad (2.7)$$

where N is the total number concentration while dN is the same parameter for

particles with radii between r and $r+\mathrm{d}r$. It follows from Eq. (2.7) that

$$\int_0^\infty \mathrm{f}(r)\,\mathrm{d}r = 1 \tag{2.8}$$

It is obvious that a similar size distribution function can be given for the surface, volume and mass of aerosol particles. Thus, e.g. the volume concentration (aerosol volume per unit volume of air) is distributed according to particle radius in the following way:

$$\frac{1}{V}\frac{\mathrm{d}V}{\mathrm{d}r} = \mathrm{F}(r) \tag{2.9}$$

with the condition

$$\int_0^\infty \mathrm{F}(r)\,\mathrm{d}r = 1 \tag{2.10}$$

Of course, the number size distribution may be converted to volume size distribution, given an assumed particle shape. Furthermore, by using a constant particle density the size distribution of particle mass can be calculated from Eq. (2.9) by a simple calculation.

It is customary, in the interconversion of these distribution functions, to assume that the particles are spherical; this simplifies the mathematics, but is somewhat questionable physically. The method of measurement determines the nature of the reported radii of these hypothetical spheres; e.g. in the case of microscopic sizing, the so-called "surface radius" is obtained, which is the radius of a circle having the same surface area as the orthogonal projection of the particle.

On the basis of his atmospheric impactor measurements JUNGE (1963) proposed a power law to describe the size distribution of large and giant particles:

$$\frac{\mathrm{d}N}{\mathrm{d}r} = C_1 r^{-(\beta+1)} \tag{2.11}$$

where C_1 and β are constants. Considering the broad range of particle size, Eq. (2.11) is best rewritten in the following form:

$$\frac{\mathrm{d}N}{\mathrm{d}\log r} = C_2 r^{-\beta} \tag{2.12}$$

In this formula C_2 is a function of concentration, while β gives the slope of the distribution curve. According to JUNGE (1963), β is about 3 under continental conditions.

More recently, WHITBY (1978) has analyzed the results of much more numerous size distribution observations carried out mainly by his group, using a combination of expansion chamber, electrical mobility and optical counter techniques. This analysis clearly shows that the complete size distribution is

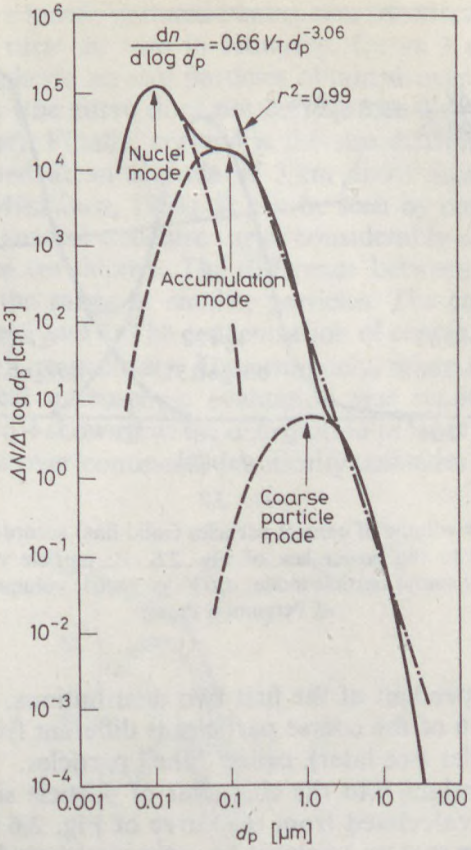

Fig. 2.6

Number size distribution of aerosol particles under urban conditions according to WHITBY (1978). *N*: number of particles; d_p: diameter of particles; V_t: total volume concentration; *r*: correlation coefficient between power law given in the figure and experimental data. (By courtesy of Pergamon Press)

composed of three separate log–normal distributions as demonstrated in Fig. 2.6. WHITBY assumes that the first distribution, the nuclei mode, is controlled by the condensation of vapor (predominantly H_2SO_4) formed by chemical reactions. Thus, the concentration of these small particles was found to be very significant in the irradiated, polluted atmosphere. On the other hand, the so-called accumulation mode is due to the coagulation of primary particles or to the vapor condensation on secondary particles formed by coagulation or on existing aerosol particles. It follows from this idea that the accumulation mode is a consequence of aging of the primary aerosol. In the air far from gaseous sources the nucleation mode may well be partly or totally missing. The third log–normal distribution consists of particles formed mostly by mechanical disintegration of the material of the Earth's surface. This is the coarse particle

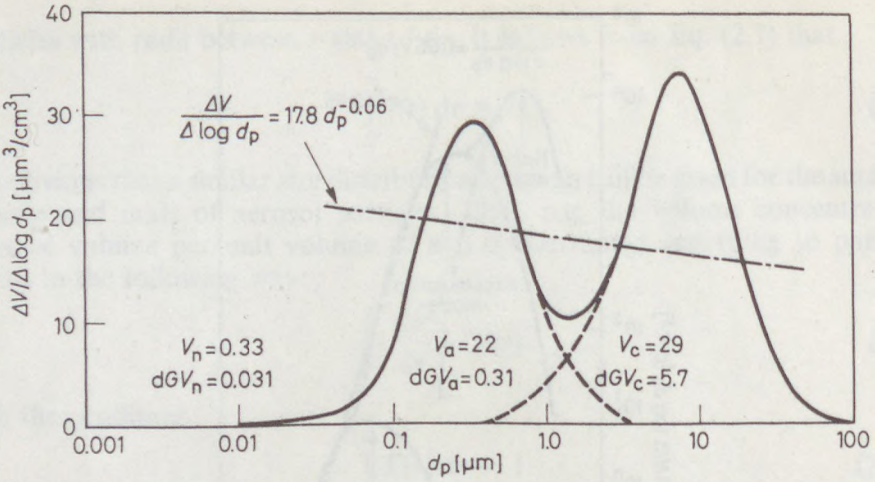

Fig. 2.7

Size distribution of the volume of aerosol particles (solid line) according to WHITBY (1978). Dotted line corresponds to the power law of Fig. 2.6. *V:* particle volune; *n:* nuclei mode; *a:* accumulation mode; *c:* coarse particle mode; d_pGV: geometric volume mean size. (By courtesy of Pergamon Press)

mode, which is independent of the first two distributions. For this reason the chemical composition of the coarse particles is different from the composition of the smaller particles (see later), called "fine" particles.

To gain further insight into the character of particle size distribution, the volume distribution calculated from the curve of Fig. 2.6 is also presented in Fig. 2.7. It can be seen that on a volume basis the nuclei mode, which determines the particle number, cannot be identified owing to the small size of the primary particles. One can also see that a large fraction of the aerosol mass is found in the range of coarse particles. However, the mass of particles in the accumulation mode is also significant. In our case the particle volume in the two modes is nearly the same. Generally speaking, 2/3 of the total mass is in the coarse and 1/3 in the accumulation mode. Finally, Figs 2.6 and 2.7 show that, while the number size distribution of large and giant particles can be well approximated by the power law, JUNGE's formula is very poor for characterizing the volume distribution. In other words this means that minor deviations from the power law in the number distribution cause significant deviations in the volume distribution.

It should be mentioned that the size distributions presented in Figs 2.6 and 2.7 are typical of a polluted atmosphere. To gain further insight into the tropospheric aerosol structure let us consider Fig. 2.8. These average size distributions were measured by A. MÉSZÁROS under various conditions by using the membrane filter technique. Particles were counted and sized in the radius range of 0.03–64 μm by optical and electron microscopy. In the figure the total concentration of these particles is also shown. Curve 1 was observed near

Budapest, Hungary in a locally polluted atmosphere (A. MÉSZÁROS, 1977), while spectrum 2 refers to rural air also in Hungary. Curve 3 represents the size distribution of atmospheric aerosol particles obtained over the oceans of the Southern Hemisphere (the curve does not contain the distribution of sea salt particles dicussed later). Finally, curve 4 is the size distribution of large and giant particles observed at an altitude of 3 km above inversion layers over Central Europe (A. MÉSZÁROS, 1969). It can be seen by comparing these size distributions that the aerosol structure varies considerably as a function of the pollution of the place considered. The difference between curve 1 and 3 is particularly great in the range of smaller particles. The coarse mode is also evident in distributions 1 and 2. The concentration of coarse (or giant) particles is 0.40 and 0.12 cm^{-3}, respectively. Unfortunately, when distribution 4 was measured, only optical microscopic evaluation was made. However, comparison of curves 3 and 4 shows that the distribution of large and giant particles at an altitude of 3 km over continents practically coincides with the spectrum

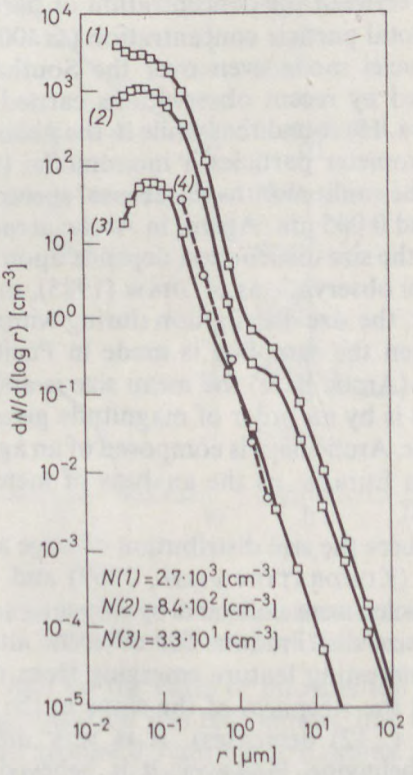

Fig. 2.8

Size distribution of atmospheric aerosol particles under various conditions. (1): urban; (2): continental; (3): tropospheric background; (4): continental at 3000 m above inversions; N: total number of particles with radius larger than 0.03 μm. (Data of A. MÉSZÁROS)

of aerosol particles measured in remote oceanic areas without the sea salt component. This fact also supports the concept of a tropospheric background aerosol.

It can also be seen that the maximum of distribution 3, referring to background conditions, occurs around 0.1 μm radius, a value in the range of the accumulation mode. It should be mentioned that the form of this spectrum agrees fairly well with the distributions found by other workers over the North Atlantic (JUNGE and JAENICKE, 1971; TYMEN *et al.*, 1975) and over other remote areas (BIGG, 1980) like Alaska, Hawaii, Tasmania and Antarctica. However, the maximum of the distribution over the Northern Hemisphere is shifted to smaller sizes probably as a result of indirect anthropogenic effects.

On this point, JUNGE and JAENICKE (1971) identified, by the diffusion channel technique, another maximum in the aerosol particle spectrum below 0.01 μm, which proves the presence of primary particles formed by reaction and subsequent condensation (nuclei mode). This finding is supported by data of HAAF and JAENICKE (1980) gained on sunny days during a North Atlantic expedition. Such measurements were not performed by A. MÉSZÁROS and VISSY (1974). However, comparison between the concentration of particles with radii larger than 0.03 μm and the total particle concentration ($\cong 400\ cm^{-3}$) makes evident the presence of the nuclei mode even over the Southern Hemisphere. This assumption is confirmed by recent observations carried out by ITO (1985) in clean air over Antarctica. He found that while in the polar night months the size distribution of submicrometer particles is monomodal (with a maximum at a radius of 0.03 μm), in the sunlit months the aerosol spectrum is bimodal, having another mode at around 0.005 μm. Again, in Arctic areas the situation is more complicated. In winter the size distribution depends upon the type of air masses, as shown by the aerosol observations of SHAW (1985), made in central Alaska. According to this work, the size distribution during winter months is similar to curve 3 in Fig. 2.8 when the sampling is made in Pacific marine air masses. However, in Arctic air (Arctic haze) the mean size is about 5 times larger and the mass concentration is by an order of magnitude greater than during intrusions of warm Pacific air. Arctic haze is composed of an aged polluted continental aerosol coming from Eurasia, as the analysis of meteorological conditions indicates (RAATZ, 1985).

In the upper troposphere the size distribution of large and giant particles was investigated by Soviet (KONDRATYEV *et al.*, 1969) and American (BLIFFORD, 1970) researchers. Particles were collected by impactors in both cases. Figure 2.9 shows BLIFFORD's size distributions for different altitudes, obtained over Nebraska, USA. An interesting feature emerging from the distributions presented is the decrease in the steepness of the slope in the distributions (that is, the value of β in Eq. (2.12) decreases). It is very difficult to explain this peculiarity of aerosol behavior. However, it is believed that the removal of aerosol particles by cloud elements (Section 2.6) plays an important role in control of the size distribution of aerosol particles in the troposphere.

The first model size distribution of stratospheric aerosol particles was con-

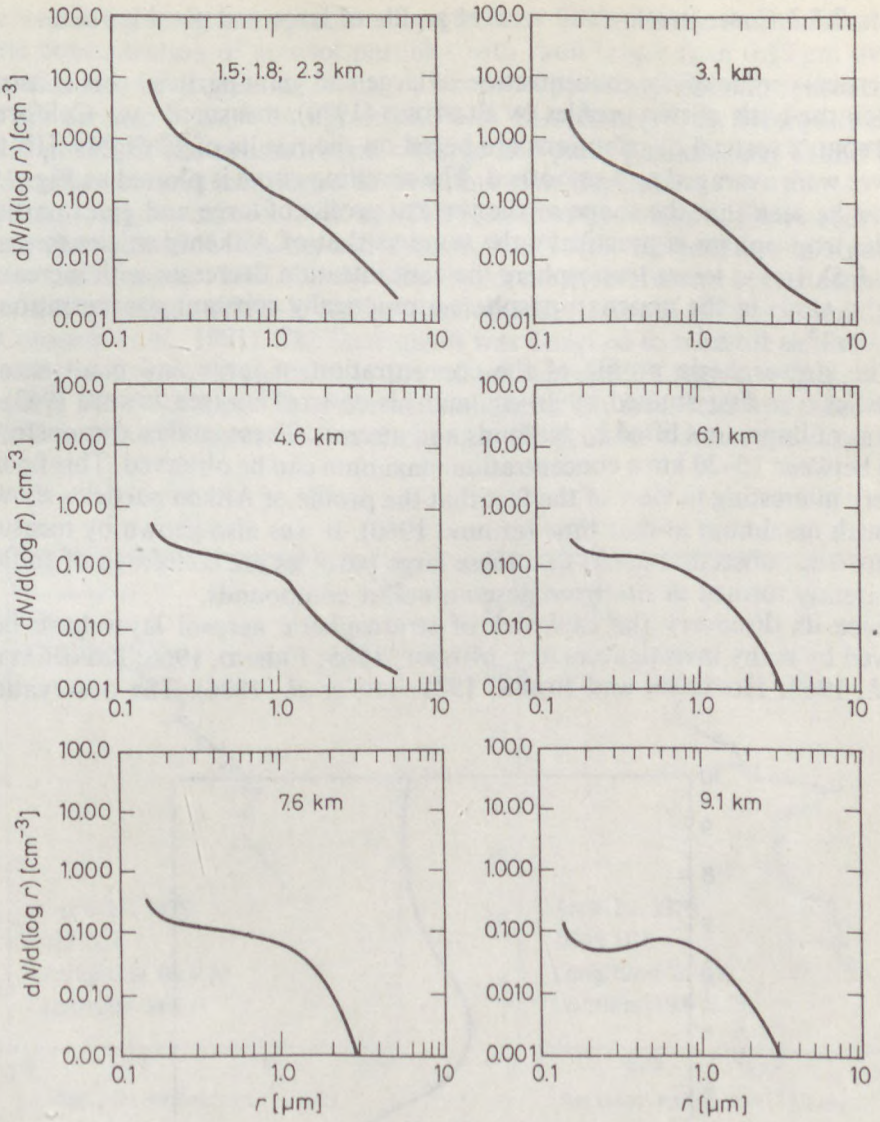

Fig. 2.9

Size distribution of large and giant particles at various altitudes (BLIFFORD, 1970). (Copyright by the American Geophysical Union)

structed by FRIEND (1966) on the basis of information available at that time. He postulated that the spectrum has two modes, one in the range of Aitken particles and the second around 0.3 μm particle radius. However, according to the results of the measurements of BIGG (1976) the distribution has its maximum at a smaller size. It is very probable that the actual size spectrum varies as a function of time and location of volcanic activity (Subsection 2.4.3) as it is shown by measurements carried out more recently (INN *et al.*, 1982).

2.3.3 Concentration and vertical profile of large and giant particles

A vertical profile of the concentration of large and giant particles was constructed on the basis of two profiles by BLIFFORD (1970), measured over California. BLIFFORD's vertical distributions are based on the results of 12 flights. His two curves were averaged and smoothed. The resulting curve is plotted as Fig. 2.10. It can be seen that the shape of the vertical profile of large and giant particles in the troposphere is practically the same as that of Aitken particles (see also Fig. 2.5). In the lower troposphere the concentration decreases with increasing height, while in the upper troposphere a practically constant concentration of 1–2 cm^{-3} is found.

The stratospheric profile of the concentration of large and giant aerosol particles was first studied by JUNGE and his co-workers (see JUNGE, 1963) by means of impactors lifted by balloons and aircraft. These studies demonstrated that between 15–20 km a concentration maximum can be observed. This finding is very interesting in view of the fact that the profile of Aitken particles showed no such maximum at that time (around 1960). It was also shown by measurements (see Subsection 2.4.3) that these large particles are composed of sulfates apparently formed *in situ* from gaseous sulfur compounds.

Since its discovery the existence of stratospheric aerosol layer have been proved by many investigators (e.g. MOSSOP, 1965; FRIEND, 1966; KONDRATYEV *et al.*, 1969; HOFMANN and ROSEN, 1981; ITO *et al.*, 1986). The observations

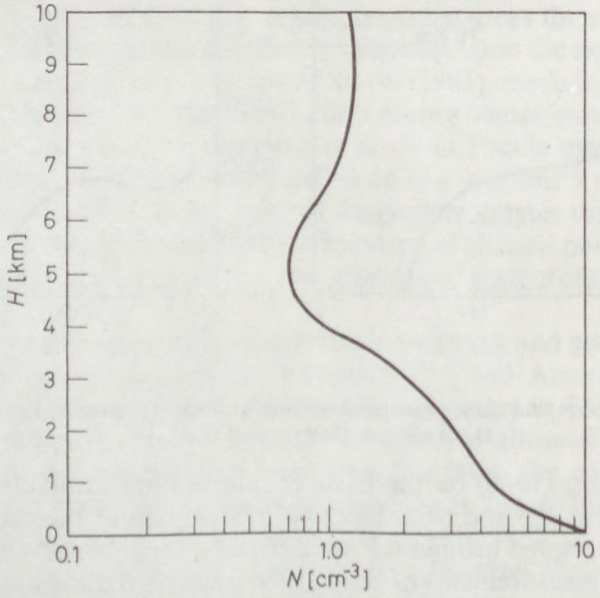

Fig. 2.10

Vertical distribution of the concentration of large particles according to BLIFFORD (1970). *H*: height; *N*: number concentration. (Copyright by the American Geophysical Union)

made with a light scattering counter by ITO *et al.* (1986) show that the stratospheric concentration of aerosol particles with radii larger than 0.15 μm over Antarctica may be as great as 15 cm^{-3}, whereas upper tropospheric concentrations are around 1 cm^{-3}, in agreement with BLIFFORD (1970). However, the vertical profile of the concentration of large and giant particles was found by the Japanese workers mentioned to be rather time-dependent.

The stratospheric aerosol layer was first identified by means of lidar observations in 1964 and 1965 (GRAMS and FIOCCO, 1967) after the emission of Agung volcano (Indonesia) in 1963. On the other hand, the measurement of stratospheric particles by using satellite-borne instruments was started in 1978 on Nimbus 7 (MCCORMICK *et al.*, 1981). The instrument was designed to measure extinction caused by stratospheric particles in the 1.0 μm wavelength region. Figure 2.11 represents the vertical profile of the aerosol extinction measured by spacecraft by MCCORMICK and his associates (INN *et al.*, 1982) under normal and volcani-

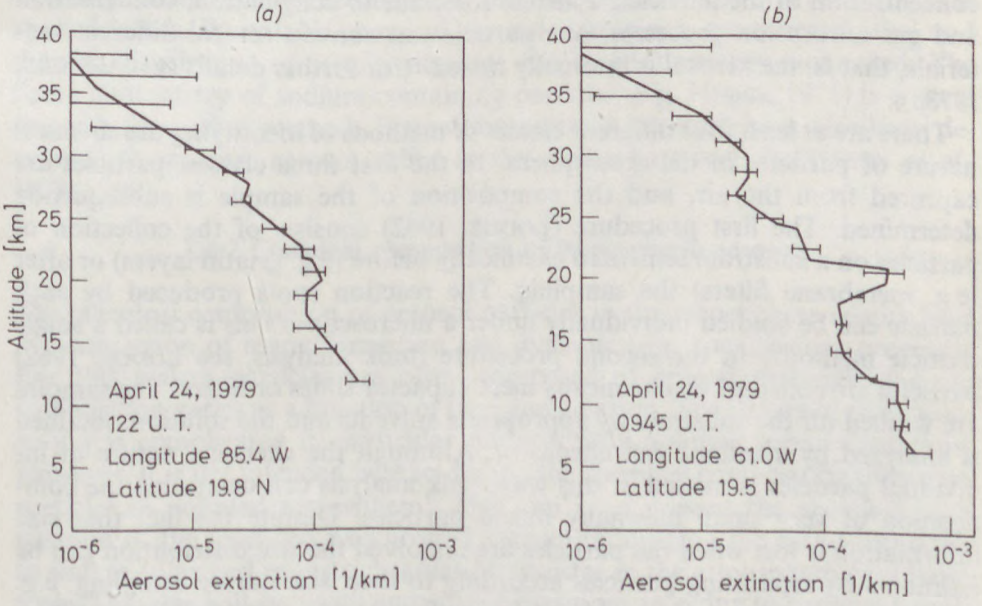

Fig. 2.11

The vertical profile of aerosol extinction with *(b)* and without *(a)* the effect of volcanic activity (INN *et al.*, 1982). (By courtesy of Springer-Verlag)

cally active conditions. The results plotted in Fig. 2.11*b* were obtained in the stratosphere influenced by the material injections from the Soufrière volcano (St. Vincent: 13.3° N, 61.2° W). In Fig. 2.11*b* an extinction maximum at 20.4 km can be seen, which is approximately four times greater than the appropriate value in Fig. 2.11*a*. Finally, stratospheric aerosol observations from Earth-

orbiting spacecraft are very promising since this procedure increases considerably the opportunities for measurements at different locations and times. Thus, the two-dimensional aerosol distribution can also be determined by satellite observations as discussed by INN *et al.* (1982).

2.4 Chemical composition of atmospheric aerosol particles

2.4.1 The main methods of identification

Effects of the atmospheric aerosol depend not only on the concentration and size but also on the chemical composition of particles. For this reason the study of the chemical nature of particulate matter in the atmosphere is of crucial importance. This study is rather complicated because of the small mass and concentration of the particles. Furthermore, due to coagulation, condensation and gas adsorption processes, one particle can contain several different materials, that is, the aerosol is internally mixed[1] (for further details see JAENICKE, 1978a).

There are at least four different classes of methods of identifying the chemical nature of particles in the atmosphere. In the first three classes, particles are captured from the air, and the composition of the sample is subsequently determined. The first procedure (LODGE, 1962) consists of the collection of particles on a substrate sensitized chemically before (e.g. gelatin layers) or after (e.g. membrane filters) the sampling. The reaction spots produced by each particle can be studied individually under a microscope. This is called a single particle method[2]. In the second procedure (bulk analysis, see LODGE, 1962) particles are collected on chemically inert impactor slides or filters. The samples are washed off the substrate by appropriate solvents and the solution obtained is analyzed by standard wet chemistry. Although the chemical nature of individual particles is missed in this way, bulk analysis can determine the composition of very small internally mixed particles. Despite the fact that size information is lost when the particles are dissolved the size distribution can be estimated by separating particles according to their size during sampling, e.g. by cascade impactors and suitable filters (see FINLAYSON–PITTS and PITTS, 1986).

Modern bulk analysis methods make possible non-destructive chemical identification, which means that the sample remains intact after analysis. Such a procedure is provided by electron microprobe or X-ray fluorescence analyses, in which the sample is irradiated by electron beams or X-rays and the elemental composition is determined on the basis of induced characteristic X-ray emis-

[1] By contrast, an external mixture contains particles, each of which is composed of a pure substance.

[2] Individual aerosol particles can also be characterized by up-to-date physical methods. The reader interested in these procedures is referred to SPURNY (1986).

sions. These methods have been successfully employed to study both stratospheric (JUNGE, 1963) and tropospheric (GILLETTE and BLIFFORD, 1971) aerosol particles. In the last decade many aerosol studies (see e.g. WINCHESTER, 1981) have been carried out by means of the proton-induced X-ray emission (PIXE) method first applied by JOHANSSON *et al.* (1975). Neutron activation analysis is also widely used to identify the chemical composition of atmospheric particulate matter (e.g. DUCE *et al.*, 1966; RAHN *et al.*, 1971); this is also a non-destructive procedure.

The third major class of analytical techniques may be called morphological methods. This identification consists of comparing the form of particles captured with the morphology of particles of known composition. Morphological similarity is a necessary but not always sufficient condition for compositional identity. In spite of this problem this procedure is widely employed mainly in clean atmosphere, since even Aitken particles can be identified morphologically (A. MÉSZÁROS and VISSY, 1974; BUTOR, 1976; PARUNGO *et al.*, 1986).

In the fourth type of identification the chemical composition of particles is studied *in situ*. By suitable chemical aerosol instruments the concentration and the size distribution of certain elements can be continuously monitored. The flame photometry of sodium-containing particles (e.g. HOBBS, 1971) is a good example for such a method. Flame photometric detectors have also been developed to measure aerosol sulfur in the atmosphere (e.g. KITTELSON *et al.*, 1978).

2.4.2 Chemical composition of tropospheric aerosols

The chemical composition of aerosol particles in the troposphere results from the interaction of many formation and dynamic (e.g. coagulation) processes. For this reason particles are often composed of several materials and the composition varies as a function of time and location. The nature of particulate matter is complicated in particular under locally polluted urban conditions. However, it is not intended here to discuss the chemical composition of aerosol particles in polluted atmosphere[1]. Our aim is to present the chemical composition of the so-called background aerosol influencing the cloud formation as well as solar and terrestrial radiation transfer in the atmosphere on a larger scale. Thus, we will deal with aerosol compositions referring to regional (rural), continental and global scales. As we will see the major part of tropospheric background aerosol consists of water-soluble substances. For this reason we begin the present section with the discussion of the water-soluble part of atmospheric particulate matter important for cloud droplet formation as we will see in the next chapter.

The investigation of the composition of water-soluble particles started with the classical measurements of JUNGE (1963), who collected particles with a

[1] The interested reader is referred to the review of CORN (1976) and to the book of FINLAYSON-PITTS and PITTS (1986).

two-stage cascade impactor, the two stages corresponded to the large and giant size range, respectively. Samples were washed off the collecting surface with a small quantity of distilled water, and the ions dissolved were analyzed by microchemical methods (bulk analysis). Measurements were carried out in continental air (Frankfurt, FRG) as well as under maritime conditions in eastern USA, Florida and Hawaii. The results indicate that in the large size range water-soluble species consist of ammonium and sulfate and their mass ratio practically coincides with the stoichiometric ratio of SO_4^{2-} to NH_4^+ in ammonium sulfate. In the size range of giant particles over maritime areas chloride and sodium predominate. The major part of nitrate ions is found in the giant size range because of the interaction of gaseous NO_x and sea salt particles[1]. The concentration of chloride ions increases, while the sulfate level decreases in the direction of more maritime environments. However, in the giant range relatively high sulfate concentrations can be detected even under oceanic conditions owing to the sulfate fraction of sea salt.

Table 2.3

Size distribution of the mass of various ions in percentage of the total mass of the ion considered (E. MÉSZÁROS, 1968). (By courtesy of *Tellus*)

Size range	NH_4^+	SO_4^{2-}	Cl
Giant	8	12	33
Large	45	45	49
Aitken	47	43	18

The measurement technique of JUNGE was extended to Aitken particles in the sixties by several workers. In these studies cascade impactors were backed up by suitable filters to capture unimpacted small particles. Table 2.3 shows the results obtained in this way by E. MÉSZÁROS (1968) under moderately polluted continental conditions. In the table the values are expressed in percentage of the total mass. It can be seen from these data that approximately half of the *mass* of sulfate and ammonium ions may be found in the Aitken size range, which means that on a *number basis* the great majority of sulfate particles have radii less than about 0.1 μm. This is hardly surprising, considering the formation mechanism of secondary aerosol particles. It is to be noted that the mass median diameter of sulfate particles identified agrees well with the geometric mean of the accumulation mode, as discussed by WHITBY (1978; see also Fig. 2.7). In contrast to sulfate- and ammonium-containing aerosol particles, only 20% of chloride ions are detected in the Aitken size range and in this case the fraction found on giant particles is also significant, in agreement with JUNGE's results discussed above. MÉSZÁROS' measurements also showed that the relative quantity of water-soluble substances increases with decreasing particle size, which

[1] During this process sodium nitrate is formed with the liberation of gaseous hydrochloric acid.

also suggests that the amount of particulate matter formed by mechanical disintegration is less significant in the range of smaller particles.

An important step in the understanding of the formation and composition of tropospheric background aerosol was provided by the work of FENN *et al.* (1963) who demonstrated that in aerosol samples collected in Greenland, 40%

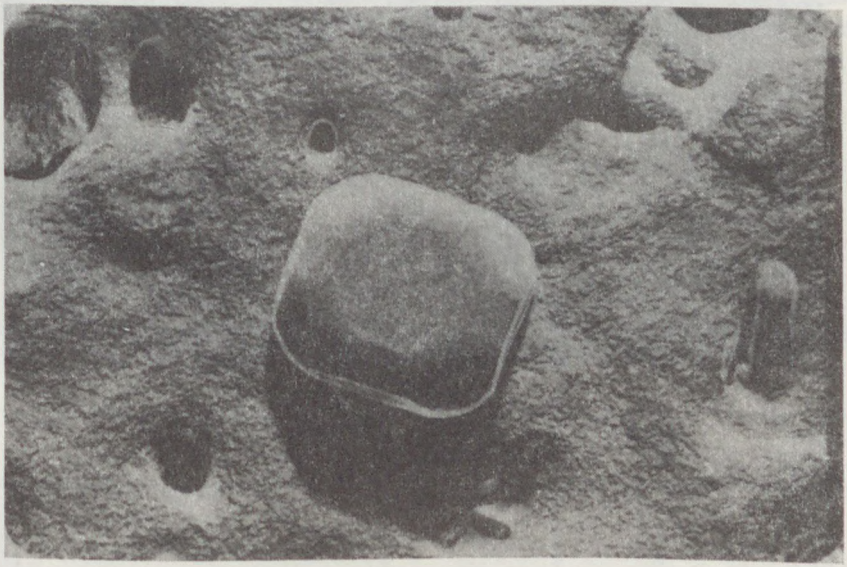

Fig. 2.12a

Fig. 2.12b

Fig. 2.12c

Fig. 2.12d

Electron micrographs of aerosol particles collected on membrane filters under remote maritime conditions (photo: A. MÉSZÁROS). *(a)* sea salt; *(b)* ammonium sulfate; *(c)* sulfuric acid; *(d)* mixed. The size of the field in the pictures is 2.4×3.6 μm. (By courtesy of Pergamon Press)

of the large particles consisted of sulfate. This finding was confirmed by American authors (CADLE *et al.*, 1968) who showed by means of special microscopic techniques (e.g. morphological identification) that in Antarctic air the large particles are formed from sulfates.

The composition of background aerosol particles, including a part of the Aitken range, was investigated by morphological identification by A. MÉSZÁROS and VISSY (1974) on the basis of membrane filter samples collected in remote oceanic air in the Southern Hemisphere. They found that 75–95% of the particles was composed of the following four substances (Fig. 2.12):

a) sea salt,
b) ammonium sulfate,
c) sulfuric acid,
d) mixture of sea salt and $(NH_4)_2SO_4$.

Table 2.4

Chemical composition of atmospheric aerosol particles expressed in percentage of the number of particles with radius larger than 0.03 μm (A. MÉSZÁROS and VISSY, 1974). (By courtesy of Pergamon Press)

	Atlantic $0 \leqq \varphi \leqq 20$	Atlantic $40 \leqq \varphi \leqq 60$	Atlantic $\varphi > 60$	Indian Ocean
$(NH_4)_2SO_4$	69	38	33	18
NaCl	1.6	15	7.3	28
H_2SO_4	–	–	7.6	3.2
Mixed	4.9	42	36	31

Note: Collections were made in remote oceanic areas. φ is the geographical latitude in the Southern Hemisphere.

In Table 2.4 the relative quantities of these substances, expressed in percentage of the number concentration of particles with $r \geq 0.03$ μm, are tabulated as a function of geographical position. It can be seen that the fraction that consists of these water-soluble substances is the smallest in the vicinity of the Equator (75%), owing to the fact that in these areas the number of insoluble particles with radii greater than 0.5 μm was relatively significant.

Figure 2.13 represents the average size distribution of sulfate and sea-salt particles observed by A. MÉSZÁROS and VISSY (1974) over different parts of the South Atlantic. One can see that on a number basis (solid lines), sulfate particles with much smaller mean radii predominate, while the major proportion of the particle volume (dotted lines) is occupied by the sea salt fraction in the coarse size range. On the basis of the data plotted, only 4% of the total volume of the particulate matter is composed of sulfates (the total volume is 6.2 $\mu m^3\ cm^{-3}$). This means that the mass concentration of aerosol particles in remote oceanic areas is also controlled by sea salt.

The quantity of sea salt particles, identified as NaCl, was found to be particularly important over the Indian Ocean. This is explained by stormy weather

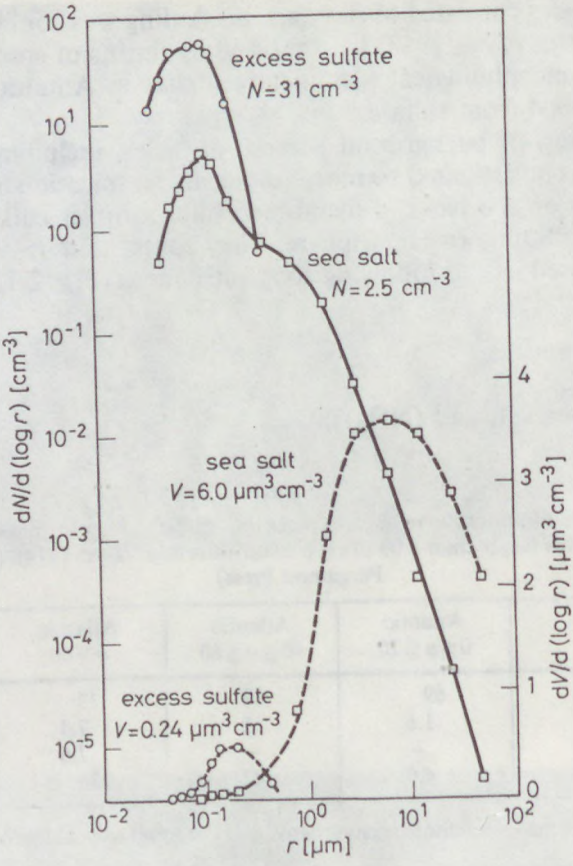

Fig. 2.13

Size distribution of the number *(N)* and volume *(V)* of excess (non sea salt) sulfate and sea salt particles with $r \geq 0.03$ μm. (Data of A. MÉSZÁROS)

conditions during the sampling period. Curve 1 in Fig. 2.14 gives the size distribution of sea salt particles measured over the Indian Ocean (the total number concentration, N, is also plotted). To represent the advection of sea salt particles over the continents, two other spectra are also shown. Curve 2 was measured by METNIEKS (1958) in Ireland, while distribution 3 was observed in the surface air in Hungary (E. MÉSZÁROS, 1964). These latter investigators used gelatin layers sensitized with silver nitrate to identify chloride particles. Figure 2.14 makes it clear that the sea salt concentration is very small in a continental environment. Furthermore, the maximum of the distribution is shifted in the direction of larger particles. However, even over the ocean very few sea salt particles have a radius smaller than 0.1 μm (3.2 cm^{-3} in this case) as compared to the total concentration of Aitken particles (Subsection 2.3.1). Finally, over the Indian Ocean practically all giant particles consisted of sea salt.

It follows from Table 2.4 that the great majority of aerosol particles consist either of ammonium sulfate or of a mixture of ammonium sulfate and sea salt. Thus, if we disregard sea salt particles we can conclude that the particulate matter in tropospheric background air consists mainly of sulfur-containing species. This finding was confirmed by BUTOR (1976) and more recently by PARUNGO *et al.* (1986) who made samplings over the North Atlantic and Pacific Ocean, respectively, and identified particles by electron microscopy. Moreover, the investigation of A. MÉSZÁROS and VISSY also shows that 70% of the number of ammonium sulfate particles are in the range of $0.03 \leqq r \leqq 0.1$ μm, in agreement with the results of continental observations (see Table 2.4) and with the direct chemical bulk analyses of WINKLER (1975) indicating that the main component of the aerosol in the Aitken size range is sulfur under oceanic background conditions.

The composition of aerosol particles in the remote atmosphere was studied

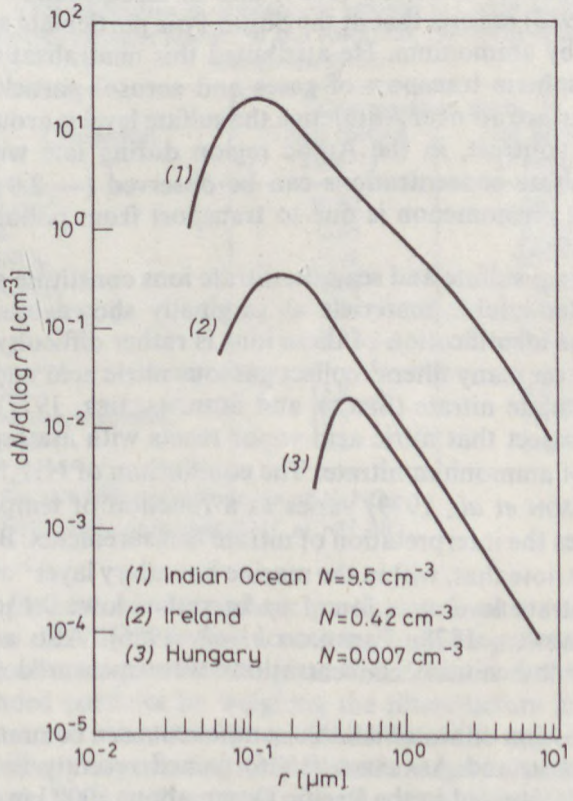

Fig. 2.14

Size distribution and concentration *(N)* of sea salt particles from different geographical regions. *(1)*: according to A. MÉSZÁROS and VISSY (1974) (by courtesy of Pergamon Press); *(2)*: according to METNIEKS (1958) (by courtesy of School of Cosmic Physics); *(3)*: according to E. MÉSZÁROS (1964) (by courtesy of *J. Recherches Atmosphériques*)

in detail by BIGG (1980) who applied electron microscopy combined with a special single-particle analysis. He collected aerosol particles by electrostatic precipitators and impactors in Alaska, Hawaii, Tasmania and Antarctica. BIGG found that, in agreement with previous discussions, smaller particles were composed mainly of sulfuric acid (Alaska and Hawaii) or ammonium sulfate (Tasmania and Antarctica). In the size range of larger particles in Alaska, a lot of mixed particles were identified which consisted of insoluble cores coated by sulfuric acid. On the other hand, in Tasmania particles larger than 0.1 μm were of oceanic origin. At the sampling site in Tasmania (Cape Grim) a mass size distribution similar to the volume spectrum presented in Fig. 2.13 was measured. In remote Everest highlands at altitudes between 5400 and 6500 m ONO *et al.* (1983) also found that in the submicrometer size range atmospheric particles consisted of sulfate particles. By using a selective single-particle method, ONO and his associates also showed that sulfate particles were in the form of hydrated sulfuric acid solution and/or in the form of supersaturated acidic droplets. In agreement with BIGG (1980) and in disagreement with Japanese workers, GRAS (1983) reports that at the South Pole particulate sulfate is nearly fully neutralized by ammonium. He attributed this neutralization to the mid- and upper-tropospheric transport of gases and aerosol particles. Finally, we note that in the surface air over Antarctica the sulfate level is around 0.1 $\mu g\ m^{-3}$ (BIGG, 1980). In contrast, in the Arctic region during late winter or spring relatively high sulfate concentrations can be observed ($\sim$ 2.0 $\mu g\ m^{-3}$). It is expected that this phenomenon is due to transport from pollution sources in Eurasia (RAHN, 1981).

Beside ammonium sulfate and sea salt, nitrate ions constitute another important class of water-soluble materials as originally shown by JUNGE (1963). Unfortunately, the identification of these ions is rather difficult due to the fact that alkaline sites on many filters[1] collect gaseous nitric acid and cause it to be reported as particulate nitrate (SPICER and SCHUMACHER, 1977). Moreover, it is reasonable to expect that nitric acid vapor reacts with atmospheric NH_3 to form an aerosol of ammonium nitrate. The equilibrium of NH_4NO_3 with NH_3 and HNO_3 (STELSON *et al.*, 1979) varies as a function of temperature, which further complicates the interpretation of nitrate measurements. Bearing in mind these problems we note that, within the marine boundary layer[2] over the Pacific, the particulate nitrate level was found to be rather low: 0.1 $\mu g\ m^{-3}$ or less (HUEBERT and LAZRUS, 1978; PARUNGO *et al.*, 1986). Also at Ny-Ålesund, Spitzbergen, very low nitrate concentrations were measured (HEITZENBERG, 1981).

The above discussion on water-soluble components can be summarized by the results of YOSHIZUMI and ASAKUNO (1986) gained recently in Chichi of the Ogasawara Islands situated in the Pacific Ocean about 1000 km from the main

[1] Teflon filters minimize sampling artefacts.

[2] Above the boundary layer even lower concentrations were observed (HUEBERT and LAZRUS, 1978).

island of Japan. During sampling in Chichi particles were separated into several size intervals by a cascade impactor. Species were analyzed by neutron activation and wet chemistry. Sodium nitrate and ammonium nitrate were separated by a method based on the difference in their thermal stability. Table 2.5 gives the concentrations measured in the coarse and fine particle size ranges. It can be seen that sea salt, constituting the majority of the total mass, is in the coarse particle size range. Nitrate ions and soil components[1] are also in the coarse mode. The Cl loss related to Na concentration (3.1%) is comparable to the quantity of $NaNO_3$ on the mole basis. Fine particles consist mostly of sulfate ions. The concentration of ammonium makes it possible that about 75% of sulfate is neutralized by NH_4^+. YOSHIZUMI and ASAKUNO note that the unknown fraction in the fine particle range is probably composed of some organics and elemental carbon not evaluated in their program. In the following we will discuss these two types of carbonaceous particles.

Table 2.5

Characterization of atmospheric aerosols in Chichi of the Ogasawara Islands (YOSHIZUMI and ASAKUNO, 1986). (By courtesy of Pergamon Press)

Component	Concentration ($\mu g\ m^{-3}$)	
	Coarse particle ($2\ \mu m <$)	Fine particle ($2\ \mu m \geq$)
Sea salt*	10.52	0.83
Soil	2.60	0.62
$NaNO_3$	0.69	0.07
NH_4NO_3	0.05	0.08
Secondary SO_4^{2-}	0.04	1.90
$NH_4^{+\dagger}$	0.01	0.54
Total	13.9	4.0
Mass con. measured	16.5	7.4
Unknown	2.6	3.4

* Sea salt does not include Na of $NaNO_3$.

† NH_4^+ does not include NH_4^+ of NH_4NO_3.

The organic fraction of atmospheric particulate matter was investigated by KETSERIDIS *et al.* (1976) at several locations, including remote oceanic areas. These authors collected particles on glass fiber filters and determined the total mass of suspended particles by weighing the filters before and after the sampling. They extracted ether-soluble materials from the samples and were able to identify chemically organic acids and phenols, organic bases, aliphatic hydrocarbons, aromatic hydrocarbons and neutral compounds. The results obtained are summarized in Fig. 2.15. The data labelled "Meteor" refer to samplings

[1] Determined on the basis of Al concentration (see later).

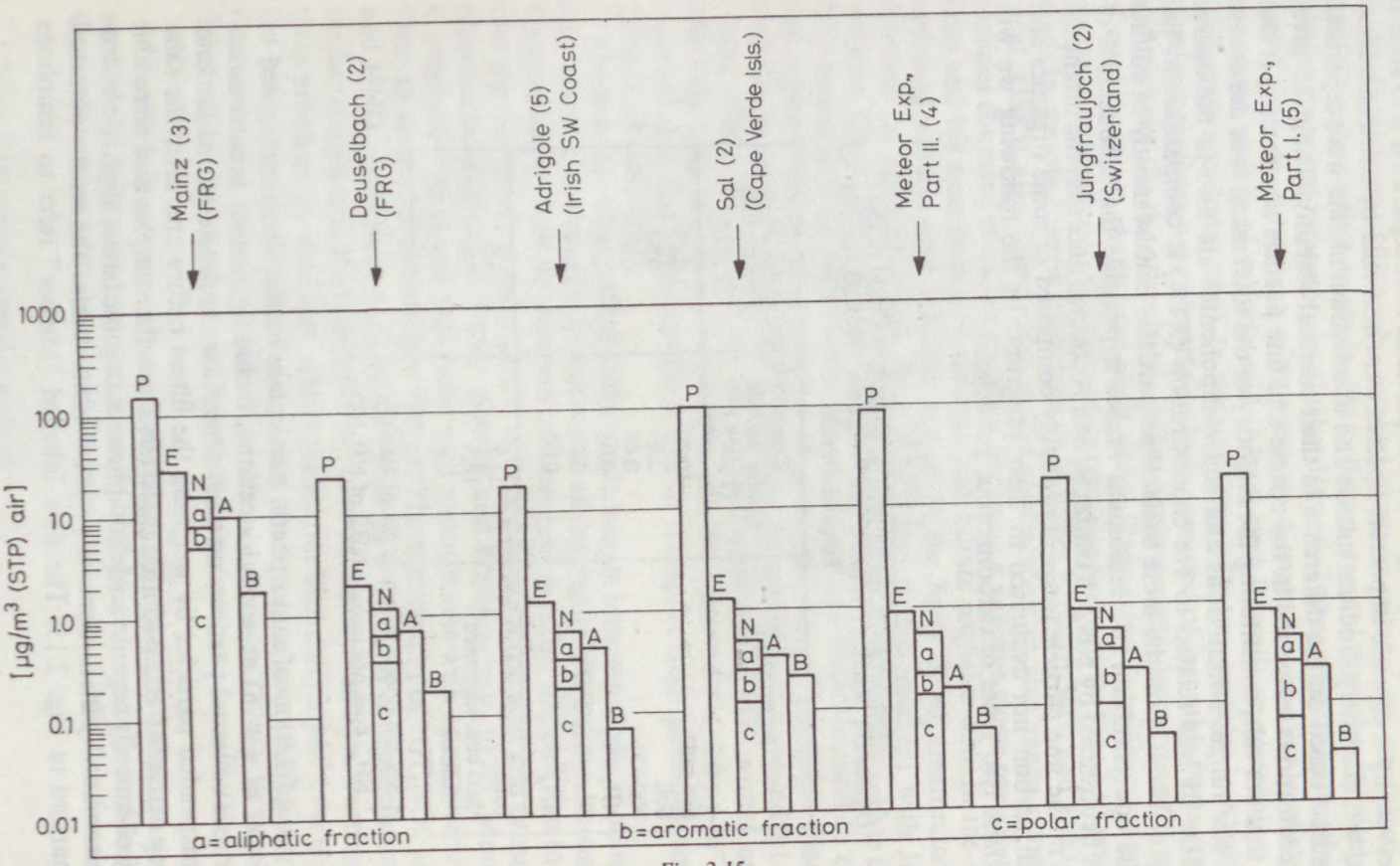

Fig. 2.15

Mass concentration of all aerosol particles *(P)* and of organic particles at different sampling sites according to KETSERIDIS *et al.* (1976). *E:* ether extractable organic material; *N:* neutral organic compounds; *A:* organic acids; *B:* organic bases. (By courtesy of Pergamon Press)

Note: The majority of the mass of all particles under marine conditions is sea salt (see Fig. 2.13). The numbers behind the names of the sampling locations give the number of samples analyzed.

carried out on board of the German research vessel Meteor in 1973 over the North Atlantic. It is to be noted that during Part II of this expedition and during sampling in Cape Verde an advection of Sahara dust was observed. One can see that, except more polluted atmospheres, the concentration of organic material extractable in ether is practically constant at about 1 $\mu g\, m^{-3}$ at standard temperature and pressure. The fraction of different components is also independent of the sampling location. At Jungfraujoch and over the Atlantic Ocean (without dust advection) about 5–10% of the aerosol particle mass is composed of organics. KETSERIDIS *et al.* (1976) assumed that this constant concentration of organic particulate matter in tropospheric background is either due to particle advection from highly populated areas or to a constant production mechanism in clean tropospheric air. In another study, KETSERIDIS and EICHMANN (1978) used an impactor to separate particles with radii smaller and larger than 1 μm. They report on the basis of their measurements carried out in Ireland, that the majority of organics are in the smaller size range where these materials comprise 25% of the aerosol mass. It is very probable that organic particles of these sizes are formed by gas-to-particle conversion.

In recent years several analyses have been made to identify organic compounds in the atmospheric aerosol (FINLAYSON–PITTS and PITTS, 1986; SIMONEIT, 1984). These studies show that higher molecular weight solvent-soluble compounds ($> C_{12}$, lipids) are common species in urban, rural and oceanic aerosols. It is demonstrated that petroleum residues predominate in urban and suburban areas, while waxes from vegetation are the main components under rural and oceanic conditions. Polycyclic aromatic hydrocarbons were also identified in urban and remote atmosphere.

The presence of elemental carbon in the particulate matter has also been demonstrated. It is expected that under polluted conditions elemental carbon particles are mostly emitted by diesel vehicles. In winter these particles are transported to long distances and they constitute an important component of the Arctic haze (ROSEN *et al.*, 1981). Moreover, significant amounts (0.01–0.1 $\mu g\, m^{-3}$) of soot carbon were observed in remote air over the tropical Atlantic and Pacific Oceans (ANDREAE *et al.*, 1984). On the basis of the concentrations of other species in the particulate matter, ANDREAE and his associates estimate that elemental carbon detected over tropical oceans is released into the air by biomass burning in the tropics and subsequently transported over oceanic areas. A. MÉSZÁROS (1984) showed by electron microscopy that elemental carbon can be internally mixed with sulfate, while COVERT and HEITZENBERG (1984) observed a high degree of external mixing between the two species.

According to recent studies of CACHIER *et al.* (1986) the average concentration of giant carbonaceous aerosol particles in remote oceanic air over the Northern and Southern Hemisphere is the same and equal to 0.07 $\mu g\, m^{-3}$ expressed in carbon equivalents. On the other hand, the mean concentration for particles with radii smaller than 0.5 μm is rather different over the two hemispheres: it is 0.45 and 0.06 $\mu g\, m^{-3}$ for the Northern and Southern Hemisphere, respectively. Carbon isotope measurements of CACHIER *et al.* indicate that carbonaceous

Table 2.6

Elemental composition of atmospheric aerosol particles under different environmental conditions expressed in ng m^{-3}

Element	Europe			Asia		Africa		N. America		S. America	Arctic		Antarctica		Pacific O.
–	K-puszta[1] Hungary	Valen[2] Sweden	Jungfraujoch[3] Switzerland	Delhi[4] India	Great Wall[5] near Beijing, China	Gezira[6] Sudan N	Gezira[6] Sudan S	St. Louis[7] USA	Twin Gorges[8] N. W. Canada	Chacaltaya[9] Bolivia	N. Greenland[10] Summer	Ny-Ålesund[11] Spitzbergen Winter	Summer[12]	Winter[12]	Enewatak Atoll[13] tropical N. Pac.
Si	1350	–	–	–	21	–	–	2260	–	200	43	110	–	–	–
Al	663	–	51	3413	–	3030	293	–	66	62	–	–	0.82	0.4	21
Ca	470	65	–	2600	–	–	–	170	–	~28	9.1	73	0.6	1.6	220
Na	–	–	22	848	–	480	197	–	18	~10	–	130	4.2	26	5200
Fe	285	72	36	2753	7.9	2996	940	960	71	58	6.4	64	0.7	0.3	15
Ti	21	4.5	2.4	–	–	–	–	–	5.0	5.2	0.9	<5	0.1	0.2	–
S	2270	650	–	–	315	767	1052	4400	–	34	27	690	78	48	–
Cl	18	130	7.2	1978	6.5	970	260	197	9.0	1.4	10	96	4.3	38	8300
Br	3.5	2.1	1.3	–	0.6	14	7.8	177	0.5	0.1	0.2	130	0.9	0.3	0.02
Pb	35	14	4.4	52	5.6	–	–	742	–	1.1	–	–	–	–	–
Cu	8.7	1.8	0.9	39	0.4	49	<9	–	0.9	0.5	–	<2	0.004	0.006	0.04
V	3.1	2.1	0.3	–	0.5	9.1	2.6	–	0.2	0.3	0.1	0.2	0.002	0.001	0.08

[1] A. MÉSZÁROS *et al.* (1984); [2] LANNEFORS *et al.* (1977); [3] elevation: 3752 m; DAMS and DE JONGE (1976); [4] KHEMANI *et al.* (1985); [5] only fine particles; WINCHESTER *et al.* (1981); [6] PENKETT *et al.* (1979a); N: north wind, S: south wind; [7] only inhalable particles ($d < 15$ µm); SPENGLER and THURSTON (1983); [8] RAHN (1976); [9] elevation: 5245 m; ADAMS *et al.* (1983); [10] FLYGER and HEIDAM (1978); [11] HEITZENBERG (1981); [12] ZOLLER *et al.* (1979); [13] DUCE *et al.* (1983)

materials in the giant size range are associated with sea salt, while fine carbonaceous particles are of continental origin.

As mentioned in Subsection 2.4.1, recent research on the composition of aerosol particles has been promoted by the application of non-destructive nuclear analytical methods (PIXE, neutron activation). These procedures have made possible to study simultaneously several elements in particulate matter. As an example, Table 2.6 contains mean concentrations of twelve elements according to the measurements carried out under different atmospheric conditions. Except some data (e.g. concentrations measured in Delhi) the values tabulated were obtained by the nuclear methods mentioned. For the sake of completeness some results for a locally pulluted place (St. Louis, USA) are also given. In this respect we note that according to KHEMANI *et al.* (1985) the samples collected in Delhi are free from the effects of local pollution sources. Thus, it is proposed that results gained at K-puszta (Hungary) and Valen (Sweden) are representatives of regional background air in Europe, while Chinese and Indian data in the table refer probably to similar conditions in Asia. Further, we believe that Jungfraujoch (Switzerland), Gezira (Sudan), Twin Gorges (Canada) and Chacaltaya (Bolivia) are suitable sites to study the continental background aerosol over Europe, Africa, North America and South America, respectively. Finally, concentrations measured at other stations, except those for Ny-Ålesund and Enewetak Atoll, give information about global tropospheric background air. As we discussed above, data observed in Arctic regions during late winter are related to Arctic haze, while values gained at the station in the Pacific Ocean represent remote oceanic conditions.

If we do not consider the concentrations measured over the Pacific Ocean (which are controlled by sea salt components) one can say that data can be divided into two groups. The first six elements (from Si to Ti) are of soil origin, which is proved by their crustal enrichment factors defined in Subsection 2.2.1. On the other hand, sulfur, chlorine, bromine, copper, lead and vanadium are typically so-called enriched elements, the concentration of which are controlled by different natural and anthropogenic emissions. (Lead and vanadium are notorius man-made elements due to exhaust materials from vehicles and to combustions processes, respectively.) In agreement with the discussion in Section 2.2, elements in the first category are in the coarse particle range, while enriched species can be detected generally in the fine size range (see the references given in the table).

As it can be seen from values tabulated, enriched elements have high concentrations under polluted conditions, while the concentration of elements of soil origin is significant particularly in the air influenced by dust particles coming from deserts (Delhi, Gezira in the case of north winds)[1]. It is interesting to note that the atmospheric level of crustal elements is rather high even at elevated altitudes (Jungfraujoch, Chacaltaya). For Gezira, Arctic and Antarctica the

[1] It is noted that in Delhi the total mass concentration of aerosol particles is about 100 and 200 $\mu g\ m^{-3}$ for monsoon and dry season, respectively (KHEMANI *et al.*, 1985), while it is only 3.1 $\mu g\ m^{-3}$ at the Jungfraujoch (DAMS and DE JONGE, 1976).

concentrations are separated into two classes. In the case of Gezira, data are separated according to the wind direction. This is explained by the fact that at this site an aerosol originating from deserts can be observed if the wind blows from north, while south winds transport to the site aerosol particles of tropical origin. Further, Antarctic concentrations are grouped according to the seasons of the year. This classification clearly shows that sulfate–sulfur, the majority of particulate matter, has a high concentration in summer, in agreement with our discussion about Aitken particles in Subsection 2.3.1. On the other hand, winter Antarctic data indicate that in winter sea salt is an important component of the atmospheric aerosol in this remote area. Finally, the comparison of summer and winter data obtained over Arctic regions makes evident the presence of the Arctic haze during late winter. Data indicate that the ratio of winter to summer concentrations is especially high in the case of sulfur.

Table 2.7

Chemical composition of aerosol particles in the upper troposphere over the Philippine Islands on November 19, 1969, from the aircraft measurements of CADLE (1973). (By courtesy of Plenum Press)

Latitude N	Longitude W	Height 10^{-3} feet	Concentration [$\mu g\ m^{-3}$ ambient air]					
			SO_4^{2-}	Si	Na	Cl	NO_3^-	NH_4^+
35°04′	139°35′	26	0.041	–	–	–	0.020	0.0064
26°21′	120°40′	26	0.051	0.011	0.055	0.085	0.019	0
19°32′	120°40′	25	0.10	0.016	0.016	0.052	0.042	0.0013
16°30′	117°00′	25	0.15	0.022	<0.001	0.029	0.022	0.013
13°00′	124°00′	25	0.073	0.009	0.010	0.013	0.039	0.0033
21°00′	127°54′	25–39	–	0.014	0.019	0.018	–	–
11°00′	119°00′	39	0.16	0	0.019	0.018	–	–
11°00′	122°00′	39	0.23	0.007	0	0.057	–	0
16°52′	117°15′	39	0.068	0.003	0.016	0.052	0.026	0

Note: 1 foot = 30.48 cm

In the upper troposphere the chemical composition of aerosol particles was widely studied by American researchers (CADLE, 1973). During aircraft flights, particles were collected on special filters, and the samples were subsequently analyzed by wet chemistry and neutron activation. The results obtained in the upper tropical troposphere near the Philippine Islands are tabulated in Table 2.7. These data show that the sulfate concentrations are much higher than those of silicon, chloride and sodium, showing that sea salt and mineral dust are unimportant at these altitudes. It is interesting that very small ammonium concentrations were found. This finding makes it likely that the majority of the sulfate consists of sulfuric acid droplets, which are less common near the Earth's surface (A. MÉSZÁROS and VISSY, 1974) owing to higher NH_3 concentrations. This result is supported by the work of ONO *et al.* (1983) mentioned above and by the observations of GEORGII (1978) and TANNER *et al.* (1984). These latter authors demonstrated that the acidity of sulfate particles increases with increas-

ing altitude in the lower troposphere. Finally, it should be mentioned that CADLE argues that the relatively high nitrate concentrations are explained by the adsorption of HNO_3 vapor by the filter material.

The vertical profile of different elements in particulate matter was investigated by GILLETTE and BLIFFORD (1971) who used cascade impactors and filters to collect particles. The sulfur profiles obtained over the Pacific Ocean near California and over the American continent (Death Valley) are represented by the data given in Table 2.8. By re-calculating their concentrations in sulfate we can say that in the upper troposphere the sulfate level is 0.1–0.2 $\mu g\, m^{-3}$ which agrees reasonably well with figures in Table 2.6 as well as with the results of near surface measurements of WINKLER (1975) carried out in remote areas. However, the sulfate concentrations observed by GILLETTE and BLIFFORD (1971) are too high as compared to the values measured over South America at an altitude of 5245 m by ADAMS *et al.* (1983, see Table 2.6). The X-ray fluorescence analyses of GILLETTE and BLIFFORD (1971) also showed that 80–90% of the sulfate (sulfur) found occurs in the Aitken size range.

Table 2.8

Vertical profile of the mass concentration of particulate sulfur according to GILLETTE and BLIFFORD (1971). (Copyright by the American Geophysical Union)

Height [km]	Pacific Ocean [$\mu g\, m^{-3}$]	Death Valley [$\mu g\, m^{-3}$]
0.015	0.24 (3)	0.31 (5)
0.915	0.09 (4)	0.32 (5)
1.5	–	0.23 (1)
1.8	0.11 (6)	0.24 (5)
3.7	0.04 (6)	0.14 (5)
4.6	–	0.03 (1)
6.1	0.05 (5)	0.07 (6)
7.6	0.03 (5)	0.12 (6)
9.1	0.06 (4)	0.06 (5)

Note: Values in parentheses give the number of observations. Samples were collected in 1967.

On the basis of the foregoing discussion it is concluded that troposheric particles in the fine size range consist mainly of water-soluble sulfates. Sulfate particles contain hydrogen or ammonium ions as a function of the amount of the ammonia gas available. It seems that the relative importance of hydrogen ions increases with increasing altitude. It is also demonstrated that sulfate particles are (externally or internally) mixed with carbonaceous materials at least near the Earth's surface[1]. In the coarse size range particles may be of

[1] According to JAENICKE (1978b), in the Aitken size range 25% of particles consist of organic materials under tropospheric background conditions.

crustal or oceanic origin. Crustal particles are composed mostly of Al, Si and Fe compounds, while sea salt particles consist of chloride and sodium in agreement with the composition of sea water.

2.4.3 Stratospheric particles

At the end of the fifties a program was started in the USA to study stratospheric aerosol particles. The results of the program were analyzed by JUNGE and his associates (JUNGE, 1963). The most important achievement of this study was the discovery of an aerosol layer between 15–20 km consisting mostly of large particles (see Subsection 2.3.3).

To investigate their chemical composition, stratospheric particles were collected by aircraft- and balloon-borne impactors. Elements with atomic numbers 12–30 were identified in the samples by electron microprobe and X-ray fluorescence techniques. Table 2.9 summarizes the results obtained (JUNGE,

Table 2.9

Chemical composition of stratospheric aerosol particles (JUNGE, 1963). (By courtesy of Academic Press)

Elements	Number of observations	Concentration [10^{-3} μg m^{-3}]	Relative composition
Mg	4	0.0	0.000
Al	4	0.43	0.056
Si	12	0.11	0.014
P	4	0.000	0.000
SO_4	11	6.82	0.89
Cl	4	0.01	0.0013
K	7	0.13	0.017
Ca	8	0.10	0.013
Ti	3	0.000	0.000
V	4	0.000	0.000
Cr	4	0.000	0.000
Mn	4	0.000	0.000
Fe	12	0.071	0.0093
Co	4	0.000	0.000
Ni	7	0.000	0.000
Cu	4	0.000	0.000
Zn	4	0.000	0.000
Total	12	7.68	1.00

1963). In this table the sulfur is given as sulfate since further wet chemical analyses showed that the sulfur occurred as sulfate particles. It can be seen from the data that 89% of the mass of the components identified is sulfate. Data also indicate that the quantity of NH_4^+ is sufficient only to neutralize about one third of the sulfate ions. Further flights carried out over a wide range of latitudes

(60° S–70° N) demonstrated that this sulfate layer can be observed everywhere in the stratosphere.

About ten years later a new stratospheric aerosol program was performed. In this case, particles were collected between 17 and 28 km by absolute filters having a collection efficiency of virtually 100% in all size ranges. Table 2.10 shows the results of a sampling day when particles were collected at an altitude of 18 km. In the last column of the table the percentage of sulfate ions possibly neutralized by NH_4^+ is also presented. It can be seen that the concentrations measured by this more recent program exceed by at least one order of magnitude the concentration found in the previous program (see Table 2.9). Furthermore, LAZRUS and his co-workers (1971) found high sulfate mass concentrations even

Table 2.10

Mass concentration of sulfate and ammonium particles sampled at an altitude of 18 km on May 11, 1970 (LAZRUS *et al.*, 1971). (Copyright by the American Geophysical Union)

Latitude	Longitude	SO_4^{2-}	NH_4^+	%
38°10′	106°50′	0.17	0.0030	5.0
42°00′	106°50′	0.22	0.0036	4.6
45°36′	106°52′	0.19	0.0030	4.5
49°30′	106°45′	0.16	0.0024	4.1
53°02′	106°56′	0.22	0.0030	3.9
54°58′	106°56′	0.24	0.0034	4.0
51°15′	106°57′	0.20	0.0043	5.9
48°05′	106°54′	0.15	0.0029	5.3
44°30′	106°53′	0.20	0.0038	5.2

Note: Values in last column give relative quantity of sulfate ions associated to ammonium. Concentrations are expressed in $\mu g\ m^{-3}$.

when the optical measurements designed to detect large particles did not indicate the presence of an aerosol layer. These data strongly suggest that the difference between the results of the two programs is caused by the different sampling techniques used. Further studies in which simultaneous impactor and filter samples were taken showed (CADLE *et al.*, 1973) that a sizeable part of the sulfate was really in the Aitken size range. However, we cannot rule out the possibility that the concentration differences may be explained partly by an increase of stratospheric sulfate burden arising from the volcanic activity between 1960 and 1970. This assumption is proved by stratospheric aerosol measurement carried out more recently. Thus, WOODS and CHUAN (1983) demonstrated that the submicrometer particles in the stratosphere consisted mainly of sulfuric acid after the El Chichón eruptions in 1982.

The first stratospheric aerosol chemical analyses showed that only a small quantity of the aerosol particles in the lower stratosphere could be of meteoritic origin (e.g. no nickel was found in the samples, see Table 2.9). This problem was studied in detail by SHEDLOVSKY and PAISLY (1966) who found by means of

neutron activation of aerosol particles collected on filters that the stratospheric Fe/Na ratio is close to that reported for the Earth's crust. They concluded that less than 10% of the iron and sodium identified at altitudes of 19–21 km come from meteorites. This is consistent with more recent observations showing that meteoritic particles are detected generally above 20 km (INN *et al.*, 1982). Numerical calculations made by means of an appropriate aerosol model indicate (TURCO, 1982) that meteoric debris has a small, but perceptible effect on the aerosol mass in the stratosphere. Finally, we note that volcanic eruptions inject a large amount of ash particles into the stratosphere having a size larger than 2 μm (KNOLLENBERG and HUFFMANN, 1983). It was also found (WOODS and CHUAN, 1983) that magmatic and lithic particles play an important temporary role in the control of the composition of stratospheric aerosol after volcanic eruptions.

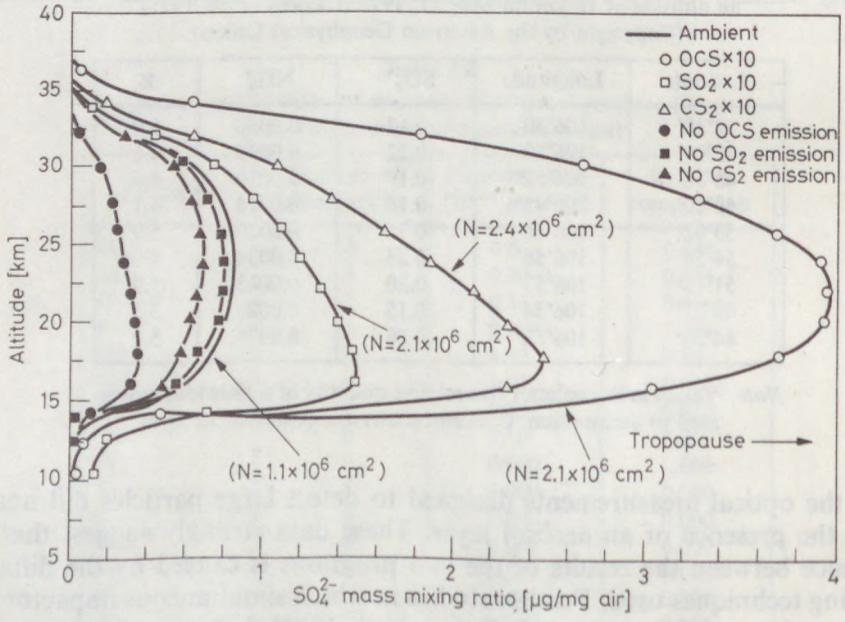

Fig. 2.16

Mixing ratio of sulfate particles in the stratosphere according to model calculations by TURCO (1982). (By courtesy of Springer-Verlag)

JUNGE (1963) assumed that the sulfate particles in the stratosphere are formed by chemical transformation of SO_2 and H_2S gases mixing into the stratosphere mostly over the tropics. On the other hand, MARTELL (1966) concluded that large stratospheric sulfate particles are due to the coagulation of Aitken-sized sulfate particles transported from the troposphere. According to our present knowledge, during volcanically active periods stratospheric particles form mostly from sulfur dioxide of volcanic origin. Thus, EVANS and KERR (1983) estimate

that the Mt. Helens eruption in 1980 injected 0.6 Tg of sulfur dioxide into the stratosphere, while the corresponding value was 13.4 Tg in the case of the El Chichón eruption. Accordingly, after El Chichón eruption GANDRUD *et al.* (1983) observed that sulfate mixing ratios were by two orders of magnitude greater than typical background values.

In volcanically inactive periods carbonyl sulfide emitted at the surface is responsible for the formation of a major part of stratospheric sulfate layer, as first proposed by CRUTZEN (1976). A less important role is played by carbon disulfide also released at the Earth's surface, while the effect of SO_2 in these time periods is insignificant. This concept is well demonstrated by model calculations carried out by TURCO (1982) illustrated in Fig. 2.16. It can be seen that the present ambient concentration is controlled primarily by carbonyl sulfide. On the basis of TURCO's calculations the possible future anthropogenic perturbations can also be estimated. These perturbations are due to the fact that increasing consumption of fossil fuels will increase the emission of sulfur gases. Assuming a tenfold increase in atmospheric carbonyl sulfide concentration[1], a fourfold increase in sulfate mixing ratio can be expected. The curves plotted in Fig. 2.16 make it probable that perturbations in carbonyl sulfide level will greatly affect the concentration of the stratospheric aerosol layer.

RUSSEL and HAMILL (1984) reviewed the literature on stratospheric aerosol composition. They concluded that sulfate particles are not neutralized and consist mostly of sulfuric acid[2]. The sulfuric acid solution droplets found in the stratosphere originate from the condensation of H_2SO_4 vapor formed by chemical reactions of precursor gases. There is some indication that this condensation takes place on existing Aitken particles. Thus, MOSSOP (1965) observed that stratospheric solution droplets frequently contain small insoluble particles. Theoretical work by HAMILL *et al.* (1977) also indicates that heterogeneous condensation of H_2SO_4 and H_2O vapors in the stratosphere is much more probable than a homogeneous phase transition. However, FARLOW *et al.* (1977) concluded on the basis of the analysis of individual particles collected in the stratosphere that imbedded undissolved materials did not act as nucleation centers for droplet formation. Without going into more detail we note that further studies are needed to clarify this point.

On the basis of the above discussion we can conclude that the composition and origin of stratospheric particles are rather well established due to recent research. It is well-documented that volcanic activity is the most important factor in the control of the aerosol cycle in the stratosphere having an influence in this way on climate variations, as is discussed in Chapter 5 of this book.

[1] The abundance of only one gas was modified for each calculation.

[2] BIGG (1986) demonstrated recently that there are occasions when ammoniated aerosols are present due to the injection of tropospheric aerosol particles and ammonia gas into the stratosphere.

2.5 Variation of the size of aerosol particles as a function of the relative humidity

2.5.1 Theoretical considerations

The size distribution of aerosol particles was presented in Subsection 2.3.2. We have not discussed, however, the relation between the size distribution and the relative humidity of the air, since for such a discussion the knowledge of the chemical composition is necessary. The aim of this section is to summarize the problem with the presentation of some results of measurements. The interested reader is referred for further details to HÄNEL (1976).

The size distribution of aerosol particles varies as a function of the relative humidity because of the presence of water-soluble materials in the particulate matter. To understand the principle of this phenomemon let us consider a single water-soluble particle consisting of a given substance. The particle, with radius r_o, is in a dry state, that is, in an environment containing no water vapor. If the relative humidity of the particle's environment is increased the radius initially remains the same, disregarding the adsorption process which is of little importance (see Fig. 2.17). At a relative humidity determined by the nature of the substance (and also somewhat by the particle size) the radius of the particle suddenly changes to a larger value. This phenomenon is due to the fact that the particle has changed to a solution droplet called haze particle. The phase change takes place at the relative humidity at which a saturated solution of the substance considered is in vapor equilibrium with its environment.

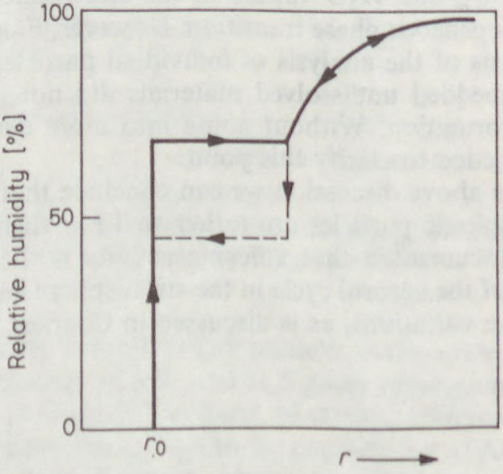

Fig. 2.17

Schematic variation of the radius *(r)* of a soluble particle as a function of relative humidity of the air. r_0: dry radius

It is known from physical chemistry that the equilibrium vapor pressure is smaller over solutions than over pure water. In the case of ideal solutions this vapor pressure decrease is proportional to the mole fraction of the solvent (Raoult's law). If the solution is real, the interaction of solvent and solute molecules cannot be neglected. For this reason a correction factor has to be applied to calculate the vapor pressure lowering. We also have to take into account that the soluble substance dissociates into ions, forming an electrolyte.

If we further raise the relative humidity after the phase change (see Fig. 2.17), the radius of the droplet increases and the solution becomes more dilute. This means that at a higher relative humidity a more dilute solution is in dynamic equilibrium with the vapor environment. It should be mentioned that the equilibrium radius is governed also by the curvature of the droplet as discussed in Section 3.2. By using Eqs (3.2) and (3.3) the variation of the droplet size as a function of the relative humidity can be calculated. The solid line of Fig. 2.17 represents schematically the results of calculations made using these equations for relative humidities below saturation. This curve was experimentally verified first by DESSENS (1949) who used a microscope to study the change of radius of atmospheric particles (droplets) captured on spider's web as the relative humidity was changed. He discovered that the phase change takes place at a lower relative humidity with decreasing than with increasing humidity (dotted line). This so-called hysteresis phenomenon was later confirmed by several other investigators (see JUNGE, 1963). It goes without saying that in the case of sulfuric acid solution droplets a sudden change in the particle radius is not observed. It was also more recently shown (WINKLER and JUNGE, 1972) that the curve is also smoothed if the particle is composed of a mixture of different salts.

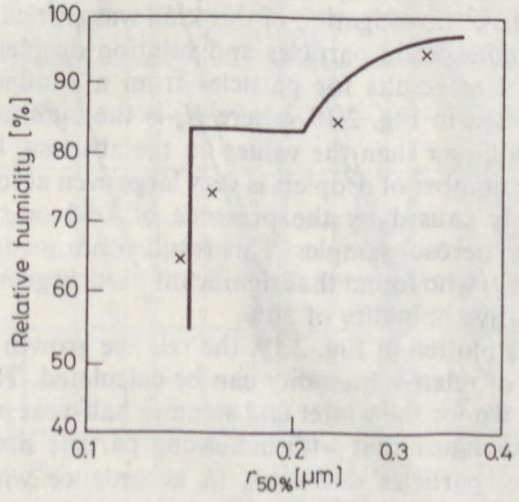

Fig. 2.18

Variation of geometric mean radius ($r_{50\%}$) of sulfate particles as a function of relative humidity (crosses). Solid line represents the theoretical growth of an ammonium sulfate particle with $r = 0.14$ μm (E. MÉSZÁROS, 1970). (By courtesy of *Tellus*)

The theory outlined is also supported by some atmospheric measurements. Thus, E. MÉSZÁROS (1970) measured the size distribution of the mass of atmospheric sulfate particles by means of a cascade impactor backed up by membrane filters. He found that the geometric mean radius of the distribution averaged by humidity intervals varies as a function of the relative humidity as shown by the points in Fig. 2.18. The solid line in this figure gives the theoretical relation calculated from Eq. (3.5) for an ammonium sulfate particle with a dry radius of 0.14 μm, the value found for the geometric mean radius at low relative humidity. The line shows that the particle radius increases by a factor of two at a relative humidity of 80%. Near 100% the droplet radius is several times larger than the dry particle size. Comparison of the curve with the experimental points indicates that the behavior of the atmospheric particle population is well approximated by the theory outlined. It cannot be excluded, however, that the real phase change is less sudden than that predicted by the theory.

2.5.2 Results of measurements

Variations of the size distribution of aerosol particles as a function of relative humidity can be observed *in situ* in the air. Changes in particle size distribution are detected by optical counters (LAKTIONOV and BOGOMOLOV, 1972), by nephelometers (CHARLSON *et al.*, 1969) or by diffusion channels (SINCLAIR *et al.*, 1974).

Another possibility is to capture particles, e.g. on impactor slides, and to study them after drying at different humidities under a microscope. Different relative humidities are generally created by different saturated salt solution (isopiestic method). An investigation of this kind was carried out by A. MÉSZÁROS (1971) who studied solid particles and solution droplets in the large and giant size ranges. Her results for particles from a continental environment (Hungary) are plotted in Fig. 2.19, where N_a is the number concentration of particles with radii larger than the values on the abscissa. It can be seen that in summertime the number of droplets is very large even at low humidities. This finding is obviously caused by the presence of acid or supersaturated salt solution droplets in aerosol samples. This result confirms optical observations of ROZENBERG (1967) who found that significant particle growth can be detected even around a relative humidity of 30%.

From the results plotted in Fig. 2.19, the relative growth of a given particle size as a function of relative humidity can be calculated. The curves obtained in this way are shown for the winter and summer half-year periods in Fig. 2.20. It follows from this figure that with increasing particle size the water-soluble fraction of aerosol particles decreases, in accordance with direct chemical observations (E. MÉSZÁROS, 1968) and considerations on particle formation (Section 2.2). It should also be noted, with respect to Fig. 2.20, that the results for 0.5-μm-radius particles are in good agreement with HÄNEL's values (HÄNEL, 1970) derived from experimental data published by WINKLER (1969).

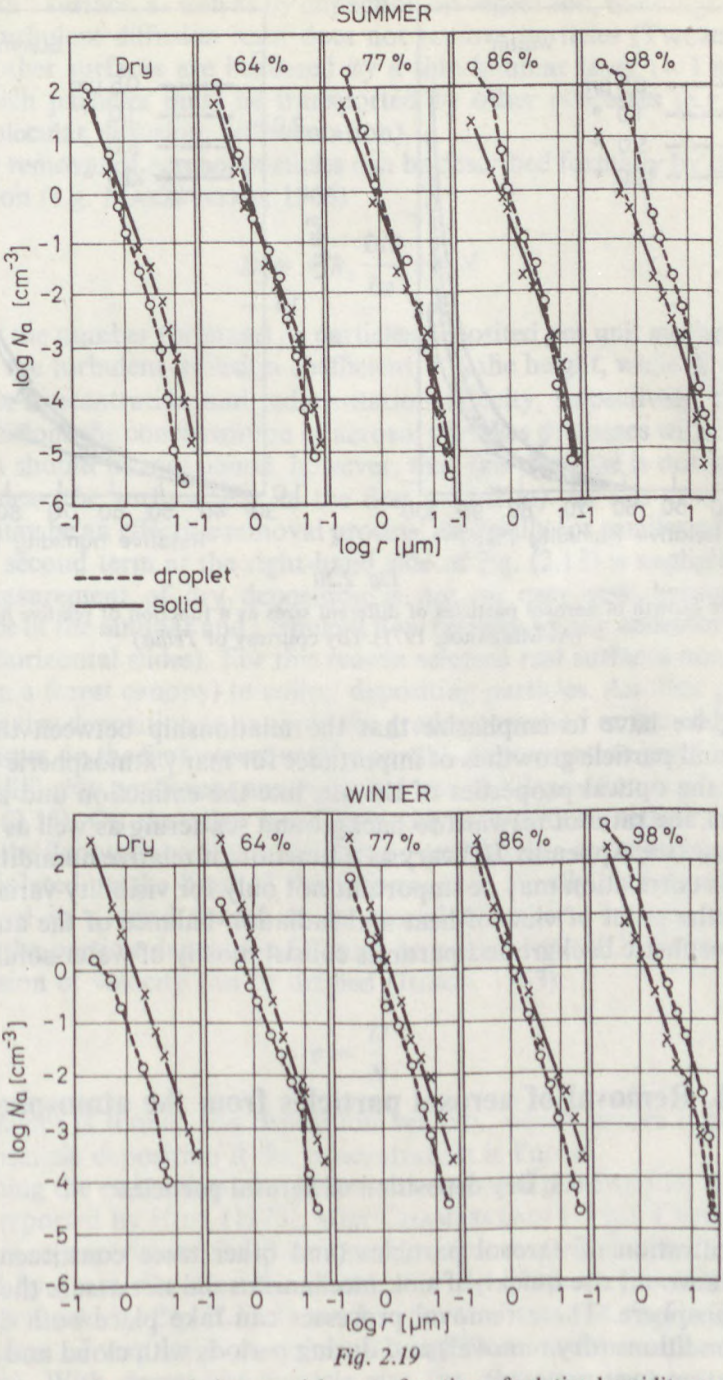

Fig. 2.19

Size distribution of large and giant particles as a function of relative humidity according to A. MÉSZÁROS (1971). N_a: concentration of particles with radius larger than the abscissa value. (By courtesy of *Tellus*)

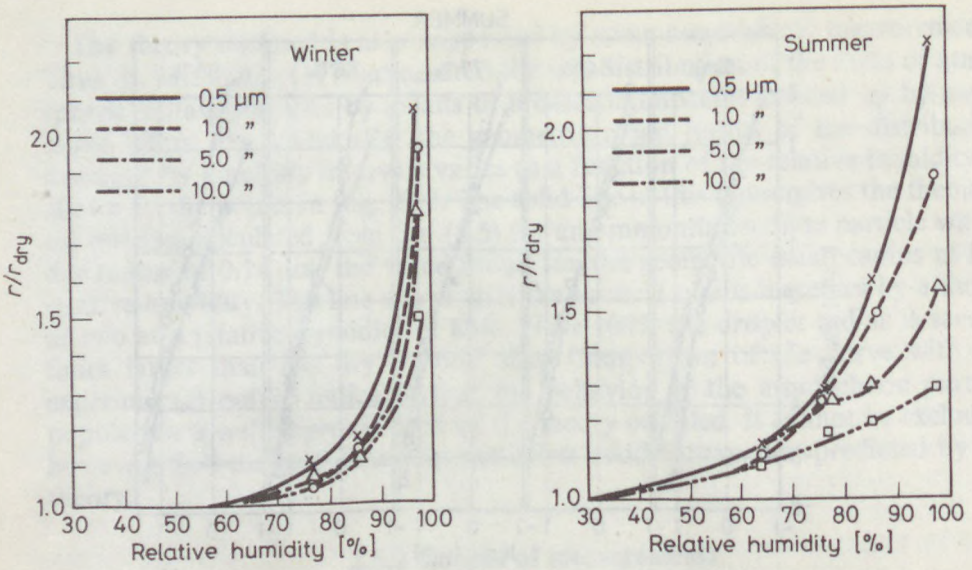

Fig. 2.20

Relative growth of aerosol particles of different sizes as a function of relative humidity (A. MÉSZÁROS, 1971). (By courtesy of *Tellus*)

Finally, we have to emphasize that the relationship between the relative humidity and particle growth is of importance for many atmospheric phenomena. Thus, the optical properties of the air, like the extinction and absorption coefficients, the ratio of forward to background scattering as well as the asymmetry factor (see Appendix III) vary as a function of relative humidity (HÄNEL, 1984). This correlation may be important not only for visibility variations, but also from the point of view of heat and radiation balance of the atmosphere, since tropospheric background particles consist mostly of water-soluble sulfate species.

2.6. Removal of aerosol particles from the atmosphere

2.6.1 Dry deposition of aerosol particles

The concentration of aerosol particles (and other trace constituents) in the atmosphere would rise quickly if sink mechanisms did not assure the cleansing of the atmosphere. These removal processes can take place both during dry weather conditions (dry removal) and during periods with cloud and precipitation formation (wet removal).

The removal of aerosol particles under dry weather conditions is caused by turbulent diffusion and gravitational sedimentation, which transport particles

to the Earth's surface, as well as by impaction on vegetation, buildings and other objects. Turbulent diffusion itself does not remove particles (TWOMEY, 1977). Soil and other surfaces are bordered by a thin laminar layer (~ 1 mm thick) across which particles must be transported by other processes (e.g. phoretic forces, molecular diffusion, sedimentation).

The dry removal of aerosol particles can be described formally by the following equation (e.g. MAKHONYKO, 1966):

$$D = -k_z \frac{\partial N}{\partial z} + v_s N \tag{2.13}$$

where D is the number (or mass) or particles deposited per unit surface per unit time, k_z is the turbulent diffusion coefficient, z is the height, while N and v_s are the particle concentration and sedimentation velocity, respectively. Under average conditions the concentration of aerosol particles decreases with increasing altitude. It should be mentioned, however, that this decrease is not necessarily observed near the surface (e.g. in the first 1 to 2 m). In this case turbulent diffusion may be an effective removal process, especially for smaller particles for which the second term at the right-hand side of Eq. (2.13) is negligible.

The measurement of dry deposition is not an easy task because of the disturbance of the laminar and turbulent flow regimes by any collector (e.g. dust fall cans, horizontal slides). For this reason selected real surfaces must be used (e.g. within a forest canopy) to collect depositing particles. Another possibility to estimate dry deposition is to apply the gradient method or the eddy correlation technique. In the first procedure the particle concentration gradient and the turbulent diffusion coefficient are measured and the deposition is calculated by using Eq. (2.13). On the other hand, the eddy correlation method consists of observing the fluctuations of vertical motion and particle concentration and the flux is calculated on the basis of this information. Finally, dry deposition can be measured in a wind tunnel or in special chambers. In any case, if we determine the particle deposition (D) and concentration (N), a parameter with the dimension of velocity can be defined (JUNGE, 1963):

$$v = \frac{D}{N}. \tag{2.14}$$

This parameter is termed the deposition velocity, which makes it possible to calculate particle deposition if the concentration is known.

Concerning the estimation of different dry removal processes let us consider Fig. 2.21, reported by HIDY (1973), after CHAMBERLAIN (1960). Curve A in this figure refers to experimental deposition velocities, measured over flat surfaces roughened by grass. On the other hand, line B represents the sedimentation velocity calculated by Eq. (2.1). It can be seen that curve A approximates line B in the range of very large particles with significant sedimentation velocities ($d_p > 10$ μm). With decreasing particle size the deviation is more and more important. It is believed that this phenomenon is caused by turbulent diffusion.

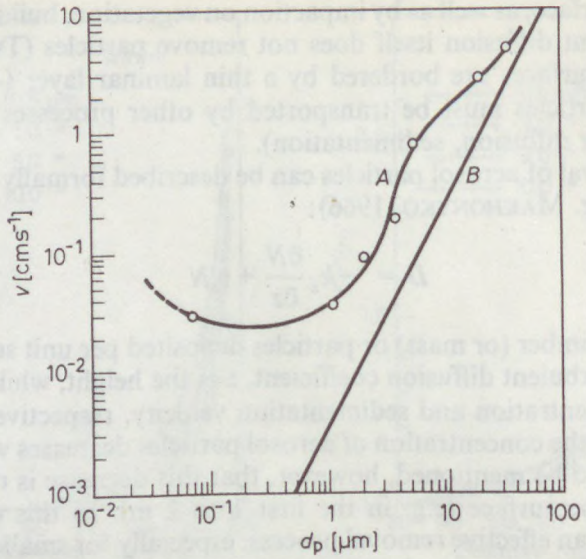

Fig. 2.21

Dry deposition velocity *(A)* and sedimentation velocity *(B)* of aerosol particles. Curve *A* refers to flow over grass (HIDY, 1973). (By courtesy of Plenum Press)

There is some indication that curve *A* begins to increase with decreasing size in the range where Brownian motion becomes important[1].

Very similar results were obtained by SEHMEL and SUTTER (1974) for a water surface during their wind tunnel investigation. However, they also found that for particles greater than 2 μm the deposition velocity increased with both an increase in particle diameter and wind speed. Thus, in the case of wind speeds higher than about 40 cm s^{-1} the deposition velocities were higher than the corresponding sedimentation velocities. While for vegetative canopies theoretical considerations (SLINN, 1982) indicate smaller deposition velocities in the 0.1–1.0 μm particle size range than CHAMBERLAIN's figures for grass surface, experimental works made over beech forests by HÖFKEN and GRAVENHORST (1982) suggest higher values for fine particles than those given in Fig. 2.21.

We have previously seen that tropospheric background aerosol particles consist mainly of ammonium sulfate and/or sulfuric acid (Subsection 2.4.2). Bearing in mind that these particles are in the fine particle range it seems to be reasonable to suppose on the basis of Fig. 2.21 that their dry deposition velocity cannot be greater than 0.1 cm s^{-1}. This figure is in a good agreement with the estimate of GARLAND (1978) and with the observations of DAVIES and NICHOLSON (1982) giving an average value of 0.08 cm s^{-1} for a rural site in eastern England. However, some recent field experiments resulted in higher deposition

[1] It is to be noted that Fig. 2.21 can be used to calculate the deposition rate of particles of different sizes if the number or mass size distribution is measured.

rates than the above value as compiled by VOLDNER *et al.* (1986). The reason for this disagreement is not clear. It is probable, however, that deposition velocity of atmospheric particles really varies as a function of surface properties (e.g. roughness) and atmospheric conditions (e.g. wind speed, thermal stability).

Finally, it is to be noted that in the foregoing discussion of dry removal we considered the total ensemble of particles. If size ranges are taken into account separately, additional sinks have to be mentioned. Thus, thermal coagulation of particles with very small size, as well as the condensation (below a relative humidity of 100%) of vapors with low saturation vapor pressure provide effective removal for Aitken particles. It is believed (HIDY, 1973) that these processes are dominant in the removal of aerosol particles in the size range below 0.1 μm radius.

2.6.2 Wet deposition

The efficiency of wet removal of aerosols is due to the fact that the falling speed of precipitation elements greatly exceeds the dry deposition velocity of particles. In a discussion of removal caused by clouds and precipitation it is reasonable to differentiate processes taking place in the cloud (in-cloud scavenging) and beneath the cloud base (sub-cloud scavenging).

In-cloud scavenging of aerosol particles is begun at the moment of cloud formation, since at the supersaturations occurring in the atmosphere ($< 1\%$ which is equivalent to a relative humidity of $< 101\%$) condensation takes place on aerosol particles called nuclei. Bearing in mind that condensation of water vapor in the atmosphere is discussed in the next chapter, we only note here that water-soluble particles are removed very effectively by condensation. Discussion in Subsection 2.4.2 clearly shows that the majority of aerosol particles in remote air consists of water-soluble sulfur species[1] and sea salt, for this reason it is obvious that a large part of these components are removed from the air during the formation of cloud droplets. It was previously noted that carbonaceous particles may be internally mixed with sulfur species, which considerably promote their in-cloud removal. However, if they are not associated with water-soluble components their in-cloud scavenging is much less significant. There is some indication that, at least under continental conditions, a substantial fraction ($\sim 50\%$ or greater) of metals in the particulate matter is soluble in water (LINDBERG and HARRISS, 1983) hence an important part of these species is also washed-out from the air by condensation.

Thermodynamic considerations also show (see Section 3.2) that larger particles are more active in condensation processes than smaller ones. This means that water-soluble particles smaller than about 0.01–0.05 μm are unaffected by condensation. The number of these particles may be very great, especially in a freshly formed aerosol. However, the Brownian motion of these small particles is rather significant (see Subsection 2.1.1). For this reason they can attach to

[1] In Chapter 3 it is also shown that condensation nuclei are composed mostly of sulfate particles.

cloud droplets very easily. Due to coagulation their concentration decreases exponentially with time. Theoretical calculations indicate (e.g. GREENFIELD, 1957) that particles with diameters smaller than 0.01 μm are almost entirely removed from cloudy air under normal conditions.

Aerosol particles may also be removed in the clouds by the different phoretic forces, e.g. by diffusiophoresis. This phenomenon involves the motion of particles due to the concentration gradient of condensing or evaporating vapor (GOLDSMITH *et al.*, 1963). In the case of condensation, particles displace towards the drop surface. According to GOLDSMITH *et al.* (1963), velocity caused by diffusiophoresis is

$$v_p = -1.9 \times 10^{-4} \frac{dp}{dx} \tag{2.15}$$

where dp/dx is the water vapor gradient expressed in hPa cm^{-1} (the dimension of v_p is cm s^{-1}). Laboratory experiments and calculations show that the role of diffusiophoresis in liquid clouds is small compared to the effect of condensation and coagulation. However, in so-called mixed clouds containing both liquid drops and ice crystals, a relatively large number of particles can be removed by growing solid cloud elements (VITTORI and PRODI, 1967).

Once a cloud is formed there are two possibilities concerning its future fate. One possibility is that the cloud partially or totally evaporates. In this case absorbed trace constituents become airborne again. However, a new aerosol spectrum is produced in this way compared to the size distribution before cloud formation, since one drop generally captures several aerosol particles and some trace gases are transformed irreversibly in cloud water (see the previous paragraph) to acids or salts. Thus, the average size of airborne particles is markedly larger after cloud evaporation than it was before cloud formation, which promotes the further removal of particulate matter.

The other obvious way is that materials imbedded in water are carried by precipitation to the surface of the Earth; that is, they are definitively removed from the air. There is no intention here to discuss the formation of precipitation. We only mention that it is believed that the coalescence of large drops with smaller ones (see Chapter 3) as well as the deposition of water vapor on ice crystals (see Chapter 4) are the predominant processes.

The wet removal of aerosol particles is continued below the cloud base, where they are captured by falling precipitation elements (snow crystals, raindrops) due to gravitational coagulation. This type of coagulation is caused by the difference between falling speeds of the aerosol particles and the raindrops or snow crystals similarly to the coalescence of larger and smaller drops (see Subsection 3.5.3 and Appendix II). For this reason precipitation elements are considered to be small impactors (see Subsection 2.1.2).

According to the theory (GREENFIELD, 1957) the mass concentration of aerosol particles below the cloud base decreases exponentially with time due to wet removal. The process is effective in particular in the coarse (giant) particle size range, caused by the fact that in the case of a given raindrop size the collection

efficiency decreases with decreasing particle size (see Appendix II). Thus, GREENFIELD demonstrated that at a rainfall rate of 2.5 mm hr^{-1}, 75–80% of particles with a radius of 10 μm are removed during one hour. On the other hand, the model calculations of SCOTT (1978) show that the sub-cloud scavenging of sulfate particles is of secondary importance compared to in-cloud removal caused mainly by condensation.

Unfortunately it is very difficult to determine the wet deposition rate of aerosol particles alone on the basis of the chemical analysis of precipitation water. The difficulty is due to the fact that gaseous trace constituents are absorbed by cloud and precipitation elements, and they are subsequently transformed in the water to species similar to those found in the particulate matter. Considering, e.g., sulfur compounds, SCOTT (1978) assumes on the basis of his removal modeling that the sulfate mass measured at the surface in rainwater can be attributed totally to the scavenging of airborne sulfate particles. On the other hand, the comparison of the ratios of ammonium to sulfate in aerosol and rainwater indicates (OPPENHEIMER, 1983) that aqueous phase oxidation of sulfur dioxide is the major pathway to the formation of precipitation sulfate. It is also reasonable to assume that the scavenging of HNO_3 vapor plays an important part in the control of nitrate content in precipitation (CHANG, 1984). There is some indication, however, that in remote oceanic air, where the SO_2 concentration is low, excess sulfate deposition rate is mostly controlled by the in-cloud scavenging of sulfate particles (E. MÉSZÁROS, 1982). In these areas the sulfate deposition rate has a magnitude of 0.1 $gm^{-2}y^{-1}$. If sulfate particles are not neutralized, they play an important part in the control of the acidity in precipitation under clean oceanic conditions (VONG *et al.*, 1988).

The deposition rate of elemental carbon, occurring only in aerosol phase, was determined by OGREN *et al.* (1984). They found that in Seattle (Washington, USA) and at a rural site in Sweden the wet deposition flux is equal to 0.05 $g\,m^{-2}y^{-1}$. In recent years many studies have been devoted to measure trace organic compounds in precipitation, including the particulate phase. LIGOCKI *et al.* (1985) demonstrated that the removal of neutral organic particles was less important than gas phase scavenging for the same compounds. They assumed that this is due to the fact that these particles are not likely to act as condensation nuclei and their scavenging is controlled by sub-cloud processes which remove only larger particles from the air.

Our knowledge about the deposition of atmospheric trace metals was summarized by GALLOWAY *et al.* (1982). According to their compilation the deposition rate of the metals studied is controlled by the particulate phase. Dry and wet deposition are of comparable magnitude. At remote places the bulk (dry + wet) deposition of both lead and copper is around 10^{-4} $g\,m^{-2}y^{-1}$. In a more recent review DUCE (1986) proposes a mean Al deposition rate of 1.2×10^{-2} $g\,m^{-2}y^{-1}$ for the air above the tropical North Pacific, while the corresponding value he gives for the tropical North Atlantic is about four times greater.

Finally, we note that while dry and wet deposition are sink mechanisms for

the particulate matter in the atmosphere, they constitute an important material input into other media of our environment. Under natural conditions undisturbed by human activities this material flow is an essential nutrient source for terrestrial and aquatic ecosystems. However, anthropogenic pollutants removed from the air by dry and wet deposition may cause serious environmental problems, like acidification of soils and waters (e.g. Swedish Ministry of Agriculture, 1982), eutrofication of lakes (e.g. HORVÁTH *et al.*, 1981b) and increasing pollution of ocean waters (DUCE, 1986).

2.6.3 Residence time of aerosol particles in the atmosphere

Atmospheric aerosol particles are continuously produced and removed. Due to the interaction of source and sink mechanisms they spend a certain time in the atmosphere, called the residence time. It is obvious that residence time is a function of the physical, chemical and dynamic state of the atmosphere as well as of the properties of the particles. As we have seen in the last subsection, the precipitation regime influences considerably the fate of atmospheric aerosols[1].

We have also seen that during dry weather periods Aitken particles coagulate rapidly to form large particles. On the other hand, coarse particles fall out relatively quickly from the atmosphere due to sedimentation. Owing to the interaction of these two processes, particles with a radius around 0.3 μm will accumulate in the air. However, particles in the large size range are removed effectively by wet removal. Figure 2.22 (after JAENICKE, 1978c) represents the residence time of tropospheric aerosol particles[2] as a function of their size. It can be seen that maximum values occur in the large size range. The residence time of these particles increases with increasing altitude because wet removal is less important at higher altitudes. It follows from the curve relative to the air below 1.5 km that the residence time of particles with a radius of 0.3 μm is around 10 days, while particles smaller than 0.1 μm remain in the air as individual particles only for at most one day. The curve also shows that the residence time of particles with a radius of 10 μm is one day.

Several attempts have been made to estimate separately the residence time of special components in the atmospheric aerosol. Thus, on the basis of budget studies RODHE (1978) proposes for particulate sulfate a residence time of about 3 days, a value essentially similar to that published by MÜLLER (1984) for nitrate particles. MÜLLER based his estimates, among other things, on the size distribution of different species. We also note that the investigation on the atmospheric cycle of elemental carbon made by OGREN and CHARLSON (1983) resulted in a residence time of 2 and 7 days for rainy and dry regions, respectively, while MÜLLER (1984) estimated a figure of 4.5 days for elemental carbon. Further,

[1] On the other hand, as we will see in the next chapters, atmospheric particles affect significantly the state of the atmosphere and the cloud and precipitation formation.

[2] We mention that the residence time of sulfate particles in the stratosphere is at least 1 year because of the lack of water and of the slow mixing between the troposphere and stratosphere.

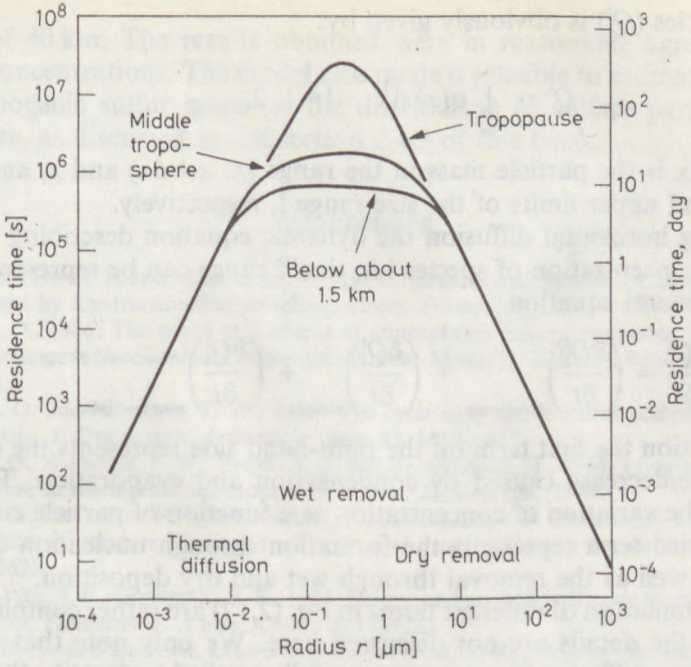

Fig. 2.22

Residence time of aerosol particles in the atmosphere as a function of their radius (JAENICKE, 1978c). (By courtesy of Bunsen Gesellschaft)

Note: While wet removal is very effective, particles in the 0.1 μm size range accumulate since precipitation falls relatively unfrequently.

DUCE (1978) assumed also using a budget approach, that fine organic aerosol particles have residence times between 4 and 7 days. On the other hand, he determined a value of 2 days for coarse organic particles. Finally, MÜLLER (1984) proposed residence times for different metals between 1 and 4 days.

2.7 Mathematical modeling of atmospheric aerosols

In recent years mathematical models have been developed to simulate the formation, evolution and removal of atmospheric particles. Since in these models all the processes we discussed are taken into account, we close this chapter with a brief summary of these numerical procedures. While the general dynamic equation for such a study was elaborated several years ago (see FRIEDLANDER, 1977) it was only very recently applied to multicomponent tropospheric systems (PILINIS *et al.*, 1987).

Consider an aerosol with continuous particle size distribution denoted by $q(x)$, where x is the natural logarithm of the mass of a particle. The total mass[1]

[1] The same approach is valid for the number of the particles.

of the particles (Q^l) is obviously given by:

$$Q^l = \int_{x_l}^{x_{l+1}} q(x)\,dx \qquad l = 1, 2, \ldots \tag{2.16}$$

where $q(x)dx$ is the particle mass in the range $(x, x+dx)$ and x_l and x_{l+1} are the lower and upper limits of the size range l, respectively.

Neglecting horizontal diffusion the dynamic equation describing the evolution of the concentration of species i in the l^{th} range can be represented by the following general equation

$$\frac{\partial Q_i^l}{\partial t} = \left(\frac{\partial Q_i^l}{\partial t}\right)_{\text{cond/evap.}} + \left(\frac{\partial Q_i^l}{\partial t}\right)_{\text{coag.}} + \left(\frac{\partial Q_i^l}{\partial t}\right)_{\text{sources/sinks}} . \tag{2.17}$$

In this equation the first term on the right-hand side represents the concentration increase/decrease caused by condensation and evaporation. The second term gives the variation of concentration as a function of particle coagulation, while the third term represents the formation through nucleation or primary emission as well as the removal through wet and dry deposition.

The determination of different terms in Eq. (2.17) are rather complicated. For this reason the details are not discussed here. We only note that Eq. (2.17), completed by a diffusion term, was successfully applied to describe the dynamics of aerosol particles in the air over the Los Angeles basin consisting (on a mass basis) of 20% sulfates, 25% nitrates, 10% elemental carbon, 20% organic carbon (primary and secondary), 25% soil, metals and water (PILINIS *et al.*, 1987). The evolution of the number size distribution of particles in the marine boundary layer was studied by mathematical modeling by FIZTGERALD and HOPPEL (1988). They considered a well-mixed boundary layer in which advection and diffusion can be neglected. Sources taken into account were sea salt production and fine particle formation by nucleation. Beside terms in Eq. (2.17) FITZGERALD and HOPPEL (1988) also took into consideration the cloud formation on the particles. While many similarities were found between the results of calculations and observations, the model was unable to simulate correctly the size distribution in the Aitken size range. This means that further research is needed to understand the behavior of the tropospheric aerosol under background conditions.

Attempts have also been made to describe the dynamics of stratospheric aerosols. Thus, TURCO (1982) used for this purpose a generalized aerosol continuity equation including the input of tropospheric Aitken particles and sulfur gases, as well as the effects of meteoric dust and galactic cosmic rays. The evolution of stratospheric sulfate particles was simulated by taking into account the following processes: adsorption, nucleation, condensation, evaporation and coagulation. The number of aerosol particles was supposed to decrease by diffusion into the troposphere.

By using a one-dimensional approach, TURCO was able to calculate the vertical profile of the concentration of sulfur gases and sulfate particles up to

a height of 40 km. The results obtained were in reasonable agreement with observed concentrations. The model also made it possible to estimate the effects of anthropogenic sulfur gases on the distribution of sulfate particles in the stratosphere, as discussed in Subsection 2.4.3 of this book.

References

ADAMS, F., Van ESPEN, P. and MAENHAUT, W., 1983: Aerosol composition at Chacaltaya, Bolivia, as determined by size-fractionated sampling. *Atmos. Environ.*, **17**, 1521–1536.

ANDREAE, M. O., 1986: The ocean as a source of atmospheric sulfur compounds. In *The Role of Air-Sea Exchange in Geochemical Cycling* (ed.: P. Buat-Ménard). D. Reidel Publ. Co., Dordrecht, 331–362.

ANDREAE, M. O. and ANDREAE, T. W., 1988: The cycle of biogenic sulfur compounds over the Amazon Basin. 1. Dry season. *J. Geophys. Res.*, **93**, 1487–1497.

ANDREAE, M. O., ANDREAE, T. W., FEREK, R. J. and RAEMDONCK, H., 1984: Long-range transport of soot carbon in the marine atmosphere. *Sci. Total Environ.*, **36**, 73–80.

ANDREAE, M. O., CHARLSON, R. J., BRUYNSEELS, F., STORMS, H., VAN GRIEKEN, R. and MAENHAUT, W., 1986: Internal mixture of sea salt, silicates, and excess sulfate in marine aerosols. *Science*, **232**, 1620–1623.

AYERS, G. P., IVEY, J. P., GOODMAN, H. S., 1986: Sulfate and methanesulfonate in maritime aerosol at Cape Grim, Tasmania. *J. Atmos. Chem.*, **4**, 173–185.

BEILKE, S., 1985: *Acid Deposition*. Umweltbundesamt (Federal Republic of Germany), Frankfurt.

BERRESHEIM, H. and JAESCHKE, W., 1983: The contribution of volcanoes to the global atmospheric sulfur budget. *J. Geophys. Res.*, **88**, 3732–3740.

BIGG, E. K., 1976: Size distributions of stratospheric aerosols and their variations with altitude and time. *J. Atmos. Sci.*, **33**, 1080–1086.

BIGG, E. K., 1980: Comparison of aerosol at four baseline atmospheric monitoring stations. *J. Appl. Meteor.*, **19**, 521–533.

BIGG, E. K., 1986: Ammonium compounds in stratospheric aerosols. *Tellus*, **38B**, 62–66.

BIGG, E. K. and TURVEY, D. E., 1978: Sources of atmospheric particles over Australia. *Atmos. Environ.*, **12**, 1643–1655.

BIGG, E. K., GRAS, J. L. and EVANS, C., 1984: Origin of Aitken particles in remote regions of the Southern Hemisphere. *J. Atmos. Chem.*, **1**, 203–214.

BLANCHARD, D. C., 1969: The oceanic production rate of cloud nuclei. *J. Rech. Atmos.*, **4**, 1–6.

BLANCHARD, D. C., WOODCOCK, A. H. and CIPRIANO, R. J., 1984: The vertical distribution of the concentration of sea salt in the marine atmosphere near Hawaii. *Tellus*, **36B**, 118–125.

BLIFFORD, J. H., 1970: Tropospheric aerosols. *J. Geophys. Res.*, **75**, 3099–3103.

BODHAINE, B. A. and DELUISI, J. J., 1985: An aerosol climatology of Samoa. *J. Atmos. Chem.*, **3**, 107–122.

BODHAINE, B. A., DELUISI, J. J., HARRIS, J. M., HAUMERE, P. and BAUMAN, S., 1986: Aerosol measurements at the South Pole. *Tellus*, **38B**, 223–235.

BRAATEN, D. A. and CAHILL, T. A., 1986: Size and composition of Asian dust transported to Hawaii. *Atmos. Environ.*, **20**, 1105–1109.

BRICARD, J., BILLARD, F. and MADELAINE, G., 1968: Formation and evolution of nuclei of condensation that appear in air initially free of aerosols. *J. Geophys. Res.*, **73**, 4487–4496.

BUTOR, J. F., 1976: Application des techniques de la microscopie électronique à l'étude de l'aérosol atmosphérique fin. Thèse 3e cycle, Brest. *Rapport C.E.A.R. 4709*.

BYERS, H. R., SIEVERS, J. R. and TUFTS, B. J., 1957: Distribution in the atmosphere of certain particles capable of serving as condensation nuclei. In *Artificial Stimulation of Rain* (eds: H. Weickmann and W. Smith). Pergamon Press, New York, 47–70.

CACHIER, H., BUAT-MÉNARD, P., FONTUGNE, M. and CHESSELET, R., 1986: Long-range transport of continentally-derived particulate carbon in the marine atmosphere: evidence from stable carbon isotope studies. *Tellus*, **38B**, 161–177.

CADLE, R. D., 1973: Particulate matter in the lower atmosphere. In *Chemistry of the Lower Atmosphere* (ed.: S. I. Rasool), Plenum Press, New York, 69–120.
CADLE, R. D., FISCHER, W. H., FRANK, E. R. and LODGE, J. P., 1968: Particles in the Antarctic atmosphere. *J. Atmos. Sci.*, **25**, 100–103.
CADLE, R. D., GRAHEK, F. E., GANDRUD, B. W. and LAZRUS, A. L., 1973: Relative efficiencies of filters and impactors for collecting stratospheric particulate matter. *J. Atmos. Sci.*, **30**, 745–747.
CALVERT, J. G., LAZRUS, A., KOK, G. L., HEIKES, B. G., WALEGA, J. B., LIND, J. and CANTRELL, C. A., 1985: Chemical mechanisms of acid generation in the troposphere. *Nature*, **317**, 27–35.
CHAMBERLAIN, A. C., 1960: Aspects of the deposition of radioactive and other gases and particles. In *Aerodynamic Capture of Particles* (ed.: E. G. Richardson), Pergamon Press, New York, 63–88.
CHANG, T. Y., 1984: Rain and snow scavenging of HNO_3 vapor in the atmosphere. *Atmos. Environ.*, **18**, 191–197.
CHARLSON, R. J., PUESCHEL, R. F. and AHLQUIST, N. C., 1969: Use of the integrating nephelometer for studying deliquescent aerosols. *Proc. 7th Internat. Conf. on Condensation and Ice Nuclei*, Prague and Vienna, 293–303.
COBB, W. E. and WELLS, H. J., 1970: The electrical conductivity of oceanic air and its correlation to global atmospheric pollution. *J. Atmos. Sci.*, **27**, 814–819.
CORN, M., 1976: Aerosols and the primary air pollutants. Noviable particles. Their occurrence, properties and effects. In *Air Pollution* (ed.: A. C. Stern) *Vol. I.* Academic Press, New York, 77–168.
COVERT, D. S. and HEITZENBERG, J., 1984: Measurement of the degree of internal/external mixing of hygroscopic compounds and soot in atmospheric aerosols. *Sci. Total Environ.*, **36**, 347–352.
COX, R. A., 1974: Particle formation from homogeneous reactions of sulphur dioxide and nitrogen dioxide. *Tellus*, **26**, 235–240.
CRUTZEN, P., 1976: The possible importance of CSO for the sulfate layer of the stratosphere. *Geophys. Res. Lett.*, **3**, 73–76.
DAMS, R. and DE JONGE, J., 1976: Chemical composition of Swiss aerosols from the Jungfraujoch. *Atmos. Environ.*, **10**, 1079–1084.
DAVIES, T. D. and NICHOLSON, K. W., 1982: Dry deposition velocities of aerosol sulphate in rural eastern England. In *Deposition of Atmospheric Pollutants* (eds: H. W. Georgii and J. Pankrath). D. Reidel Publ. Co., Dordrecht, 31–42.
DAY, J. A., 1963: Small droplets from rupturing air-bubble films. *J. Rech. Atmos.*, **1**, 191–196.
DESSENS, H., 1949: The use of spiders threads in the study of condensation nuclei. *Quart. J. Roy. Meteor. Soc.*, 75, 23–27.
DUCE, R. A., 1978: Speculations on the budget of particulate and vapor phase non-methane organic carbon in the global troposphere. *Pure and Appl. Geophys.*, **116**, 244–273.
DUCE, R. A., 1986: *Air-sea Interchange of Pollutants*. WMO Environmental Pollution Monitoring and Research Programme, No. 37, Geneva.
DUCE, R. A., WINCHESTER, J. W. and VAN NAHL, T. W., 1966: Iodine, bromine and chlorine in winter aerosols and snow from Barrow, Alaska. *Tellus*, **18**, 238–248.
DUCE, R. A., ARIMOTO, R., RAY, B. J., UNNI, C. K. and HARDER, P. J., 1983: Atmospheric trace elements at Enewetak Atoll: 1. Concentrations, sources, and temporal variability. *J. Geophys. Res.*, **88**, 5321–5342.
EVANS, W. F. J. and KERR, J. B., 1983: Estimates of the amount of sulphur dioxide injected into the stratosphere by the explosive volcanic eruptions: El Chichón, mystery volcano, Mt. St. Helens. *Geophys. Res. Lett.*, **10**, 1049–1051.
FALL, R. D. L. ALBRITTON, F. C. FEHSENFELD, W. C. KUSTER and P. D. GOLDAN, 1988: Laboratory studies of some environmental variables controlling sulfur emissions from plants. *J. Atmos. Chem.*, **6**, 341–362.
FARLOW, N. H., HAYES, D. M. and LEM, H. Y., 1977: Stratospheric aerosols: undissolved granules and physical state. *J. Geophys. Res.*, **82**, 4921–4929.
FARLOW, N. H., OBERBECK, V. R., SNETSINGER, K. G., FERRY, G. V., POLKOWSKI, G. and HAYS, D. M., 1981: Size distributions and mineralogy of ash particles in the stratosphere from eruptions of Mt. St. Helens. *Science*, **211**, 832–834.

FENN, R. W., GERBER, H. E. and WASSHAUSER, D., 1963: Measurements of the sulfur and ammonium component of the arctic aerosol of the Greenland icecap. *J. Atmos. Sci.*, **20,** 466–468.
FINLAYSON-PITTS, B. J. and PITTS, J. N. Jr., 1986: *Atmospheric Chemistry. Fundamentals and Experimental Techniques*. J. Wiley and Sons. New York.
FITZGERALD, J. W. and HOPPEL, W. A., 1988: Numerical simulation of the evolution of the particle size distribution in the marine boundary layer. In *Atmospheric Aerosols and Nucleation* (eds: P. E. Wagner and G. Vali). Springer-Verlag. Berlin, 245–248.
FLETCHER, N. H., 1962: *The Physics of Rainclouds*. Univ. Press, Cambridge.
FLYGER, H. and HEIDAM, N. Z., 1978: Ground level measurements of the summer tropospheric aerosol in northern Greenland. *J. Aerosol Sci.*, **9,** 157–168.
FRIEDLANDER, S. K., 1977: *Smoke, Dust and Haze. Fundamentals of Aerosol Behavior*. J. Wiley and Sons, New York.
FRIEDLANDER, S. K., 1978: A review of the dynamics of sulfate containing aerosols. *Atmos. Environ.*, **12,** 187–195.
FRIEND, H. P., 1966: Properties of the stratospheric aerosol. *Tellus* **18,** 463–473.
FUCHS, N. A., 1964: *The Mechanics of Aerosols*. Pergamon Press, Oxford.
GALLOWAY, J. N., THORNTON, J. D., NORTON, S. A., VOLCHOK, H. L. and MCLEAN, R. A. N., 1982: Trace metals in atmospheric deposition: a review and assessment. *Atmos. Environ.*, **16,** 1677–1700.
GARLAND, J. A., 1978: Dry and wet removal of sulfur from the atmosphere. *Atmos. Environ.*, **12,** 349–362.
GANDRUD, B. W., KRITZ, M. A. and LAZRUS, A. L., 1983: Balloon and aircraft measurements of stratospheric sulfate mixing ratio following the El Chichón eruption. *Geophys. Res. Lett.*, **10,** 1037–1040.
GEORGII, H. W., 1978: Large scale spatial and temporal distribution of sulfur compounds. *Atmos. Environ.*, **13,** 681–690.
GILLETTE, D. A. and BLIFFORD, I. H., 1971: Composition of tropospheric aerosols as a function of altitude. *J. Atmos. Sci.*, **28,** 1199–1210.
GOLDSMITH, P., DELAFIELD, H. J. and COX, L. C., 1963: The role of diffusiophoresis in the scavenging of radioactive particles from the atmosphere. *Quart. J. Roy. Meteor. Soc.*, **89,** 43–61.
GRAMS, G. W. and FIOCCO, G., 1967: Stratospheric aerosol layer during 1964 and 1965. *J. Geophys. Res.*, **72,** 3523–3542.
GRAS, J. L., 1983: Ammonia and ammonium concentrations in the Antarctic atmosphere. *Atmos. Environ.*, **17,** 815–818.
GRAS, J. L. and ADRIAANSEN, A., 1985: Concentration and size variation of condensation nuclei at Mawson, Antarctica. *J. Atmos. Chem.*, **3,** 93–106.
GREENFIELD, S. M., 1957: Rain scavenging of radioactive particulate matter from the atmosphere. *J. Meteor.*, **14,** 115–125.
GROSJEAN, D. and LEWIS, R., 1982: Atmospheric photooxidation of methyl sulfide. *Geophys. Res. Lett.*, **9,** 1203–1206.
HAAF, W. and JAENICKE, R., 1980: Results of improved size distribution measurements in the Aitken range of atmospheric aerosols. *J. Aerosol Sci.*, **11,** 321–330.
HAMILL, P., KIANG, C. S. and CADLE, R. D., 1977: The nucleation of H_2SO_4–H_2O solution aerosol particles in the stratosphere. *J. Atmos. Sci.*, **34,** 150–162.
HÄNEL, G., 1970: Die Grösse atmosphärischer Aerosolteilchen als Funktion der relativen Luftfeuchtigkeit. *Beitr. Phys. Atmos.*, **43,** 119–132.
HÄNEL, G., 1976: The properties of atmospheric aerosol particles as functions of the relative humidity at thermodynamic equilibrium with the surrounding moist air. *Adv. Geophys.*, **19,** 73–188.
HÄNEL, G., 1984: Parameterization of the influence of relative humidity on optical aerosol properties. In *Aerosols and Their Climatic Effects* (eds: H. E. Gerber and A. Deepak). A. Deepak Publ., Hampton, 117–122.
HEGG, D. A., HOBBS, P. V. and RADKE, L. F., 1980: Observations of the modification of cloud condensation nuclei in wave clouds. *J. Rech. Atmos.*, **14,** 217–222.
HEITZENBERG, J., 1981: The chemical composition of arctic haze at Ny-Ålesund, Spitzbergen. *Tellus*, **33,** 162–171.

HEITZENBERG, J., 1984: Physical and chemical aerosol characteristics in extremely clean air masses at Cape Grim, Tasmania. *11th Internat. Conf. on Atmos. Aerosols, Condensation and Ice Nuclei, Pre-print Volume I.*, Budapest, 128–132.

HEITZENBERG, J., 1985: What we can learn from aerosol measurements at baseline stations. *J. Atmos. Chem.*, **3,** 153–169.

HIDY, G. M., 1973: Removal processes of gaseous and particulate pollutants. In *Chemistry of the Lower Atmosphere* (ed.: Rasool, S. I.). Plenum Press, New York, 121–176.

HIDY, G. M. and BROCK, J. R., 1970: *The Dynamics of Aerocolloidal Systems.* Pergamon Press, Oxford.

HOBBS, P. V., 1971: Simultaneous airborne measurements of cloud condensation nuclei and sodium-containing particles over the ocean. *Quart. J. Roy. Meteor. Soc.*, **97,** 263–271.

HOBBS, P. V., RADKE, L. F., ELTGROTH, M. W. and HEGG, D. A., 1981: Airborne studies of the emissions from volcanic eruptions of Mount St. Helens. *Science*, **211,** 816–818.

HÖFKEN, K. D. and GRAVENHORST, G., 1982: Deposition of atmospheric aerosol particles to beech- and spruce forest. In *Deposition of Atmospheric Pullutants* (eds: H.-W. Georgii and J. Pankrath). D. Reidel Publ. Co., Dordrecht, 191–194.

HOFMANN, D. J. and ROSEN, J. M., 1981: On the background stratospheric aerosol layer. *J. Atmos. Sci.*, **38,** 168–181.

HOFMANN, D. J. and ROSEN, J. M., 1983: Sulfuric acid droplet formation and growth in the stratosphere after the 1982 eruption of El Chichón. *Science*, **222,** 325–327.

HOGAN, A. W., 1986: Aerosol exchange in the remote troposphere. *Tellus*, **38B,** 197–213.

HOGAN, A. W. and BERNARD, S., 1978: Seasonal and frontal variation in Antarctic aerosol concentrations. *J. Appl. Meteor.*, **17,** 1458–1466.

HOGAN, A. W., MOHNEN, V. A. and SCHAEFER, V. J., 1973: Comments "Oceanic aerosol levels deduced from measurements of the electrical conductivity of the atmosphere". *J. Atmos. Sci.*, **30,** 1455–1460.

HORVÁTH, L., MÉSZÁROS, E., ANTAL, E. and SIMON, A., 1981a: On the sulfate, chloride and sodium concentration in maritime air around the Asian continent. *Tellus*, **33,** 382–386.

HORVÁTH, L., MÉSZÁROS, A., MÉSZÁROS, E. and VÁRHELYI, G., 1981b: On the atmospheric deposition of nitrogen and phosphorus into Lake Balaton. *Időjárás*, **85,** 194–200.

HUEBERT, B. J. and LAZRUS, A. L., 1978: Global tropospheric measurements of nitric acid vapor and particulate nitrate. *Geophys. Res. Lett.*, **5,** 577–580.

HUNTEN, D. M., TURCO, R. P. and TOON, O. B., 1980: Smoke and dust particles of meteoric origin in the mesosphere and stratosphere. *J. Atmos. Sci.*, **37,** 1342–1357.

HUSAR, R. B. and WHITBY, K. T., 1973: Growth mechanisms and size spectra of photochemical aerosols. *Environ. Sci. Technol.*, **7,** 241–247.

INN, E. C. Y., FARLOW, N. H., RUSSEL, P. B., MCCORMICK, M. P. and CHU, W. P., 1982: Observations. In *The Stratospheric Aerosol Layer* (ed.: R. C. Witten). Springer-Verlag, Berlin, 15–68.

ITO, T., 1985: Study of background aerosols in the Antarctic troposphere. *J. Atmos. Chem.*, **3,** 69–91.

ITO, T., MORITA, Y. and IWASAKA, Y., 1986: Balloon observation of aerosols in the Antarctic troposphere and stratosphere. *Tellus*, **38B,** 214–222.

JACOB, D. J. and HOFFMANN, M. R., 1983: A dynamic model or the production of H^+, NO_3^- and SO_4^{2-} in urban fog. *J. Geophys. Res.* **88,** 6611–6621.

JAENICKE, R., 1978a: Physical properties of atmospheric particulate sulfur compounds. *Atmos. Environ.*, **12,** 161–169.

JAENICKE, R., 1978b: The role of organic material in atmospheric aerosols. *Pure Appl. Geophys.*, **116,** 283–292.

JAENICKE, R., 1978c: Über die Dynamik atmosphärischer Aitkenteilchen. *Ber. Bunsen-Gesellschaft für phys. Chemie*, **82,** 1198–1202.

JAENICKE, R. and SCHÜTZ, L., 1982: Arctic aerosols in surface air. *Időjárás*, **86,** 235–241.

JOHANSSON, T. B., VAN GRIEKEN, R. E., NELSON, J. W. and WINCHESTER, J. W., 1975: Elemental trace analysis of small samples by proton induced X-ray emission. *Anal. Chem.*, **47,** 855–860.

JUNGE, C. E., 1963: *Air Chemistry and Radioactivity.* Academic Press, New York.

JUNGE, C. E. and JAENICKE, R., 1971: New results in background aerosol studies from the Atlantic expedition of the R. V. Meteor, spring 1969. *J. Aerosol Sci.*, **2**, 305–314.

KÄSELAU, K. H., FABIAN, P. and RÖHRS, H., 1974: Measurements of aerosol concentration up to a height of 27 km. *Pure Appl. Geophys.*, **112**, 877–885.

KEESER, R. G. and CASTLEMAN, A. W. Jr., 1982: The chemical kinetics of aerosol formation. In *The Stratospheric Aerosol Layer* (ed.: R. C. Whitten). Springer-Verlag, Berlin, 69–92.

KETSERIDIS, G. and EICHMANN, R., 1978: Organic compounds in aerosol samples. *Pure Appl. Geophys.*, **16**, 274–282.

KETSERIDIS, G., HAHN, J., JAENICKE, R. and JUNGE, C. E., 1976: The organic constituents of atmospheric particulate matter. *Atmos. Environ.*, **10**, 603–610.

KHEMANI, L. T., NAIK, M. S., MOMIN, G. A., KUMAR, R., CHATTERJEE, R. N., SINGH, G. and RAMANA MURTY, Bh. V., 1985: Trace elements in the atmospheric aerosols at Delhi, North India. *J. Atmos. Chem.*, **2**, 273–285.

KIANG, C. S., STAUFFER, D., MOHNEN, V. A., BRICARD, J. and VIGLA, D., 1973: Heteromolecular nucleation theory applied to gas-to-particle conversion. *Atmos. Environ.*, **7**, 1279–1283.

KITTELSON, D. B., MCKENZIE, R., VERMEERSCH, M., DORMAN, F., PUI, D., LINNE, M., LIU, B. and WHITBY, K., 1978: Total sulfur aerosol concentration with an electrostatically pulsed flame photometric detector system. *Atmos. Environ.*, **12**, 105–111.

KNOLLENBERG, R. G. and HUFFMAN, D., 1983: Measurements of the aerosol size distribution in the El Chichón cloud. *Geophys. Res. Lett.*, **10**, 1025–1028.

KONDRATYEV, K. J., BADINOV, I. J., IVLEV, L. S. and NIKOLSKI, G. A., 1969: Aerosol structure of the troposphere and stratosphere (in Russian). *Fiz. Atmos. Okeana*, **5**, 480–493.

LAKTIONOV, A. G. and BOGOMOLOV, Yu. P., 1972: Dependence of the particle size of natural aerosol on the humidity of the air (in Russian). *Fiz. Atmos. Okeana*, **8**, 291–297.

LANNEFORS, H. O., JOHANSSON, T. B., GRANAT, L. and RUDELL, B., 1977: Elemental concentrations and particle size distributions in an atmospheric background aerosols. *Nuclear Instruments and Methods*, **142**, 105–110.

LAWSON, D. R. and WINCHESTER, J. W., 1979: Atmospheric sulfur aerosol concentrations and characteristics from the South American continent. *Science*, **205**, 1267–1269.

LAZRUS, A. L., GANDRUD, B. and CADLE, R. D., 1971: Chemical composition of air filtration samples of the stratospheric sulfate layer. *J. Geophys. Res.*, **76**, 8083–8088.

LEGRAND, M. R. and DELMAS, R. J., 1986: Relative contributions of tropospheric and stratospheric sources to nitrate in Antarctic snow. *Tellus*, **38B**, 236–249.

LIGOCKI, M. P., LEUENBERGER, C. and PANKOW, J. . 1985: Trace organic compounds in rain. – III. Particle scavenging of neutral organic compounds. *Atmos. Environ.*, **19**, 1619–1626.

LINDBERG, S. E. and HARRISS, R. C., 1983: Water and acid soluble trace metals in atmospheric particles. *J. Geophys. Res.*, **88**, 5091–5100.

LOPEZ, A., SERVANT, J. and FONTAN, J., 1973: Variation des concentrations et caractéristiques physiques des noyaux d'Aitken dans un site non pollué. *Atmos. Environ.*, **7**, 945–965.

LOPEZ, A., SERVANT, J. and FONTAN, J., 1974: Méthode de mesure de l'intensité des sources de noyaux d'Aitken dans l'atmosphère. *Atmos. Environ.*, **8**, 733–754.

LOPEZ, A., PRIEUR, S. and FONTAN, J., 1984: Study of the formation of particles from natural hydrocarbons released by vegetation. *11th Internat. Conf. on Atmos. Aerosols, Condensation and Ice Nuclei. Pre-print Volume I*, Budapest, 35–51.

LODGE, J. P., 1955: A study of sea-salt particles over Puerto Rico. *J. Meteor.*, **12**, 493–499.

LODGE, J. P., 1962: Identification of aerosols. *Adv. Geophys.*, **9**, 97–130.

LOGAN, J. A., PRATHER, M. J., WOFSY, S. C. and MCELROY, M. B., 1981: Tropospheric chemistry: a global perspective. *J. Geophys. Res.*, **86**, 7210–7254.

MAKHONYKO, K. P., 1966: Selfcleaning of the lower troposphere from radioactive particles (in Russian). *Fiz. Atmos. Okeana*, **2**, 508–522.

MARTELL, E. A., 1966: The size distribution and interaction of radioactive and natural aerosols in the stratosphere. *Tellus*, **18**, 486–498.

MCCORMICK, M. P., CHU, . P., GRAMS, G. W., HAMILL, P., HERMAN, B. M., MCMASTER, L. R., PEPIN, T. J., RUSSEL, P. B., STEELE, H. M. and SWISSLER, T. J., 1981: High-latitude stratospheric aerosols measured by the SAM II satellite system in 1978 and 1979. *Science*, **214**, 328–331.

McWILLIAMS, S., 1969: The concentration of atmospheric condensation nuclei at Valentia observatory. *Irish Meteorological Service, Techn. Note* No. 33, Dublin.
MENDONCA, B. G., HANSON, K. J. and DELUISI, J. J., 1978: Volcanically related secular trends in atmospheric transmission at Mauna Loa Observatory, Hawaii. *Science,* **202,** 513–515.
MÉSZÁROS, A., 1969: Vertical profile of large and giant particles in the lower troposphere. *Proc. 7th Internat. Conf. on Condensation and Ice Nuclei.* Academia, Prague, 364–368.
MÉSZÁROS, A., 1971: On the variation of the size distribution of large and giant atmospheric particles as a function of the relative humidity. *Tellus,* **23,** 436–440.
MÉSZÁROS, A., 1977: On the size distribution of atmospheric aerosol particles of different composition. *Atmos. Environ.,* **11,** 1075–1081.
MÉSZÁROS, A., 1984: The number concentration and size distribution of the soot particles in the 0.02–0.5 μm radius range at sites of different pollution level. *Sci. Total Environ.,* **36,** 283–288.
MÉSZÁROS, A. and VISSY, K., 1974: Concentration, size distribution and chemical nature of atmospheric aerosol particles in remote oceanic areas. *J. Aerosol Sci.,* **5,** 101–110.
MÉSZÁROS, A., HASZPRA, L., KISS, I., KOLTAY, E., LÁSZLÓ, S. and SZABÓ, Gy., 1984: Trace element concentrations in atmospheric aerosol over Hungary. *11th Internat. Conf. on Atmos. Aerosols, Condensation and Ice Nuclei. Pre-print Volume I,* Budapest, 113–117.
MÉSZÁROS, E., 1964: Répartition verticale de la concentration des particules de chlorures dans les basses couches de l'atmosphère. *J. Rech. Atmos., 1* (2e année), 1–10.
MÉSZÁROS, E., 1968: On the size distribution of water soluble particles in the atmosphere. *Tellus,* **20,** 443–448.
MÉSZÁROS, E., 1970: Seasonal and diurnal variations of the size distribution of atmospheric sulfate particles. *Tellus,* **22,** 235–238.
MÉSZÁROS, E., 1982: On the atmospheric input of sulfur into the ocean. *Tellus,* **34,** 277–282.
METNIEKS, A. L., 1958: The size spectrum of large and giant sea-salt nuclei under maritime conditions. *Geophys. Bull.,* **15,** 1–50.
MIRABEL, P. J. and JAECKER-VOIROL, A., 1988: Binary homogeneous nucleation. In *Atmospheric Aerosols and Nucleation* (eds.: P. E. Wagner and G. Vali). Springer-Verlag, Berlin. 3–14.
MOORE, D. J. and MASON, B. J., 1954: The concentration, size distribution and production rate of large salt nuclei over the oceans. *Quart. J. Roy. Meteor. Soc.,* **80,** 583–590.
MOSSOP, S. C., 1965: Stratospheric particles at 20 km altitude. *Geochim. Cosmochim. Acta,* **29,** 201–207.
MÜLLER, J., 1984: Atmospheric residence time of carbonaceous particles and particulate PAH-compounds. *Sci. Total Environ.,* **36,** 339–349.
NGUYEN, B. C., BONSANG, B. and GAUDRY, A., 1983: The role of the ocean in the global atmospheric sulfur cycle. *J. Geophys. Res.,* **88,** 10903–10914.
NOVAKOV, T., 1984: The role of soot and primary oxidants in atmospheric chemistry. *Sci. Total Environ.,* **36,** 1–10.
OGREN, J. A. and CHARLSON, R. J., 1983: Elemental carbon in the atmosphere: cycle and lifetime. *Tellus,* **35B,** 241–254.
OGREN, J. A., GROBLICKI, P. J. and CHARLSON, R. J., 1984: Measurement of the removal rate of elemental carbon from the atmosphere. *Sci. Total Environ.,* **36,** 329–338.
OHTA, S. and ITO, T., 1974: Method of measurement of very low concentrations of submicron aerosols. *WMO Special Environ. Rep.,* **3,** 387–393.
ONO, A., YAMATO, M. and YOSHIDA, M., 1983: Molecular state of sulfate aerosols in the remote Everest highland. *Tellus,* **35B,** 197–205.
OPPENHEIMER, M., 1983: The relationship of sulfur emissions to sulfate in precipitation. *Atmos. Environ.,* **17,** 451–460.
PARUNGO, F. P., NAGAMOTO, C. T., RISINSKI, J. and HAAGELSON, P. L., 1986: A study of maritime aerosols over the Pacific Ocean. *J. Atmos. Chem.,* **4,** 199–226.
PENKETT, S. A., JONES, B. M. R., BRICE, K. A. and EGGLETON, A. E. J., 1979: The importance of ozone and hydrogen peroxide in oxidising sulphur dioxide in cloud and rainwater. *Atmos. Environ.,* **13,** 123–137.
PILINIS, C., SEINFELD, J. H. and SEIGNEUR, C., 1987: Mathematical modeling of the dynamics of multicomponent atmospheric aerosols. *Atmos. Environ.,* **21,** 943–955.

PODZIMEK, J., 1984: Size spectra of bubbles in the foam patches and of sea salt nuclei over the surf zone. *Tellus*, **36B**, 192–202.

PODZIMEK, J., SEDLACEK, W. A. and BROOKS HABERL, J., 1977: Aitken nuclei measurements in the lower stratosphere. *Tellus*, **29**, 116–127.

PROSPERO, J. M., 1968: Atmospheric dust studies on Barbados. *Bull. Amer. Meteor. Soc.*, **49**, 645–652.

PROSPERO, J. M., 1984: Aerosol particles. In *Global Tropospheric Chemistry*. National Academy Press, Washington D.C., 136–140.

RAATZ, W. E., 1985: Meteorological conditions over Eurasia and the Arctic contributing to the March 1983 Arctic haze episode. *Atmos. Environ.*, **19**, 2121–2126.

RAHN, K. A., 1976: *The Chemical Composition of the Atmospheric Aerosol*. University of Rhode Island, Technical Report.

RAHN, K. A., 1981: Relative importances of North America and Eurasia as sources of Arctic aerosol. *Atmos. Environ.*, **15**, 1447–1455.

RAHN, K. A., DAMS, R., ROBBINS, J. A. and WINCHESTER, J. W. 1971: Diurnal variations of aerosol trace element concentrations as determined by non-destructive neutron activation analysis. *Atmos. Environ.*, **5**, 413–422.

RODHE, H., 1978: Budgets and turn-over times of atmospheric sulfur compounds. *Atmos. Environ.*, **12**, 671–680.

ROSEN, H., NOVAKOV, T. and BODHAINE, B. A., 1981: Soot in the Arctic. *Atmos. Environ.*, **15**, 1371–1374.

ROZENBERG, G. V., 1967: Characteristics of the atmospheric aerosol on the basis of optical research (in Russian). *Fiz. Atmos. Okeana*, **3**, 936–949.

RUSSEL, P. B. and HAMILL, P., 1984: Spatial variation of stratospheric aerosol acidity and model refractive index: implications of recent results. *J. Atmos. Sci.*, **41**, 1781–1790.

SAIGNE, C. and LEGRAND, M., 1987: Measurements of methanesulphonic acid in Antarctic ice. *Nature*, **330**, 240–242.

SALTZMAN, E. S., SAVOIE, D. L., ZIKA, R. G. and PROSPERO, J. M., 1983: Methanesulfonic acid in marine atmosphere. *J. Geophys. Res.*, **88**, 10897–10902.

SCHNELL, R. C., 1984: Condensation nuclei and aerosol size distribution measurements in Arctic haze. *11th Internat. Conf. on Atmospheric Aerosols, Condensation and Ice Nuclei. Pre-print Volume I.* Budapest, 143–147.

SCOTT, B. C., 1978: Parameterization of sulfate removal by precipitation. *J. Appl. Meteor.*, **17**, 1375–1389.

SEHMEL, G. A. and SUTTER, S. L., 1974: Particle deposition rates on a water surface as a function of particle diameter and air velocity. *J. Rech. Atmos.*, **8**, 911–920.

SELEZNEVA, E. S., 1966: The mean features of condensation nuclei distribution over the European territory of the USSR. *Tellus*, **18**, 525–531.

SHAW, G. E., 1985: Aerosol measurements in central Alaska, 1982–1984. *Atmos. Environ.*, **19**, 2025–2031.

SHEDLOVSKY, J. P. and PAISLY, S., 1966: On the meteoritic component of stratospheric aerosols. *Tellus*, **18**, 499–503.

SIMONEIT, B. R. T., 1984: Application of molecular marker analysis to reconcile sources of carbonaceous particulates in tropospheric aerosols. *Sci. Total Environ.*, **36**, 61–72.

SINCLAIR, D., COUNTESS, R. J. and HOOPES, G. S., 1974: Effect of relative humidity on the size of atmospheric aerosol particles. *Atmos. Environ.*, **8**, 1111–1117.

SLINN, W. G. N., 1982: Predictions for particle deposition to vegetative canopies. *Atmos. Environ.*, **16**, 1785–1794.

SMIC, 1971: *Inadvertent Climate Modification*. MIT Press, Cambridge, Massachusetts.

SPENGLER, J. D. and THURSTON, G. D., 1983: Mass and elemental composition of fine and coarse particles in six U.S. cities. *J. Air Pollution Control Association*, **33**, 1162–1171.

SPICER, C. W. and SCHUMACHER, P. M., 1977: Interferences in sampling atmospheric particulate nitrate. *Atmos. Environ.*, **11**, 873–876.

SPURNY, K. R. (ed.), 1986: *Physical and Chemical Characterization of Individual Airborne Particles*. Ellis Horwood Limited, Chichester.

STELSON, A. W., FRIEDLANDER, S. K. and SEINFELD, J. H., 1979: A note on the equilibrium relationship between ammonia and nitric acid and particulate ammonium nitrate. *Atmos. Environ.*, **13**, 369–371.

Swedish Ministry of Agriculture, 1982: *Acidification Today and Tomorrow*. Risbergs Tryckeri A. B., Uddevalla.

TANNER, R. L., KUMAR, R. and JOHNSON, S., 1984: Vertical distribution of aerosol strong acid and sulfate in the atmosphere. *J. Geophys. Res.*, **89**, 7149–7158.

TOON, O. B. and KASTING, J. F., 1987: The sulfur cycle in the marine atmosphere. *J. Geophys. Res.*, **92**, 943–963.

TURCO, R. P., 1982: Models of stratospheric aerosols and dust. In *The Stratospheric Aerosol Layer* (ed.: R. C. Whitten). Springer-Verlag, Berlin, 93–119.

TWOMEY, S., 1955: The distribution of sea-salt nuclei in air over land. *J. Meteor.*, **12**, 81–86.

TWOMEY, S., 1977: *Atmospheric Aerosols*. Elsevier, Amsterdam.

TYMEN, G., BUTOR, J. F., RENOUX, A. and MADELAINE, G., 1975: Quelques caractéristiques de l'aérosol situé au-dessus de l'Atlantique (Campagne Midlante A, avril–mai 1974). *Chemosphere*, **6**, 357–360.

VITTORI, O. A. and PRODI, V., 1967: Scavenging of atmospheric particles by ice crystals. *J. Atmos. Sci.*, **24**, 533–538.

VOHRA, K. G., VASUDEVAN, K. N. and NAIR, P. V. N., 1970: Mechanism of nucleus-forming reactions in the atmosphere. *J. Geophys. Res.*, **75**, 2951–2960.

VOLDNER, E. C., BARRIE, L. A. and SIROIS, A., 1986: A literature review of dry deposition of oxides of sulphur and nitrogen with emphasis on long-range transport modelling in North America. *Atmos. Environ.*, **20**, 2101–2123.

VONG, R. J., HANSSON, H.-C., COVERT, D. S. and CHARLSON, R. J., 1988. Acid rain: simultaneous observations of natural marine background and its acidic sulfate aerosol precursor. *Geophys. Res. Lett.*, **15**, 338–341.

WEICKMANN, H., 1957: Recent measurements of the vertical distribution of Aitken nuclei. In *Artificial Stimulation of Rain* (eds: H. Weickmann and W. Smith), Pergamon Press, New York, 81–88.

WENT, F. W., 1966: On the nature of Aitken condensation nuclei. *Tellus*, **18**, 549–556.

WHITBY, K. T., 1978: The physical characteristics of sulfur aerosols. *Atmos. Environ.*, **12**, 135–159.

WHITBY, K. T., HUSAR, R. B. and LIU, B. Y. H., 1972: The aerosol size distribution of the Los Angeles smog. *J. Colloid Interfac. Sci.*, **39**, 211.

WINCHESTER, J. W., 1981: Particulate matter and sulfur in the natural atmosphere. *Nuclear Instruments and Methods*, **181**, 367–381.

WINCHESTER, J. W., LÜ WEIXIU, REN LIXIN and WANG MINGXING, 1981: Fine and coarse aerosol composition from a rural area in North China. *Atmos. Environ.*, **15**, 933–937.

WINKLER, P., 1969: Untersuchungen über das Grössenwachstum natürlicher Aerosolteilchen mit der relativen Feuchte nach einer Wägemethode. *Ann. Meteor.*, **4**, (Neue Folge), 134–137.

WINKLER, P., 1975: Chemical analysis of Aitken particles (< 0.2 μm radius) over the Atlantic Ocean. *Geophys. Res. Lett.*, **2**, 45–48.

WINKLER, P. and JUNGE, C., 1972: The growth of atmospheric aerosol particles as a function of the relative humidity. Part I: Method and measurements in different locations. *J. Rech. Atmos.*, **6**, 617–638.

WIRTH, E. and PRODI, F., 1972: The concentration and size distribution of airborne ferromagnetic particles. *Tellus*, **24**, 561–567.

WOODCOCK, A. H., 1953: Salt nuclei in marine air as a function of altitude and wind force. *J. Meteor.*, **10**, 362–371.

WOODS, D. C. and CHUAN, R. L., 1983: Size-specific composition of aerosols in the El Chichón volcanic cloud. *Geophys. Res. Lett.*, **10**, 1041–1044.

YOSHIZUMI, K. and ASAKUNO, K., 1986: Characterization of atmospheric aerosols in Chichi of the Ogasawara (Bonin) islands. *Atmos. Environ.*, **20**, 151–155.

ZOLLER, W. H., CUNNINGHAM, W. C. and DUCE, R. A., 1979: Trends and composition of atmospheric aerosols from South Pole station, Antarctica. *WMO Special Environ. Rep.*, No. 14, Geneva, 245–258.

3. Cloud condensation nuclei

3.1 Statement of the problem

The supersaturations which accompany cloud formation in the atmosphere are quite low (see later). Consequently cloud droplets form on a special class of aerosol particles called cloud condensation nuclei (CCN).

The results discussed in Chapter 2 show that the number of aerosol particles in the atmosphere varies approximately from 10^2 cm^{-3} to 10^5 cm^{-3} as a function of the interaction of particle sources and removal processes. On the other hand, according to atmospheric observations the concentration of water droplets in clouds of different types is between 10 cm^{-3} and 10^3 cm^{-3} (MASON, 1971). This implies that cloud droplets form only on a fraction of the aerosol particles. Thus, the aim of the research in this field is to determine the nature of particles which can serve as CCN under atmospheric conditions.

The problem can be approached in the following way. If we determine the physical and chemical properties of the aerosol particles as discussed in Chapter 2 and we calculate the critical supersaturations corresponding to those characteristics by using a thermodynamic theory (see Section 3.2), the fraction of particles active in condensation can be estimated: the lower the critical supersaturation of a particle, the higher is the probability for its participation in cloud formation. To understand the significance of critical supersaturation in more detail let us consider an expanding air parcel in an updraft. Because of cooling, the relative humidity of the air parcel becomes higher and higher. After passing the saturation level (relative humidity of 100 per cent), cloud droplets begin to form on aerosol particles[1]. By the further increase of saturation (called supersaturation) more and more nuclei become active. Due to water vapor consumption by nuclei the supersaturation begins to decrease at a certain time (at a certain level in the cloud). For that given parcel of air, only those particles can serve as condensation nuclei whose critical supersaturation is equal to or less than the maximum supersaturation which was reached. Hence, the cloud-physical importance of a particle can be characterized by its critical supersaturation, which in turn is a function of the physical and chemical properties of the particle.

The concept of critical supersaturation also gives a possibility for measuring

[1] It is to be noted that water-soluble (hygroscopic) aerosol particles can occur in the air in liquid phase even below the saturation level. However, these liquid particles cannot be considered cloud droplets since they are in stable equilibrium (see later).

atmospheric nuclei. If in a suitable volume of air, generally in a chamber, a given low supersaturation is created, the number of CCN having a critical supersaturation equal to or lower than the supersaturation in the chamber can be determined by counting the cloud droplets formed (see Section 3.3). If this measurement is carried out at different supersaturations, the so-called supersaturation spectrum is obtained, which is the number of active nuclei as a function of supersaturation. The value of such observations is particularly high if they are combined with other measurements of the physical and chemical characteristics of the particles as discussed in Section 3.4.

It follows from the above discussion that the concentration of droplets in a cloud, at a given updraft speed, depends primarily on the number of CCN. If the number of particles with low critical supersaturation is large, the concentration of cloud droplets is high and their average size is small since the amount of water vapor available is divided among the large number of nuclei. On the contrary, if the number of CCN is small, a droplet population of low concentration and large average size will be produced. Since the formation of precipitation in a cloud depends, among other factors, on the size of cloud droplets, the CCN stongly influence the ability of clouds to precipitate. For this reason the last section of this chapter is devoted to the presentation of the relationship between CCN and cloud and precipitation formation.

3.2 Theory of condensation

Condensation is a form of nucleation in which liquid water is formed from water vapor. Generally speaking, nucleation is the initiation of the phase change of a substance during which a more condensed state is formed at certain points within the less condensed state. If only molecules of the condensing substance (water in our case) are involved in the process, the condensation is called homogeneous. In contrast, if the phase change takes place on nuclei composed of other substances, the process is termed heterogeneous. As it was mentioned, in the atmosphere cloud droplets form on CCN at low supersaturations, hence atmospheric condensation is a heterogeneous process. The basic theory of heterogeneous condensation is based on the theory of homogeneous condensation. These concepts are presented in Appendix I.

3.2.1 Condensation on water-soluble nuclei

Based on the theory of homogeneous condensation (see Appendix I), the role of condensation nuclei can be readily understood. The nuclei decrease the supersaturation necessary for germ[1] formation. On the other hand, on certain nuclei germs can form spontaneously. From the point of view of water con-

[1] Also called an embryo of critical size: a droplet in unstable equilibrium with its environment.

densation, atmospheric particulate matter can be classified as: water-insoluble or water-soluble substances, or mixtures of the two. In this subsection the theory of the water vapor condensation on water-soluble nuclei is briefly presented. This theory can easily be applied even for mixed particles.

For understanding the role of water-soluble particles in condensation let us consider a system which consists of water vapor and of a soluble nucleus. Let the dry radius and the mass of the nucleus be denoted by r_o and m_o, respectively. If we raise the relative humidity in the system, the nucleus becomes a saturated solution (consequently its radius becomes larger) even before the relative humidity reaches 100%. This is due to the fact, well-known from physical chemistry, that the equilibrium vapor pressure over a solution is lower than over pure water. While there is also a slight dependence on the dry particle radius, the phase change from dry particle to saturated solution droplet (called deliquescence) takes place very near a relative humidity characteristic of the substance of the nucleus, namely, the relative humidity at which the saturated solution is in equilibrium with its vapor environment (it is about 75% and 80% for sodium chloride and ammonium sulfate, respectively). The change in free energy of the system during droplet formation (before and after deliquescence of the nucleus) can be calculated using a thermodynamic approach. The principles of such a calculation can be summarized as follows (for the mathematical details see KÖHLER, 1950 and MÉSZÁROS, 1969).

Suppose that the vapor pressure (p_1) is between the equilibrium values for the saturated solution of the substance ($p'_{2\infty}$) and for pure water ($p_{2\infty}$). If we represent the free energy change as a function of the radius fo the solution droplet, the curve labelled by $p'_{2\infty} < p_1 < p_{2\infty}$ in Fig. 3.1 is obtained. At this vapor pressure the nucleus grows spontaneously until its radius reaches r_a. For further growth (and also for shrinking) free energy is needed since ΔF increases with increasing (or decreasing) droplet radius. Considering that ΔF has a minimum, the droplet with radius r_a is in a stable equilibrium with the vapor[1]. This means that in spite of the fact that we have a droplet it cannot be considered as a germ of condensation (which is in unstable equilibrium). If such a stable droplet gains or looses water molecules by random fluctuations, it will tend to regain its original size again by subsequent fluctuations. In contrast, if a small supersaturation is created in the system ($p_{2\infty} < p_1 < p_1^*$; the physical explanation of p_1^* is given below) the soluble particle can have two equilibrium radii: one of them (r_b) represents a stable, the other (r_c) an unstable state. Thus, the free energy of germ formation (δF^*) is given by the difference $\Delta F_c - \Delta F_b$ and the requirement for germ formation at $p_1 < p_1^*$ would be the growth of the droplet from r_b to r_c by random fluctuations. If the supersaturation is further increased, the difference between r_b and r_c becomes smaller and smaller. Finally, at a vapor pressure p_1^* the critical supersaturation is reached at which $r_b = r_c = r^*$, that is the minimum and the maximum coincide. Under this

[1] Such a droplet is called haze particle.

condition $\Delta F^* = 0$ and the curve has an inflection point. Above the critical supersaturation condensation takes place spontaneously on soluble nuclei with dry radius of r_0; clearly, S^* and r^* are functions of r_0.

The relationship between supersaturation and droplet radius for water-soluble nuclei can be obtained if we take into account the presence of soluble material in the liquid droplet. It can be demonstrated (DUFOUR and DEFAY, 1963; MÉSZÁROS, 1969) that this relationship can be given by the following expression[1]:

$$\ln \frac{p_1}{p_{2\infty}} = \frac{2\sigma'_{12}}{n'_2 kTr} + f \ln x \tag{3.1}$$

where σ'_{12} is the specific surface energy of the liquid–vapor interface, n'_2 is the number of molecules in unit volume of the solution, k is the Boltzmann constant (1.381×10^{-23} J K^{-1}), T is the temperature, while f and x are the osmotic coefficient and the concentration of water molecules in the solution, respectively. In Eq. (3.1) the solution is considered "real", which means that the interaction of solvent and solute molecules is not neglected, by inclusion of a correction factor, the so-called osmotic coefficient of water.

The numerical values of σ'_{12} and f for ammonium sulfate are listed in Table 3.1 as a function of x:

$$x = \frac{n_2 \left(\frac{4}{3} \pi \frac{\varrho'}{\varrho} r^3 - \frac{m_0}{\varrho} \right)}{n_2 \left(\frac{4}{3} \pi \frac{\varrho'}{\varrho} r^3 - \frac{m_0}{\varrho} \right) + \nu n_0 \frac{m_0}{\varrho_0}},$$

while n'_2 in Eq. (3.1) is as follows[2]:

$$n'_2 = \frac{n_2 \left(\frac{4}{3} \pi \frac{\varrho'}{\varrho} r^3 - \frac{m_0}{\varrho} \right)}{\frac{4}{3} \pi r^3}.$$

In these latter two formulae ϱ, ϱ' and ϱ_0 are the density of pure water, solution and dry soluble material, respectively, n_0 is the number of molecules in unit volume of soluble material, and ν is the number of ions formed during the dissociation of one molecule of the solute (3 for ammonium sulfate, 2 for sodium chloride). For ammonium sulfate $\varrho_0 = 1.769$ g cm^{-3}, $n_0 = 4.559 \times 10^{21}$ cm^{-3}, while the values of ϱ' are given in Table 3.1.

After a simple mathematical transformation, Eq. (3.1) yields

$$\frac{p_1}{p_{2\infty}} - 1 = \frac{2\sigma'_{12}}{n'_2 kTr} - f\nu x' \tag{3.2}$$

[1] An equation of this type was first developed by KÖHLER (1926). For this reason it is frequently referred to as the KÖHLER's formula.

[2] Note that for pure water at 0° C: $n_2 = 3.3 \times 10^{22}$ cm^{-3}.

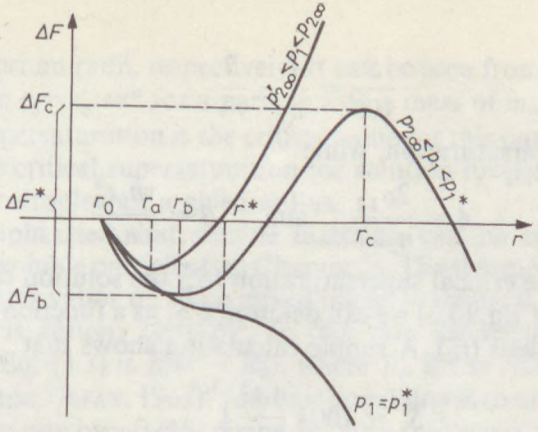

Fig. 3.1

Variation of the free energy change *(ΔF)* of droplet formation as a function of droplet radius in the case of a soluble particle with radius r under different vapor pressure conditions (see the text)

Table 3.1

Specific surface energy (σ'_{12}), osmotic coefficient (f) and density (ϱ') of ammonium sulfate solutions as a function of the concentration of water molecules in the solution at a temperature of 0 °C

x	σ'_{12} [10^{-3} Jm^{-2}]	f	ϱ'[10^{-3} kg m^{-3}]
1	75.60	–	0.9999
0.9997	75.61	0.87	1.0077
0.9994	75.62	0.84	1.0081
0.9985	75.66	0.79	1.0091
0.997	75.72	0.76	1.0107
0.994	75.84	0.73	1.0140
0.985	76.20	0.68	1.0240
0.97	76.81	0.65	1.0405
0.94	78.03	0.62	1.0733
0.85	81.66	0.57	1.1698
0.79	84.09	0.56	1.2326

since $x-1 = -\nu x'$, where x' is the concentration of solute molecules in the solution:

$$x' = \frac{n_0 \dfrac{m_0}{\varrho_0}}{n_2\left(\dfrac{4}{3}\pi\dfrac{\varrho'}{\varrho}r^3 - \dfrac{m_0}{\varrho}\right) + \nu n_0 \dfrac{m_0}{\varrho_0}}$$

If the solution becomes dilute ($x' \to 0$), then $f \to 1$, $\varrho' \to \varrho$, $n'_2 \to n_2$ and $\sigma'_{12} \to \sigma_{12}$. Further, in this case the second term in the denominator becomes negligible relative to the first one and also m_0/ϱ in the parenthesis can be neglected. Thus, Eq. (3.2), for a particle of given size and nature, transforms to[1]

[1] It is to be noted, however, that this is true only in a first approximation. The error made by assuming that CCN form dilute (weak) solutions is discussed by SAXENA and FISHER (1984).

$$\frac{S}{100} = \frac{A}{r} - \frac{B}{r^3} \tag{3.3}$$

where S it the supersaturation, while

$$A = \frac{2\sigma_{12}}{n_2 kT} \quad \text{and} \quad B = \frac{\nu n_0 r_0^3}{n_2}.$$

Since around the critical supersaturation (S_c) the solution can be considered dilute, by means of Eq. (3.3) we can determine S_c as a function of the dry radius of the soluble nucleus (r_0). A simple calculation shows that

$$S_c = 100\left(\frac{4A^3}{27B}\right)^{1/2}. \tag{3.4}$$

This formula makes it possible to obtain the supersaturation spectrum from the size distribution of particles, and *vice versa* (see later) if all particles are of the same soluble substance. On the other hand, if both spectra are simultaneously measured B can be calculated for estimating the solubility of the aerosol and for checking the theory (FITZGERALD and HOPPEL, 1982).

The results of calculations, using Eq. (3.2), for ammonium sulfate nuclei are illustrated in Fig. 3.2. These calculations were made for a temperature of 273 K. The curve calculated for pure water droplets is also plotted for comparison. To interpret the curves let us suppose that the supersaturation is 0.006 (as given by the horizontal dotted line). An ammonium sulfate particle with a mass of $m_0 = 10^{-17}$ g has two equilibrium radii at this supersaturation. In agreement with the curve labelled by $p_{2\infty} < p_1 < p_1^*$ in Fig. 3.1, r_b and r_c give the stable and

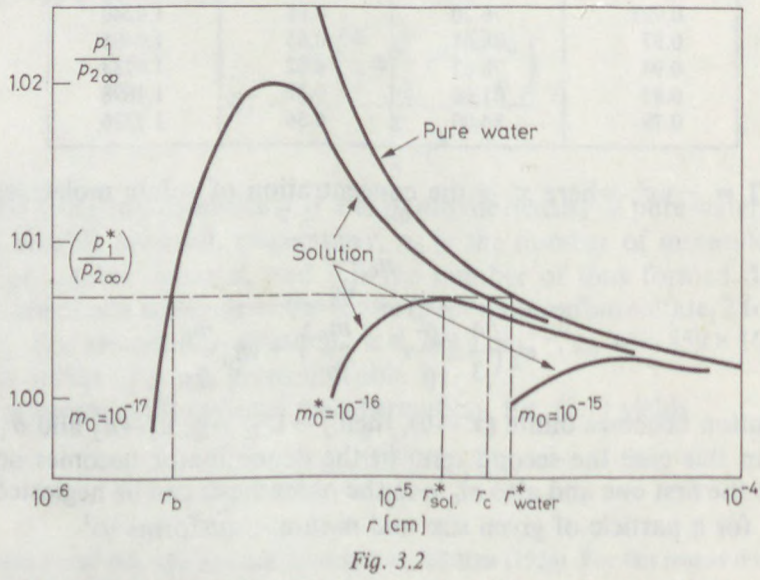

Fig. 3.2

Relationship between supersaturation ($p_1/p_{2\infty}$) and equilibrium droplet radius (r) for pure water and $(NH_4)SO_4$ solutions (m_0 is the dry mass of ammonium sulfate nuclei)

the unstable equilibrium radii, respectively. It can be seen from Fig. 3.2 that at this supersaturation $r_b = r_c = r^*$ for a particle with a mass of $m_0 = 10^{-16}$ g. This means that 0.6% supersaturation is the critical value for this particle. Figure 3.2 also shows that the critical supersaturation for solution droplets is lower than that for pure water droplets of a given radius.

It should be emphasized that soluble materials can be combined in the atmosphere with insoluble particles (see Chapter 2). The thermodynamics of the condensation of water vapor on these mixed nuclei is simple if we assume that the insoluble core is entirely wettable. In this case the second term on the right-hand side of Eq. (3.3) is $B/(r^3 - R_0^3)$, where R_0 is the radius of insoluble particles (DUFOUR and DEFAY, 1963). Another possibility is to multiply the value of B in the same equation by a factor giving the mass fraction of soluble material in the particle (FITZGERALD and HOPPEL, 1982). This factor is equal to 0 for insoluble and to 1 for soluble nuclei.

For mixed nuclei in which the insoluble core is not entirely wettable (MÉSZÁROS, 1969) and/or if it has an uneven surface (LEVKOV, 1970) the theory is more complicated. These cases are not discussed in this volume because of the lengthy mathematics needed. We only note that these formal complications do not change our main conclusion: the presence of a soluble substance reduces considerably the free energy of germ formation.

3.2.2 Condensation on insoluble particles

As we will see in Section 3.4, CCN are composed mostly of hygroscopic materials. However, for the sake of completeness, the principles of condensation on insoluble particles are briefly outlined in this subsection. For further details the interested reader is referred to Appendix I of this book.

The theory of condensation on plane insoluble substrate was first elaborated in the thirties (see VOLMER, 1939). It was extended to the case of curved surfaces by KRASTANOV and his associates (see KRASTANOV and MILOSHEV, 1963) as well as by FLETCHER (1962). Condensation on insoluble particles can be readily analyzed if we assume that the surface of the nucleus is completely wettable with liquid water, that is, the contact angle between the liquid and the solid is equal to zero. This situation would correspond to the case when there is no change in free energy associated with replacing the surface between the vapor and solid phases by a solid–liquid and liquid–vapor surface of infinitesimal thickness, since $\sigma_{13} = \sigma_{12} + \sigma_{23}$ in this case (where 1, 2 and 3 refer to vapor, liquid and solid phase, respectively). In other words, a water-insoluble but wettable particle behaves exactly like a pure water droplet of the same size.

It then also follows that the relationship between supersaturation and critical germ radius for pure water[1] is valid for this case, too. The activities of soluble

[1] This relationship is given by Eq. (3.1) if we do not consider the second term at the right-hand side ($f \ln x$). For insoluble particles the radius of the water droplet must be substituted by the radius of the particles.

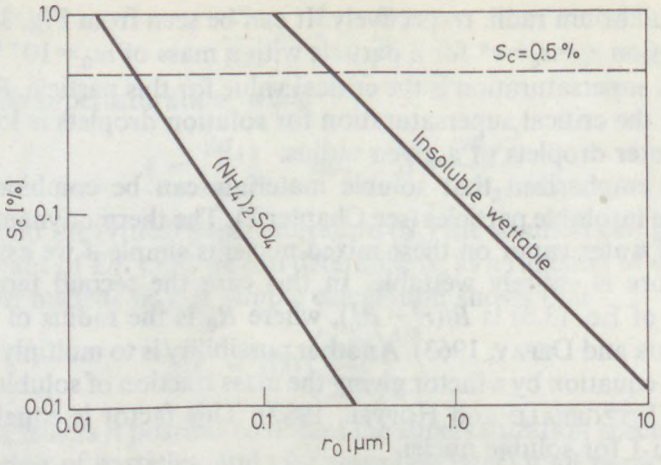

Fig. 3.3

Variation of the critical supersaturation for soluble $(NH_4)_2SO_4$ and insoluble, wettable particles as a function of the radius of nuclei

and insoluble particles may be compared on the basis of Fig. 3.2. This comparison makes it evident that the critical supersaturation for soluble nuclei is lower than for insoluble particles. This fact is further illustrated in Fig. 3.3 where the critical supersaturation (S_c) is plotted as a function of the radius of insoluble particles and of the dry radius of soluble nuclei. One can see from this figure that at a supersaturation of 0.5%, for example, ammonium sulfate particles with a dry radius larger than 0.02 μm serve as active CCN. For insoluble nuclei the corresponding value is larger by an order of magnitude.

It should be noted that the theory outlined above have some shortcomings. First, it is valid only for wettable nuclei. The problem is much more complicated if the substance of the nucleus is not completely wettable with water. Without going into details we mention that the thermodynamics of condensation for this case was elaborated by FLETCHER (1962) and independently by KRASTANOV and MILOSHEV (1963). The main result is that for such particles higher supersaturation is needed for a given radius. Second, it was assumed that particles are spherical. This assumption simplifies the mathematics, but is physically questionable since aerosol particles may have variable forms. Third, small-scale surface properties can also play an important role in condensation processes as discussed by KRASTANOV and MILOSHEV (1980). These authors also demonstrated theoretically that the absorption of foreign molecules on the surface of nuclei modifies the condensation activity. Further research is needed, however, to clarify these points.

The theory of water vapor condensation on insoluble substrates was tested for plane surfaces and for aerosol particles of different nature. Thus, TWOMEY (1959c) found good agreement between theory and experiment in the case of plane surfaces. However, HUDSON *et al.* (1982) demonstrated that the critical

supersaturation of both silver iodide and fly ash particles was much lower than the theoretical values. Whether this discrepancy is caused by the contamination of aerosol samples with some soluble material remains an open question.

3.3 Concentration and supersaturation spectra of cloud condensation nuclei

3.3.1 Principle of diffusion chambers

The first observations on condensation nuclei were carried out with expansion chambers (see 2.2.1). Since the supersaturations in the expansion chambers are typically several hundred percent, practically all the particles in the air are activated to form water droplets of detectable size. The particles detected in this way are termed the Aitken nuclei.

Theoretical work (HOWELL, 1949; MORDY, 1959) and observations made in clouds (WARNER, 1968a) and fogs (GERBER, 1982; SAXENA and FUKUTA, 1982) have shown that supersaturations in nature are very low compared to those in expansion chambers. Low supersaturations (fraction of a percent to a few percent) can be created in so-called diffusion chambers. These chambers, used previously in cosmic physics (LANGSDORF, 1936), were first applied in the fifties to measure the concentration of cloud condensation nuclei in the atmosphere (HOLL and MÜHLEISEN, 1955; WIELAND, 1955; TWOMEY, 1959a).

In a diffusion chamber a steady state flux of water vapor is maintained between two wet surfaces having either different temperatures or different solute concentrations. The former type is called the thermal-gradient diffusion chamber, while the latter constitutes the class of chemical diffusion chambers. Except for some early work (e.g. TWOMEY, 1959a), thermal diffusion chambers have been generally used.

Figure 3.4 illustrates the operating principle of a thermal diffusion chamber. First, the chamber is filled with sample air through an inlet. Water vapor diffuses from the warmer surface with temperature T_w toward the cold surface with temperature T_c. The steady-state temperature gradient and vapor pressure gradient established in the chamber are linear (solid line). However, the relationship between saturation vapor pressure and temperature is non-linear (dotted line). For this reason a supersaturation is created at all levels in the chamber, the maximum supersaturation occurring nearly midway between the two surfaces. This maximum supersaturation (S_m) can be approximately calculated as a function of the temperature difference:

$$S_m = \frac{(T_w - T_c)^2}{25}$$

By illuminating the chamber at a level where S_m occurs, the droplets in a given volume may be photographed to determine the concentration of CCN with a critical supersaturation less than or equal to S_m. From a series of measurements

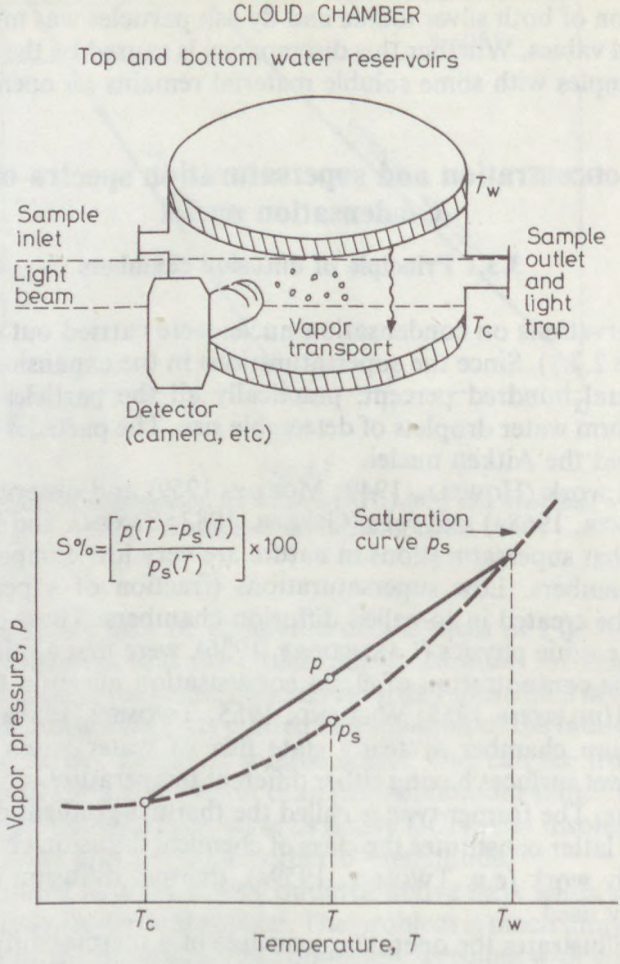

Fig. 3.4

Operating principle of a thermal diffusion chamber according to RADKE and JIUSTO (1981). The lower part of the figure represents the relationship between vapor pressure *(p)* and temperature *(T)* in the chamber (solid line) as well as for plane water surface (dotted line). The indices w and c denote the warm and cold surfaces, respectively. (By courtesy of Galway University Press)

with different $(T_w - T_c)$ and hence different S_m values, we can determine the concentration of CCN as a function of supersaturation. In this way the so-called supersaturation spectrum is obtained. The chamber illustrated in Fig. 3.4 is called the static diffusion chamber referring to the air sample being kept without motion in the chamber. Without going into details we note that the tedious analysis of photographic images can be avoided by using an automatic image analyzer or by measuring the intensity of light scattered by the droplets (RADKE and JIUSTO, 1981).

The slow sampling rate of static diffusion chambers can be improved by maintaining a continuous flow of air through the chamber. In these instruments,

called dynamic flow chambers (LAKTIONOV, 1968; HUDSON and SQUIRES, 1976) droplets existing in the chamber after activation and growth are generally counted by measuring the light impulses scattered by individual droplets. The dynamic flow chambers can be designed to sustain a range of supersaturations (FUKUTA and SAXENA, 1979). This makes it possible to measure the supersaturation spectrum with a high resolution in space and time.

A general drawback of the chambers discussed so far is the fact that they can be used only for supersaturations exceeding about 0.15%. For measurements at supersaturation below this value isothermal haze chambers are used (LAKTIONOV, 1972; HUDSON, 1980). The principle of this type of device is very simple. In a chamber the air sample is saturated with water vapor so that hygroscopic nuclei can grow to their equilibrium radii at 100% relative humidity (r_{100}). The distribution of r_{100}-values is measured for a sample by means of an optical device. On the basis of the thermodynamic theory outlined in the last section the critical supersaturation (S_c) of a nucleus can be inferred from its size at 100% humidity:

$$S_c = \frac{0.04}{r_{100}} \tag{3.5}$$

where r_{100} is given in μm and S_c is in percent. Hence, from the size distribution of r_{100} the supersaturation spectrum can be constructed if all particles are assumed to have the same chemical composition. If the proportion of insoluble and hydrophobic particles in some sample is high this method is a bit questionable. However, the method has enabled to construct supersaturation spectra down to about 0.01%.

Diffusion chambers of various types and design are widely used by research groups all over the world. To obtain a unified data set, comparison of the different devices is of crucial importance. The results of the International Cloud Condensation Nuclei Workshop held in 1980 in Reno (Nevada, USA) showed (KOCMOND *et al.*, 1982) that static diffusion chambers and dynamic flow diffusion chambers of good quality agreed with each other to within about 15%. However, for isothermal haze chambers the agreement was not so good: only two of four isothermal haze chambers agreed to within about 40%. This indicates the need for further improvement of haze chambers.

3.3.2 Results of CCN measurements

Many atmospheric observations have been carried out by means of the diffusion chambers discussed. Figure 3.5 shows the classical results of TWOMEY (1959a) obtained at ground level near Sydney, Australia. The ordinate gives the concentrations of CCN at the supersaturations plotted on the abscissa. We note that in continental air the concentration of CCN is higher than in maritime air masses. This indicates that a major part of CCN is of continental origin. The number of CCN is significant in particular under drought conditions.

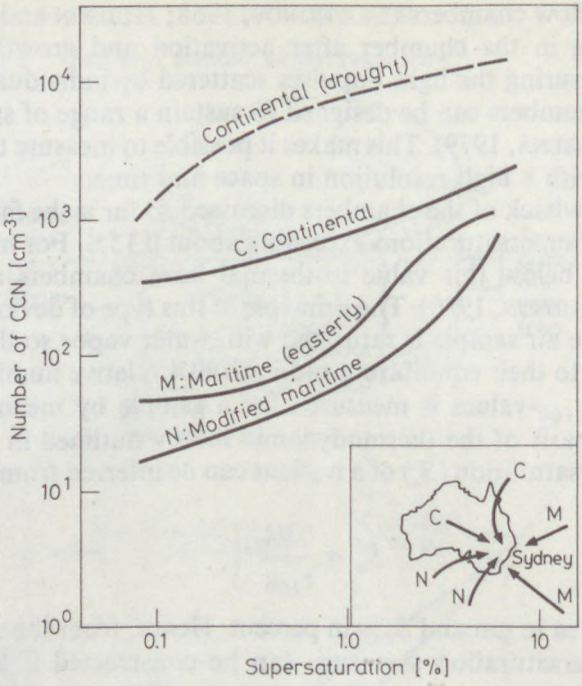

Fig. 3.5

Supersaturation spectra of cloud condensation nuclei measured at the ground level near Sydney, Australia, by TWOMEY (1959a) in air masses of different origin. (By courtesy of Birkhäuserr Verlag)

Figure 3.6 summarizes the results of another set of measurements made by JIUSTO and KOCMOND (1968) under different conditions. Beside TWOMEY's conclusions these curves demonstrate that in polluted air at Buffalo (New York, USA) the concentrations are more significant than in country air over Southern France (Lannemezan). This raises the possibility that some CCN are produced by human activities, as discussed in more detail in Subsection 3.3.4.

As it was first proposed by TWOMEY (1959b), several supersaturation spectra observed can be approximated by a power law of the form

$$N = C\,S^k \tag{3.6}$$

where N is the number of CCN active at S, while C and k are constant. For example, corresponding to Fig. 3.5, TWOMEY gives $C = 2000\ \mathrm{cm}^{-3}$ and $k = 0.4$ for continental air masses, and $C = 125\ \mathrm{cm}^{-3}$ and $k = 0.3$ for maritime air masses. However, many authors report (e.g. LAKTIONOV, 1975; HUDSON, 1980; ALOFS and LIN, 1981) that k varies as a function of S if supersaturation below 0.1% is also included in the study. For example, in 22 series of measurements near Moscow in surface air during the period 1966–1972 LAKTIONOV (1975) obtained $k = 2.3$ for supersaturations below 0.1% and $k = 0.96$ for supersatura-

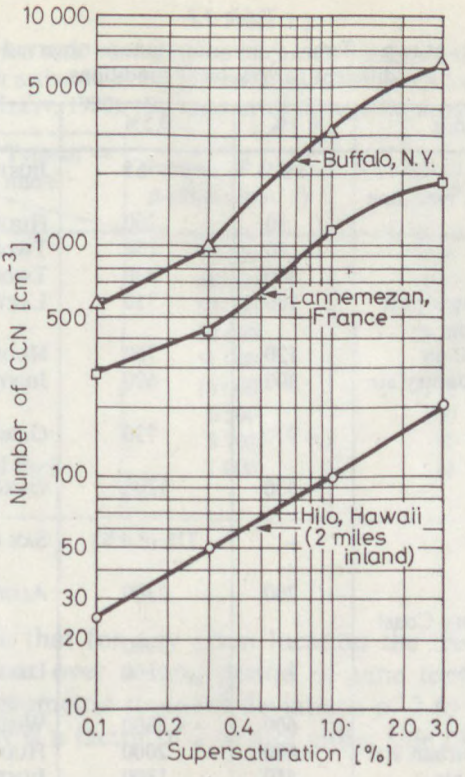

Fig. 3.6

Supersaturation spectra of cloud condensation nuclei observed under different conditions (JIUSTO and KOCMOND, 1968). (By courtesy of *J. Recherches Atmosphériques*)

tions in the range of 0.16–1.0%. The corresponding standard deviations were found to be 0.85 and 0.54, respectively.

Table 3.2 contains the results of CCN observations carried out at ground level under different conditions. In the table the concentrations at supersaturations of 0.1% and 0.5% are tabulated. One can see that at 0.5% the concentration of CCN in maritime air is below 200 cm^{-3}, while it lies between 300 and 1000 cm^{-3} under continental conditions. We may also note that in polluted atmosphere over continents the concentrations at $S = 0.5\%$ are above 10^3 cm^{-3}. Since the CCN concentrations in maritime and continental air are different, it is reasonable to anticipate that the number of droplets in maritime and continental clouds will also be different. This conclusion is in excellent agreement with the results of droplet samplings carried out in clouds formed under maritime and continental conditions, as discussed in Section 3.5.

It can also be seen from Table 3.2 that under sub-equatorial conditions surprisingly high concentrations of CCN were measured. As discussion in Subsection 3.3.4 shows this is due to CCN produced by vegetation.

Table 3.2

The concentration of CCN at two different supersaturations as observed at the ground level under different geographical conditions

Location/Conditions	0.1%	0.5%	Author (s)
Hawaii, oceanic air	25	65	JIUSTO (1967)
Yaquina Head, Oregon, maritime air	80	200	HUDSON (1980)
Sydney, maritime air	80	150	TWOMEY (1959a)
Sydney, continental air	300	630	TWOMEY (1959a)
Vicinity of Moscow, country air	100	310	LAKTIONOV (1975)
Trinidad Head, California unpolluted continental air	120	700	HUDSON (1980)
Lannemezan, France, country air	300	670	JIUSTO and KOCMOND (1968)
Valladolid, Spain country air, W winds	~370	730	GARCIA *et al.* (1981)
Valladolid, Spain country air, E winds	~520	1200	GARCIA *et al.* (1981)
Florida region, continental influence	–	718 (0.4%)	SAX and HUDSON (1981)
Rolla, Missouri, nonindustrial town	700	2300	ALOFS and LIN (1981)
Vicinity of Abidjan, Ivory Coast, dry season	–	1960	
subequatorial monsoon	–	1660	DÉSALMAND *et al.* (1982)
Switzerland, mixed continental air	600	3800	WIELAND (1955)
San Diego, California, urban air	400	2000	HUDSON (1980)
Buffalo, N.Y., polluted air	550	1800	JIUSTO and KOCMOND (1968)
Near Jerusalem, winter season	180	930	TERLIUC and GAGIN (1971)
Pune, India, modified maritime air	250–450	400–650 (0.3%)	KHEMANI (private commun.)
Nagoya, Japan	–	200–1000	OKADA *et al.* (1986)

Since specific characteristics are required for an aerosol particle to be a cloud condensation nucleus (i.e. to have $S_c < 1\%$) it is to be expected that only a fraction of the aerosol particles serves as cloud condensation nuclei. This statement can be verified if we compare the observed number of CCN to the total particle (Aitken nucleus) concentration. In Table 3.3 these two parameters are given for different locations as compiled by PRUPPACHER and KLETT (1980). It can be seen that the relative number of CCN activated at $S = 1\%$ lies between 0.4% and 14%. It also follows from the data listed that a high total aerosol concentration does not necessarily coincide with large concentration of CCN.

The concentration of CCN varies with time at a given location. TWOMEY's (1977) results from five years of CCN observations carried out near the Australian east coast (Robertson, New South Wales) indicate that the seasonal and yearly fluctuations of CCN concentration are very significant. Even during one day important variations (between about 20 cm^{-3} and 200 cm^{-3} at $S = 1\%$) were observed by RADKE and HOBBS (1969) in Olympic Mts (Washington, USA) at an elevation of 2025 m as a function of meteorological conditions.

Table 3.3

Comparison between total concentration of aerosol particles and concentration of cloud condensation nuclei activated at 1% supersaturation at various locations (PRUPPACHER and KLETT, 1980). (By courtesy of Kluwer Academic Press)

Location \ Type of nuclei →	Number of Aitken particles (cm^{-3})	Number of CCN (cm^{-3})	Ratio CCN/Aitken
Washington D.C.	78 000	2000	0.026
	68 000	2000	0.029
	57 000	5000	0.088
	50 000	7000	0.14
Long Island (N.Y.)	51 000	220	0.0043
	18 000	110	0.0061
	6 500	150	0.023
	5 700	30	0.0052
Yellowstone National Park (Wyoming)	1 000	15	0.015

Finally, we note that for any given location the frequency distribution of CCN concentrations over a long period of time tends to be a log-normal distribution with geometric standard deviations of 2 to 4. This means that the range of variability is a factor of 2 to 4 of either side of the median in 67% of the occasions.

3.3.3 Aircraft observations

It is self-evident that observations made at different altitudes are of crucial importance for cloud-physical studies. The first aircraft measurements of the concentration of CCN were made by SQUIRES and TWOMEY (1966) in continental air over Colorado, USA and in maritime air over the Caribbean sea. Figure 3.7 represents their results at $S = 0.35\%$. The important finding examplified in these data is that while in the air layers near the surface the differences between continental and maritime air masses are significant, upper tropospheric air tends to have more uniform concentrations of CCN. One can also see that the average concentrations decrease with increasing height over continents while they remain constant over the sea. These findings, confirmed subsequently, among others, by HOPPEL *et al.* (1973) and TWOMEY and WOJCIECHOWSKI (1969), support the conclusion that the major sources of CCN can be found over the continent. TWOMEY and WOJCIECHOWSKI (1969) also found that supersaturation spectra measured aloft under oceanic conditions are largely independent of geographical locations. The value of k in the power law of the supersaturation spectrum is equal to 0.5, while the nearly constant oceanic CCN concentration at a supersaturation of 1% is around 100 cm^{-3}.

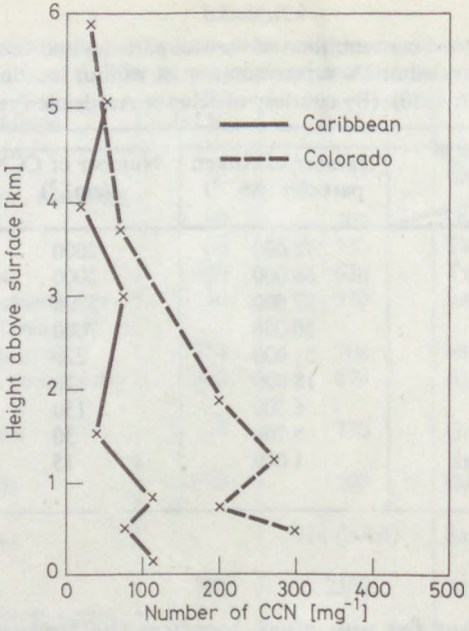

Fig. 3.7

Vertical profiles of cloud condensation nuclei at a supersaturation of 0.35% over Colorado and over the Caribbean Sea (SQUIRES and TWOMEY, 1966). (Copyright by the American Meteorological Society)

The spectrum of CCN at very low supersaturations ($S < 0.1\%$) were extensively measured by aircraft samplings in the Soviet Union. Figure 3.8 represents the results obtained by LAKTIONOV (1975) over the central region of the European territory of the USSR. We note that between 200 m and 2000 m the shape of the spectra practically does not change. In the supersaturation range of $0.16 \leq S_c < 1\%$ the k value is equal to 0.7 at these altitudes, in an excellent agreement with TWOMEY and WOJCIECHOWSKI (1969). In the range between 0.025% and 0.16%, k is slightly larger: it is between 0.9 and 1.1. Above the mixing layer (> 2000 m) the decrease with height of the number of most active CCN ($S_c \leq 0.1\%$) is more significant than the concentration decrease of nuclei with a critical supersaturation above the value mentioned. For this reason the slope of the spectrum becomes steeper and steeper with increasing height. LAKTIONOV (1975) assumes that this is due to the more intense removal of larger nuclei by cloud and precipitation. LAKTIONOV's results also demonstrate that the concentration of CCN in the air layer near the ground depends on the character of the underlying surface. Thus, over the taiga in the Komi ASSR much lower concentrations were found than over the steppe in the central part of the European territory of the USSR.

The vertical profile of the CCN at low supersaturations ($S < 0.1\%$) above the

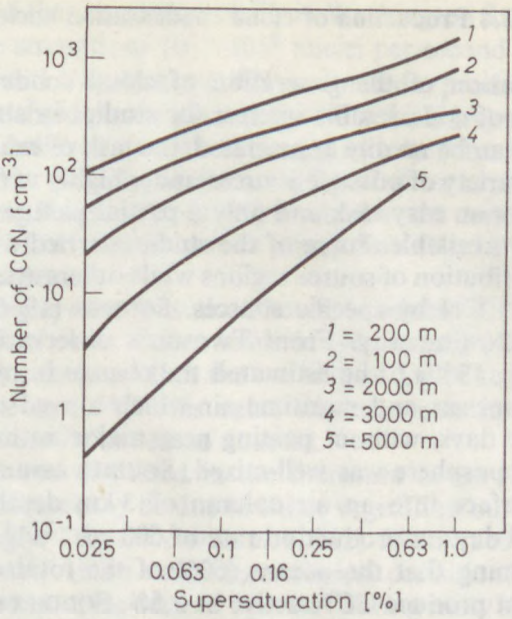

Fig. 3.8

Supersaturation *(S)* spectra of cloud condensation nuclei (CCN) at different altitudes over the central part of the European territory of the USSR (LAKTIONOV, 1975)

sea was measured recently by HINDMAN and SINCLAIR (1982). They found that in the marine boundary layer near California the concentration of CCN decreased with increasing height. This implies that larger nuclei with lower critical supersaturation are probably of maritime origin in contrast to nuclei active at supersaturations above 0.1%. This point is discussed in more detail in the next section of this chapter.

The aircraft observations of HUDSON (1984) are of interest in particular for cloud-physical considerations. This author was able to make in-cloud measurements of CCN. In some of the measurements, the nuclei within cloud droplets were excluded giving the spectra of the so-called interstitial CCN, i.e. nuclei which were not activated in cloud formation. By comparing these supersaturation spectra with the spectra of all nuclei (including nuclei involved in cloud droplets) HUDSON found that the droplets were indeed formed on nuclei with the lower range of critical supersaturation, in agreement with theoretical predictions. He also found that fewer nuclei with higher critical supersaturation were activated in stratus clouds than in cumulus clouds. This finding indicates that higher updraft velocities and consequently higher supersaturations occur in cumulus clouds.

3.3.4 Production of cloud condensation nuclei

Quantitative evaluation of the generation of cloud condensation nuclei by different sources is of considerable interest for studies in atmospheric physics and chemistry. As can be readily appreciated, the task of evaluating the contributions of a large variety of possible sources under highly variable meteorological conditions is not an easy task and only a partial picture can be assembled from the data now available. Some of the studies carried out so far aimed at estimating the contribution of source regions while others attempted to examine the production of CCN by specific sources. SQUIRES (1966) approached the problem in the following way. From TWOMEY's observations near Sydney, Australia (TWOMEY, 1959a,b) he estimated the change in nucleus content between clean maritime air and maritime air which moved over the continent during about three days, without passing near major anthropogenic sources. Since the lower troposphere was well-mixed, SQUIRES assumed a spreading of CCN from the surface into an air column of 3 km depth. Taking a mean residence time of 3 days, a production rate of 500 $cm^{-2}s^{-1}$ was estimated for $S = 0.5\%$. By assuming that the oceans (60% of the total over the Northern Hemisphere) do not produce CCN active at 0.5%, SQUIRES concluded that the average natural source strength of CCN over the Northern Hemisphere is 200 $cm^{-2}s^{-1}$.

SQUIRES (1966) estimated the intensity of anthropogenic production of CCN from observations made upwind and downwind of Denver (Colorado, USA). He obtained an anthropogenic CCN production rate of 0.55×10^4 $cm^{-2}s^{-1}$ for this city. SQUIRES generalized this estimate by making the reasonable assumption that the anthropogenic production rate is proportional to the consumption of fuels within any area. In this way he derived 68 $cm^{-2}s^{-1}$ and 9 $cm^{-2}s^{-1}$ for the average anthropogenic source strength over the USA and the Northern Hemisphere, respectively. This means that the production rate due to human activities is 14% of the intensity of natural sources in the USA. The corresponding figure for the Northern Hemisphere as a whole is 5%. This conclusion is also supported by the results of TWOMEY and WOJCIECHOWSKI (1969).

However, the foregoing evaluation does not exclude the possibility that anthropogenic production can be significant on a local scale. In addition to SQUIRES (1966), several authors demonstrated that cities produce CCN: for example, KOCMOND and MACK (1972) observed larger CCN concentrations in air downwind of Buffalo (New York, USA) than upwind. On the basis of their observations they calculated a CCN production rate of 0.68×10^4 $cm^{-2}s^{-1}$ for a supersaturation of 0.3%. According to a similar study made over St. Louis (Missouri, USA) AUER (1975) estimated, in agreement with SQUIRES, a production rate of 0.43×10^4 $cm^{-2}s^{-1}$ at 0.5%. Also over St. Louis, FITZGERALD and SPYERS-DURAN (1973) found, at a level of 600 m, downwind concentration increases of 52% and 94% at supersaturations of 0.17% and 1.0%, respectively. Recently KHEMANI (1985) obtained similar results in the vicinity of Bombay, India. Individual industrial complexes were also found to generate CCN: HOBBS

et al. (1970) reported that large paper mills in Washington State (USA) emitted CCN with a source strength of 10^{17}–10^{19} nuclei per second active at $S_c = 1\%$. Further, PUESCHEL and VAN VALIN (1978) estimated a production rate of 10^{16} per second for a coal-fired power plant (New Mexico, USA) with a total output of 2175 MW. It is believed that these nuclei mostly form by gas-to-particle conversion from sulfur dioxide, as discussed by WHITBY *et al.* (1978). In agreement with this finding HOBBS *et al.* (1980) found that the concentration of CCN in plumes from coal-fired electric power plants was about 2 to 5 times higher than outside the plumes.

The burning of sugar cane was also shown to release CCN into the atmosphere. On the basis of observations made in Queensland (Australia) WARNER and TWOMEY (1967) calculated that the burning of 1 g of sugar cane produces 8×10^{12} CCN active at 0.5%. This value was also confirmed by laboratory experiments carried out by the same authors.

Another CCN source discussed in the literature is the release by natural vegetation. Such a release may be due to either vegetation burning or biological processes. Accordingly, DÉSALMAND *et al.* (1982) determined two major CCN sources in Ivory Coast, Africa under intertropical conditions. The first source is active during dry season, the second operates during rainy saison. During dry season CCN are produced by bush fires. For rainy periods, DÉSALMAND and her co-workers postulated that two phenomena are responsible for nucleus generation. They believe that high humidity is favorable for the bacterial decomposition of plants and consequently for the release of sulfur gases and formation of sulfur-containing particles. On the other hand, under humid conditions plants emit droplets which are rich in soluble substances. It was found that these sources are so intense that during the rainy season the CCN concentration increases in spite of particle scavenging by precipitation.

3.4 Size and nature of CCN

3.4.1 Estimation of the size and nature of CCN on the basis of the measurements of aerosol characteristics

Theoretical considerations on water vapor condensation outlined in Section 3.2 show that there is a well-determined relationship between the physical and chemical properties of the particles and their activity in condensation processes. Larger and more hygroscopic nuclei have lower critical supersaturations than smaller and less water-soluble particles. Thus, by measuring the characteristics of the particles their role in cloud and fog droplet formation can be estimated. The size distribution of aerosol particles can be converted into a supersaturation spectrum if the chemical composition is known for particles of different sizes. The aim of this subsection is to discuss these problems in more detail.

The first issue to be mentioned is whether the number of large and giant hygroscopic particles is sufficient to explain condensation in atmospheric clouds. This question is interesting mostly because of historical reasons; it was believed in the past that large sea salt particles (see Chapter 2) play an essential role in cloud formation even above the continents (e.g. KÖHLER, 1936). This hypothesis was questioned on the basis of the low production rate of sea salt particles relative to the figure necessary to explain the removal of nuclei from the atmosphere by precipitation (see MASON, 1957). Further, the results of direct observations of chloride (sea salt) particles in the atmosphere showed, mainly under continental conditions, that their number is generally much lower than the concentration of cloud droplets (RAU, 1955; MÉSZÁROS, 1964). Finally, results of direct observations on CCN have demonstrated that their concentration is much higher under continental conditions than over oceanic areas (see Subsection 3.3.2). This does not exclude the possibility, however, that sea salt particles constitute an important class of CCN under oceanic conditions if the supersaturation is low. Thus, by re-calculating the sea salt size distributions measured by A. MÉSZÁROS and VISSY (1974) into supersaturation spectra, MÉSZÁROS *et al.* (1975) showed that at small supersaturations ($S < 0.03\%$) chloride particles have a dominant role in droplet formation over oceanic areas. These authors also reported that with increasing supersaturation the importance of sea salt nuclei decreases. For example in the air over the Atlantic Ocean between latitudes of 40°–60° S only about 16% of the cloud nuclei active at a supersaturation of 0.3% are composed of sodium chloride.

Another possibility is that large and giant particles ($r > 0.1$ μm) constitute the majority of CCN, independently of their chemical composition. This hypothesis was proposed by JUNGE (1963) on the basis of his aerosol observations. A necessary (but not sufficient) condition for the correctness of this hypothesis is that the number of large and giant particles exceed the concentration of cloud droplets. However, results of simultaneous aircraft observations made over Hungary (A. MÉSZÁROS, 1969) and the USA (HIDY *et al.* 1970) indicate that the concentration of large and giant particles is rather low compared to that of cloud droplets. In Table 3.4 the results obtained by A. MÉSZÁROS (1969) are tabulated. The first line gives the number of large and giant aerosol particles under the base of freshly formed summer cumuli, while the second line contains the droplet concentration measured above the cloud base. These observations indicate that in the highest case (cloud number 2) one-third of the droplets could

Table 3.4

Concentration of large and giant aerosol particles (N) and cloud droplets (n) in five different cases (A. MÉSZÁROS, 1969). (By courtesy of Academia – Prague)

	1	2	3	4	5
N [cm^{-3}]	330	350	300	220	500
n [cm^{-3}]	2300	1080	1660	1100	2300
N/n [%]	14	32	18	20	22

have formed on large and giant aerosol particles. The average of the five sets of observations is around 20%. On the basis of these data we can conclude that some fraction of Aitken particles ($r < 0.1$ μm) also contribute to cloud nuclei under atmospheric conditions. It follows from thermodynamic calculations (see Fig. 3.4) that these particles must consist of water-soluble materials.

Measurements of the chemical composition of the water-soluble fraction of Aitken-sized aerosols (in dry state) show that these particles are mainly composed of sulfur species, like ammonium sulfate and sulfuric acid, as discussed in more detail in Chapter 2. This means that small sulfate particles play an important role in the condensation of atmospheric water vapor. It should be mentioned in this respect that according to the calculations of MÉSZÁROS *et al.* (1975) at a supersaturation of 0.3% the number of CCN, calculated on the basis of the size distribution of sulfate particles with a radius larger than 0.03 μm, is comparable to the concentration of cloud droplets, both measured under oceanic conditions. In a more recent study CLARK *et al.* (1987) also found that sulfate particles in the fine size range constitute the class of CCN in oceanic air.

However, the problem is more complicated if water-soluble materials (e.g. sulfur species) are mixed with insoluble substances. This can be the case mostly above continental locations. The question was studied by JUNGE and MCLAREN (1971) who converted measured aerosol size distributions into supersaturation spectra for assumed mass fractions of soluble materials in the particles of between 0.1 and 1.0. They found that while the shape of the CCN spectrum is independent of the mass fraction, the chemical composition strongly influences the CCN concentration at a given supersaturation. Similar results were obtained by MAZIN (1980) and FITZGERALD (1973). FITZGERALD compared the observed and calculated CCN spectra. These latter spectra were determined on the basis of aerosol size distribution measurements carried out in Fort Collins, Colo. (USA). FITZGERALD found good agreement between observed and calculated spectra by using $(NH_4)_2SO_4$ mass fractions between 15 and 35% for the natural aerosol samples consisting of Aitken-sized particles. This finding is supported by the results of direct aerosol observations of MÉSZÁROS (1968) made under continental conditions near Budapest, Hungary, indicating that the ammonium sulfate mass fraction of particles with radii smaller than 0.14 μm is 20%.

3.4.2 Combination of diffusion chamber observations with other experiments

Observations carried out in the atmosphere by means of diffusion chambers make it possible to determine the number and the supersaturation spectra of CCN. As it was mentioned previously this information is of crucial importance for the study of cloud formation. However, the results obtained in this way do not give any direct experimental evidence on the size and nature of active nuclei. For this reason the combination of diffusion chamber observations with other measurements, to estimate the characteristics of the nuclei, is also of interest. In the following the results of such combined experiments are summarized.

The first step in this direction was made by TWOMEY (1965). He sampled air either directly into a diffusion chamber or the samples were first passed through a tube array in which a fraction of the particles was removed from the air due to diffusion to the tube walls. Since the diffusion coefficient is a function of particle size (see Chapter 2) TWOMEY was able to estimate the mean size of CCN on the basis of the difference between concentrations in the "normal" air and in the "decayed" air. In air sampled on the western shore of Chesapeake Bay (USA) he found that the average radius of CCN at a supersaturation of 0.35% was most probably 0.03–0.04 μm. He concluded that "the results mean that these nuclei must be soluble, or partially soluble, since even water droplets of this size have critical supersaturations considerably higher than 0.35%". Practically the same results were obtained by TWOMEY (1972) using Nuclepore filters of different pore sizes in front of the diffusion chamber to remove aerosol particles of different radii from air.

The chemical nature of CCN was also studied by TWOMEY (1968, 1971). During these experiments air samples were passed through a tube[1] heated to several hundred degrees Celsius by an electric heater prior to introduction into the thermal diffusion chamber. Depending on their volatility, some particles evaporated in the tube leading to reduced concentrations of CCN. Since the temperature of volatility is a function of chemical composition, this experiment made it possible to estimate the nature of CCN by varying the degree of heating. Experiments carried out with ambient air samples were compared to those with artificial nuclei of known composition. These studies, made in northeastern United States, suggest that ammonium sulfate may be the main constituent of cloud condensation nuclei. Very few nuclei were found to behave similarly to artificial sodium chloride particles which are practically non-volatile. Sometimes this type of nucleus was found to be entirely absent. This is little surprising if we take into account that the average radius of CCN is 0.03–0.04 μm at a supersaturation of 0.35%, while the majority of sea salt particles can be found in the coarse size range as discussed in Chapter 2.

Similar experiments were conducted by DINGER *et al.* (1970) by means of aircraft flying over the North Atlantic and over the east coast of Barbados (West Indies). Figure 3.9 shows the results obtained by these workers. The curve labelled "unheated" represents the concentration of CCN activated at 0.75% supersaturation. The other curve gives the vertical profile of the same parameter in air samples collected at the same altitudes, but heated to about 320 °C. It can be seen that the concentration of non-volatile CCN, reasonably assumed to be sea salt, decreases rapidly with increasing altitude. The relative proportion of volatile nuclei (presumably consisting of ammonium sulfate) to the sea salt fraction increases with increasing height. Above a stable air layer (about 3 km) all CCN were found to be volatile. The form of the vertical profile of CCN in untreated air samples indicates that active nuclei cannot be of surface origin.

[1] It should be noted that in this experiment the length of the tube was much less while the diameter of the tube was much larger than in the previous case.

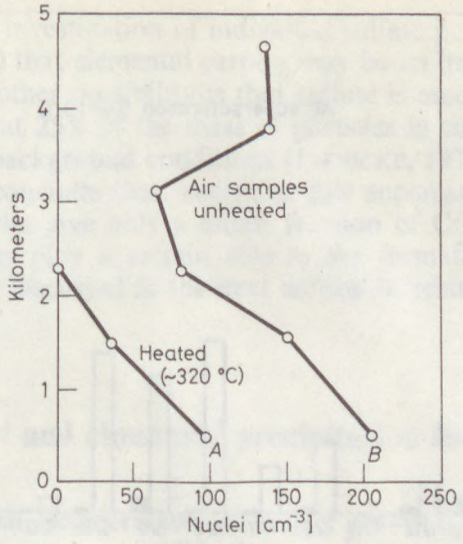

Fig. 3.9

Vertical profile of cloud condensation nuclei in the air ("unheated") at a supersaturation of 0.75%. The curve labelled "heated" represents the same parameter in air samples heated to about 320 °C (DINGER *et al.*, 1970). (Copyright by the American Meteorological Society)

The results of DINGER *et al.* (1970) are consistent with the findings of A. MÉSZÁROS and VISSY (1974) demonstrating that even near the ocean surface the number concentration of ammonium sulfate particles formed from gaseous precursors exceeds that of sea salt components (see Chapter 2).

A more direct determination of the nature of CCN was carried out recently by ONO and OHTANI (1980) in Japan. These authors compared atmospheric particles which passed through a diffusion chamber without taking part in the condensation with those sampled directly from the original air. The particles were collected in both cases by an electrostatic sampler on a thin film containing barium chloride to identify sulfate particles. Between the diffusion chamber and the aerosol sampler an impactor removed from the air water droplets formed in the chamber. Their results are represented in Fig. 3.10. This figure shows that while many sulfate particles were found in the original air, in the air which passed through the diffusion chamber maintained at supersaturations between 0.4 and 1% sulfate particles were nearly entirely absent. This is obviously caused by the fact that sulfate particles were activated in the chamber as CCN. ONO and OHTANI were also able to determine that at supersaturations less than 1%, particles having masses larger than 10^{-17} g took part in the condensation. By assuming that sulfate particles consisted of ammonium sulfate this gives a dry radius equal to 0.011 μm, in rough agreement with findings discussed previously.

Finally, we note that according to SHAW (1986) cloud condensation nuclei associated with Arctic haze (see Chapter 2) are soluble salts. The supersaturation spectra measured in Arctic haze are very close to that calculated from

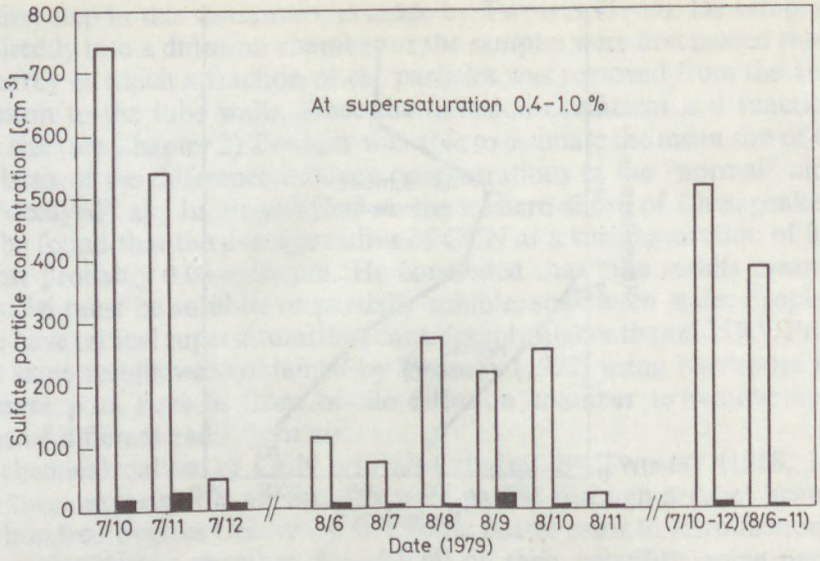

Fig. 3.10

Sulfate particle concentration in original air samples (left columns) and in the air passed through a cloud chamber maintained at supersaturations of 0.4–1% (right columns) according to ONO and OHTANI (1980). (By courtesy of *J. Recherches Atmosphériques)*

aerosol size measurements by assuming that particles consist of ammonium sulfate. SHAW assumes that soluble nuclei with a radius larger than $3–4 \times 10^{-2}$ μm are activated in Arctic stratiform clouds.

3.4.3 Conclusion

All the experimental evidence presented in this section point in the direction that a major part of CCN consists of sulfur species, mostly of ammonium sulfate.

As we have seen in Chapter 2, under clean conditions sulfate particles form from dimethyl sulfide of biogenic origin. This involves the possibility that the biosphere regulates the number of CCN and consequently the structure of clouds, through the emission of DMS from the ocean (CHARLSON *et al.*, 1987). We have also mentioned in Chapter 2 that the oceanic emission of DMS exceeds the magnitude of the continental release. Thus, one has to assume that, in some disagreement with our discussion in Subsection 3.3.4, higher CCN concentrations above the continents are due entirely to the anthropogenic production of sulfur dioxide. Unfortunately, the interesting hypothesis of CHARLSON and his co-workers can be neither proved, nor disproved on the basis of our present knowledge. Further research is needed in this field.

We must also note the sulfate particles serving as CCN can be mixed with other materials mainly under continental (more polluted) conditions. Direct

electron microscopic investigation of individual sulfate particles demonstrates (A. MÉSZÁROS, 1984) that elemental carbon may be an important component in this respect. The other possibility is that sulfate is associated with organic materials giving about 25% of the mass of particles in the Aitken size range under tropospheric background conditions (JAENICKE, 1978).

Finally, one can conclude that, except at low supersaturations in oceanic areas, sea salt particles give only a minor fraction of CCN. However, giant chloride particles can play a certain role in the formation of larger cloud droplets as it will be discussed in the next section in relation to precipitation formation.

3.5 CCN and cloud and precipitation formation

3.5.1 Theoretical considerations on droplet growth by condensation

As it was discussed in Section 3.1, the characteristics of the droplets in a cloud depend, among other parameters, on the number and size of CCN. Since the precipitation-forming ability of a given cloud is strongly dependent on its microstructure, the above statement means that precipitation formation is related to the CCN population. The aim of this section is to clarify these points; however, before going into details some theoretical considerations on the condensational growth of cloud droplets seem to be appropriate.

If we want to examine how a given soluble (or mixed) nucleus grows in and updraft we must first recognize that the thermodynamic equations (see Eqs 3.1–3.3) giving the relationship between supersaturation and nucleus properties do not explicitly involve a time variable. In other words, in formulating the equations we implicitly assumed that there is enough time for the nuclei to attain their equilibrium sizes. However, in an updraft this is not generally the case. Actually the growth rates of nuclei and of droplets are determined by the difference between the supersaturation in the cooling air (S) and the equilibrium supersaturation (S') for the nuclei or droplets. The equation relating the growth rate and supersaturation difference is as follows[1] (for further details see Appendix II, as well as FLETCHER, 1962; MASON, 1971):

$$r\frac{\mathrm{d}r}{\mathrm{d}t} = G(S-S') \tag{3.7}$$

where t is the time, while G is a coefficient given in Appendix II. In the above equation

$$S = \ln\frac{p_1}{p_{2\infty}} \approx \frac{p_1 - p_{2\infty}}{p_{2\infty}}$$

[1] This equation represents the growth of one droplet. The concentration of cloud drops formed on nuclei with radius r is given by the number of such nuclei.

$$S' = \ln \frac{p_1'}{p_{2\infty}} \approx \frac{p_1' - p_{2\infty}}{p_{2\infty}}$$

where p_1 is the actual vapor pressure in the air, while p_1' is the equilibrium vapor pressure for a solution droplet of radius r calculated by Eq. (3.3). This implies that the size of the solution droplets increases with time if $p_1 > p_1'$, while it evaporates in the opposite case. An important consequence of Eq. (3.7) is that the growth rate of the droplet is inversely proportional to its size. That is: the larger the droplet the lower its growth rate by condensation.

The second point to be considered is that the supersaturation varies in a cloud updraft as

$$\frac{dS}{dt} = Q_1 v - Q_2 \frac{dw}{dt} \tag{3.8}$$

where v is the updraft speed[1], w is the liquid water content, and Q_1 and Q_2 are physical parameters which can be found in Appendix II. It follows from the definition of the liquid water content (the mass of liquid water in unit volume of the cloudy air) that dw/dt is given by

$$\frac{dw}{dt} = 4\pi \sum_r N_r r^2 \frac{dr}{dt} \varrho'. \tag{3.9}$$

In this formula N_r is the concentration of droplets with radius r, while ϱ' is the density of water. Equation (3.8) physically means that the cooling rate, characterized by the updraft speed, tends to increase the saturation. On the other hand, supersaturation is reduced by the mass of the water vapor condensed in the air parcel.

By using the above concept and the results of his observations, TWOMEY (1959b) was able to derive a relationship between maximum supersaturation (S_{max}) on the one hand and updraft speed (in cm s^{-1}) and CCN characteristics on the other hand. He reported that this relationship can be given in the following form

$$S_{max} = \left[\frac{1.63 \times 10^{-3} v^{3/2}}{CkB(3/2, k/2)} \right]^{\frac{1}{k+2}} \tag{3.10}$$

where C and k are the constants in the supersaturation spectrum (see Eq. 3.6), while B is the complete Beta-function. Substituting S_{max} from (3.10) into (3.6) yields the number of cloud droplets which form in given updraft speed for a given supersaturation spectrum.

Equations (3.7–3.9) make the conversion of the size distribution/supersaturation spectrum of CCN into cloud droplet characteristics possible. This is of considerable importance if we want to study the cloud microstructure as a

[1] In the case of fog formation it can be replaced by the cooling rate (see e.g. Low, 1975). Thus, the first term on the right-hand side of Eq. (3.8) will be: $Q'(dT/dt)$.

function of the size and nature of CCN. The results of such calculations will be presented in the next subsection. It is to be noted in advance, however, that by using the above model we assume that the rising air cools adiabatically. This problem can be avoided by using a so-called entrainment model, first proposed by MASON and CHIEN (1962), in which mixing with the environment is taken into account.

3.5.2 Relationship between CCN and droplet characteristics

The first calculations of the formation of a droplet population on a prescribed distribution of CCN were carried out by HOWELL (1949). He assumed that the cooling rate was uniform and the temperature and pressure were practically constant during cloud formation. He also assumed, which was accepted at that time, that nuclei consisted of sea salt particles[1]. The variables in his calculations were: the relative humidity (supersaturation), the masses of the nuclei, the droplet radius, and the time (for a known updraft speed, time is equivalent to the height of rise of the parcel).

Some of HOWELL's results are illustrated in Fig. 3.11. Firstly, the droplets (nuclei) grow slowly in parallel with the increase of supersaturation. In this phase the size of droplets, except some large nuclei in the case of high cooling rates, is near the equilibrium value. After reaching the maximum supersaturation, the growth becomes very rapid. However, due to the consumption of vapor by the condensing drops, the growth rate slows down and finally it is characterized again by nearly steady growth rate. HOWELL's calculations also indicate that sizes of activated droplets converge toward a common value with time, that is the droplet spectrum narrows. As it follows from Fig. 3.11 the droplets formed on inactive nuclei (with mass of 10^{-18} mole and 10^{-19} mole) begin to evaporate when the maximum supersaturation is surpassed. For high cooling rates larger maximum supersaturations are created and consequently more smaller nuclei are activated.

Similar calculations were made later by MORDY (1959) as well as by NEIBURGER and CHIEN (1960) by using large electronic computers. Their results are generally in good agreement with those obtained by HOWELL (1949) by tedious hand calculations (MORDY repeated two of HOWELL's computations). MORDY used four updraft speeds of 5, 15, 50 and 100 cm s^{-1} and nucleus spectra of maritime type containing some giant hygroscopic nuclei. He found that the concentrations of fog and cloud droplets calculated were very similar to the data observed. The dividing line between active and inactive nuclei was calculated to be between 0.05–0.5 μm as a function of the conditions used. For a given updraft speed, higher numbers of nuclei resulted in higher cloud droplet concentrations.

[1] The calculations carried out by using ammonium sulfate nuclei give similar results (BÓNIS *et al.*, 1977) if we take into account differences in size distribution and solubility.

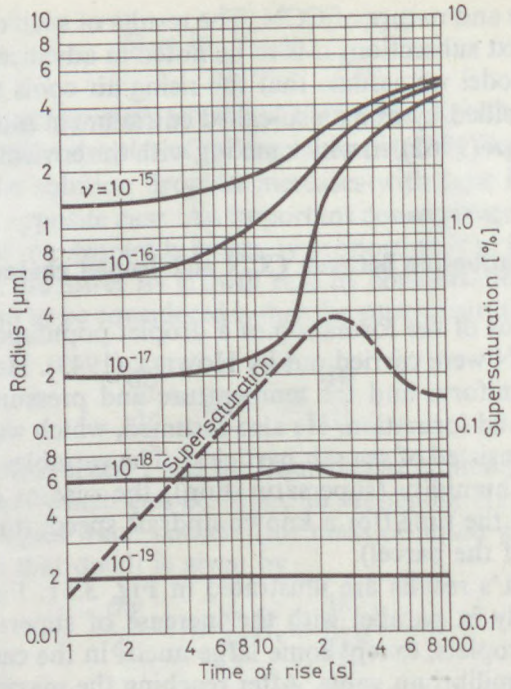

Fig. 3.11

The growth of sodium chloride nuclei of different masses (expressed in moles: ν) with an ascent of 60 cms^{-1} according to HOWELL (1949). (Copyright by the American Meteorological Society)

The latter result involves that in continental air, where the number of CCN at a certain supersaturation is higher than over the oceans (see Section 3.3), cloud droplet concentrations exceed those formed under oceanic conditions. Consequently, the average size of cloud droplets over the oceans is larger than in continental clouds. This conclusion is supported by the observations of SQUIRES (1958a,b) and of many other workers (e.g. BATTAN and REITAN, 1957) demonstrating that the microstructure of maritime clouds is different from the microstructure of continental clouds (see Fig. 3.12). Since this result is very important from the point of view of precipitation formation, it will be discussed in more detail in the next subsection.

An important test of the relation between CCN and cloud droplet characteristics was carried out by SQUIRES and TWOMEY (1960) in 1958 over Australia (near Sydney). They simultaneously measured the cloud nucleus spectra below cumulus clouds and the cloud droplet concentrations above the cloud base. The number of cloud droplets was calculated on the basis the CCN measurements by using the method outlined in Subsection 3.5.1. The calculated and measured cloud droplet concentrations are compared in Fig. 3.13 by assuming a reasonable updraft speed of 1 m s^{-1}. One can see that the agreement between cal-

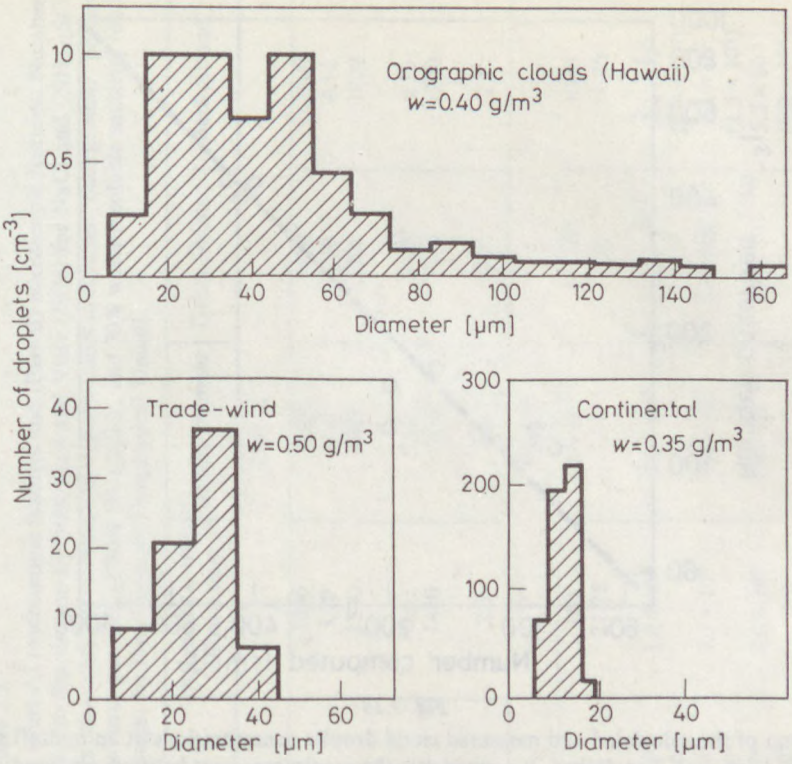

Fig. 3.12

Size distribution of cloud droplets under different conditions (SQUIRES, 1958a). (By courtesy of *Tellus*)

culated and measured figures is excellent. In a more recent paper LEAITCH *et al.* (1986) found that the concentration of cloud droplets was directly proportional to the number of aerosol particles (with a diameter larger than 0.18 μm) measured at the cloud base. However, they observed this relationship only under adiabatic conditions when the particle concentration was < 750 cm^{-3}. For particle concentrations greater than 750 cm^3, the cloud droplet number did not increase as fast as the particle concentration.

As we said already, in closed parcel models we assume that there is no mixing between the rising air and its environment. However, this assumption is not supported by observation in clouds indicating that the liquid water content in clouds without precipitation is generally much lower than the adiabatic value. MASON and CHIEN (1962) assume, which seems to be reasonable, that this is due to the fact that rising air exchanges heat, momentum and water vapor with the environment. In addition, owing to mixing, a part of the droplets leaves the cloud and evaporates in the surroundings, why in dry air fresh condensation nuclei enter the cloud. This means in part that the liquid water content decreases, and, also that the lifetime of the droplets in the cloud can be rather

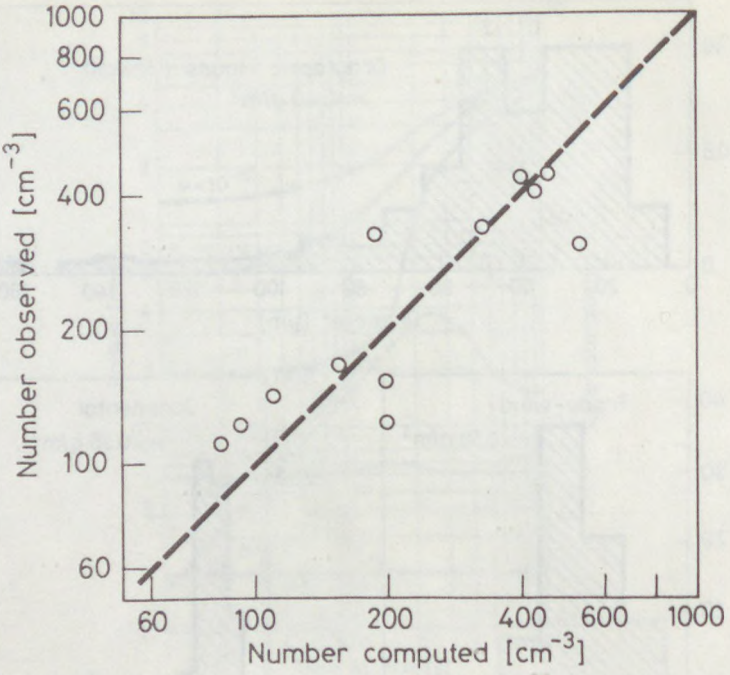

Fig. 3.13

Comparison of the calculated and measured cloud droplet concentrations at an updraft speed of 1 m s^{-1} (points). The dashed line represents the exact agreement between observed and computed values (SQUIRES and TWOMEY, 1960)

different. The difference in lifetime and supersaturation histories results in the broadening of the droplet spectrum. This concept was further developed by MANTON (1979) and BAKER *et al.* (1980) showing theoretically and by model calculations that turbulent mixing plays an important role in the formation of raindrop embryos.

Another possibility for broadening the droplet spectrum was proposed by KORNFELD (1970) who assumes that cloud droplet spectra are broader if nucleus population contains hygroscopic and insoluble substances together. In his numerical study KORNFELD assumed that the nucleus population consists of three components: chloride nuclei, wettable but insoluble nuclei of disc form and a mixture of these two types of particles. Contrary to these results, FITZGERALD (1974) concluded that in the case of mixed nuclei containing 1, 5, 10, and 50% of soluble material the droplet size distributions are not broader than for particles of homogeneous composition.

There is no intention here to discuss in further detail the differences between the results obtained by adiabatic and entrainment models (interested readers are referred e.g. to WARNER, 1973a and LEE and PRUPPACHER, 1977). However, it seems appropriate to summarize the conclusion of a numerical study in which an entrainment model was used to investigate the effects of different aerosols

Table 3.5

Cloud characteristics of aerosol types considered by LEE *et al.* (1980): (Part A) macroscopic features and (Part B) microscopic features. Numbers in parentheses in column "Atlantic O." pertain to results based on the size distribution by MÉSZÁROS and VISSY (1974) for NaCl and $(NH_4)_2SO_4$ particles over oceans with no NaCl above 2000 m (data from LEE and PRUPPACHER, 1977). Numbers in parentheses in column "Background" pertain to results based on the JUNGE size distribution for mixed continental aerosol particles of 70% $(NH_4)_2SO_4$ and 30% water-insoluble material (data from LEE and PRUPPACHER, 1977). (Copyright by the American Geophysical Union)

	Atlantic O.	Atlantic O. with Sahara dust	Urban, summer	Urban, winter	Background
	Part A				
Cloud depth (m)	3000	3000	3200	3200	3100
Maximum updraft velocity ($m\ s^{-1}$)	3.95	3.70	4.30	4.30	4.10
Level above cloud base where the updraft velocity is maximum (m)	1450	1500	1600	1700	1800
Maximum supersaturation (%)	0.36	0.40	0.09	0.09	0.15
Level above cloud base where supersaturation is maximum (m)	1440	1440	1100	1100	1200
Maximum liquid water content ($g\ kg^{-1}$)	2.6	2.3	3.0	3.1	2.8
	Part B				
Total drop concentration (cm^{-3})	155	160	2×10^4	1×10^5	1000
Mode drop radius at the top of the clouds (μm)	22.25	21.75	7.75	7.25	11.25
Drop concentration 3000 m above cloud base (L^{-1})					
$r > 10$ μm	9.7×10^4 (1.2×10^5)	1.0×10^5	9.1×10^4	5.2×10^4	3.4×10^5 (2.9×10^5)
$r > 15$ μm	7.3×10^4 (8.1×10^4)	7.1×10^4	7.4×10^0	1.4×10^2	7.6×10^3 (1.5×10^4)
$r > 20$ μm	5.0×10^4 (3.7×10^4)	4.7×10^4	1.2×10^{-1}	3.4×10^1	5.5×10^{-1} (6.8×10^1)
$r > 25$ μm	3.0×10^3 (7.4×10^2)	2.4×10^3	–	5.2×10^0	–
$r > 30$ μm	9.6×10^{-1}	6.7×10^{-1}	–	–	–
Bulk density of aerosol material	2.45	2.64	3.03	2.85	1.85

on the evolution of cloud droplet spectra. The authors of this study (LEE *et al.*, 1980) did not make any assumption on the chemical composition of aerosol particles. They used data obtained by measuring the amount of water deposited on particles under different equilibrium conditions[1]. On the other hand, they used particle size distributions actually observed in different environments (e.g. maritime, urban and continental background aerosols). The results of this set of numerical calculations (see Table 3.5) show that the maximum supersaturation reached in maritime clouds considerably exceeds the values determined for urban aerosols (the background case is somewhere in-between). This results from the fact that urban aerosol particles contain a large amount of hygroscopic material. In clouds formed in polluted air the drop size spectrum is the most narrow, while it is the broadest in maritime clouds. Also in agreement with our previous discussion the modal radius of cloud droplets is larger and the droplet concentration is lower in maritime clouds than in continental cases.

The calculations of LEE *et al.* (1980) also indicate that the spectrum of cloud droplets has a double mode, as is observed in a large number of clouds (see e.g. ELDRIDGE, 1957). The concentration of large droplets with $r > 20$ μm at a level of 3000 m above the cloud base is higher than 1 l^{-1} in maritime clouds and in clouds formed under polluted conditions during wintertime. This is a very important result from the point of view of precipitation formation as discussed in the next subsection.

3.5.3 CCN and precipitation formation

The observations carried out in different clouds at different altitudes indicate that the typical concentration of water droplets varies around from 100 to 1000 cm^{-3}, while their radius lies generally between 5 and 20 μm. On the other hand, the number of raindrops with sizes exceeding. 0.1 mm is lower by several orders of magnitude than the above value. The falling velocity of the larger drops is sufficient to reach the ground level even if the updraft is important. It is believed at present (for further details see textbooks on cloud physics: FLETCHER, 1962; MASON, 1971; PRUPPACHER and KLETT, 1980) that two microphysical mechanisms are responsible for this phenomenon: the ice crystal mechanism (discussed in Chapter 4) and the coalescence of cloud elements of different sizes.

In the case of coalescence, cloud droplets of different falling velocities collide to form larger drops. During their fall larger drops "overtake" smaller ones and even though air flows around the falling drop, the smaller droplets are impacted against the drops due to their inertia.

Let us suppose that a cloud consists of large drops with radius R and small drops with radius r. If r is much smaller than R, the large drop will grow

[1] Accordingly, they modified the thermodynamic equations elaborated for a given substance.

according to the following equation (see Appendix II, Part B):

$$\frac{dR}{dt} = \frac{E(V-v)}{4\varrho_2} w \tag{3.11}$$

where t is the time, V and v are the falling velocity of the large and small drops, respectively, ϱ_2 is the density of water, w is the liquid water content of the cloud, while E is the collection efficiency defined in Appendix II.

It follows from Eq. (3.11) that the growth of large drops is fast if the difference between the falling velocities of the two drops is large, the liquid water content in the cloud is high and the value of the collection efficiency is significant.

The collection efficiency as a function of R and r was first determined by LANGMUIR (1948) and consequently by HOCKING (1959). These calculations show that the value of E is zero if R is less than about 20 μm. More recent studies (see MASON, 1971) gave non-zero values for the size range of $R < 20$ μm. However, they also indicated very low figures. This means that even now it is believed that the formation of droplets larger than about 20 μm in radius is a necessary condition for the initiation of coalescence, and consequently for the release of precipitation in water clouds[1]. Thus, the study of the formation of such large droplets is of crucial importance and since the formation process is related to the characteristics of CCN, this subsection is devoted to a brief discussion of this problem.

WOODCOCK (1952) was probably the first who proposed that large cloud droplets form on giant sea salt nuclei. He observed the concentration and size distribution of giant hygroscopic particles ($m > 10^{-12}$g) of maritime origin over Miami, Florida (USA). By also measuring the chloride content of rain as a function of precipitation intensity, WOODCOCK calculated the water quantity necessary for the nuclei to become drops with the same chloride concentration as the value observed. Since in this way he obtained drop size distributions similar to the raindrop spectra observed by MARSHALL and PALMER (1948), he concluded that each sea salt nucleus grows to raindrop size through coalescence with smaller, more numerous droplets formed on non-saline particles. This theory was forwarded by WOODCOCK and BLANCHARD (1955) who determined over Hawaii that the mass of giant chloride particles in unit volume of air is equal to the chloride content of raindrops found in the same volume. The numerical calculations of MASON and GHOSH (1957) also seemed to support the WOODCOCK hypothesis. According to the results of their calculations the presence of droplets (100 droplets per liter) with radii exceeding 30 μm in small cumulus clouds in maritime environment can be explained by giant hygroscopic nuclei ($m > 10^{-11}$ g) provided that the clouds last at least one hour.

[1] Water clouds are frequently termed "warm clouds". This means that all parts of the clouds are warmer than 0 °C. In other words: there are no ice crystals in them and their microphysical processes are determined by condensation and coalescence. This does not mean, however, that coalescence cannot be important in clouds containing ice phase as well.

Another explanation for the formation of large cloud droplets was published by SQUIRES (1952). By studying the condensation phase of the droplet growth he concluded that the size of CCN is not a determining factor in the process. CCN size determines only whether at a given maximum supersaturation a nucleus becomes a cloud droplet or remains a stable solution droplet. The SQUIRES' theory is very attractive since it explains the difference in precipitation-forming ability of oceanic and continental clouds without the necessity of the presence of special giant nuclei. To explain this issue in further detail, typical parameters of maritime and continental clouds are given in Table 3.6.

It can be seen that the updraft speeds and the liquid water contents are equal in the two types of clouds. However, droplet concentrations and average droplet sizes are rather different due to the differences in the number of CCN. Droplets with a radius of 30 μm, the concentration of which is 1 l^{-1}, grow by coalescence into drops of 0.55 mm during 40 minutes before falling out from a maritime cloud of 1000 m depth. The corresponding time for a continental cloud is three times longer; during which time the cloud reaches 3800 m depth, while droplets with a radius of 19 μm, having a concentration of 1 l^{-1}, grow to a size of 0.9 mm (the larger size is explained by the longer time for coalescence). Under maritime conditions, a droplet of 40 μm becomes a raindrop of 0.45 mm during 30 minutes by rising 600 m in the cloud. In contrast, in a continental cloud a droplet of 40 μm reaches a size of 0.40 mm during a time period of 65 minutes. Moreover, a much deeper cloud is necessary for this growth. Thus, we can conclude that the probability of precipitation formation in continental and maritime clouds is rather different.

It should also be noted that WOODCOCK's theory was also criticized by

Table 3.6

Formation of precipitation (see the text) in typical maritime and continental clouds (FLETCHER, 1962). (By courtesy of Cambridge University Press and the author)

		Maritime	Continental
Updraft speed		100 cm s^{-1}	100 cm s^{-1}
Liquid water content		1 g m^{-3}	1 g m^{-3}
Supersaturation		0.2%	0.2%
Drop concentration		50 cm^{-3}	200 cm^{-3}
Mean drop radius		17 μm	11 μm
Radius of drops with a concentration of 1/l		30 μm	19 μm
1/liter	Final radius	0.55 mm	0.9 mm
	Time	40 min	120 min
	Height	1000 m	3800 m
30 μm	Final radius	0.55 mm	0.55 mm
	Time	40 min	85 min
	Height	1000 m	2400 m
40 μm	Final radius	0.45 mm	0.40 mm
	Time	30 min	65 min
	Height	600 m	1400 m

WOODCOCK himself. In a more recent study WOODCOCK and his associates (WOODCOCK *et al.*, 1971) determined the ratio of iodine to chlorine both in sea salt particles and in raindrops of different sizes in marine air of Hawaii. They found that in sea salt particles the I/Cl ratio varies as a function of particle size, whereas in raindrops the ratio is constant and independent of drop size. This constant ratio is equal to 2×10^{-3} which corresponds to smaller ($10^{-12} < m < 10^{-8}$ g) salt nuclei. On the basis of these data they rejected the idea according to which each raindrop forms on a giant sea salt nucleus under maritime conditions.

The possible role of giant salt nuclei in rain formation was also studied by numerical modeling. Thus, TAKAHASHI (1976) reports that giant salt nuclei are important only for the chemical balance during cloud formation. This conclusion is based on his result indicating that the salt content of rainwater determined by calculating the removal of sea salt nuclei in the air is in good agreement with observations. At the same time these giant nuclei are unimportant for rain initiation in warm clouds. TAKAHASHI (1976) also concluded that cloud droplet concentration, determined by the number of CCN, is the critical factor in initiating rain because of the inverse relationship between the number of CCN and cloud droplet size. Practically similar results were obtained by HINDMAN *et al.* (1977c) who measured the parameters of CCN beneath non-raining water clouds in Washington State (USA) and on the basis of these data they calculated theoretically the cloud droplet size distributions by applying the theory outlined above. Their size distributions calculated were found to be in a good agreement with the droplet spectra observed in clouds. HINDMAN and his co-workers found that high concentrations of large ($0.1 \leq r \leq 1.0$ μm) and giant ($r \geqq 1$ μm) nuclei result in droplet size distributions containing large droplets only if the concentration of small, Aitken-sized nuclei ($0.03 \leq r \leq 0.1$ μm) is low (e.g. under maritime conditions). If the concentration of small CCN is high, the cloud droplet size distribution does not contain large droplets even if the number of giant nuclei is significant.

Finally, we note that over the continents the concentration of giant sea salt nuclei is generally much lower then over the oceans (see e.g. MÉSZÁROS, 1963). However, under continental conditions giant particles as large as 100 μm can be found in relatively high concentrations (see e.g. JAENICKE and JUNGE, 1967). As we discussed in Chapter 2, these giant insoluble particles are of soil origin. On the basis of this information, JOHNSON (1982) assumes that particles larger than about 20 μm can initiate coalescence growth independently of their solubility and surface properties. He carried out a series of numerical calculations showing that these particles can produce a tail of large drops in droplet size distributions which is an important factor from the point of view of precipitation formation by coalescence. JOHNSON also states that "high droplet concentrations do not preclude precipitation development". Since this statement is in a disagreement with our previous discussion we can conclude that further research is needed to elucidate the relationship between CCN and precipitation formation.

3.5.4 Modification of clouds by artificial CCN

It follows from the above discussion that man can modify the evolution of clouds and precipitation by releasing into the atmosphere either giant hygroscopic nuclei or aerosol particles in general. These modifications can be divided into two categories:

1) Deliberate weather modification experiments carried out by the introduction of giant nuclei into clouds to provoke the release of more precipitation from warm clouds[1];
2) Inadvertent cloud modification due to emission of different air pollutants.

The aim of this subsection is to summarize our present knowledge on these two kinds of modification processes. Here we will deal only with warm clouds. The principles of the artificial stimulation of precipitation from supercooled clouds are given in the next chapter. The possible climatic effects of particulate pollution are discussed in Chapter 5.

The experiments to modify warm clouds by means of giant hygroscopic nuclei was begun in the fifties by using ground-based particle generators (e.g. FOURNIER D'ALBE *et al.*, 1955). This technique became wide-spread in India to increase rainfall during the monsoon months (ROY *et al.*, 1961). The results gained during 18 experiment-seasons were published by BISWAS *et al.* (1967). These experiments were carried out by releasing particles of common salt with dry radius of 7–10 μm into the air. Water was added to the salt to produce solution droplets wich are in equilibrium with the vapor phase at a relative humidity of 95%. The production rate was equal to 10^9 particles per second. In a generator of other type, common salt was mixed with soapstone in a ratio of 9 : 1 to emit dry particles of radius 5 μm at a rate of 2500 g/min. The experiments were made in a randomized way near Delhi, Agra and Jaipur. The precipitation quantity over the experimental territories was compared to that observed in upwind control areas which are climatologically similar to experimental ones. Statistical analysis of the data showed that the rainfall amount increased by 41.6%, 58.5% and 18.6% over Delhi, Agra and Jaipur, respectively.

These excellent results were criticized on both physical and statistical bases. WARNER (1973b) noted that, among other things, the natural concentrations of giant hygroscopic particles were similar to those produced artificially even if each salt particle generated at the ground level would have entered the clouds, which seems to be very unprobable. On the other hand, SIMPSON and DENNIS (1972) believe that the positive results were probably obtained because of the fluctuation of precipitation amount over the control areas. In spite of this criticism, work in this direction has continued in India. RAMACHANDRA MURTY (private communication) reported that under suitable conditions 1000–1500 kg

[1] Similar experiments can be made by using water drops. However, the discussion of this type of cloud seeding is not in the frame of this book. We also do not deal with the experiments made in warm fogs to improve the visibility.

of salt in dispersed by aircraft in the form of particles with a size of 10 μm over an area of 40×40 km^2. A similar area serves as control area. Several cloud-physical and chemical parameters are measured. The distribution of precipitation is also carefully observed. It is found that cloud droplet distribution, electric field intensity in the clouds and cloud chemistry are modified by the seeding. According to the results of different evaluation procedures it is estimated that the rainfall is increased by 17–32%. A detailed analysis of Indian data by an independent scientific group would appear to be very useful in order to evaluate these results.

Similar experiments were carried out in South Dakota (USA) by BISWAS and DENNIS (1971). A line of stratocumulus cloud formed in a polar air mass was seeded, in contrast to the experiments in India where tropical clouds were modified. The preliminary numerical calculations of BISWAS and DENNIS demonstrated that cloud seeding by giant hygroscopic nuclei can be efficient only if the updraft speed is strong enough to make the LANGMUIR (1948) chain reaction[1] possible.

The operation of South Dakota was carried out on 23 July 1970 under stratocumulus clouds whose growth was limited by an inversion layer. The updraft speed was found to be about 3 m s^{-1}. 150 kg of salt of different sizes ($r > 5$ μm) was released. During the operation (13 minutes after seeding started) radar echos appeared demonstrating that drops of raindrop size were created[2]. Taking into account the results of their numerical calculations BISWAS and DENNIS (1971) stated on the basis of this result that the LANGMUIR chain reaction can be initiated by artificial hygroscopic nuclei of proper sizes. The paper of BISWAS and DENNIS (1971) was criticized by several authors. BLANCHARD (1972) remarked that it is very improbable that the artificial salt nuclei grew into raindrop size in a cloud of 3 km depth. To solve at least partially this problem subsequent numerical simulations were performed. The calculations of FARLEY and CHEN (1975) show that, in agreement with BISWAS and DENNIS (1971), without the LANGMUIR-type chain reaction salt seeding essentially does not influence the precipitation formation. Their study also indicates that the dynamics of clouds is very important in this respect. Thus, updraft speeds greater than 10 m s^{-1} are needed for the efficiency of drop breakup. This conclusion makes the results of BISWAS and DENNIS very questionable.

It should also be mentioned that cloud seeding by giant hygroscopic particles can also modify atmospheric dynamic processes due to the latent heat released by vapor condensation on nuclei. This idea was first proposed by WOODCOCK

[1] Due to the coalescence process large drops ($r > 5$ mm) form in the cloud e.g. on giant nuclei present. Because of hydrodynamic instability they break up to create more raindrop embryos.

[2] The echo intensity on the radar screen is proportional to the following expression

$$\frac{1}{\lambda^4} \sum N d^6$$

where λ is the wavelength used ($\lambda \gg d$), d is the diameter of drops, while N is their concentration. By using wavelengths with a magnitude of cm only the raindrops can be detected.

et al. (1963) and later confirmed by the same author and his associate (WOODCOCK and SPENCER, 1967). In this later study salt particles of 0.25–10 μm dry radius were dispersed by aircraft generators at a level of 400–500 m above the sea surface (Hawaii). The concentration of the salt was 40 mg kg^{-1} in the air. According to the results of 41 experiments, in the salt-laden air the temperature was found to be higher by 0.35 °C than in the environment. On the basis of this result WOODCOCK and SPENCER assumed that in this way artificial clouds can be created under some circumstances. However, this assumption has never been proved experimentally. Moreover, RAMACHANDRA MURTY *et al.* (1975) observed in warm cumulus clouds subjected to cloud seeding over India that the temperature rise was 1–2 °C and the liquid water content increased by 20% relative to unseeded clouds. They also found that the top of seeded clouds was higher by 60% than that of unseeded clouds.

On the basis of this discussion[1] we can conclude that, the possibility of the modification of warm clouds to produce rain has not been scientifically proved. However, as a report of the World Meteorological Organization states (WMO, 1984) "...this subject has not had the benefit of large-scale research programmes and very few warm cloud modification projects have been conducted using modern methods including in-cloud measurement capability and radar techniques. Accordingly, it is unwise to abandon this subject. Rather a wiser course would be to encourage scientifically designed, executed and evaluated studies (both theoretical and field) in order to base judgements on a much firmer foundation".

As we noted at the beginning of this discussion man can inadvertently modify cloud formation by emitting into the air aerosol particles and gaseous components which may be converted in the air into particulates. In this respects two types of particulate pollutants are of interest. First, large hygroscopic nuclei can result in an increase of precipitation amount. Second, fine water-soluble particles in high concentrations may increase the stability of clouds and result in decrease of precipitation[2].

Concerning the possible inadvertent effects of human activities on the formation of precipitation we begin our discussion by mentioning the famous paper published by CHANGNON (1968). In this paper he reported that during the time period between 1951 and 1965 in downwind of La Porte (near Chicago), a large industrial complex (mainly steelworks), the precipitation amount was higher by 31% than at stations which were not influenced by human activities. The publication of this result, called the La Porte anomaly, initiated a lively scientific debate including the nature of the particles (ice nuclei or CCN, see OGDEN, 1969) which might cause the anomaly. To gain further insight into the problem, a climatological study of precipitation records was made at different places. This

[1] For further details the interested reader is referred to the review of COTTON (1982) and its references.

[2] Clouds can also be altered by human activities by releasing ice-forming nuclei into the air (see the next chapter).

research revealed (see CHANGNON *et al.*, 1976) that in the six largest cities in USA the precipitation amount increased by 10–30% during the time period between 1901 and 1970 in and downwind of urban locales. Following this study a program entitled *Metro*politan *M*eteorological *Ex*periment (METROMEX) was organized in the St. Louis area with sophisticated instrumentation for obtaining information on the physical causes of the phenomenon.

The results of METROMEX show that for 1971–1974 the summertime downwind rainfall was significantly higher than that observed in upwind areas. In their paper discussing the METROMEX results CHANGNON *et al.* (1976) mention three causes for this precipitation increase. The first cause is thermal (heat release), while the second is mechanical in nature, so that confluence zones are created where cloud formation is enhanced. The third reason, the most important for the scope of this book, is the enhancement of the coalescence process owing to giant hygroscopic nuclei emitted by urban sources. The authors assumed that the observed lower altitudes of first radar echos in clouds are caused by raindrops formed on artificial giant nuclei. However, the model calculations of OCHS and SEMONIN (1979) do not support this conclusion. According to these calculations the appearance of the first radar echos in downwind clouds over St. Louis could not be created by giant nuclei or by variations in their chemical composition. Further, in agreement with observations (FITZGERALD and SPYERS-DURAN, 1973; BRAHAM, 1974), calculations indicate higher droplet concentration over St. Louis urban–industrial complex than in upwind clouds which tend to stabilize cloud systems. On the basis of their results OCHS and SEMONIN (1979) conclude that differences in cloud parameters between upwind and downwind clouds over St. Louis are explained first of all by dynamic processes caused by heat release.

HOBBS *et al.* (1970) also published a description of a case of precipitation increase which was attributed to artificial nuclei. They compared precipitation data gained in Washington State (USA) during 1929–1946 with those obtained between 1947 and 1966. In the second time period the precipitation amount was found to be higher by 30% than for the first interval. Taking into account the circulation patterns, HOBBS and his associates assumed that this increase is due to the emission of giant hygroscopic particles by paper mills. The emission of such particles are proved by observations. Thus, airborne measurements of HINDMAN *et al.* (1977a) showed that the concentration of large and giant CCN (see also Subsection 3.3.4) was higher in the plume of a paper mill than in the background air, while the number of Aitken-sized cloud condensation nuclei was similar to that in uninfluenced air. Accordingly, the concentration of the droplets with radii larger than 15 μm was also higher in clouds formed in the plume. However, again, calculations based on warm cumulus and stratus cloud models did not support the concept that changes in rainfall were caused by large and giant CCN alone (HINDMAN *et al.*, 1977b). Thus, HINDMAN and his coworkers concluded that "the heat and moisture emitted by the mill, in combination with the CCN, may have been responsible for the increased rainfall".

A reduction of precipitation associated with the increase of the concentration

of CCN was reported by WARNER (1968b). By using precipitation data obtained in eastern Australia he demonstrated that rainfall amounts decreased during years when sugar cane production increased (see also Subsection 3.3.4). This reduction, revealed by rainfall measurements carried out in the harvesting season, was not detected over a control area. WARNER's concept was checked independently by WOODCOCK and JONES (1970) by analyzing precipitation records from Hawaii in a similar manner. No significant difference was detected between influenced and control areas which makes WARNER's conclusions doubtful.

Very few studies have been performed to examine the possible effects of artificial CCN on precipitation formation over a larger area. MÉSZÁROS and VÁRHELYI (1982) estimated the mass ratio of sulfate particles of natural origin to the mass of sulfate particles due to human activities. On the basis of their European sulfur budget calculations they found that only 20% of the sulfate particles, giving a major part of CCN (see Section 3.4), is of natural origin[1]. This result implies that the number of CCN over Europe is practically five times more at present than before the industrial revolution. Taking into account an analysis of long-term European precipitation records (KOFLANOVITS, 1974) MÉSZÁROS and VÁRHELYI assume that the variation in the amount of precipitation for a period between 1871 and 1970 can be neglected as compared to the change of the mass (number) of CCN from sulfate. It should be noted, however, that this conclusion needs further support because of the difficulties involved in sulfur budget calculations.

We can conclude that while inadvertent anthropogenic effects on cloud microstructure have been revealed by some studies, the modification of precipitation amount by particulate pollutants has never been demonstrated in a rigorous manner. This conclusion is true in particular if we speak about the precipitation regime over a large area like a continent. We do not want to exclude the possibility, however, that artificial nuclei have influenced the rainfall on a local scale in interaction with other effects of human activities (e.g. heat and moisture release). Taking into account that the pollution level of the atmosphere including aerosol particles will probably increase in the future over certain parts of the world, this question has to be answered by the scientific community on a more solid basis.

Finally, we note that aerosol particles of anthropogenic origin can also modify the radiation properties of a cloud, as discussed in Chapter 5. Here we only mention that this effect is probably more important from the point of view of weather and climate modifications than the changes in precipitation.

[1] Note that this result is not consistent with that of SQUIRES (1966) discussed in Subsection 3.3.4. The reason for this discrepancy remains an open question.

References

ALOFS, D. J. and LIN, T. H., 1981: Atmospheric measurements of CCN in the supersaturation range 0.013–0.681. *J. Atmos. Sci.*, **38,** 2772–2778.

AUER, A. H., 1975: The production of cloud and Aitken nuclei by the St. Louis metropolitan area (Project METROMEX). *J. Rech. Atmos.*, **9,** 11–22.

BÓNIS, K., KOFLANOVITS, E., MÉSZÁROS, A. and MÉSZÁROS, E., 1977: A felhőképződés kezdeti szakaszának numerikus modellezése. *Időjárás,* **81,** 1–10.

BATTAN, L. J. and REITAN, C. H., 1957: Droplet size measurements in convective clouds. In *Artificial Stimulation of Rain* (eds: H. Weickmann and W. Smith). Pergamon Press, New York. 184.

BAKER, M. B., CORBIN, R. G. and LATHAM, J., 1980: The influence of entrainment on the evolution of cloud droplet spectra: I. A model of inhomogeneous mixing. *Quart. J. Roy. Meteor. Soc.*, **106,** 581–598.

BISWAS, K. R. and DENNIS, A. S., 1971: Formation of rain shower by salt seeding. *J. Appl. Meteor.*, **10,** 780–784.

BISWAS, K. R., KAPOOR, R. K. and KANUGA, K. K. 1967: Cloud seeding experiment using common salt. *J. Appl. Meteor.*, **6,** 914–923.

BLANCHARD, D. C., 1972: Comments on "Formation of shower by salt seeding". *J. Appl. Meteor.*, **11,** 556–557.

BRAHAM, R. R. Jr., 1974: Cloud physics of urban weather modification: A preliminary report. *Bull. Amer. Meteor. Soc.*, **55,** 100–105.

CHANGNON, S. A. Jr., 1968: The La Porte weather anomaly—fact or fiction. *Bull. Amer. Meteor. Soc.*, **49,** 4–11.

CHANGNON, S. A. Jr., SEMONIN, R. G. and HUFF, F. A., 1976: A hypothesis of urban rainfall anomalies. *J. Appl. Meteor.*, **15,** 544–560.

CHARLSON, R. J., LOVELOCK, J. E., ANDREAE, M. O. and WARREN, S. G., 1987: Oceanic phytoplankton, atmospheric sulfur, cloud albedo and climate. *Nature,* **326,** 655–661.

Clark, A. D., AHLQUIST, N. C. and COVERT, D. S., 1987: The Pacific marine aerosol: evidence for natural acid sulfates. *J. Geophys. Res.*, **92,** 4179–4190.

COTTON, W. R., 1982: Modification of precipitation from warm clouds — a review. *Bull. Amer. Meteor. Soc.*, **63,** 146–159.

DÉSALMAND, F., BAUDET, J. and SERPOLAY, R., 1982: Influence of rainfall on the seasonal variations of cloud condensation nuclei concentrations in a subequatorial climate. *J. Atmos Sci.*, **39,** 2076–2082.

DINGER, J. E., HOWELL, H. B. and WOJCIECHOWSKI, T. A., 1970: On the source and composition of cloud nuclei in a subsident air mass over the North Atlantic. *J. Atmos. Sci.*, **27,** 791–797.

DUFOUR, L. and DEFAY, R., 1963: *Thermodynamics of Clouds.* Academic Press, New York.

ELDRIDGE, R. G., 1957: Measurement of cloud drop size distributions. *J. Meteor.*, **14,** 55–59.

FARLEY, R. C. and CHEN, C. S., 1975: A detailed microphysical simulation of hygroscopic seeding on the warm rain process. *J. Appl. Meteor.*, **14,** 718–733.

FITZGERALD, J. W., 1973: Dependence of supersaturation spectrum of CCN on aerosol size distribution and composition. *J. Atmos. Sci.*, **30,** 628–634.

FITZGERALD, J. W., 1974: Effect of aerosol composition on cloud droplet size distribution: A numerical study. *J. Atmos. Sci.*, **31,** 1358–1367.

FITZGERALD, J. W. and HOPPEL, W. A., 1982: Measurements of the relationship between the dry size and critical supersaturation of natural aerosol particles. *Időjárás,* **86,** 242–248.

FITZGERALD, J. W. and SPYERS-DURAN, P. A., 1973: Changes in cloud nucleus concentration and cloud droplet size associated with pollution from St. Louis. *J. Appl. Meteor.*, **12,** 511–516.

FLETCHER, N. H., 1962: *The Physics of Rainclouds.* University Press, Cambridge.

FOURNIER D'ALBE, E. M., LATEEF, A. M. A., RASOOL, S. I. and ZAIDI, I. H., 1955: The cloud-seeding trials in the central Punjab, July–Sept. 1954. *Quart. J. Roy. Meteor. Soc.*, **18,** 574–581.

FUKUTA, N. and SAXENA, V. K., 1979: The principle of a new horizontal thermal gradient cloud condensation nucleus spectrometer. *J. Rech. Atmos.*, **13,** 169–188.

GARCIA, J. A., PEREZ, P. J., FERNANDEZ, J. F., GAYA, M., DE GRADO, J. R. and SERPOLAY, R., 1981: Analyse statistique des résultats d'une campagne de mesures de noyaux de condensation nuageuse. *J. Rech. Atmos.*, **15,** 143–148.

GERBER, H., 1982: Nature of fog nuclei from measurements of relative humidity. *Időjárás*, **86**, 175–178.

HIDY, G. M., BLECK, R., BLIFFORD, I. H., BROWN, P. M., LANGER, G., LODGE, J. P., ROSINSKY, J. and SHEDLOVSKY, J. P. 1970: *Observations of aerosols over Northeastern Colorado*. NCAR Technical Notes 49, Boulder.

HINDMAN, E. E. and SINCLAIR, P. C., 1982: Airborne measurements of cloud condensation nuclei active at a supersaturation $\leq 0.15\%$. *Időjárás*, **86**, 200–208.

HINDMAN, E. E., HOBBS, P. V., RADKE, L. F., 1977a: Cloud condensation nuclei from a paper mill. Part I: Measured effects on clouds. *J. Appl. Meteor.*, **16**, 745–752.

HINDMAN, E. E., TAG, P. M., SILVERMAN, B. A., HOBBS, P. V., 1977b: Cloud condensation nuclei from a paper mill. Part II: Calculated effects on rainfall. *J. Appl. Meteor.*, **16**, 753–755.

HINDMAN, E. E., HOBBS, P. V. and RADKE, L. F., 1977c: Cloud condensation nuclei and their effects on cloud droplet size distributions. *J. Atmos. Sci.*, **34**, 951–956.

HOBBS, P. V., RADKE, L. F. and SHUMWAY, S. E., 1970: Cloud condensation nuclei from industrial sources and their apparent influence on precipitation in Washington State. *J. Atmos. Sci.*, **27**, 81–89.

HOBBS, P. V., SMITH, J. L. and RADKE, L. F., 1980: Cloud-active nuclei from coal-fired electric power plants and their interactions with clouds. *J. Appl. Meteor.*, **19**, 439–451.

HOCKING, L. M., 1959: The collision efficiency of small drops. *Quart. J. Roy Meteor. Soc.*, **85**, 44–50.

HOLL, W. and MÜHLEISEN, R. A., 1955: A new condensation nuclei counter with continuous oversaturation. *Geofis. Pura Appl.*, **31**, 21–25.

HOPPEL, W. A., DINGER, J. E. and RUSKIN, R. E., 1973: Vertical profiles of CCN at various geographical locations. *J. Atmos. Sci.*, **30**, 1410–1420.

HOWELL, W. E., 1949: The growth of cloud drops in uniformly cooled air. *J. Meteor.*, **6**, 134–149.

HUDSON, J. G., 1980: Relationship between fog condensation nuclei and fog microstructure. *J. Atmos. Sci.*, **37**, 1854–1867.

HUDSON, J. G., 1984. Cloud condensation nuclei measurements within clouds. *J. Clim. Appl. Meteor.*, **23**, 42–51.

HUDSON, J. G. and SQUIRES, P., 1976: An improved continuous flow diffusion chamber. *J. Appl. Meteor.*, **15**, 776–782.

HUDSON, J. G., ROGERS, C. F. and KOCMOND, W. C., 1982: Measurements with an instantaneous CCN spectrometer. *Időjárás*, **86**, 209–216.

JAENICKE, R., 1978: The role of organic material in atmospheric aerosols. *Pure Appl. Geophys.*, **116**, 283–292.

JAENICKE, R. and JUNGE, C. E., 1967: Studien für oberen Grenzgrösse des natürlichen Aerosoles. *Beitr. Phys. Atmos.*, **40**, 129–143.

JIUSTO, J. E.; 1967: Aerosol and cloud microphysics measurements in Hawaii. *Tellus*, **19**, 359–368.

JIUSTO, J. E. and KOCMOND, W. C., 1968: Note on cloud nucleus measurements in Lannemezan, France. *J. Rech. Atmos.*, **3**, (2^{e} année), 101–104.

JOHNSON, D. B., 1982: The role of giant and ultragiant aerosol particles in warm rain initiation. *J. Atmos. Sci.*, **39**, 448–460.

JUNGE, C. E. 1963: *Air Chemistry and Radioactivity*. Academic Press, New York.

JUNGE, C. E. and MCLAREN, E., 1971: Relationship of cloud nuclei spectra to aerosol size distribution and composition. *J. Atmos. Sci.*, **28**, 382–390.

KHEMANI, L. T., 1985. *Characteristics of Atmospheric Gaseous and Particulate Pollutants and Their Influence on Cloud Microphysics and Rain-Formation*. Doctor thesis. University of Poona, India.

KOCMOND, W. C. and MACK, E. J., 1972: The vertical distribution of cloud and Aitken nuclei downwind of urban pollution sources. *J. Appl. Meteor.*, **11**, 141–148.

KOCMOND, W. C., ROGERS, C. F., KATZ, U., HUDSON, J. G. and JIUSTO, J. E. 1982: The 1980 International Cloud Condensation Nuclei Workshop. *Időjárás*, **86**, 160–168.

KOFLANOVITS, E., 1974: Hosszú csapadéksorok trendjének elemzése Európa területén. *Időjárás*, **78**, 88–96.

KÖHLER, H., 1926: Zur Thermodynamik der Kondensation an hygroskopischen Kernen und Bemerkungen über das Zusammenfliessen der Tropfen. *Meddn St. met.-Hydrogr. Anst.*, **3**, No. 8.

KÖHLER, H., 1936: The nucleus in and the growth of hygroscopic droplets. *Trans. Faraday Soc.*, **32,** 1152.

KÖHLER, H., 1950: On the problem of condensation in the atmosphere. *Nova Acta Reg. Soc. Sci. Upsaliensis.* Ser. IV., **14,** No. 9.

KORNFELD, P., 1970: Numerical solution for condensation of atmospheric vapor on soluble and insoluble nuclei. *J. Atmos. Sci.*, **27,** 256–264.

KRASTANOV, L. and MILOSHEV, G., 1963: On the mechanism of condensation process in the atmosphere. *J. Rech. Atmos.*, **1,** 165–172.

LAKTIONOV, A. G., 1968: Photoelectric measurements of condensation cloud nuclei. *J. Rech Atmos.*, **3** (2e année), 63–72.

LAKTIONOV, A. G., 1972: Isothermal method of the determination of the concentration of cloud condensation nuclei (in Russian). *Fiz. Atmos. Okeana,* **8,** 672–677.

LAKTIONOV, A. G. 1975: Spectra of cloud condensation nuclei in the supersaturation range 0.02–1%. *Proc. VIII. International Conference on Nucleation.* Gidrometeoizdat, Moscow, 437–444.

LANGMUIR, I., 1948: The production of rain by a chain reaction in cumulus clouds at temperatures above freezing. *J. Meteor.*, **5,** 175–192.

LANGSDORF A., 1936: A continuously sensitive cloud chamber. *Phys. Rev.*, **49,** 422.

LEAITCH, W. R., STRAPP, J. W., ISAAC, G. A. and HUDSON, J. G., 1986: Cloud droplet nucleation and cloud scavenging of aerosol sulphate in polluted atmospheres. *Tellus,* **38** B, 328–344.

LEE, J. Y. and PRUPPACHER, H. R., 1977: A comparative study on the growth of cloud drops by condensation using an air parcel model with and without entrainment. *Pure Appl. Geophys.*, **115,** 523–545.

LEE, I. J., HÄNEL, G. and PRUPPACHER, H. R., 1980: A numerical determination of the evolution of cloud drop spectra due to condensation on natural aerosol particles. *J. Atmos. Sci.*, **37,** 1839–1853.

LEVKOV, L., 1970: On the formation of liquid embryos upon mixed nuclei. *Comptes rendus de l'Académie Bulgare des Sciences,* **23,** 671–673.

LOW, R. D. H., 1975: Microphysical and meteorological measurements of fog supersaturation. *Tellus,* **27,** 507–513.

MANTON, M. J., 1979: On the broadening of a droplet distribution by turbulence near cloud base. *Quart. J. Roy. Meteor. Soc.*, **105,** 899–914.

MARSHALL, J. S. and PALMER, W. McK., 1948: The distribution of raindrops with size. *J. Meteor.*, **5,** 165–166.

MASON, B. J., 1957: *The Physics of Clouds* (first edition). Clarendon Press, Oxford.

MASON, B. J., 1971: *The Physics of Clouds* (second edition). Clarendon Press, Oxford.

MASON, B. J. and CHIEN, C. W., 1962: Cloud droplet growth by condensation in cumulus. *Quart. J. Roy. Meteor. Soc.* **88,** 136–142.

MASON, B. J. and GHOSH, D. K., 1957: The formation of large droplets in small cumulus. *Quart. J. Roy. Meteor. Soc.*, **83,** 501–507.

MAZIN, I. P., 1980: Some theoretical problems of cloud condensation nuclei (in Russian). *Meteor. i Gidrol.* No. 8, 5–12.

MÉSZÁROS, A., 1969: Vertical profile of large and giant particles in the lower troposphere. *Proc. 7th Internat. Conf. on Condensation and Ice Nuclei.* Academia, Prague, 364–368.

MÉSZÁROS, A., 1984: The number concentration and size distribution of the soot particles in the 0.02–0.5 μm radius range at sites of different pollution levels. *Sci. Total Environ.*, **36,** 283–288.

MÉSZÁROS, A. and VISSY, K., 1974: Concentration, size distribution and chemical nature of atmospheric aerosol particles in remote oceanic areas. *J. Aerosol Sci.*, **5,** 101–109.

MÉSZÁROS, E., 1964: Répartition verticale de la concentration des particules de chlorures dans la basses couches de l'atmosphère. *J. Rech. Atmos.*, **1,** (2e année), 1–10.

MÉSZÁROS, E., 1968: On the size distribution of water soluble particles in the atmosphere. *Tellus,* **20,** 443–448.

MÉSZÁROS, E., 1969: On the thermodynamics of the condensation on water soluble and mixed nuclei. *Időjárás,* **73,** 1–11.

MÉSZÁROS, E. and VÁRHELYI, G. 1982: An evaluation of the possible effect of anthropogenic sulfate particles on the precipitation ability of clouds over Europe. *Időjárás,* **86,** 76–81.

MÉSZÁROS, E., MÉSZÁROS, A. and VISSY, K., 1975: Estimation of the size and nature of cloud nuclei from aerosol measurements carried out in pure maritime air. *Proc. VIII. Internat. Conf. on Nucleation.* Gidrometeoizdat, Moscow, 431–436.

MORDY, W., 1959: Computation of the growth by condensation of cloud droplets. *Tellus*, **11**, 16–44.

NEIBURGER, M. and CHIEN, C. W., 1960: Computations of the growth of cloud drops by condensation using an electronic digital computer. In *Physics of Precipitation* (ed. H. Weickmann) American Geophysical Union, Washington D.C., 191–210.

OCHS, H. T. and SEMONIN, R. G., 1979: Sensitivity of a cloud microphysical model to an urban environment. *J. Appl. Meteor.*, **18**, 1118–1129.

OGDEN, T. L., 1969: The effect on rainfall of a large steelworks. *J. Appl. Meteor.*, **8**, 585–591.

OKADA, K., ISHIZAKI, Y. and TAKEDA, T., 1986: Features and behavior of submicrometer aerosol particles in the urban atmosphere of Nagoya. *J. Meteor. Soc. of Japan*, **64**, 755–763.

ONO, A. and OHTANI, T., 1980: On the capability of atmospheric sulfate particles as cloud condensation nuclei. *J. Rech. Atmos.*, **14**, 235–240.

PRUPPACHER, H. R. and KLETT, J. D., 1980: *Microphysics of Clouds and Precipitation.* D. Reidel Publ. Co., Dordrecht.

PUESCHEL, R. F. and VAN VALIN, C. C., 1978: Cloud nucleus formation in a power plant plume. *Atmos. Environ.*, **12**, 307–312.

RADKE, L. F. and HOBBS, P. V., 1969: Measurement of cloud condensation nuclei, light scattering coefficient, sodium-containing particles, and Aitken nuclei in the Olympic Mountains of Washington. *J. Atmos. Sci.*, **26**, 281–288.

RADKE, L. F. and JIUSTO, J. E., 1981: Cloud condensation nucleus counters: a review. In *Atmospheric Aerosols and Nuclei* (eds A. F. Roddy and T. C. O'Connor). Galway University Press, Galway, 85–95.

RAMACHANDRA MURTY, A. S., SELVAM, M. and RAMANA MURTY, BH. V., 1975. Summary of observations indicating dynamic effect of salt seeding in warm cumulus clouds. *J. Appl. Meteor.*, **14**, 629–637.

RAU, W., 1955: Grösse und Häufigkeit der Chloridteilchen in kontinental Aerosol und ihre Beziehung zum Gefrierkerngehalt. *Meteor. Rundsch.*, **8**, 169–176.

ROY, A. K., RAMANA MURTY, BH. V., SRIVASTAVA, R. C. and KHEMANI, L. T., 1961: Cloud seeding trials at Delhi during monsoon months, July to Sept. (1957–1959). *Indian J. Meteor. Geophys.*, **12**, 401–412.

SAX, R. I. and HUDSON, J. G., 1981: Continentality of the South Florida summertime CCN aerosol. *J. Atmos. Sci.*, **38**, 1467–1479.

SAXENA, V. K. and FISHER, G. F., 1984: Water solubility of cloud-active aerosols. *Aerosol Sci. and Technology*, **3**, 335–344.

SAXENA, V. K. and FUKUTA, N., 1982: The supersaturation in fogs. *J. Rech. Atmos.*, **16**, 327–335.

SHAW, G. E., 1986: Cloud condensation nuclei associated with Arctic haze. *Atmos. Environ.*, **20**, 1453–1456.

SIMPSON, J. and DENNIS, A. S., 1972: *Cumulus Clouds and Their Modification.* NOAA Technical Memo., ERLOD–14, Washington, D.C.

SQUIRES, P., 1952: The growth of cloud drops by condensation. *Austral J. Sci. Res.*, **A5**, Part I: General characteristics: 59–86, Part II. The formation of large cloud drops: 473–499.

SQUIRES, P., 1958a: The microstructure and colloidal stability of warm clouds. I. The relation between structure and stability. *Tellus*, **10**, 256–261.

SQUIRES, P., 1958b: The microstucture and colloidal stability of warm clouds. II. The causes of variations in microstructure. *Tellus*, **10**, 262–271.

SQUIRES, P., 1966: An estimate of the anthropogenic production of cloud nuclei. *J. Rech. Atmos.*, **2** (2e année), 297–308.

SQUIRES, P. and TWOMEY, S., 1960: The relation between cloud droplet spectra and the spectrum of cloud nuclei. In *Physics of Precipitation* (ed.: H. Weickmann). American Geophysical Union, Washington, D.C., 211–219.

SQUIRES, P. and TWOMEY, S., 1966: A comparison of cloud nuclei measurements over North America and Caribbean Sea. *J. Atmos. Sci.*, **23**, 401–404.

TAKAHASHI, T., 1976: Warm rain, giant nuclei and chemical balance—a numerical model. *J. Atmos. Sci.*, **33**, 269–286.
TERLIUC, B. and GAGIN, A., 1971: Cloud condensation nuclei and their possible influence on precipitation. *J. Appl. Meteor.*, **10**, 474–481.
TWOMEY, S., 1959a: The nuclei of natural cloud formation. Part I: The chemical diffusion method and its application to atmospheric nuclei. *Geofis. Pura Appl.*, **43**, 227–242.
TWOMEY, S., 1959b: The nuclei of natural cloud formation. Part II: The supersaturation in natural clouds and the variation of cloud droplet concentration. *Geofis. Pura Appl.*, **43**, 243–249.
TWOMEY, S., 1959c: Experimental test of Volmer theory of heterogeneous nucleation. *J. Chem. Phys.*, **30**, 941.
TWOMEY, S., 1965: Size measurements of natural cloud nuclei. *J. Rech. Atmos.*, **2**, 113–119.
TWOMEY, S., 1968: On the composition of cloud nuclei in North-Eastern United States. *J. Rech. Atmos.*, **4**, 281–285.
TWOMEY, S., 1971: The composition of cloud nuclei. *J. Atmos. Sci.*, **28**, 377–381.
TWOMEY, S., 1972: Measurements of the size of natural cloud nuclei by means of Nuclepore filters. *J. Atmos. Sci.*, **29**, 318–321.
TWOMEY, S., 1977: *Atmospheric Aerosols*. Elsevier, Amsterdam.
TWOMEY, S. and WOJCIECHOWSKI, T. A., 1969: Observation of the geographical variation of cloud nuclei. *J. Atmos. Sci.*, **26**, 684–688.
VOLMER, M. 1939: *Kinetik der Phasenbildung*. Steinkopff, Dresden and Leipzig.
WARNER, J., 1968a: The supersaturation in natural clouds. *J. Rech. Atmos.*, **3** (2e année), 233–237.
WARNER, J., 1968b: A reduction in rainfall associated with smoke from sugar can-fires—An inadvertent weather modification? *J. Appl. Meteor.*, **7**, 247–251.
WARNER, J., 1973a: The microstructure of cumulus clouds. Part IV. The effect on the droplet spectrum of mixing between cloud and environment. *J. Atmos. Sci.*, **30**, 256–261.
WARNER, J., 1973b: Rainfall enhancement—A review. *Proc. WMO/IAMAP Sci. Conf. on Weather Modification*, Tashkent, 43–50.
WARNER, J. and TWOMEY, S., 1967: The production of cloud nuclei by cane fires and the effect on cloud droplet concentration. *J. Atmos. Sci.*, **24**, 704–706.
WHITBY, K. T., CANTRELL, B. K. and KITTELSON, D. B., 1978: Nuclei formation rate in a coal-fired power plant plume. *Atmos. Environ.*, **12**, 313–321.
WIELAND, W., 1955: Eine neue Methode des Kondensationskernzählung. *Eid. Kom. Stud. Hagenbildung, Hagelabwehr*. ETH Pub. No. 6, Zürich.
WMO, 1984: *Modification of Precipitation from Cumulus Clouds*. Precipitation Enhancement Project, Rep. No. 31, Geneva.
WOODCOCK, A. H., 1952: Atmospheric salt particles and raindrops. *J. Meteor.*, **9**, 200–212.
WOODCOCK, A. H. and BLANCHARD, D. C., 1955: Tests of the salt-nuclei hypothesis of rain formation. *Tellus*, **7**, 437–448.
WOODCOCK, A. H. and JONES, R. H., 1970: Rainfall trends in Hawaii. *J. Appl. Meteor.*, **9**, 690–696.
WOODCOCK, A. H. and SPENCER, A. T., 1967: Latent heat released experimentally by adding sodium chloride particles to the atmosphere. *J. Appl. Meteor.*, **6**, 95–101.
WOODCOCK, A. H., BLANCHARD, D. C. and ROTH, C. G. H., 1963: Salt-induced convection in clouds. *J. Atmos. Sci.*, **20**, 159–169.
WOODCOCK, A. H., DUCE, R. A. and MOYERS, J. L., 1971: Salt particles and raindrops in Hawaii. *J. Atmos. Sci.*, **28**, 1252–1257.

4. Nucleation of ice

4.1 Introduction

The existence of ice—the solid phase of water—is of unmeasurable importance for the world as we know it. The range of conditions under which ice is the stable phase of water (as determined by the properties of the substance) coincides with conditions found over large portions of the Earth's surface and in its atmosphere.

All three phases of water are in stable equilibrium at 0.000 °C and 101.32 kPa. The liquid–ice equilibrium condition changes very slowly with pressure, so slowly that it requires a pressure of 10^4 kPa to lower the melting point by 1 °C. In the atmosphere, the variation of the melting point is <0.01 °C, so it is neglected in practically all calculations. At temperatures below the melting point, the stable phases of water are the vapor and the solid, the equilibrium condition being defined by the vapor pressure of the solid. That vapor pressure decreases with decreasing temperatures in an exponential fashion: from 610.7 Pa at 0 °C, to 259.7 Pa at −10 °C, to 103.2 Pa at −20 °C, and so on (vapor pressure tables can be consulted for the full set of values). Hence, ice can stably exist (without evaporating) at any temperature at or below 0 °C, if the vapor pressure has the values indicated above. Of course, at higher vapor pressures the ice will be growing, and at lower ones it will be evaporating.

What makes the formation of ice an interesting and complex phenomenon is that both the vapor and the liquid phases can exist, metastably, at temperatures lower than 0 °C, and at vapor pressures equalling or exceeding the limits described in the preceding paragraph. The metastable phases—supercooled water and supersaturated vapor—are transformed into the stable phase, ice, following the nucleation of that stable phase. One therefore deals with the nucleation of freezing and the nucleation of deposition depending on whether the parent phase is the liquid or the vapor. This chapter will discuss the theory describing these phenomena, and the empirical evidence related to them, with emphasis on the role of atmospheric aerosol as freezing nuclei and as deposition nuclei (the term ice nuclei will also be used as a collective name for the two types of nuclei).

The role that ice nuclei play in the atmosphere is, potentially, very great, because of the importance of ice particles which might form on them. Perhaps most importantly, ice particles forming in supercooled clouds can rapidly develop into precipitation (snow, hail or, after melting, rain). Less directly

noticable, but of great significance for climate are the impacts ice clouds have on the radiation balance of the Earth–atmosphere system. Also, the development of ice in clouds influences the removal of trace substances from the atmosphere, thereby impacting the global cycles of those substances, including the fate of pollutants. In turn, changes in atmospheric aerosol numbers, or in composition, might influence ice formation in clouds. Many of these connections are not yet sufficiently well known. Ice processes in clouds are quite complex, so their study is not easily accomplished, and there are very large variabilities among different atmospheric situations. Furthermore, since ice formation in clouds can occur either from ice nuclei (primary mechanism), or from interactions between hydrometeors (secondary mechanism), the question of what role ice nuclei play in the atmosphere is only a subset of the questions associated with the role of ice particles in general.

One important way to examine the role of nucleation in the formation of ice particles is to compare the concentration of ice crystals in clouds with the concentration of ice nuclei. This is a difficult comparison to make; as far as present data allows a conclusion to be drawn, it appears that secondary processes are indeed involved in many clouds, but that there are numerous cloud types where the primary mechanism is not followed by a secondary one (cf. Section 4.5). For those cases, the impacts of ice particles on precipitation, radiation, chemistry, cloud electrification, etc., can be directly referred back to ice nuclei. In other cases, where secondary processes become important, the role of nuclei is less clear: the secondary ice generation might completely overwhelm whatever effects nuclei might have. Alternatively, it might be that the role of nuclei become amplified by the secondary process. Current thinking leans toward the former possibility, but this is more a guess at this point than scientific fact. It is clear, that a great deal of research is still required to elucidate the situation.

Mention should also be made of the use of artificial ice nuclei for the initiation of ice formation in clouds. "Cloud seeding" has been extensively studied and is widely practiced. There is little doubt that artificial nuclei can form ice particles in clouds. It is more difficult to ascertain what the evolution and impact of those ice particles will be within the overall cloud system. Artificial ice nuclei will be discussed in Section 4.6; the broader question of cloud modification is left to specialized texts on that subject.

4.2 Basic description of ice nucleation

Fundamentally, the nucleation of ice is similar to the nucleation of other phase transitions: embryos of the new phase form by the aggregation of molecules (into an ice lattice in this case), with the bulk energy of the embryo per unit volume being lower than for the parent phase, but with the creation of new interfaces requiring additional energy. The balance of these two energies favors the dissipation of the embryo when the embryo is small. Increased supercooling or supersaturation increases the average size of the embryo, and when random

fluctuations bring about the formation of a critical size embryo, the probability of growth becomes equal to the probability of dissipation. Beyond that size, growth becomes the more likely event, and growth becomes energetically favorable so that it will proceed at a very high rate, limited only by factors related to the transport of molecules to the growing interface and by the micro-scale heat balance at that interface.

The general pattern described above applies both to the homogeneous and to the heterogeneous nucleation of ice, and can be put into an analytical framework along the same lines as was done in Chapter 3 for condensation, and as is elaborated in Appendix I. However, there are some additional factors which have to be dealt with. Ice has two principal axes of symmetry, and therefore the surface energy and the bulk energy of the embryo depend on the specific shape of the embryo, and the embryos are often so small that the molecular interactions between it and the substrate have to be considered explicitly instead of using bulk properties. Further difficulties relate to the paucity of meaningful data on interface energies, especially for specific surface sites on substrates and for the very small embryo sizes involved.

The result of the added complexities is that theoretical formulations designed to deal with them often reach a stage of practical intractability. Observational difficulties are equally formidable, since the scale of the phenomenon is beyond the reach of available observational methods (techniques requiring high vacuum cannot be used). Consequently, agreement between theory and observation has been quite elusive in the field of ice nucleation, and neither theory, nor empirical data are sufficiently reliable for predicting ice nucleation behavior. This situation necessitates that a large amount of material be presented in the subsequent sections, providing the reader with a broad enough range of evidence for properly judging the relative importances of various facets of the available knowledge.

4.3 Homogeneous nucleation of ice

An examination of the homogeneous nucleation of ice can serve not only to study that phenomenon, which in itself is of substantial importance in the atmosphere, but also to illustrate how the difficulties mentioned in the preceding section can be dealt with. In the following, we will present a number of alternative treatments of the problem, then discuss the empirical evidence for the homogeneous freezing of water, and conclude with a brief discussion of the atmospheric contribution of the process.

The main characteristic of homogeneous nucleation is that the critical embryo of ice forms by spontaneous, random fluctuations in molecular arrangements. The phenomenon is thus intrinsically probabilistic, with the probability of occurrence depending on external variables like temperature and vapor pressure, and the size of the sample. It is also dependent, of course, on the nature of the molecular interactions in the parent phase and in the embryos. Since water is a substance with many surprising characteristics, especially at tem-

peratures below 0 °C (ANGELL, 1982), and since its structure in the condensed phases (liquid and solid) is not fully known, studies of the homogeneous nucleation of ice are often a combination of attempting to learn about the phase transition and about the characteristics of the material itself.

In principle it is possible, at temperatures below 0 °C, for ice to be nucleated homogeneously from either supersaturated vapor or from supercooled liquid. The fact that at a given vapor pressure the supersaturation with respect to ice is higher than that with respect to water might suggest that homogeneous deposition would have a higher rate (or probability) than homogeneous freezing. However, there are both theoretical arguments and empirical evidence for homogeneous freezing being the only process actually realized.

The most general indication for freezing to predominate over deposition is the Ostwald phase rule, which states that from any metastable state the phase of next closest level of ordering will form. In the case of supersaturated vapor, this rule predicts that the formation of the liquid phase precedes the formation of the solid phase.

The same result is obtained in the framework of classical nucleation theory by comparing the probability of formation of an ice embryo from the vapor with the probability that a liquid embryo will form. Since the interfacial energy σ_{sv} between ice and the vapor is much larger than between liquid and vapor σ_{lv}, the rate of nucleation for ice from the vapor is lower by factors of 10^{10} or more than the rate for liquid drop formation.

The molecular theory of nucleation, in which the energy of molecular clusters is calculated directly from the interaction energy between molecules and specific cluster geometries are taken into account, further corroborates that the formation of small ice-like structures have a higher free-energy barrier to overcome than clathrate structures of equivalent size (PLUMMER, 1973).

The nucleation of liquid prior to the nucleation of ice (for homogeneous nucleation only) means that ice will form from supersaturated vapor only when the supersaturation is high enough to nucleate drops (see Section 3.2.1) and if, simultaneously, the temperature is low enough for freezing to be initiated. Thus, the homogeneous nucleation of ice from the vapor is a two-stage process, but the processes follow in such rapid progression that the stages may not be distinguishable in practical situations (like a rapid expansion in a chamber at cold temperatures). If liquid drops are already in existence, the requirement for the homogeneous nucleation of ice is in terms of temperature only. This is the only case of importance for the atmosphere and for that reason the following discussion treats only homogeneous freezing.

To formulate estimates of the free energy of formation of ice embryos using a thermodynamic (classical) approach it is necessary to assume that the ice–water interface is a sharp one. In reality, the change from the water structure to the ice structure is gradual, extending over several molecular distances. For small clusters (tens of molecules) it can be imagined that none of the interior is free from surface influences. The thermodynamic theory cannot take such complexities into account, so that the assumption of an ideal surface defining

a discontinuity in structure is a necessary one. With that model, as detailed in Appendix I, and assuming spherical embryo shape, the critical free energy and critical embryo radius are

$$\Delta F^* = \frac{16\pi\sigma_{sl}^3}{3(\Delta F_v)^2} \quad \text{and} \quad r^* = \frac{-2\sigma_{sl}}{\Delta F_v} \tag{4.1}$$

where ΔF_v is the bulk free energy change of solidification per unit volume, and σ_{sl} is the solid–liquid interfacial energy. In order to make practical use of these equations it is necessary to make appropriate choices for the quantities involved. The procedure suggested by FLETCHER (1970) is to make use of the entropy relation $\psi = -(\partial F/\partial T)_p$ to yield

$$\Delta F_v = -\Delta\psi_v \, dT = -<\Delta\psi_v>\theta \tag{4.2a}$$

and gives the average entropy of fusion $\langle\Delta\psi_v\rangle$ for the temperature range T_0 to T, with the supercooling $(T - T_0)$ designated by the symbol[1] θ as

$$\langle\Delta\psi_v\rangle = (1.13 - 0.004\theta)\ \mathrm{J\,m^{-3}\,°C^{-1}}. \tag{4.2b}$$

The combination of Eqs (4.1) and (4.2) provides a basis for the calculation of homogeneous freezing rates. The value of σ_{sl} is usually left as an adjustable parameter to fit the experimental results (the value is roughly around 0.02 $\mathrm{J\,m^{-2}}$). A similar expression was derived by MCDONALD (1964):

$$\Delta F_v = \frac{-L_m\theta}{T_0} \tag{4.3}$$

with L_m being the mean value of the latent heat of solidification between T_0 and T. Both (4.2) and (4.3) show the proportionality of ΔF_s to supercooling, $\theta = T - T_0$, as would be expected, since the two phases are in equilibrium at $T = T_0$.

If the approximation of a spherical embryo is replaced by more realistic assumptions of crystalline shapes, then the free energy expression can be modified by inclusion of "shape factors" for volume and area of the embryo. Yet further refinements can be included by using different values of σ_{sl} for the different crystal faces of the embryo. In general, such modifications amount to little more than formal exercises, since the numerical values for the parameters are not known and the experimental data cannot yield values for more than one adjustable parameter.

The calculation of the rate of homogeneous freezing nucleation follows the general procedure described in Appendix I, taking the form

[1] Since for pure water $T_0 = 0$ °C, the numerical value of θ is equal to the Celsius temperature. This will not be the case when considering solutions, or other substances whose melting point is not at 0 °C. In some ways it would be convenient to use a positive number to describe supercooling, but retaining the equivalence to Celsius temperature makes it easier to visualize the discussion relating to ice.

$$J = K \exp \frac{-\Delta F^*}{kT} \tag{4.4a}$$

where ΔF^* is the energy of formation of a critical size embryo and the pre-exponential factor, K, for the case of ice formation includes the rate of addition of molecules to the (sub-critical size) embryo. This rate reflects the transfer of water molecules across the water–ice boundary and may be estimated either from the activation energy of viscous flow of water (FLETCHER, 1970; WOOD and WALTON, 1970) or from the self-diffusion coefficient of water (PRUPPACHER and KLETT, 1978). In either case the data are derived from measurements of the transport properties of water at subzero temperatures (ANGELL, 1982); since those measurements do not extend to the temperature of homogeneous nucleation, the data are extrapolated. The numerical value of the pre-exponential factor is found to be in the range 10^{32} to 10^{38} $m^{-3}s^{-1}$ depending on the form and numerical inputs to the calculations. The uncertainty in this factor is of less concern, since the major interest lies in the dependence of the nucleation rate on temperature. That dependence is with θ^{-2}, as seen when (4.2a) is substituted into (4.2b) to yield

$$J = K \exp(-B'\tau'), \quad \tau' = (T\theta^2)^{-1} \tag{4.4b}$$

where B' is a constant. Taking into account the temperature dependence of the entropy of fusion changes the expression to

$$J = K \exp(-B\tau), \quad \tau = (T^3\theta^2)^{-1} \tag{4.4c}$$

as was given by WOOD and WALTON (1970). The temperature dependences predicted by (4.4b) and (4.4c) are nearly identical since T^{-2} changes only slightly over the few degrees in T over which J is observable in practice.

A 1 °C change in θ corresponds (at typical values of the other variables) to a one and a half order of magnitude change in J. The rapid increase in J with slight changes in θ is typical of many nucleation phenomena and lends credence to the frequent use of "threshold" values to describe the point where J becomes appreciable.

Experimental studies of homogeneous freezing nucleation developed along two lines: the use of cloud chambers and the observations of small droplets which are either freely falling, are supported on solid surfaces or are dispersed as emulsions. In any experiment, the volume of the samples (droplets) are made small, so as to reduce the chance of having contaminants present and introducing heterogeneous nucleation into the observations.[1]

In the cloud chamber experiments, a rapid expansion is used to create the cloud; by suitably large expansions the temperature can be lowered sufficiently to have ice crystals develop. These experiments followed from the classical

[1] The role of foreign matter in initiating the crystallization of supercooled liquids became established by the 1920's. The first observation of homogeneous freezing of water might be that of MEYER and PFAFF (1935), after filtration of the water through colloidon membrane.

studies of C. T. R. WILSON during the early years of this century. CWILONG (1947) undertook a systematic study of expansions to low temperatures, pursuing WILSON's observation that liquid drops and not ice formed even when condensation took place at temperatures around −15 °C. CWILONG found that when the lowest temperature in an expansion reached −41.2 °C a shower of ice crystals appeared, which he detected by either letting them fall into supercooled water at the bottom of his apparatus or by observing the scintillation from the crystals.

The most recent in the long series of experiments of this type is that reported by ANDERSON *et al.* (1980). Their photographic records could be evaluated to yield quantitative results on the proportion of water droplets and ice crystals shortly after expansion. An example of their results is shown in Fig. 4.1; the diagram illustrates the rapid increase in the number of ice crystals at temperatures below −43 °C. The indicated temperature refers to the calculated minimum value which is reached for a very short time (~0.01 s) immediately after the sudden expansion in the chamber. The nucleation rate in these experiments became high enough to produce observable concentrations of ice crystals at temperatures between −41 and −42 °C. In this experiment, the fact that ice formed by the freezing of liquid droplets was demonstrated by the lack of any discontinuity in the total number (liquid or ice) of particles formed as the final

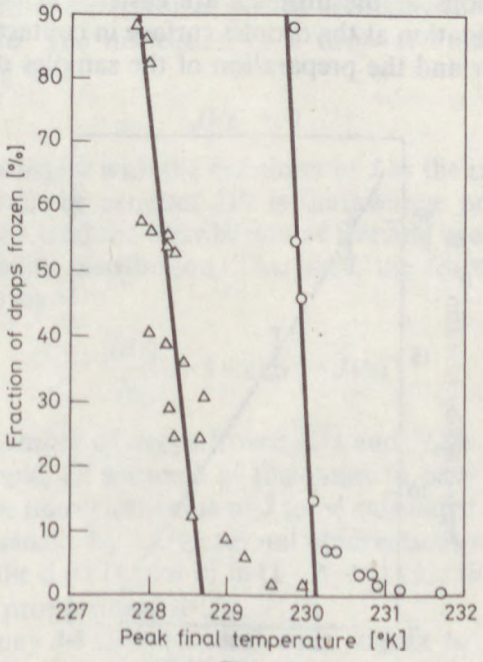

Fig. 4.1

Expansion chamber results from ANDERSON *et al.* (1980). The frozen fraction of droplets increases sharply as the final temperatures of expansion reach 230° K and 228.5° K, for initial conditions of −9° C in He, and −12° C in Ar, respectively

temperature was gradually decreased in a series of expansions past the onset of ice formation. By evaluating the experimental data as a sequence of homogeneous condensation, droplet growth and homogeneous freezing of the droplets, HAGEN *et al.* (1981) derived the nucleation rate as a function of temperature. This result is shown in Fig. 4.2 exhibiting the very rapid rise in J with decreasing temperatures.

Cloud chamber experiments produce droplets of only a few micrometer diameter but in very large numbers. Other techniques have been developed for studies with larger droplets; the main advantage of larger droplet sizes is that the volumes of the droplets can be directly measured, as opposed to the use of calculated values in the cloud chamber studies. Often, these techniques allow droplets to be individually observed and, also, to be subjected to repeated cycles of freezing and melting. The droplets are allowed to freely fall in air (KUHNS and MASON, 1968), are enclosed in glass capillaries (MOSSOP, 1955), are suspended in one (BUTORIN and SKRIPOV, 1972), or at the interface of two immiscible liquids (BIGG, 1953; LANGHAM and MASON, 1958), or are dispersed as an emulsion within a carrier oil (RASMUSSEN and MACKENZIE, 1972; MICHELMORE and FRANKS, 1982; CLAUSSE *et al.* 1983; TABOREK, 1985). With supported droplets the rate of change of temperature can be controlled, avoiding the rapidly changing conditions of expansion chambers or of free-fall droplets. These methods also allow the temperature to be controlled with greater accuracy and observations of the droplets are easier. On the other hand, the possibility of contamination at the droplet surface in contact with the supporting medium is greater and the preparation of the samples requires great care.

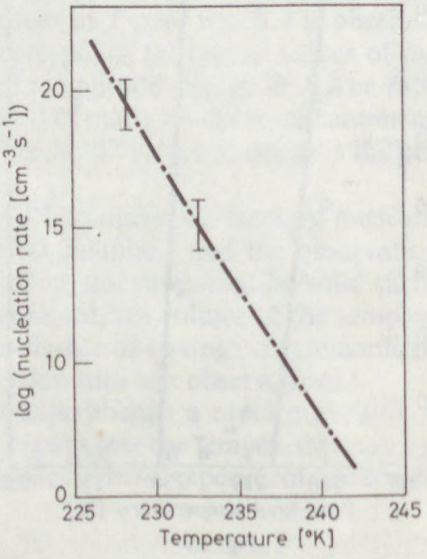

Fig. 4.2

Observed rates of ice nucleation, from HAGEN *et al.* (1981). The nucleation rate (error bars, and solid line) increases exponentially with decreasing temperatures

For all methods, water of the greatest possible purity is used, but even so, the main factor that allows homogeneous nucleation to be studied in droplets is the partition of the sample in many small droplets. The limited number of impurities in the water are thereby sequestered into an equally limited number of droplets, so that the larger the number of droplets is into which the sample is divided, the smaller is the fraction of droplets influenced by the impurities. This measure works as long as there is no interference by the supporting medium even though for smaller drops the surface to volume ratio becomes higher.

It is necessary at this point to digress a little and deal with the methods applicable to the evaluation of droplet freezing experiments. What the freezing of a given droplet evidences is the formation of at least one critical size embryo within the volume of that droplet over the time of observation. Once an embryo reaches critical size and goes through the rapid next step of adding one more molecule to become stably growing, the rest of the droplet freezes within a short enough interval of time that other embryos are likely to form within the same droplet. The observed freezing events are linked to the nucleation rate, J, by the external variables volume, time and temperature. For a population with a large number of droplets there will be a distribution of freezing temperatures due to the chance occurrence of nucleation in each, even if all are of identical volume and are at identical conditions.

The simplest case to consider is that of a set of droplets held at a constant temperature, neglecting the transient period necessary for bringing the sample to that temperature. The nucleation of a drop of volume V at time t' is equivalent to saying that

$$JVt' = 1 \tag{4.5}$$

for that droplet, consistent with the definition of J as the rate of nucleation per unit time. In general, the product JVt is the average probability of a drop freezing within time t, and the distribution of freezing events is describable by the Poisson probability distribution. Therefore, the fraction of drops frozen after time t is given by

$$\frac{N(t)}{N_0} = 1 - \exp(-JVt) \tag{4.6}$$

where $N(t)$ is the number of drops frozen at t and N_0 is the total number of droplets in the sample, all assumed at this point to have identical sizes. This equation permits the numerical value of J to be calculated, for the temperature of the experiment, usually by taking several observations at different times and fitting Eq. (4.6) to the data (a plot of $\ln(1 - N/N_0)$ vs. t should yield a straight line whose slope is proportional to J).

Equation (4.6) may be differentiated with respect to time to express the numbers of freezing events, dN, which are expected within an interval of time dt:

$$dN = N_0 [\exp(-JVt)] [JV\,dt] \tag{4.7}$$

where the terms have been grouped to show that the probability of freezing of a droplet within dt is given as the probability of it not yet being frozen at time t, times the probability that it will freeze within dt. This equation is the starting point for describing experiments in which the temperature is not constant with time. A steady lowering of the temperature (constant cooling rate) is the most convenient experimental procedure and it has the potential of yielding values of J over a range of temperatures, not just at a single point. For a cooling rate $dT/dt = \alpha$, Eq. (4.7) can be integrated, after substituting for the exponential factor from Eq. (4.6), to give

$$\frac{1}{N_0 - N} dN = \frac{V}{\alpha} J(T)\, dT \tag{4.8}$$

where the left-hand side is equal to $\ln (1 - N/N_0)$. To render this equation usable some simplifying assumption is needed, usually based on the fact that $J(T)$ increases very rapidly with decreasing temperature.

Experiments with constant cooling rate yield frequency distributions of freezing events with temperature which are strongly skewed toward lower temperatures. Since J increases exponentially and so the number of drops freezing increases at an accelerating rate, this is expected to be offset and eventually dominated by the decrease in the number of drops remaining unfrozen. By matching the frequency distribution to the approximate solution of Eq. (4.8), values of $J(T)$ can be derived for the temperature range covered by the distribution (e.g. BIGG, 1953; BUTORIN and SKRIPOV, 1972). The range of temperatures over which the freezing events take place can be changed, within limits, by varying either V, or α: lower temperatures of freezing result from small V and from large α-values. Experiments agree with Eq. (4.8) in producing frequency distributions which do not change in shape but are shifted in temperature in response to changes in V or in α. The shape of the distribution is governed by the temperature-dependence of J. While the precise form of that temperature dependence, as predicted by Eqs (4.1) to (4.4), is more complex, the empirical data can be well represented by linear plots of $\ln J$ vs. T (as will be shown in the following paragraphs). For such an exponential increase in J with decreasing T, the mean freezing temperature of a set of droplets, T_m, corresponding to $N = N_0/2$, varies with $-\ln V$ and with $\ln \alpha$ (LANGHAM and MASON, 1958). These dependences are supported by the empirical data and can be effectively used to distinguish between homogeneous and heterogeneous nucleation.

Returning now to the discussion of homogeneous nucleation experiments, a few recent data sets will be presented. Summaries of the large body of earlier studies can be found, for example, in MASON (1958) or FLETCHER (1970).

The method of allowing droplets to fall in a gas through a gradient in temperature, and detecting the point of nucleation by the accompanying change in opacity was used by KUHNS and MASON (1968). After correcting the observed freezing temperatures for the lag due to thermal inertia, the nucleation temperatures of 10 μm diameter drops was near − 38 °C and those of 40 μm droplets

near −36 °C. By assuming that at the rate at which droplets were cooling (several degrees C per minute) the freezing events can be taken to indicate nucleation within 1 second, the observations could be converted to nucleation rates; these results are included in Fig. 4.4.

The freezing of single drops suspended in oil, and detecting freezing events by the temperature rise accompanying the release of latent heat, was utilized by BUTORIN and SKRIPOV (1972) in experiments both at constant temperatures and at constant rates of cooling. Typical results for the two kinds of tests are shown in Fig. 4.3, both clearly exhibiting the expected trends described in the foregoing

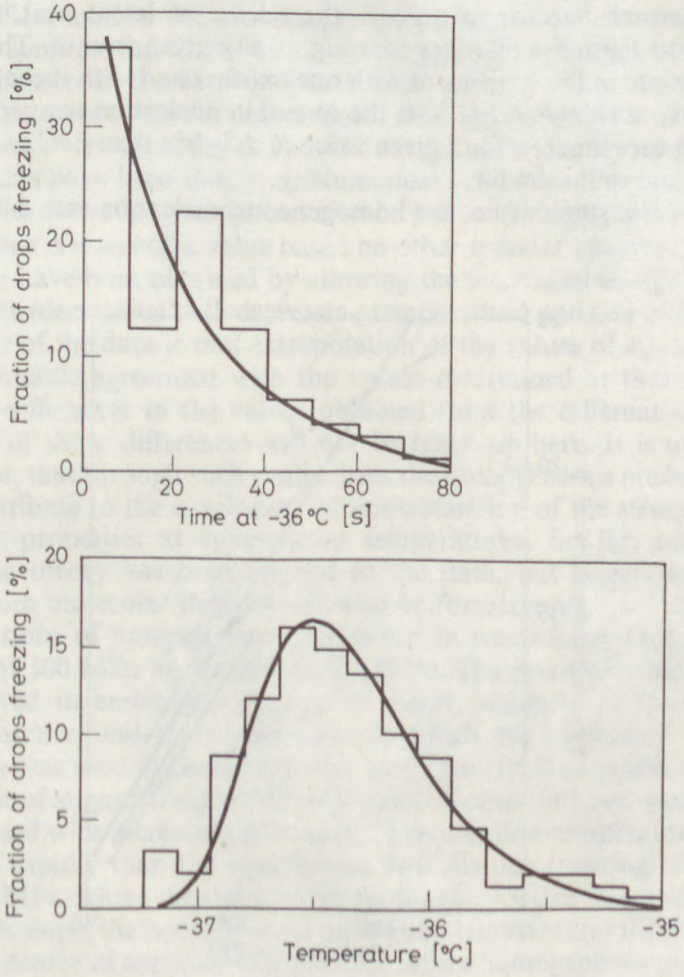

Fig. 4.3

Examples of the results of experiments for two sets of conditions. Upper diagram: constant temperature of −36 °C (96 droplets of 115 μm diameter). Lower diagram: continuous cooling of 0.15 °C s^{-1} (150 droplets of 150 μm diameter). The histograms show the numbers of droplets frozen within given time intervals. The smooth curves are based on equations similar to Eqs (4.7) and (4.9). (After BUTORIN and SKRIPOV, 1972)

discussion for droplet freezing experiments. The derived nucleation rates are shown in Fig. 4.4.

Emulsions of water in oil offer the possibility of observing very large numbers of droplets although present a fairly broad range of droplet sizes as a result of the mechanical dispersion process. WOOD and WALTON (1970), MICHELMORE and FRANKS (1982) and TABOREK (1985), among others, made effective use of emulsions to study homogeneous freezing nucleation. The droplets were photographed through a microscope to determine droplet sizes and to detect freezing in the experiments of WOOD and WALTON. MICHELMORE and FRANKS utilized a differential scanning calorimeter, and TABOREK used a specially designed sensitive thermal detector to observe the release of latent heat, which is in proportion to the mass of water freezing at any given instant. The results of these studies are in fair agreement with one another and with those of BUTORIN and SKRIPOV, as shown in Fig. 4.4; the spread in nucleation temperatures from the different experiments, for a given value of J, is less than 2 °C and the slopes of the lines are quite similar.

Figure 4.4 is a summary of the homogeneous nucleation rate data discussed

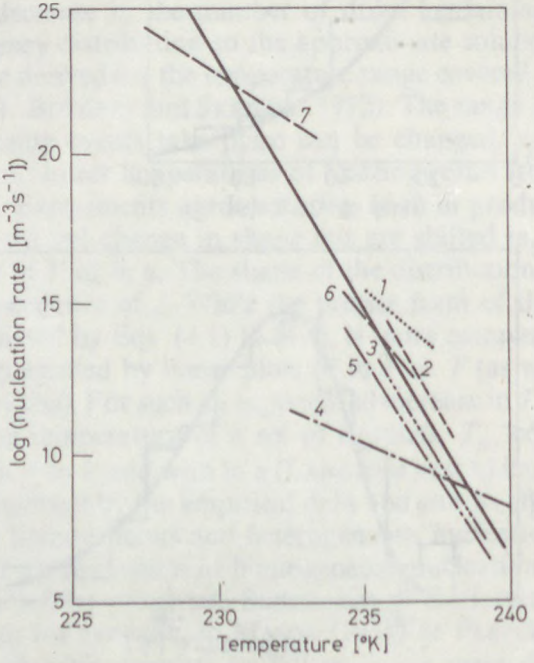

Fig. 4.4

Homogeneous nucleation rate, J ($m^{-3}s^{-1}$), as a function of temperature, as determined by: A – KUHNS and MASON (1968); B – WOOD and WALTON (1970); C – RAVDELY and KOZLOV (1970); D – BUTORIN and SKRIPOV (1972); E – MICHELMORE and FRANKS (1982); F – HAGEN *et al.* (1981); and G – TABOREK (1985). The heavy long line is an indication of the average trend, which can be described by the equation $J = 6.8 \times 10^{-50} \exp(-3.9\Theta)$

in this section. The cloud chamber results of HAGEN *et al.* (1981) fall at the high values of J (10^{21} to 10^{26} nuclei per m^3 per second), whereas the data obtained with larger drops are at a lower range of values. The relatively good fit of all of the data to a single line is quite reassuring although there are some clear systematic differences among the data sets; some of those differences result from experimental errors, some from the methods of interpretation of the observations. The trend toward a linear increase of $\ln J$ with decreasing temperature is supported by the data displayed in Fig. 4.4, but it must be remembered that this is only an empirical trend and not a rigorous analytical dependence. Also, while the emulsion experiments have been very productive, there is evidence that the emulsifiers used in the experiments produce heterogeneous nucleation, at least after some period of time (CLAUSSE *et al.*, 1983; MATHIAS *et al.*, 1985).

Reconciliation of the empirical data with the theoretical formulations was attempted in each of the references cited; with the relatively narrow ranges of temperatures over which any of the data sets extend, reasonably good fits with the equations have been obtained. Numerical values for the interfacial energy σ_{sl} or for the activation energy can also be extracted from the data depending on which one is assigned a value based on other types of observations. Best fits to the data have been obtained by allowing the interfacial energy to vary with temperature (decreasing with decreasing temperature) and one of the checks on the validity of the data is that extrapolation of the values of σ_{sl} to 0 °C should show reasonable agreement with the values determined at that temperature. There are differences in the values obtained from the different studies and a discussion of those differences will not be taken up here. It is useful to note nonetheless, that through such evaluations the homogeneous nucleation experiments contribute to the developing of understanding of the structure of water and of its properties at supercooled temperatures. So far, only the thermodynamic theory has been applied to the data, but hopefully some comparisons with molecular theories will also be forthcoming.

Observations of homogeneous nucleation in water have been extended to pressures of 300 MPa by KANNO *et al.* (1975). The point of rapid heat release was observed in emulsified samples of water, similarly to the experiments discussed earlier, and the temperature at which the nucleation rate became appreciable was used to characterize each experiment. The results revealed that the amount of supercooling possible before the onset of homogeneous nucleation increased with increasing pressures, i.e. nucleation temperatures decreased even more rapidly than the equilibrium liquidus line (melting temperatures). Below 200 MPa, where the stable ice phase is cubic ice (Ice III), and the liquidus line changes slope, the homogeneous nucleation temperatures followed the same trend. The degree of supercooling possible before homogeneous nucleation was found to increase to nearly 70 °C for pressures of 300 MPa; nearly double the value for atmospheric pressure. There are interesting, and not fully understood, implications of these findings regarding the structure of supercooled water. KNIGHT (1976) compared the results of KANNO *et al.* with the predictions of the thermodynamic theory by accounting for the pressure dependences of density,

melting temperature and the entropy of fusion, and by assuming that the interfacial energy between ice and water, the heat capacities of ice and of water, and the pre-exponential term in Eq. (4.4) are independent of pressure. The agreement was found to be quite good for the Ice I region (the comparison was not extended to the Ice III region). While this result does give further confidence in the theory, it does not constitute a very severe test. The fundamental objections to the thermodynamic approach which were mentioned earlier certainly remain valid.

In summary, experimental results from several different kinds of tests show reasonable agreement in indicating that the homogeneous nucleation of ice takes place from the liquid at supercoolings of roughly 40 °C at normal atmospheric pressure. The rate of nucleation, as shown in Fig. 4.4 rises very rapidly when those temperatures are reached, so that the dependence of the nucleation temperatures on the rate of cooling and on the volume of a given sample (droplet), although well quantifiable based on the empirical data, is only a second-order effect, causing small differences from the −40 °C point. The thermodynamic theory of homogeneous nucleation has been shown to be capable of explaining the main features of the empirical data and to yield numerical values for the interfacial energy which are comparable with values derived by other methods. Thus, there is no reason to be overly sceptical of the validity of the theory, in spite of its fundamental limitations.

The atmospheric role of homogeneous ice nucleation is quite tangible, in contrast with homogeneous condensation, as the abundance of heterogeneous ice nuclei is restricted in comparison to the numbers of cloud droplets (see following section). Many cloud droplets can reach temperatures near −40 °C in the liquid state and have ice form in them via homogeneous nucleation. This process is most evident in deep convective clouds. The most readily perceived example of homogeneous ice formation is the rapid glaciation of the tops of cumulonimbi and the formation of anvil clouds. While some ice elements form in these clouds via heterogeneous nucleation at temperatures between 0 °C and −40 °C as the cloud rises through the corresponding levels, an appreciable fraction (perhaps a few to a few tens of percent) of the cloud droplets arrives at the −40 °C level unfrozen. The small temperature range in which homogeneous freezing is initiated and the presence of the tropopause near those temperatures combine to produce the characteristic appearence of anvil clouds.

The majority of cirrus clouds also forms at temperatures where homogeneous ice nucleation becomes probable, but the concentration of cloud elements in cirrus is much lower than in convective clouds and so the contribution from heterogeneous nucleation may be more important. There are as yet no good measurements which would allow a quantitative description of the initiation of ice particles in cirrus. The same may be said of deep nimbostratus clouds which can extend to the temperatures of homogeneous nucleation, but where cloud formation and the growth of particles are slow and difficult to observe in sufficient detail to characterize the nucleation process involved.

Whatever is the type of cloud considered, there is an additional factor to

account for when discussing the homogeneous nucleation of ice in the atmosphere. As cloud droplets form on soluble (or partially soluble) nuclei and existing droplets collect gases and aerosols from the air at fairly rapid rates, cloud droplets cannot be considered to consist of pure water until they grow to large sizes by condensation. The influence of dissolved substances on the homogeneous nucleation of ice has been examined both theoretically (e.g. BÓNIS, 1971) and experimentally (e.g. WOOD and WALTON, 1969; RASMUSSEN and MACKENZIE, 1972). The simple effect of melting-point depression gets supplanted by additional effects due to changes in interfacial energies, non-idealities of solutions, etc. In clouds, the effects become especially large when the droplet size is small and the concentration of solute high. The resulting changes in nucleation temperatures can range from several degrees to perhaps in excess of ten degrees. The most extreme influence on ice nucleation can be expected in haze particles (soluble aerosol at humidities above that of deliquescence)—unfrozen haze particles probably account for the sketchy but noteworthy observations of "liquid water" at temperatures as cold as −65 °C in the atmosphere. There is considerable scope for extending nucleation research to such conditions.

4.4 Heterogeneous nucleation

4.4.1 General comments

The role of foreign materials in initiating the nucleation of ice at temperatures warmer than that required for homogeneous nucleation is very well demonstrated. Some materials can initiate ice formation at just a few tenth of degrees below the melting point, which is a remarkable fact, in comparison with the nearly 40 °C supercooling required for homogeneous nucleation. In addition, on some foreign materials ice can be nucleated directly from the vapor phase. The range of materials which are effective ice nucleators is also quite surprising, going from substances like silver iodide (AgI) to organic macromolecules in the cell membranes of some bacteria. As a result, there is a truly fascinating variety of phenomena in which heterogeneous ice nucleation is a key element. The formation of ice in lakes, rivers, puddles, and so on, is usually started at barely noticeable supercoolings by some material with which the water is in contact at its boundaries. In clouds, on the other hand, water droplets readily supercool, but ice is nucleated in some fraction of the droplets over the broad temperature range from about −5 to −40 °C. Certain plants and insects would not have ice form in or on them until quite low temperatures, except that some accompanying bacteria might nucleate ice on them, or in them, at just a few degrees supercooling. Some organism have special strategies for preventing ice nucleation. Thus, the reasons to study and understand heterogeneous ice nucleation are indeed manyfold.

Accordingly, the subject of ice nucleation received the attention of many scientists, with systematic studies carried out at least since the middle of the last century[1]. Especially since about the 1930's experimental investigations of ice nucleation have been pursued with many different methods and with many different combinations of conditions. Tests have been conducted with a wide diversity of substances, but understandable focus fell on materials of greater effectiveness. Theoretical developments derive mainly from the thermodynamic treatment of homogeneous nucleation, with attempts to incorporate models of the factors important to heterogeneous nucleation. These theories are not specific to water substance, but have general validity to other substances as well. At the molecular level, the interaction and ordering of water molecules on surfaces has been modelled, with the prospect of extending the calculations to the formation of critical embryos.

In spite of the intense efforts to understand heterogeneous ice nucleation, the accomplishments can still only be viewed as initial developments. Theory and observation have not yet been matched with any generality. The main complication arises from the fact that specific variations of details of the processes appear to be important enough to make formulations that ignore them of little utility; in most cases, observations are capable of yielding phenomenological descriptions only, not quantitative analyses of the processes involved.

4.4.2 Basic theory

The fundamental effect in heterogeneous nucleation is that the embryo of the new phase forms on the foreign substrate, so that the embryo shape is approximated by a portion of a sphere attached to the substrate (as shown in detail in Appendix I). The result is that the critical embryo radius is reached at smaller values of the free-energy difference which is associated with the formation of the embryo. Hence, critical size embryos can be realized at smaller supercoolings or supersaturations. The parameter describing the interaction of the substrate with the embryo is reduced, in the macroscopic description of the process, to the contact angle parameter, m. The predictions of this formulation are shown in Fig. 4.5 for ice nucleation from the vapor (deposition), and in Fig. 4.6 for nucleation from the liquid (freezing), both as functions of the parameter m and of the radius of curvature of the substrate. The latter factor is considered, because, especially in atmospheric applications, the nuclei are usually in the

[1] Interestingly, the first clear demonstration of the phenomenon of supercooling was with water, in 1724, by FAHRENHEIT. Subsequent studies of metastable systems and the triggering of phase transitions focussed on supersaturated solutions, and the crystallization of various organic crystals. Experiments with supercooled water were then reported well over a century after FAHRENHEIT's discovery (MOUSSON, 1858; DUFOUR, 1861). However, the fact that fogs consist of water droplets even at temperatures much below 0 °C appears to have been common knowledge in 1858. Studies of ice nucleation took on a new impetus in the 1930's, by which time many of the important basic concepts of nucleation have been established from studies with substances other than water.

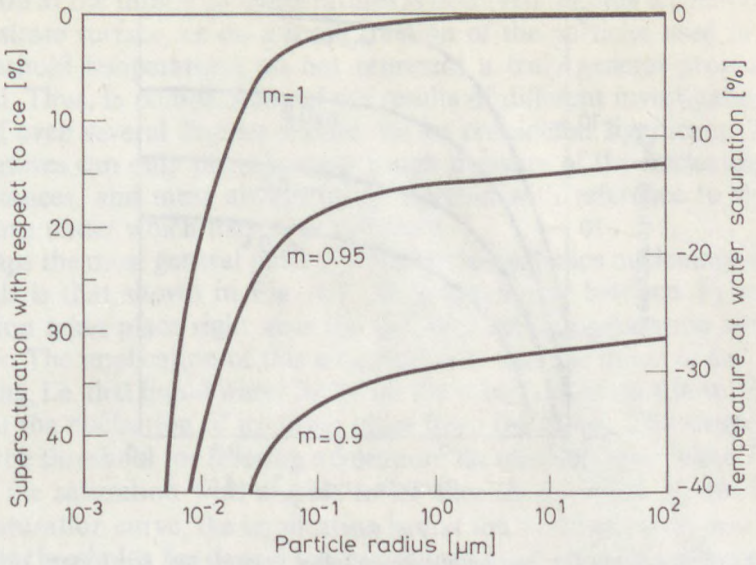

Fig. 4.5

Calculated dependence of the critical supersaturation on particle radius, for deposition nucleation at a rate of $J = 10^6$ $m^{-3}s^{-1}$. The parameter m characterizes the interfacial energies of the system, as defined in Eq. (I.6) of Appendix I (After FLETCHER, 1958)

form of small particles whose size may be comparable to the critical embryo radius. Somewhat simpler equations apply to nucleation on flat surfaces (cf. Appendix I). Equivalent relationships are given for cylindrical substrate forms by KNIGHT and WEINHEIMER (1987), and for liquid substrates by COOPER and KNIGHT (1975). There is considerable similarity in the trends given by the different assumptions about the geometric shape of the substrate.

As can be seen by comparing Figs 4.5 and 4.6 (using the right-hand ordinate in 4.5) for given values of m and r_p, deposition nucleation reaches the $J = 10^{-6}$ $m^{-3}s^{-1}$ rate, for example, at considerably lower temperatures than freezing nucleation. In reality, this comparison is not as meaningful as it appears because m will have different values for deposition and for freezing for a given substrate material.

Agreement between these theoretical predictions and observations is not easily tested, as will be discussed later, but there is at least partial experimental support for the trend, shown in Fig. 4.6, that materials which have small interfacial energies with ice (i.e. are more "ice-like" in their structure), giving m-values near unity, can indeed be quite effective ice nuclei. This factor will be examined in more detail in a following section. The dependence on r_p shown in Figs 4.5 and 4.6 has not been verified by experiments, except in the general sense that larger particles are indeed more likely to be effective nuclei. That fact, however, has other explanations also; namely, that the probability of finding an active site on a particle increases with the size of that particle (see Section 4.4.4).

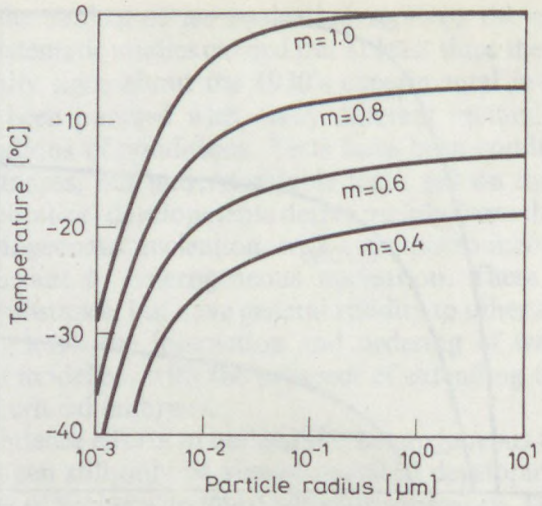

Fig. 4.6
Same as Fig. 4.5, but for freezing nucleation (after PRUPPACHER and KLETT, 1978)

4.4.3 Characteristics of ice nuclei

Before discussing the specific factors which are important in ice nucleation, it is worth clarifying what is meant by "effective", or "active", ice nuclei. These terms have been used with varieties of connotations, and therefore have largely lost the chance for rigorous definitions. It is perhaps preferable that way, and in this text too the phrases will be used in different contexts. In all cases, the intention is to indicate that ice nucleation is facilitated by the hetero-nucleus to a substantial degree. Most simply, this means that ice is formed at some relatively small supercooling or supersaturation. In another sense, effectiveness might mean a higher number concentration of nuclei at given conditions. Quantitative differences will always be expressed in terms of better-defined properties, such as mean temperature, sites per unit area, etc.

Ice nucleating materials

There are many substances known to be capable of initiating heterogeneous ice nucleation, as shown, for example, in the compilations of MOSSOP (1963) and of PRUPPACHER and KLETT (1978). Ice nucleating materials range from minerals to alkali halides to metal oxides and to varieties of organic compounds. For simplicity, each substance is usually characterized in terms of the "threshold temperature" of nucleation. Threshold temperatures can be viewed most simply as relative measures which emerged from specific series of experiments; they roughly correspond to a fixed, but only poorly known, value of J. Since ice

formation at the threshold temperatures is observed on only a small fraction of the substrate surface, or on a small fraction of the particles used in the tests, the threshold temperatures do not represent a truly general property of the material. Thus, in comparisons of the results of different investigations, differences of even several degrees should not be considered significant. Threshold temperatures can only provide some rough measure of the nucleating abilities of substances, and must always be interpreted with reference to the specific conditions under which they were obtained.

Perhaps the most general pattern characterizing the ice nucleating abilities of materials is that shown in Fig. 4.7. At temperatures between T_1 and T_2 ice nucleation takes place right near the line representing saturation with respect to water. The implication of this observation is that the mode of ice formation is freezing, i.e. that liquid water forms on the substrate, at least in small clusters, and that the nucleation of ice takes place from the liquid. The temperature T_1 is then the threshold for freezing nucleation. At temperatures below T_2, ice can form if the saturation with respect to ice exceeds S_2. Since S_2 lies below the water saturation curve, the implication is that the mode of nucleation is deposition. The thresholds for deposition are defined by T_2 and S_2, although the two are not independent, since $S_2 = f(T_2)$. This type of observation was first reported by BRYANT *et al.* (1959) for silver iodide and cadmium iodide. Later studies showed these characteristics to be quite general. There will be further discussion of this pattern in the section on ice nucleation modes. The main point

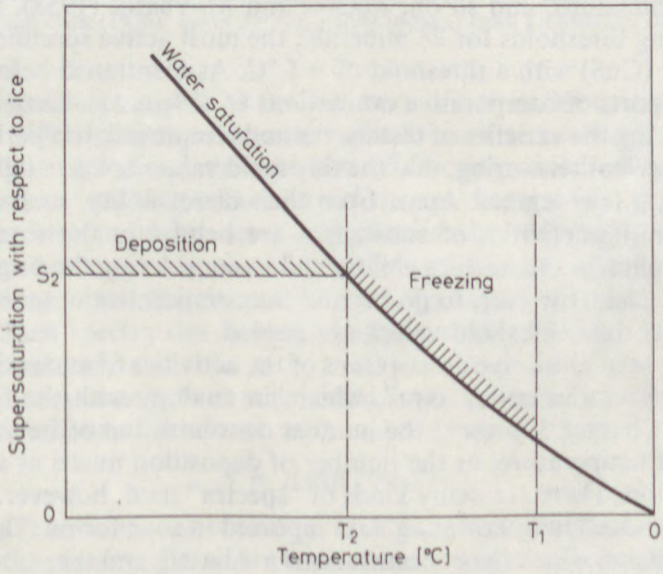

Fig. 4.7

Schematic depiction of the temperature and supersaturation conditions which are observed to lead to deposition and freezing nucleation on common substrates

is that the theoretical prediction that freezing nucleation is possible at temperatures higher than those assigned to deposition nucleation is born out by the observations. The dependence of ice nucleation, for $T < T_2$, on both temperature and vapor pressure is also evident.

Values of T_1 and S_2 are listed in Table 4.1 for selected materials, to show the approximate range of values observed. The first three materials in the list are among the most effective ice nucleators known; kaolinite is important because of its abundance.

Table 4.1

Examples of freezing and deposition thresholds (after SCHALLER and FUKUTA, 1979)

Material	Freezing T_1 °C	Deposition S_2%
Silver iodide	−4.5	9.5
1,5-dihydroxynaphthalene	−5.0	12.0
Phloroglucinol	−4.8	10.0
Kaolinite	−9.9	20.3

All the materials mentioned above are purified or synthetized substances. For ice nucleation in the atmosphere, there is, of course, considerable interest in the activities of naturally-occurring substances, and there are many published sets of measurements on the nuclei found in natural water samples, in different soils, in volcanic emissions, and so on. MASON and MAYBANK (1958), for example, report freezing thresholds for 28 minerals; the most active specimen in that set was covellite (CuS) with a threshold of −5 °C. As mentioned before, there are numerous reports of comparative evaluations of different potential ice nucleators. Considering the varieties of testing methods employed, it is perhaps surprising, and somewhat reassuring, that the threshold values are generally repeatable within about a few degrees. Apart from their direct utility, such comparisons of the nucleating activities of substances are helpful in the search for what factors determine ice nucleating ability, and in considering the origins of atmospheric ice nuclei. However, to go beyond the comparative observations, other measurements than threshold values are needed.

More precise quantitative descriptions of the activities of nucleating materials are given by "ice nucleus spectra", which, in analogy with the CCN spectra discussed in Chapter 3, present the number concentration of freezing nuclei as a function of temperature, or the number of deposition nuclei as a function of supersaturation. There are many kinds of "spectra" used, however, so that care should be exercized in interpreting data reported in such forms. The differences are in the units on which the concentrations are based, and there are differential (per temperature interval) and cumulative spectra. The type of spectrum used is tied to the method of measurement from which the data are derived, and each type conveys different information.

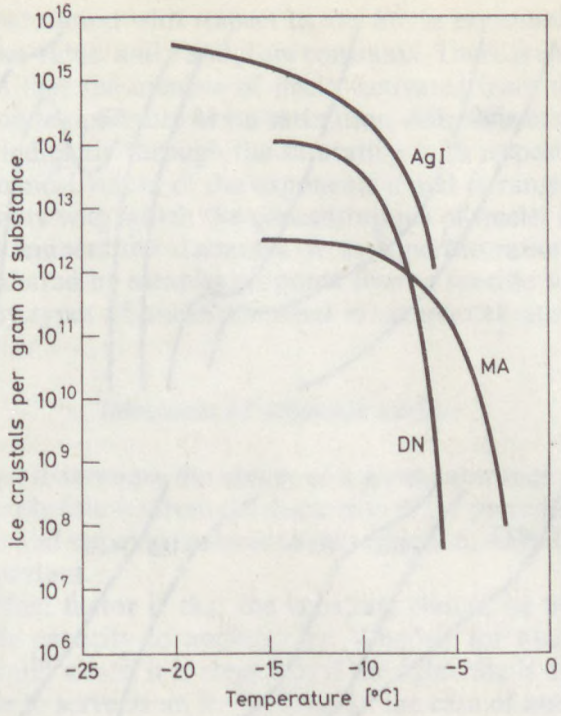

Fig. 4.8

Examples of ice initiation observed in cloud chambers for aerosols of three different nucleating substances. Curves *1* = DN (1,5-dihydroxynaphthalene,) and *2* = MA (metaldehyde) taken from FUKUTA and PAIK (1976); curve *3* = AgI (silver iodide,) from DEMOTT *et al.* (1983)

Figure 4.8 shows examples of the numbers of ice nuclei detected in cloud chambers for different materials tested in the form of aerosols injected into the chambers. Figure 4.9 shows the numbers of freezing nuclei per unit mass of material for some naturally-occurring substances dispersed in distilled water. Even though these examples are taken from rather different systems, they illustrate some common features of cumulative ice nuclei spectra, i.e. curves which for a temperature T indicate the concentrations of nuclei active between 0 °C and T. Such spectra rise monotonically, and usually quite sharply at the warmer temperatures.

At least for measurements at substantial supercoolings, say below − 10 °C, exponential functions of the form

$$N = a \exp(-bT) \tag{4.9}$$

with a and b as constants and with T in °C, often give a good fit to the empirical data. Better fits, covering a wider temperature range and also including the sharp initial rise of the spectra, can be obtained with power-law equations of the form

$$N = c\,(-T)^{d} \tag{4.10a}$$

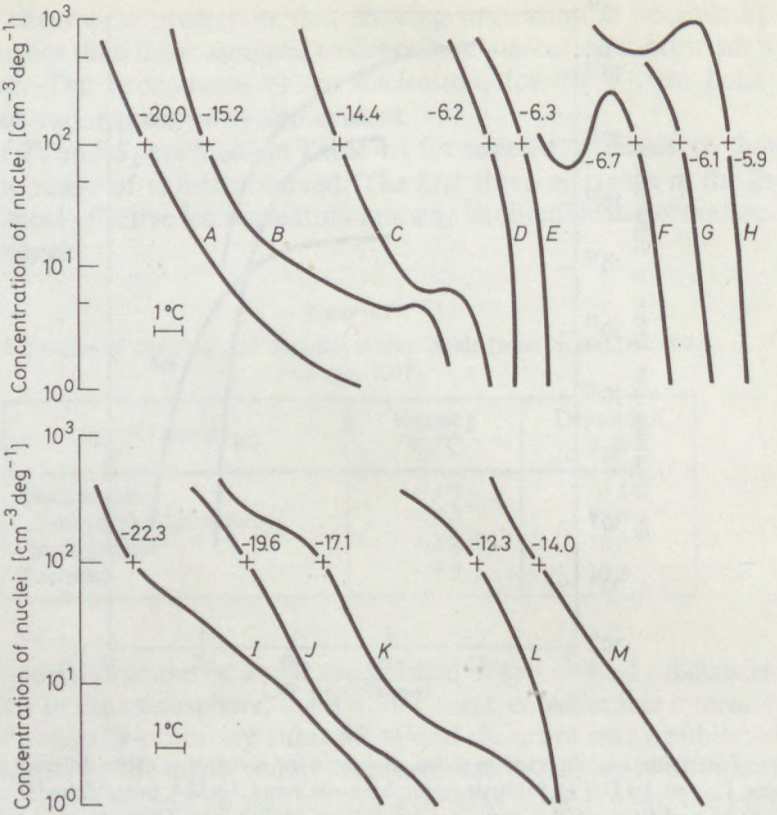

Fig. 4.9

Freezing nucleus concentrations for soil samples in 0.05% (by volume) suspensions. There are large differences among the samples: surface soils, and those with high organic content, show the warmest temperature of nucleation. (VALI, 1968)

where c and d are fitted constants, and T is in °C. Equation (4.10a) is not dimensionally consistent, so a more rigorous form is

$$N = c\,(T/T_1)^d \tag{4.10b}$$

where T_1 is a reference temperature (not 0 °C) conveniently chosen somewhere in the middle region of the spectrum (VALI, 1975). These functions have no *a priori* foundations, but provide simple descriptions for data which are smoothed by long-term averaging or by poor instrumental resolution. At times spectra of much greater complexity are observed.

HUFFMAN (1973) showed that the supersaturation spectra of ice nuclei (for deposition) can also be best represented by power-law relationships of the form

$$N = \varepsilon \left(\frac{SS}{SS_1} \right)^{\beta} \tag{4.11}$$

where the supersaturation with respect to ice, SS, is expressed in percent, SS_1 is again a reference value, and ε and β are constants. There is special significance in this finding in that the number of nuclei activated from the vapor do not directly depend on temperature or on saturation with respect to water (relative humidity), only indirectly through the saturation with respect to ice.

The large numerical values of the exponents d and β, ranging from 4 to 12, indicate the rapidity with which the concentrations of nuclei in a sample typically rise as the temperature decreases or as supersaturation increases. This characteristic is shared by samples prepared from a specific substance, and by mixtures of many types of nuclei obtained in samples of atmospheric air (cf. Section 4.5).

Influences of substrate surface

The question what determines the ability of a given substance to be an effective ice nucleus obviously follows from the discussion of the preceding section. While there is no simple and universal answer to that question, some factors have been shown to be important.

One fairly evident factor is that the substrate should be water-insoluble in order to have the capacity to nucleate ice. Whether for nucleation from the vapor or from liquid water, it is clear that if the substrate is dissolved in water it will not be able to serve as an ice nucleus. In the case of nucleation from the vapor, especially at subsaturations with respect to water, there is a possibility that a nonhygroscopic but soluble substance might nucleate ice. For any real aerosol, which is never of one pure substance, even this possibility is remote. In any case, it has been found that most ice-nucleators have low solubilities in water. This is certainly true for the chemically identified nucleating substances; one assumes that the same holds for naturally occurring ice nuclei whose composition is not known. For some water-soluble substances it is possible to get ice nuclei when the solution becomes supersaturated upon cooling and solid particles precipitate (Montefinale and Papee, 1978). In a general sense, one might argue that the question can be reduced to the relative magnitudes of the rate of dissolution of the substrate and the rate of formation of ice embryos. There is no totally water-insoluble substance and some slight etching of the surface might even facilitate nucleation. The indications are that ice embryo formation is not so fast as to allow moderately soluble substances to be good nucleators.

Perhaps the most clearly demonstrated factor in ice nucleation is the role of crystal structure of the substrate, i.e. the degree of similarity of crystal structure between ice and the substrate. Growth of a crystal on another crystal, with a close relationship between the two crystal structures is called epitaxial growth. The effect is intuitively readily acceptable: if the crystal structure of the substrate resembles closely that of ice, the water molecules in the embryo will be more readily arranged into the ice structure. The prime example for this effect is silver iodide, which has a hexagonal crystal structure differing from that of ice by only

a few percent in the spacing of the atoms. VONNEGUT (1947) selected AgI for experimentation as an ice nucleant to be used in weather modification based on this fact.

A quite evident illustration of epitaxial growth is in the observation that when ice crystals grow on a substrate of similar crystal structure the orientation of the ice crystals coincides with that of the substrate (BRYANT *et al.*, 1959; KOBAYASHI, 1965, and many others). Another proof for the importance of lattice fit was provided by the experiments of EVANS (1965): by examining the supercooling required for nucleation of ice on silver iodide as a function of pressure, they found that even at pressures exceeding 2×10^5 kPa where the stable ice form is cubic, not hexagonal as at lower pressures, there was no discontinuity in the nucleation threshold with respect to the extrapolation of the melting point of hexagonal ice. The implication is that hexagonal ice was nucleated, because of the crystal fit to the hexagonal AgI lattice.

The influence of lattice fit was further shown by VONNEGUT and CHESSIN (1971), and PASSARELLI *et al.* (1973, 1974a, 1974b). By preparing solid solutions of Br and Cu in AgI, they obtained materials whose match of crystal parameters

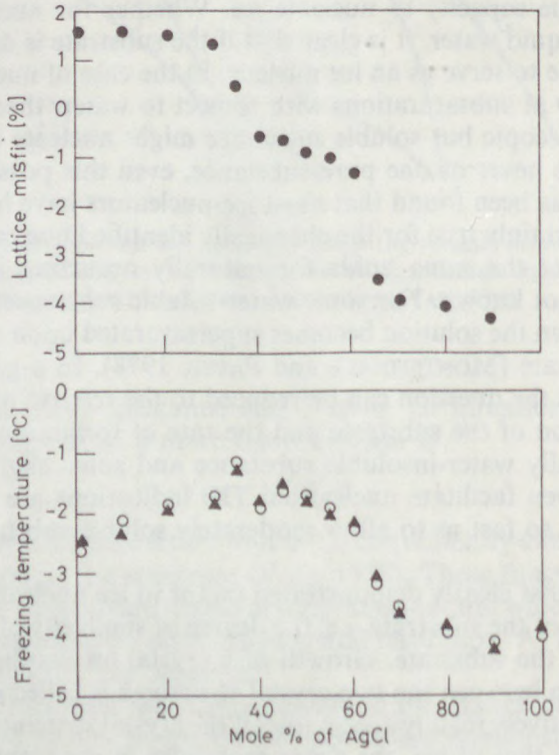

Fig. 4.10

The freezing temperature for various composition AgI–AgCl nuclei is closest to 0° C when the lattice misfit with respect to ice is nearest to zero. (PALANASAMY *et al.*, 1986)

to ice could be varied by adjustments of the composition. A direct relationship between the closeness of fit of lattice parameters to ice and ice nucleating ability was found. Similar experiments were reported for AgI–AgCl solutions by PALANASAMY *et al.* (1986) with the same conclusions. Their results are reproduced in Fig. 4.10. The upper diagram shows the variation of the percent difference between the ice lattice and the AgI–AgCl lattice parameter, which was measured by X-ray diffraction. The lower diagram shows the corresponding nucleation thresholds for 1:1000 suspensions of the sample in water. The highest freezing temperatures were observed for the closest match between ice and the substrate.

A special case of epitaxial growth is observed on some organic crystals, which have lattice dimensions quite different from that of ice, yet ice crystals grow with uniform orientations, and the nucleation thresholds are just few degrees below 0 °C. FUKUTA and MASON (1963) suggested that the arrangements of the hydrogen-bonding groups determine the nucleating abilities of such crystals.

A theoretical argument can be made for the influence of the substrate in terms of the influence it has on the entropy of the water molecules in the embryo. Hydrogen atoms are continually changing positions from near one to near the other oxygen atom along any O—H—O bond, so that ice has a certain inherent residual entropy, or disorder. If interaction with a substrate tends to restrict the hydrogen atoms then the entropy of the embryo is decreased and the bulk free energy of the ice away from the surface is increased. That, in turn, means a reduced possibility for ice nucleation. Calculations of the ordering effect of the substrate have been given by FLETCHER (1959) and by FUKUTA and PAIK (1973) showing that the entropy effect may alter the effectiveness of crystal surfaces, giving, for example, better nucleation on the prism faces of AgI and PbI_2 then on their basal faces. Clearly, this is an important factor in substrate–embryo interactions, but very difficult to quantify, and even more difficult to isolate from the other factors which come into play. Consequently, no direct experimental proofs of the effect have emerged.

At least for some effective ice nucleators, there is evidence that the formation of ice embryos should not be viewed as taking place in a three-dimensional spherical cap shape, but rather to be proceeding via the formation of two-dimensional ice. The presence of a layer of ice, one or two molecules deep, was invoked by EVANS (1967) and EDWARDS *et al.* (1970) to interpret the observations that once water drops containing certain nucleants were exposed to temperatures below T_w while maintained in the liquid state by high pressures, and not heated to above T_M, they subsequently froze right at the melting point (without supercooling). The values of T_W were, for example, −15 °C and −20 °C for phloroglucinol-dihydrate and mercuric iodide, respectively, while T_M was 0 °C for both. The insensitivity of $(T_M - T_W)$ to pressure, for any given substance, and the apparent presence of ice on the substrate surface within the bulk liquid sample led to the suggestion that a two-dimensional layer of ice is involved. Lowering the temperature below the melting point allows the two-dimensional ice layer to nucleate the rest of the volume without supercooling.

The implications of these observations, in terms of modifications of nucleation theory by the inclusion of line tension, are presented by KNIGHT (1973) and EVANS and LANE (1973). To what extent would the tendency toward the formation of two-dimensional ice patches play a role in the nucleation of ice without the preconditioning used in EVANS' experiments, is a matter of conjecture at this time. In fact there are a number of other observations of memory effects, i.e. where the previous temperature or humidity history of the sample influences its nucleating ability. Some of these phenomena are probably due to modifications of the substrate surface itself, while others are probably related to something akin to the two-dimensional ice.

Influences of surface irregularities

In the foregoing discussion, surfaces were treated as if they were totally uniform, so that ice nucleation would have an equal chance of starting at any point on the surface. This is a simplification, since even in the epitaxial nucleation observations mentioned above it was noted that the growth of ice crystals on the substrate surfaces starts, and repeatably takes place, at certain specific locations, such as steps in the crystal face, dislocations, pits, etc. In fact, only the epitaxial growth experiments from the vapor, which can be carried out under a microscope, allow direct visual identification of the areas where nucleation has taken place. Even in these experiments considerable growth has to take place after nucleation for the crystals to become visible. The nucleation event itself is of the scale of only tens or hundreds of molecules, and there are no methods available to observe those events. Hence, the specific locations of nucleation events cannot be subjected to examination. In the following, we discuss the evidence which demonstrates the role of surface sites in nucleation, the empirical evidence regarding the properties of the sites, and the theoretical analyses attempting to provide a general description of this mode of nucleation.

That steps and other crystal irregularities can be the sites of ice nucleation on silver iodide and other crystalline substrates was already noted by BRYANT *et al.* (1959), and subsequently confirmed by numerous authors. In material science the phenomenon was well established even before that (e.g. TURNBULL, 1950). FLETCHER (1960) incorporated the geometries of steps and corners into the calculation of the free energy of embryo formation. ANDERSON and HALLETT (1976) showed that, for CuS and AgI, nucleation sites for ice formation from the vapor occurred at the same locations on the surface in many repeated tests.

Another interesting way that sites can arise was discovered by observing changes in the ability of silver iodide to nucleate ice when silver iodide is irradiated with ultraviolet light. Metal halides in general, and silver iodide in specific, are light sensitive; the effect being a dissociation of the molecules followed by oxidation or other chemical reactions, depending on impurities present in the material, or on other species in contact with the surface. The experiments of ROWLAND *et al.* (1964) showed the photolytic effect very clearly.

Silver iodide crystals prepared and maintained in dark, or under red light only, were ineffective as ice nucleants, but when exposed to ultraviolet light, nucleating ability rose rapidly. The effect reversed after about five or ten minutes of irradiation – an observation which was reported previously by many authors. The loss of activity due to sunlight was of particular concern in the use of AgI as a cloud nucleating agent. GARVEY (1973) reported that, for AgI particles in water drops, the activation effect of UV radiation was reversible; within minutes of irradiation the activity rose, and within minutes of near-darkness the activity decayed. ANDERSON and HALLETT (1976) observed that the numbers of sites for ice nucleation from the vapor increased with illumination, but the specific locations of the sites were not always the same in repeated tests. The evidence points toward the formation of clusters of silver or silver oxide molecules which are better nucleation sites than the pure surface. Many aspects of this phenomenon are still not clarified, but the conclusion is clear that crystallographic fit is not a sufficient criterion for ice nucleation activity.

Substrate surfaces exposed to water vapor will have some adsorbed water molecules on the substrate. There appears to be an improved chance for ice nucleation when the adsorbed water is in small clusters, due to the presence of hydrophilic patches on a generally hidrophobic surface (ZETTLEMOYER *et al.*, 1961). The hydrophilic (water-attracting) sites were thought to be steps, or oxide sites. By treatments silica surfaces could also be made to have hydrophilic sites over about half of the total surface, with a corresponding increase in ice nucleating effectiveness (BASSETT *et al.*, 1970). On the other hand, the formation of more complete adsorbed layers have the opposite effect, probably due to lesser likelihood of ice embryo formation in a more strongly held water layer than in the small patches which are surrounded by areas where the water molecules interact only weakly with the substrate (MORACHEVSKY *et al.*, 1972; LEVKOV and KONSTANTINOV, 1975).

From the experiments of FEDERER (1968) and of PRUPPACHER and PFLAUM (1975) it also became evident that the electrical properties of the surfaces also influence their ice-nucleating ability. FEDERER showed that the doping of semiconductor materials, which change its electric conductivity, altered the adsorption of water and the density of sites for nucleation of ice from the vapor. Working with a ferroelectric substance, PRUPPACHER and PFLAUM found that the most active nucleation sites were located at the boundaries of positive and negative charge regions, and related this finding to the surface diffusion of water molecules toward these regions.

It should be recognized that the concept of nucleation sites does not imply just one type of specific configuration with a corresponding well-defined temperature of nucleation. ANDERSON and HALLETT (1976), for example, observed that each site on the substrate surface tended to nucleate ice at a given supersaturation, with good repeatability of those values over several nucleation and evaporation cycles. DORSEY (1948), VALI (1968), GENADIEV (1971), and many others have noted that water droplets taken from the same sample might freeze at different temperatures, and there is a strong tendency for each drop to retain

its freezing temperature in many repeated tests. It seems clear that even on apparently uniform surfaces, or in populations of apparently uniform particles, there is always a diversity of different nucleation sites present. The activity of each site might be defined by a "characteristic temperature" which corresponds to an arbitrarily chosen value of the nucleation rate on that site (VALI and STANSBURY, 1966). There is clear connection between the relative numbers of sites at different characteristic temperatures in a sample and the activity spectra defined by Eqs (4.9), (4.10) and (4.11). The connection is then established by considering the probability distributions of sites on particles of various sizes which are present in the particular sample. There is also a certain degree of time dependence in the connection between site characteristics and the activity spectra; this will be discussed in more detail later.

The influence of sites was included in the thermodynamic theory of ice nucleation by FLETCHER (1969). He modelled sites as circular paths with $m = 1$ (i.e. ice-like), the sizes of the sites having a statistical distribution leading to a corresponding distribution of nucleation temperatures. By assuming a fixed form of that distribution, and with the portion of particle surface covered by sites as an adjustable parameter, the fraction of aerosol particles becoming ice nuclei at given temperatures could be calculated. These predictions have not been subjected to empirical verification, due to the lack of information about the parameters used in the calculations, but the treatment effectively illustrates the concept of nucleation by sites.

In total, the evidence is strong that the nucleation of ice takes place on specific surface sites. There are many different kinds of sites, some major types having been identified, so that the activities of materials have to be considered in terms of the distributions of characteristic temperatures. The threshold temperatures discussed earlier can be viewed as indicators of the temperature at which the number of active sites increases, usually quite rapidly, past the detection threshold of the experiment.

Other influences

The fact, that relatively minor surface features on a substrate can form nucleation sites, demonstrates that embryo formation can be significantly influenced by subtle interactions on the scale of small numbers of molecules. In that light, it is not surprising that nucleation can also be influenced in several other ways, principally by alterations in the time variations of temperature and supersaturation, and by changes in the chemical environment of the nucleating site. Where they occur, these effects can be substantial, so that they deserve mention, but of their many different manifestations only a few can be discussed here.

The so-called memory effect has been best examined for minerals (ROBERTS and HALLETT, 1968). The effect is similar to that discussed earlier for two-dimensional ice formation, except that in this case the formation of bulk ice appears to be required. Observations show, that once ice has formed on a sample from the vapor, evaporation of that ice appears to leave small patches of ice in

cavities, or other features, so that ice nucleation can take place at smaller supersaturations on subsequent occassions. Whereas the values of T_2 and S_2 (referring to Fig. 4.5) were in the vicinity of -20 °C and 20% for most of the minerals for the formation of ice the first time, those values changed to around -12 °C and 14% after all visible ice was evaporated but the sample not exposed to relative humidities less than about 30–40%. The duration of exposure to low humidities also had an influence; longer times were more likely to destroy the memory effect. Similar observations of a memory effect for ice formation from the liquid were reported, for example, by REISCHEL (1987). One interpretation for the memory effect, originally given by TURNBULL (1950), is that small volumes of solids can remain in thermodynamic equilibrium above the bulk melting or vaporization points if they are held in cavities, so that the curvature of the surface toward the liquid or vapor is negative (concave). Adsorbed layers are also known to have lower vapor pressures than the bulk material. While these alternative explanations are both plausible, without the ability to study nucleation sites in detail, the precise mechanism of the memory effect cannot be established either. The effects here discussed are not unique to ice; similar phenomena have been observed with the phase changes of other materials.

The nucleation of ice can be significantly influenced by the presence of a third component in addition to the substrate and water. This might be anticipated, since the presence of the other substance can lead to modifications of the substrate surface, for example by partial dissolution, or there may be competition between the substance and water molecules for adsorption (nucleation) sites. Studies of such three-component systems show some strong influences on nucleating activity. For freezing nucleation, REISCHEL and VALI (1975) showed that the influence of dissolved substances depends on the composition and concentration of the dissolved species, and on the type of nucleating substrate involved. For example, organic soil nuclei used in their tests were practically insensitive to twenty or so species of dissolved salts. Silver iodide, on the other hand, could be influenced very strongly: at the extremes, NH_4I at 0.1 molal concentration increased the freezing temperatures of the suspension by over 4 °C, while CsI at the same concentration decreased freezing temperatures by nearly 12 °C. The soil nuclei and the AgI suspension by themselves had very similar nucleus spectra in these tests. Some even stronger effects were reported by REISCHEL (1987). PARUNGO and LODGE (1967), and REISCHEL (1984) showed that some dissolved gases can also change nucleating temperatures, by as much as 3 °C. There is no clear evidence yet for similar effects with deposition nucleation, but the addition of gases to cloud chambers (where nucleation may take place by either by freezing or by deposition) has been found to alter nucleation, but the addition of gases to cloud chambers (where nucleation may take place either by freezing or by deposition) has been found to alter lead to strong changes in the nucleating ability of the substrate. Explanations for these effects probably lie in the adsorption or formation of reaction products at specific locations on the substrate; the result might be the creation of ice nucleating sites of superior effectiveness, or the covering of sites in the substrate

so as to reduce their ability to nucleate ice. The importance of three-component systems in the atmosphere can be expected to be considerable, in view of the fact that most atmospheric aerosols contain both soluble and insoluble components. There is also the potential for pollutants to influence ice nucleation, by activation or deactivation of natural ice nuclei. Information on these matters from atmospheric observations is very scant at this time, because of the difficulties of isolating these effects from the many others influencing ice nucleation. This remains an important area to study in the future, as the chemistry of clouds becomes better known.

Early literature on the supercooling of water and the nucleation of ice frequently discussed the common observation that sudden mechanical disturbance of supercooled water can lead to solidification. A definitive study of this dynamic nucleation phenomenon has never emerged, since it is practically impossible to seperate the effect of the mechanical disturbance from modifications of the surfaces in contact with the water (the container and the suspended particles). The most likely explanation for the observations is, in fact, that nucleation is initiated at the moving interface between the water and some foreign surface. Whether there are practical manifestations of such phenomena outside the laboratory is not known, even though it is not difficult to imagine situations where that could be the case.

4.4.4 Some macroscopic factors

The preceding section focussed on the factors determining the formation of ice embryos on the scale of the embryos themselves, i.e. the molecular scale. In practical terms, ice nucleation is controlled, in addition to the molecular-scale phenomena, by the sizes of the nucleating particles, by the volume of the sample and other macroscopic factors.

The size-dependence of ice nucleation is of special concern in experiments or practical situations where the nucleating material is in the form of small particles—aerosols or colloids. The question is how does nucleation activity depend on the size of the particles. Intuition would suggest that smaller particles are less likely to be effective, but there could be various manifestations, and various underlying reasons, of that trend. Theoretical basis exists to expect that the curvature of the surface plays a role, as was shown in Figs 4.5 and 4.6; this effect derives from the change in embryo volume depending on the shape of the contact surface with the substrate. As the figures show, the radius-dependence is not simple. Another expectation, most widely held, is that the surface area of a particle is the prime factor, by determining the numbers of nucleating sites to be found on it. This follows directly from the earlier discussion in which the areal density of nucleating sites was considered. The manifestation of this dependence in terms of size vs. nucleation temperature is then determined by (i) the spectrum of site density as a function of temperature, and (ii) the probability distribution of finding sites of given characteristic temperatures on

particles of given sizes. The latter can be deduced from a Poisson distribution, if the surfaces of all particles are assumed to have the same average properties; the former needs to be determined empirically. The problem thus becomes quite complex, exacerbated by the fact that particles of different sizes derived from the same material might in fact differ in surface structure, and that crystalline surfaces are not isotropic. Perhaps the best experimental evidence for activity in proportion to surface area was provided by EDWARDS *et al.* (1962), for monodisperse preparations of AgI particles. For natural samples, from the atmosphere or from precipitation, for example, size dependence takes on the added complexity that particles of different sizes will have rather different chemical compositions and physical structures. Empirical evidence for such systems will be presented in Section 4.5.

A more readily answered question is how does nucleation depend on the volume of the sample being examined. There is a long history of speculations and observations on this point, but, finally, the answer turns out to be quite simple. If the nucleation of a sample is caused by particles suspended in its interior, then the volume of the sample determines the probability of finding nuclei of given characteristic temperatures in it. For samples in contact with a surface of greater nucleating activity than the particles suspended in it, then the area of contact is the determining factor. Many of the confusing findings of early experiments came from not knowing which of the cases applied. The situation of greater importance is that of samples isolated from nucleating surfaces; certainly that is the case with cloud and rain drops, and that is what is attempted in laboratory experiments. Making the assumption that a population of samples, let's say drops, are all derived from the same bulk sample, the probability that a given drop will contain nuclei with certain characteristic temperature can be calculated if one knows the average concentration of such nuclei per unit volume of the bulk sample (LANGHAM and MASON, 1958; VALI, 1971; PITTER and PRUPPACHER, 1973). The mean freezing temperatures of drops of different size groups will vary depending on the spectrum of nucleus concentration with temperature. For an exponential spectrum, the average freezing temperature varies with ln V, where V is the volume for the size range considered. For more complex spectra, the volume-dependence is also more complex.

Up to this point, emphasis was placed on the determination of nucleation temperatures, or supersaturations, by the distribution of characteristic temperatures of the nucleating sites, even though it was recognized at the onset that nucleation has to be considered in terms of the rate of critical embryo formation. That implies a time-dependence of the process, which is totally inherent to nucleation under all circumstances. The reason why this fundamental aspect is of lesser importance than site characteristics is that the rate of nucleation for a given site is a very rapidly varying function of temperature, quite similar to that shown for homogeneous nucleation in Section 4.3. To translate that time-dependence to the typical situation where the temperature is lowered at some steady rate, the impact of the probabilistic nature of embryo growth is about 1 °C change in average nucleation temperature for a tenfold increase in the rate

of cooling (VALI and STANSBURY, 1966). Faster cooling results in colder nucleation temperatures. There is a more apparent impact of time-dependence in a sample held at constant temperature: whereas, if nucleation depended solely on temperature, there would be no nucleation taking place at a constant temperature, observations in fact show small numbers of nucleation events taking place over periods of tens of minutes, with the frequency of events diminishing as time goes on. Time-dependence of freezing nucleation is well demonstrated by the experiments of VONNEGUT and BALDWIN (1984) and WANG and VONNEGUT (1984): if a sample is held at some temperature < 0 °C until nucleation takes place, then melted, and this cycle is repeated many times, it is observed that the lapse of time until nucleation is initiated varies from a few seconds to tens of minutes in an apparently random fashion. The relationship between this type of time-dependence and the activity expressed in terms of temperature spectra has not yet been clearly formulated; it appears that time is an important factor if a sample is held at a temperature where there are many nuclei with slightly lower characteristic temperatures.

It is evident from an overview of this chapter that heterogeneous nucleation is a very complex phenomenon, easily influenced by numerous factors. Experimental studies of heterogeneous nucleation are faced with considerable difficulties in attempting to vary independently only one or two of the parameters of importance. Theoretical descriptions have developed considerable power of generalization, but they need more concrete conceptual pictures of the physical configurations of nucleation sites. Careful experimentation and theoretical advances will hopefully lead to some unification of apparently disparate nucleation phenomena.

4.5 Ice nucleation in the atmosphere

4.5.1 Modes of atmospheric ice nucleation

The concepts of ice nucleation, the characteristics of ice nuclei, and the factors influencing ice nucleation—topics described in the preceding section—apply in their full generality to the atmosphere. In fact, much of the study of ice nucleation was motivated by interest in the formation of ice in the atmosphere, and by the expectation that clouds and precipitation can be influenced by seeding with artificial ice nuclei. Yet, to maintain a greater degree of generality, the discussion of ice nucleation up to this point was not given with specific focus on atmospheric processes. This section takes that turn, and presents aspects of the problem which pertain specifically to the atmosphere.

The two fundamental modes of ice nucleation have already been introduced: freezing of supercooled liquid water, and deposition of supersaturated water vapor. The temperatures required for homogeneous freezing are reached in the upper troposhere and in the stratosphere, so there is every reason to expect that some ice in the atmosphere could be formed by that process. Less certain is

whether droplets free of hetero-nuclei can indeed exist or not. The relative scarcity of ice nucleating particles, in comparison with cloud condensation nuclei and other aerosols, would suggest that homogeneous nucleation in pure systems is unlikely, but we do not have good information on which to base the comparison for temperatures lower than about −20 °C and those approaching the homogeneous threshold. Homogeneous nucleation in haze droplets (high-concentration solution droplets) is suggested by some observations, but, for those situations also, the role of insoluble materials remains to be resolved.

The behavior of nucleating materials with respect to the freezing and deposition was illustrated in Fig. 4.7. Actual data, for specific substances, differ in details from the pattern shown in that figure (SCHALLER and FUKUTA, 1979; FUKUTA, 1985; DETWILER and VONNEGUT, 1981; and many others), but that scheme can serve as a good first approximation and generalization.

Examples of the two basic modes of ice nucleation are easy to find in the atmosphere. Cloud droplets or raindrops may freeze due to nucleation of ice on a particle contained within them. A particle exposed to supersaturation with respect to ice, but subsaturation with respect to water, may have deposition nucleation take place on it, followed by continued growth of the ice from the vapor. On the other hand, looking at a snow crystal, or other form of ice particle, one can not readily tell what mode of nucleation was involved in its formation. There are quite a large number of possibilities beyond the basic ones of freezing and deposition, and all the different modes of nucleation have to be dealt with distinctly, as shown by experience. The reason for the added complexities lies with the sensitivities of nucleating materials to their history of interactions with water, either in liquid or vapor form. Some of these relatively subtle processes have been described in Section 4.4. Because the vast majority of atmospheric aerosol particles are of mixed composition (not single chemical compounds), their interactions with water are even more varied, leaving yet more room for variations in the way ice nucleation proceeds on them. Much is yet to be learnt about these processes; the description to be given here emerged from many decades of studies, but even so, it is clearly not complete.

One of the extensions of the modes of ice nucleation is needed to allow for the possibility that a particle, at some temperature below 0 °C, might serve as a condensation nucleus (CCN), and have ice nucleate on it immediately. By nucleating ice at an early stage of condensation, when both the chemical and physical state of the water might be different from bulk, pure water, or by avoiding partial dissolution of the particle following condensation, the ice-nucleating activity of the particle might be greater than it would be with the same particle immersed in bulk liquid. These mechanisms are not yet proven; they are broad hypotheses, which correspond to likely sequences in cloud formation, and which warrant consideration of condensation-freezing nuclei as a separate class. Over the last few years, attempts have been made to isolate this mode of ice nucleation in measuring instruments (see Section 4.5.2), but there is not enough information yet to gauge the significance of this mode. A possibility of considerable significance was recognized by ROSINSKI *et al.* (1975), and

GAGIN and NOZYCE (1984): in the vicinity of growing hailstones, and near large drops at their moment of freezing, there is a region of high supersaturations, so that there is a potential for condensation-freezing nucleation to take place on aerosol within that zone. Deposition nucleation can also take place there, but the majority of aerosol particles are likely to act as condensation nuclei at the high supersaturations present in these situations.

Another mode, whose importance is more clearly established, is contact-freezing, which is nucleation of ice at the instant when a particle makes contact with a supercooled water droplet. Clearly, the number of such contact-freezing events depends both on the concentration of nuclei in the air, and on the rate at which those nuclei collide with cloud droplets. The collisions may be brought about by diffusion, inertial capture, phoretic forces, etc.; processes which are dependent on particle size, and on environmental conditions. Since the collision processes are relatively well known, experimental results which conform to the predicted rates of particle collection can be interpreted as being due to contact freezing (e.g. DEMOTT *et al.*, 1983). Experiments in which nucleating AgI aerosol was tagged with a flourescent tracer, and the tracer particles were detected in the ice crystals, were also interpreted as evidence for contact-freezing (KATZ and PILIE, 1974).

The mechanism of contact-freezing is not clearly established. One possibility is that nucleation might be favoured when the nucleating particle is in the somewhat ordered surface layer of the droplet. COOPER (1974) recognized that while particles are in the air within a cloud (colder than 0 °C), they are exposed to supersaturations with respect to ice, and will have an equilibrium population of ice embryos. When such a particle comes into contact with a water droplet an embryo of subcritical size for deposition might be large enough to nucleate ice in the water, since the critical size for freezing is smaller than for deposition. The predictions of this theory seem to be in fair agreement with the limited sets of observations with which it can be compared. FUKUTA (1975) criticized COOPER's suggestion and put forth a theory based on the movement of the liquid-air interface at the moment of contact and the associated high transient free energy condition. The only specific test of this theory is the prediction that contact-freezing nucleation would be preferred on hydrophobic materials. For the organic materials in FUKUTA's tests this condition was fulfilled. Additionally, it may be surmised that the phenomenon of contact-freezing is related to the initiation of phase change by a dynamic disturbance (vibration, shock, etc.), although it is certain that contact-freezing is also a function of the specific property of the nucleating substance, not just of the mechanical action of the contact. Clarification of the alternative lines of explanation will require further experimental evidence.

To distinguish the simplest form of freezing nucleation from the others just described, the case when freezing is initiated from a particle suspended in the interior of the water (droplet or other bulk volume) is called immersion-freezing. There is not much more to be added to the discussions of this process given in the previous chapter. For a full description of how immersion freezing would

be manifested in a cloud, one has to also consider how the particles originally enter the droplets. This is the same question as for contact-freezing, but here the two processes are independent except that collection has to precede freezing.

The nucleation modes described above are, it is easy to realize, limiting cases of a continuum of intermediate possibilities in which the precise duration of contact, immersion, etc., the amount of water involved, the position of the particle within the drop, and other conditions, can vary. There is considerable uncertainty about how each of those factors affect nucleation probability. It was observed, for example, that AgI particles impacted unto supercooled water drops produced freezing events over a period of several minutes following the contact yet continued immersion led to a loss of activity (VALI, 1976b). Were the AgI particles in these experiments changing with time due to the contact with water (like dissolution); or, were they penetrating the surface film of the drops only gradually; or, was it simply a matter of the time-dependence discussed in Section 4.4.4? Such phenomena are difficult to interpret, and will require careful experimentation to elucidate. In any case, the distinctions among nucleation modes are necessary and useful approximations for describing the mechanisms of ice nucleation in the atmosphere. In modeling cloud and precipitation processes, each mode has to be considered separately and specifically, because of the differences in how they depend on environmental and cloud conditions. As the next section will show, there is yet a dearth of empirical data for such detailed modeling, but hopefully the situation will improve rapidly.

4.5.2 Measurements of atmospheric ice nuclei[1]

In view of having to consider different ice nucleation modes, measurements of atmospheric ice nuclei can follow one of two general approaches: (1) to attempt to recreate particular atmospheric conditions in an apparatus and observe the numbers of ice crystals which develop, or (2) to perform separate measurements for each mode of nucleation, with appropriate variations of the controlling conditions, and superpose the results for given atmospheric conditions. The former is termed the simulation approach, and the latter the mechanistic approach.

The simulation approach was at the heart of the earliest ice nucleus measurements (FINDEISEN and SCHULZ, 1944) conducted in a cloud chamber. In such instruments a cloud is created inside a refrigerated enclosure (of about 0.1 to 1 m^3 volume) either by mixing of humid and cold air or by expansion and the numbers of ice crystals which form are counted by one of several methods. Depending on the method of cloud formation distinction is made between "mixing chambers", rapid or slow "expansion chambers", and others. Temperature is the main adjustable variable in these instruments, with about -6 to

[1] The material in this section, and the following one, is drawn, in part, from the review of VALI (1985).

– 25 °C as the practicable range. In the use of many subsequent cloud chamber devices adequate simulation of atmospheric conditions was assumed to be assured simply by the presence of numerous cloud droplets. However, intercomparisons of different cloud chambers and calculations showed that normally uncontrolled variables influence the results to significant degrees. The concentrations and sizes of cloud droplets, the duration of the cloud, the supersaturation involved in forming the cloud, and other parameters, were found to alter the results by large factors (BIGG, 1971; HALLETT, 1972; KNIGHT, 1979; FUKUTA, 1982; and others). Hence, the conclusion became inescapable that different atmospheric cloud conditions have to be reproduced very carefully in order to obtain valid measurements, but there are major instrumental difficulties in controlling the numerous relevant parameters. Even without adequate simulation of atmospheric clouds, the cloud chambers can yield relative measurements, and are in frequent use for the assessment of artificial ice nuclei sources (AgI generators, etc.). Extrapolation of cloud chamber results to atmospheric clouds can also be attempted, but requires quite detailed knowledge of conditions in the chamber and assumptions about the relative contributions of different nucleation modes to natural ice nuclei. The approach which appears to hold most promise toward realistic simulations is to use large chambers in which the air can be expanded at rates corresponding to realistic updraft velocities in clouds and to adjust the initial CCN concentration to well represent the natural situation. Such controlled-expansion measurements have a good possibility of reproducing ice initiation in convective updrafts. Slower updraft velocities and longer cloud lifetimes which correspond to other cloud types are more difficult to simulate. For the measurement of natural ice nuclei an important limitation arises from the fact that sampling is restricted to the location of the installation due to the large size and complexity of the chambers.

Cloud chambers are one of the main laboratory techniques for investigations of the activities of materials. Careful evaluation of processes within the chambers have led to clearer interpretation of the results. DEMOTT *et al.* (1983), GORBUNOV *et al.* (1987) and PASHENKO and GORBUNOV (1987), among others, show how the cloud chamber results can be refined by analyses of the time rates of development of ice crystals, and by accounting for the competition of particles for available vapor. These results are encouraging, and perhaps will lead to renewed application of cloud chambers to atmospheric measurements.

Of the individual ice nucleation modes, immersion-freezing can perhaps be studied most readily experimentally. As mentioned before, partition of a sample into many small drops allows the observation of nuclei of different characteristic temperatures. More active nuclei cause freezing of the drops in which they happen to be located, while leaving other portions of the sample to be frozen at lower temperatures. Of course, with high concentrations of nuclei per unit volume, the probability that more than one nucleus is found in a drop has to be accounted for. The method of determination of nucleus spectra (number of nuclei per unit volume as a function of temperature) has been presented by VALI (1971).

Freezing experiments with rain and snow samples have a tradition of over a hundred years; they gave the first indication of the degree of supercooling which might be expected in clouds. Even today, this method of atmospheric sampling —considering precipitation as both an active and a passive sampler—yields the best indication that the atmosphere has ice nuclei active at temperatures as high as -5 °C. Clearly though, interpretation of the measured nucleus concentrations in precipitation in terms of nucleus concentrations in the air is far from simple and can never be really unambiguous. Precipitation elements may be initiated in clouds by ice nuclei, but they may also collect from the air some aerosol, and hence nuclei, during their growth. Plus, the nuclei may undergo changes in the water either before or after collection. Cloud droplets provide better samples because of their less complex history, but the collection of cloud liquid water is not done with the same ease as the collection of precipitation. Cloud water collection as rime, on mountain peaks immersed in supercooled clouds, is a relatively easy procedure which could probably see more extensive use, but collection of cloud water from aircraft, with good efficiency and without contamination, has proven to be quite a difficult task.

Deposition nucleation measurements have been most widely attempted by the so-called filter method originally introduced by BIGG *et al.* (1963). While often viewed as a general method of activation of ice nuclei not restricted to deposition, the best use of the method is for the activation of nuclei from the vapor. Aerosols are sampled with high-efficiency membrane filters, and are placed into a chamber in which temperature and humidity can be independently controlled. The filters rest on a lower cold-plate of the chamber, while the upper plate, in close vicinity to the filter, is coated with ice and is kept at a slightly warmer temperature than the lower plate. A supersaturation with respect to ice is created thereby at the filter surface; the magnitude of the supersaturation can be controlled by the difference in temperature between the two plates. Water saturation can also be reached, and perhaps slightly exceeded. The number of ice crystals which grow on the filter, after 10 to 20 minutes of development, divided by the volume of air which was sampled, yields the concentration of nuclei for the given supersaturation. Because of the ease with which filter samples can be collected, and the possibility of processing the samples subsequently, the method is well suited for field work, and has been widely used, including a worldwide network for a period of time.

As always, there are drawbacks to the filter method. Most serious are the problems which arise from the fact that aerosols, which were widely dispersed in space originally, become compressed on the filter surface. Since some of the particles are hygroscopic, they are sinks of water vapor and therefore diminish the supersaturation produced by the ice source in the chamber. This volume effect (so called since the degree of vapor depletion depends on the number of hygroscopic aerosol on the filter, and in turn, on the volume of air which was sampled) has been extensively investigated, and various correction schemes have been worked out to remove the interference (KING, 1978; ZAMURS *et al.*, 1977; BEREZINSKII *et al.*, 1980; TANAKA, 1982). Continuous, laminar airflow in the

chamber has also been used in order to reduce the depletion effect (e.g. LANGER and RODGERS, 1975). The success of even that measure is limited though, since chemical interactions between the dissolved aerosol and the ice nuclei introduce further complications. Overall, because of variabilities in the hygroscopic component and chemical composition of natural aerosols, and because of suspected variabilities in the sensitivities of ice nuclei to the interactions on the filter, no scheme has been found adequate for all applications. The development of haze particles, or of water drops, on the filter also calls into question the specificity of the method for deposition nucleation. Other modes may also contribute to the observed ice crystal count, and the unknown degree of contribution makes interpretation of the results difficult.

Impactors have been also employed as an alternative to filters for collecting atmospheric aerosol samples. This technique allows the aerosol to be divided into size categories (by using a multi-stage impactor of varying impaction velocities), so that the size-dependence of ice nucleation can be examined together with the temperature and supersaturation dependence (e.g. BEREZINSKII and STEPANOV, 1986). However, the problems discussed above are not circumvented in this method either, so that the results are not unambiguous.

Measurements of contact-freezing nuclei have been attempted by allowing particles to contact supercooled water drops in a cooled chamber, and observing the freezing of the drops either by noting the signal from the thermocouple on which the drops are supported, or by other methods. The mechanism relied on for producing the collection of particles by the detector drops can be Brownian diffusion (GUENADIEV, 1970; DESHLER, 1982), or the aerosol can be forced into contact with the drops by electrostatic forces (VALI, 1976b). These methods simulate the atmospheric process of contact between aerosol and droplets reasonably well, but the calculation of collection efficiencies is somewhat uncertain. The instruments have been used only in the laboratory up to this point; field application awaits further development of the method. The specificity of this approach is somewhat limited by the possibility that deposition nuclei also become activated in the vicinity of the sample drops prior to making contact with the drop. While this is a detraction as far as separation of nucleation modes is concerned, it is likely, that the same process takes place in the atmosphere also, although perhaps not with the same time scale. Another method is explored with the two-section chamber of GORBUNOV *et al.* (1986): a fog is formed and precooled in an upper chamber, forced to enter the lower chamber where the test aerosol was previously admitted. The resulting ice crystals are formed, most probably, via contact nucleation, but the activation of deposition nuclei cannot be excluded, so the evaluation of nucleation modes is not completely clear here either.

In order to properly account for contact nucleation in clouds, it will be necessary to determine activity as a function of particle size, since the rates of collision between cloud droplets and particles is strongly dependent on the size of the aerosol. For small particles, diffusion is the main mechanism leading to collisions, whereas large particles make contact with cloud droplets as a result of inertial impaction. Near 0.1 μm diameter neither mechanism is very effective.

Condensation-freezing nuclei are perhaps the most difficult to measure, since a two-step process is postulated. Attempts at developing instruments which are specific to this process have shown promise, but have not yet reached the stage of field use. The basic idea used in these instruments is to produce a flow of air between two plates, or cylinders which form a diffusion chamber, just as in CCN counters. The two boundary surfaces are covered with uniform ice layers and are maintained at slightly different temperatures to produce a supersaturated region near midway between the two plates. Ice crystals which develop in the air stream are counted at the exit from the chamber. Detection of the crystals is either by collection in a supercooled sugar solution layer (in which crystals grow slowly enough not merge, and can therefore be counted visually), or by optical scattering (relying on the fact that ice crystals grow faster in the chamber than cloud droplets). TOMLISON (1980), ROGERS (1982) and AL-NAIMI and SAUNDERS (1985) have described such continuous-flow diffusion chambers. By

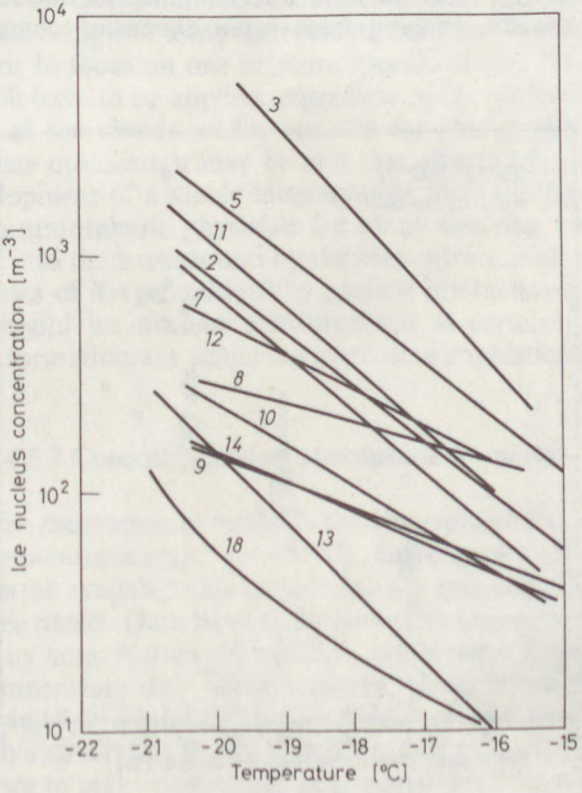

Fig. 4.11

A comparison of the ice nucleus concentrations observed with different instruments which were sampling outdoor air simultaneously during the Second International Workshop on Condensation and Ice Nuclei. Each line represents the average spectrum for a given device, for observations taken during the four days of intercomparisons. Descriptions of the instruments can be found in the original report. (BIGG, 1971)

varying the temperature difference between the plates, these instruments can be used for activation of deposition nuclei at a range of subsaturations with respect to water, or just at water saturation. Observations with these instruments confirm the noteworthy finding made first with filter measurements that there is no discontinuity in the numbers of activated nuclei when water saturation is reached. This result must have a fundamental significance regarding the way ice nuclei become activated, but, at the same time, raise a fundamental question about the validity of attempting to distinguish between different modes of activation. Once again, the problem will have to be investigated in much more detail than has been done so far.

It is clear from the foregoing, that the mechanistic approach as well as the simulation approach have many limitations, and that neither is yet capable of providing reliable information on atmospheric ice nucleus concentrations. The magnitude of the problem of ice nucleus measurements can be illustrated by the results of intercomparisons of instruments carried out in two international workshops. Figure 4.11, from the 1970 workshop, shows nucleus spectra from several different devices, ranging from rapid expansion chambers to filters

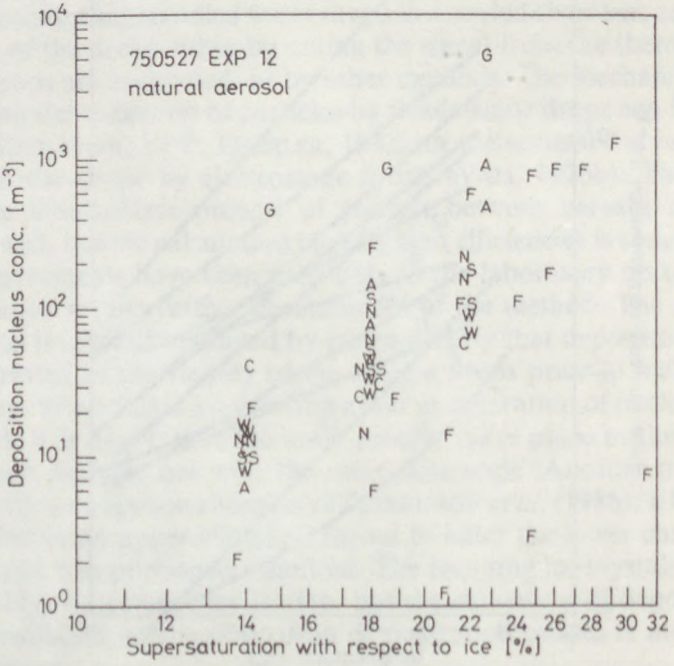

Fig. 4.12

Comparison of the ice nucleus concentrations measured on filter samples which were processed in different chambers during the Third International Workshop on Ice Nucleus Measurements. The filter samples of outdoor air were taken over a 15-minute period, and were processed over the next few hours. Each letter code denotes a different instrument. See the original report for descriptions of the instruments. (VALI, 1976a)

processed in diffusion chambers. Each line represents a variable number of measurements (20–50) over four days. The scatter of values, at any given temperature, is roughly a factor of 30; if the individual data points were included instead of the mean values for each temperature, then the scatter would increase by an additional factor of 10. Figure 4.12 is from the 1975 workshop, and shows a comparison for filter samples only; the scatter in this figure is considerably less, but still very troublesome. While some of the systematic differences among instruments have been explained in the course of analyses of the intercomparisons, it is evident that it is difficult to place much confidence in the absolute values of the measurements from any of the devices. The data shown in these figures prompted careful examinations of the detailed workings of ice nucleus measuring instruments. Those analyses would perhaps ensure that an intercomparison carried out now would yield better results than those shown in Figs 4.11 and 4.12. It is becoming clear that the first problem is to better understand the activation mechanisms of ice nuclei in general, and those of atmospheric ice nuclei (aerosol of mixed composition) in specific. That information is basic for designing and using instruments either to simulate the full range of mechanisms, or to focus on one or more specific modes. The results of the measurements will have to be applied, regardless of the approach taken, using detailed models of the clouds which account for the specific conditions of interest. With some optimism it may be said that efforts will perhaps increase toward the development of a viable measurement methodology. The solution has been eluding atmospheric physicists for many decades, and the problem itself was pushed into the background by the concentration of efforts to clarify secondary processes of ice generation (by particle interactions). Yet, the need to obtain meaningful ice nucleus measurements is certainly increasing, as models of cloud formation are achieving increasing sophistication.

4.5.3 Concentrations of atmospheric ice nuclei

The lack of reliable measurement methods for atmospheric ice nuclei, especially at the higher temperatures (say, > -15 °C), make it very difficult to extract conclusions from the available data concerning the concentrations and sources of atmospheric ice nuclei. Data have to be viewed as tentative; absolute values may be in error by large factors. In addition, while most data are reported as a function of temperature only (since temperature is, undoubtedly, the most fundamental parameter), it must be born in mind that the other factors influencing ice nucleation also have to be taken into account when using data obtained with a given device to make predictions of atmospheric ice nucleation. For the most part, this requirement cannot be fulfilled at present, so all data are used at face value as a first approximation.

One of the most comprehensive attempts to compile a global distribution of ice nuclei was that of BIGG and STEVENSON (1970). A network of 44 stations performed daily collections of filter samples. The samples were processed in one

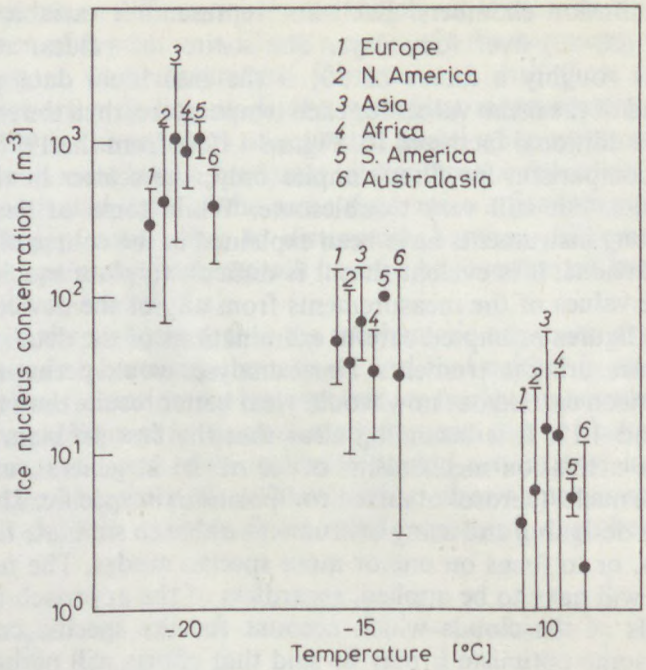

Fig. 4.13

Results of world-wide sampling of ice nuclei at 44 stations during January, February and March of 1969. Samples were taken on filters, and processed at the temperatures of −10, −15 and −20° C. Ice nucleus concentrations are expressed per m^3 of air sampled. (After BIGG and STEVENSON, 1970)

central laboratory; while this approach removed many of the usual instrumental variabilities, some doubts remained about the stability of the samples between the time of collection and processing, and about the performance of the processing system used. Even with those reservation, the results provide an indication of the differences in concentrations among the sampling sites. The results are shown in Fig. 4.13. Perhaps the most striking information is that the differences across six continents are quite small. One could deduce from the results that the median concentrations are highest in Africa and lowest in Australia, but the factor 3 difference between the two sets of data is small in comparison with the greater than tenfold variability for any of the regions. Variability appears greatest at −10 °C, and least at −20 °C. The increase in concentration with decreasing temperature is well shown in these data: about one order of magnitude increase for each 5 °C lowering of temperature.

Another comparison is shown in Fig. 4.14, this one derived from measurements with different kinds of instruments. Each data set in this figure represents observations over a period of at least several weeks at fixed sites. The differences among the various data sets appear significant since they exceed the variabilities of the individual data sets (shown, where available, as geometric standard

deviations). Whether these differences are due to instrument performance, or are true differences, cannot be determined at this point. It is noteworthy that the slopes of the spectra are relatively uniform, again indicating factor 10 concentration changes for 5 to 6 °C temperature changes. The range of concentrations shown in this graph may be giving as good an indication as is currently available of the tropospheric concentrations of ice nuclei.

The variability of ice nucleus concentrations with time is well documented in many data sets. Over longer periods of time—days to weeks—factors of 15 to 100 in concentration encompass 90% of the data. More extreme variations are also noted occasionally. Over periods of hours, relatively steady values have been found in many observations, but sudden changes, which might amount to hundredfold in a matter of minutes, have been also recorded, for example at thunderstorm gustfronts. The reasons for most changes in nucleus concentrations are not evident in correlations with meteorological conditions.

Overall, the concentrations of atmospheric ice nuclei are only sketchily known. There is a large body of data supporting the finding that concentrations

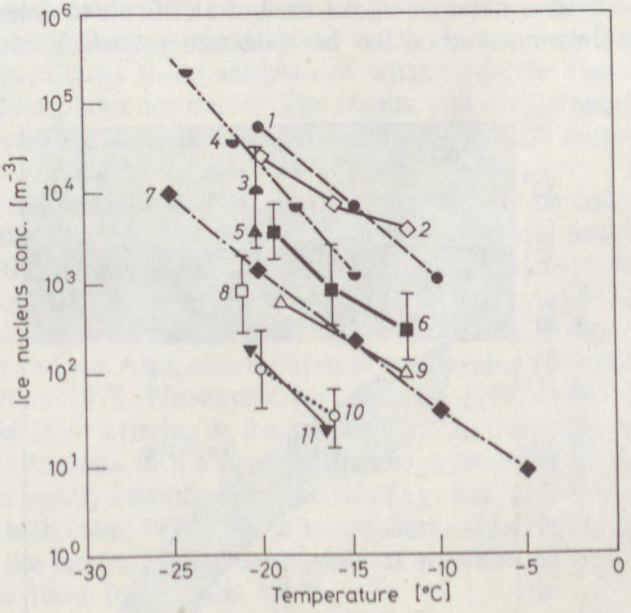

Fig. 4.14

Ice nucleus concentrations measured at different locations. The ranges of measured values are also given in some cases, as vertical bars. There are apparently significant differences among the data sets, but the contribution of differences in measurement techniques is unknown. Instruments responding to different modes of nucleation are included in this comparison. *1* – Admirat (1978); *2* – Al-Naimi and Saunders (1986); *3* – Vychuzhanina *et al.* (1984); *4* – Perez *et al.* (1985); *5* – Bertrand *et al.* (1973); *6* – Vali *et al.* (1984); *7* – Gagin (1975); *8* – Zamurs and Jiusto (1982); *9* – Stein and Georgii (1985), for Southern Germany; *10* – Bowdle *et al.* (1985); *11* – Dye and Breed (1979)

increase with decreasing temperatures, just as would be expected for any nucleating material or mixture of materials. The temperature-dependence of concentrations is usually described using exponential or power-law functions (Eq. 4.10) since concentrations increase very rapidly with decreasing temperatures: tenfold increases in concentrations for each 4 to 10 °C lowering of temperature are typical. There is also a strong dependence of concentrations on supersaturation (Eq. 4.11): for a doubling of the saturation ratio with respect to ice the numbers of atmospheric ice nuclei increase 10 to 100-fold. Since water saturation (or just a slight excess over that) is the most common condition within supercooled clouds, the concentrations of atmospheric ice nuclei are usually given for that condition. Indicated concentrations at -15 °C cluster around 10^2 to 10^3 m^{-3}. Measurements at temperatures higher than -10 °C, and also at temperatures lower than -20 °C, are few and indirect. These general trends are depicted in Fig. 4.15. Typical values of the concentrations of CCN and total aerosol are also shown, to emphasize the relative scarcity of ice nuclei: at the higher temperatures ice nuclei may be $1 : 10^6$ or fewer of the total aerosol population. That is, of course, one of the reasons that their study is wrought with so many difficulties.

The sizes of atmospheric ice nuclei are quite difficult to determine by direct measurement since no method has been devised yet which could successfully

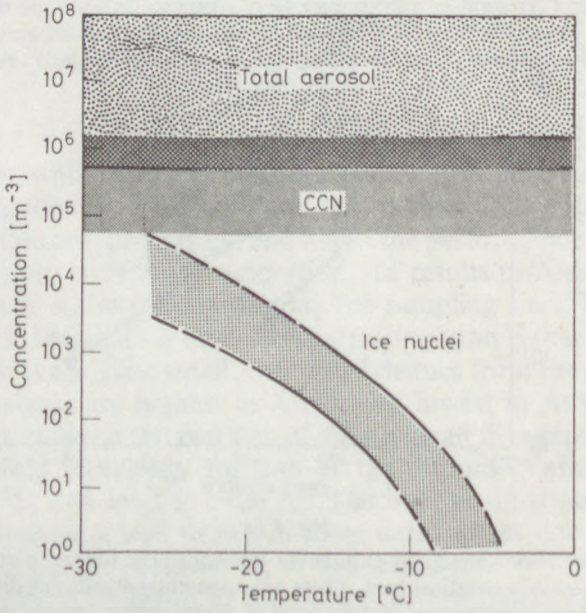

Fig. 4.15

The general trend in ice nucleus observations in the lower troposphere is shown as a function of temperature. For comparison, concentration ranges for CCN and for total aerosol are also shown. For all three components of the atmospheric aerosol, there are large variabilities in space and time, at times falling considerably outside the indicated ranges

separate ice nuclei from other, much more numerous, aerosol particles. When ice nucleus measurements were made simultaneously with measurements of the concentrations of aerosols of > 0.1 μm and of > 0.005 μm radius, the correlation with the larger particles was found to be stronger. In contrast, in rainwater most ice nuclei were found to be < 0.01 μm in size. In snowflakes, the center particles, which are assumed to be the nuclei, are > 0.1 μm when present, but there are also many smaller particles near the same location. In a recent study (BEREZINSKII and STEPANOV, 1986), it was found that the fraction of aerosol particles which were ice nuclei decreased with decreasing particles sizes: the active fraction was near 0.1 for 100 μm diameter particles and decreased to near 10^{-6} for 0.1 μm particles. However, since the concentration of 0.1 μm particles is generally a factor 10^9 greater than that of 100 μm particles, the smaller ice nuclei would still outnumber larger ones. Clearly, it is too early to make general statements; there is a need for more extensive observations.

4.5.4 Sources of atmospheric ice nuclei

Accepting measurements obtained with a given device over a limited range of atmospheric conditions as yielding, at least, *relative magnitudes* of nucleus concentrations, allows some analyses of what might be the most important sources of atmospheric ice nuclei. The results that are summarized here must be viewed, nonetheless, as provisional, especially because most of the observations refer to lower activation temperatures.

In spite of suggestions that meteoritic material may be contributing significantly to atmospheric ice nucleus populations, terrestrial sources of ice nuclei appear to be the most important. Concentrations of nuclei are observed to either be roughly constant, or to decrease with altitude above land (VALI *et al.*, 1982; BOWDLE *et al.*, 1985; BEREZINSKII *et al.*, 1986), as would be expected for sources located at the surface. Also, observations at coastal sites (BERTRAND *et al.*, 1973; BORYS and DUCE, 1979; WISNIEWSKI and LANGER, 1980) show higher concentrations of nuclei in air arriving at the station from an overland trajectory than in maritime air. Particles in the centers of snow crystals which might have been ice nuclei are mostly identified as minerals (e.g. KIKUCHI *et al.*, 1982), even at the South Pole (KUMAI, 1976). These atmospheric observations are given further credence by the laboratory measurements of activities of various natural substances as ice nuclei (cf. Section 4.4.3).

Oceanic sources are little explored. While indications are that oceans are weak sources in comparison to land areas, it seems little warranted to ignore the possibility that some important sources might exist in specific areas. Just such indications are evident in the data of BIGG (1973), SCHNELL and VALI (1976) and of ROSINSKI *et al.* (1986).

Both for terrestrial and oceanic sources, attention has been directed over the last decade to the contributions of organic, biogenic sources. Ice nucleation by organics has been the subject of investigation for some time. Several examples

are mentioned in the discussion of nucleating abilities of substances (Section 4.4.3), and there were, in addition, experiments with leucine, proteins, steroids, amino acids, and so on. Moderate activity was found with many of these materials, but none appeared of exceptional interest. The new direction of recent years was set by findings of very active ice nucleation in soils of high organic content, and by the identification of some common epiphytic bacteria on natural vegetation and on agricultural crops which are capable of developing ice nucleating ability (SCHNELL and VALI, 1972, 1976; MAKI *et al.*, 1974; VALI *et al.*, 1976; ARNY *et al.*, 1976). The fact, that in natural soils ice nucleating activity appears to be related to the organic content of the soils, is roughly evident in Fig. 4.9 also. A quantitative correlation can also be demonstrated. Vegetation has been found to carry bacteria which nucleate ice at small supercoolings, and these bacteria are, in fact, responsible for the initiation of frost on plants (ARNY *et al.*, 1976; LINDOW *et al.*, 1978). The possibility of reducing frost damage to plants, by removal, or reduction of the ice nucleating bacteria, has led to intense studies of these bacteria. The most common species, *Pseudomonas syringae,* is a common plant pathogen, and is found on the majority of plants worldwide. The other species having high ice-nucleating activity is *Erwinia herbicola.* Beyond these two major species there are only minor variants of the same which are ice nucleating—a very surprising fact when considering the thousands of species normally associated with plants.

Ice nucleation at warm temperatures is usually associated with only a small fraction of the total bacterial population, and sites occupy only a small fraction of the outer membrane of the bacterial cells. The precise composition of the sites is still unknown. A gene fragment responsible for the formation of the ice nucleating site has been identified (ORSER *et al.*, 1985). Cloning that gene fragment into common *E. coli* bacteria transferred the ability to form ice nucleating sites to those bacteria as well. The composition of the ice nucleating membrane component is narrowed down to be a lipoprotein of about 200,000 molecular weight, whose structure can be postulated (GREEN and WARREN, 1985). Many other fascinating aspects of the bacterial ice nuclei have emerged in the studies. Dead bacterial cells are being used extensively as artificial ice nuclei for improving the quality of man-made snow in ski resorts. Methods for the reduction of frost damage have been developed, including the use of a non-nucleating clone of the native bacteria. The field use of these genetically modified bacteria has progressed to the stage of limited experimentation in 1988 —more widespread use may be forthcoming. There are, of course, important related questions about the possibility of an atmospheric impact from the removal of natural ice-nucleating bacteria over large agricultural areas.

The question just raised, namely, whether ice-nucleating bacteria on plants are sources of atmospheric ice nuclei, is broader than the possible impact of frost prevention measures. Research is less advanced in this area than in investigating the population dynamics and nucleating characteristics of the bacteria. There are some measurements of the fluxes of bacteria into the air from crops (LINDEMANN *et al.*, 1982, 1985) and there are some reports of bacteria sampled from

the air, but the case is not convincing yet, and quantifying the sources is not yet possible. It can be hypothesized that the importance of bacterial ice nucleators for the atmosphere will manifest itself indirectly, rather than by direct dispersion of bacterial cells into the atmosphere. The link is likely to be through the nuclei found in soils; these nuclei may turn out to be decay products of the ice-nucleating bacterial cells.

That is not the only possibility though, which can be envisaged for the origin of nuclei in soils; other processes in which nucleating substances are formed as part of the overall scheme of cycling of organic matter in the soils might be found to be more important. In any case, it seems likely, that many of the mineral particles found in the atmosphere, and in snow crystals specifically, in fact carry a small organic component, and that ice nucleation on such particles initiates on the organic component. This is more likely to be true for soil particles originating from mid-latitudes, than for aerosol from tropical areas or from deserts.

Oceans also harbor ice nucleating bacteria (e.g. FALL and SCHNELL, 1985), a finding which reinforces the possibility that some ocean areas—those of high productivity—may be sources of atmospheric ice nuclei. There is some convergence between this possibility and the observations of nuclei in marine environments which were mentioned earlier.

Much of the story of biogenic ice nuclei in the atmosphere is still only known in vague outlines. However, the potential implications of the emerging finding are so important that there is every reason to hope for significant clarifications in the not too distant future.

Turning from natural sources to anthropogenic ones, their contribution to atmospheric ice nucleus populations must also be recognized. Specific sources, such as copper smelters, sugar-cane fires and others have been documented. Automobiles were not proven to be producing ice nuclei, although lead iodide was suspected to form from leaded gasolines, and lead iodide is an active ice nucleator. The complex mixtures of pollutants from urban areas were found to alter ambient ice nucleus concentrations in either direction; in some situations increases were reported (e.g. HOBBS and LOCATELLI, 1970; KITAGAWA-KITADE and MARUYAMA, 1979), while decreases were observed in some others (BRAHAM and SPYERS-DURAN, 1974). Extensive burning of vegetation, as is practiced for the conversion of tropical rain forests to agricultural lands, is another potentially large source of ice nuclei, but this possibility has not yet been examined empirically. In total, since there are so many uncertainties about the sources, concentrations and lifetimes of atmospheric ice nuclei, and since so little attention has been paid to this problem, one cannot now make, even rough, estimates of the impacts of anthropogenic sources of ice nuclei. Due to the suspected role of the ice nuclei in clouds, one should probably be cautious in dismissing a significant impact; the potential is there for unpleasant surprises when it will become possible to make the appropriate measurements.

4.6 Artificial ice nuclei—cloud seeding

4.6.1 Historical note

Attempts to influence atmospheric processes have a long and varied history, but for the present discussion it is sufficient to look back a little over half a century. By about 1930, studies of clouds and of precipitation have progressed to a recognition that the ice phase has more prevalent roles than the readily perceived ones of snow and hail formation. It became evident that many clouds contain supercooled water droplets, and that in such clouds ice crystals can grow rapidly. These crystals have a high condensation (deposition) rate, since ice has a lower vapor pressure than water, and they can collect supercooled droplets by impaction (riming) once they have grown large enough to develop appreciable fall velocities. These mechanisms can lead to faster, more efficient development of precipitation than is possible by the coalescence of water droplets alone. Based on these arguments, it was anticipated that most rainfall across the globe, specially in temperate climates, originated as ice in the clouds and melted before reaching the ground.

Observations during the 1930's and 1940's continued to add support to the theory, or rather, hypothesis outlined above, but quantitative examinations of the hypothesis were not then possible. The importance of ice in atmospheric precipitation processes naturally lead to the notion that the concentrations of ice nuclei exert a controlling role in the development of rain, and in the formation of snow and hail. Furthermore, since ice nucleus concentrations are quite low in comparison with condensation nuclei or total aerosol concentrations (cf. Fig. 4.15), and, since supercooled clouds were in fact observed, it could readily be argued that the possibility exists to significantly modify clouds by adding artificial ice nuclei to them.

By the mid-1940's practical methods were discovered for inducing ice crystals in supercooled clouds. The discoveries were rapidly transplanted from the laboratory to the atmosphere, and the possibility of converting portions of a supercooled cloud layer to ice crystals was convincingly shown in 1946. Widespread application of cloud seeding—coupled with intense efforts to investigate the processes and to develop improved methods—followed rapidly and continue to this day.

Now it can be easily recognized that the expectations of forty years ago were overly simplistic, and overly optimistic. Addition of artificial ice nuclei to clouds which are substantial enough to have a reasonable chance to produce precipitation does not yield clear and unequivocal results. So, while some important successes due to cloud seeding can be claimed, these cases represent but a small fraction of the numerous attempts made. Consequently, there is now, in general, a much more cautious attitude toward cloud seeding; there is an emphasis on careful consideration of the scientific and social questions involved instead of embarking on full-scale efforts on the basis of imprecise expectations. The

reasons for this situation can be placed in two groups: (1) Natural precipitation processes are more efficient than was anticipated, because of secondary ice generation, and because of a greater contribution by coalescence; and, (2) The variabilities and complexities of clouds, and the possibilities of both positive and negative effects due to seeding, demand that cloud seeding be performed with considerable *a priori* knowledge of the cloud system to be seeded, and with appropriate design of the seeding procedures. These statements cannot be elaborated in any detail here, so the reader is referred to the reviews of HESS (1974), KACHURIN (1978), DENNIS (1980), BRAHAM (1986), and others.

It should also be said that the quantitative foundations of cloud seeding are still under development; its ranges of applicability, methods of execution, and methods of testing are not clearly established. New concepts continue to emerge in response to new findings in cloud physics and in mesoscale meteorology. From the point of view of possibilities for future progress, on the positive side there is a large body of empirical results to learn from, there are improved methods for observing cloud behavior, and there are powerful numerical models for synthesizing available knowledge about cloud processes. On the negative side, development of the kind of detailed knowledge which is necessary for the purposeful modification of precipitation processes, with allowance for the natural variabilities of cloud systems, can only be gained with gradual progress.

In Section 4.5 we examined the current state of knowledge with respect to ice nucleation in the atmosphere; the uncertainties about natural ice nuclei constitute basic problems in cloud seeding also. The generation, testing, and delivery of artificial ice nuclei form another, closely related problem area; discussions of these topics are taken up in this section.

4.6.2 Cloud seeding with coolants

One approach to creating large numbers of ice crystals in a cloud, or in any zone (below 0 °C) where saturation with respect to ice is exceeded, is to cool small portions of the volume of air to temperatures of homogeneous ice nucleation. As originally discovered by SCHAEFER (1946)—thereby setting off the era of practical cloud seeding efforts—introducing dry ice into a supercooled cloud in the laboratory produces spontaneous transformation of the cloud to ice crystals.

Dispersing small pellets of solid CO_2 (dry ice), or droplets of highly volatile liquids (N_2, propane, etc.) leads to the rapid sublimation of the pellets and evaporation of the droplets, so that their surface temperatures cool to, or well below, their temperatures of vaporization. The temperature of sublimation for dry ice is −78 °C; the boiling points of liquid nitrogen and liquid propane are −196 and −45 °C, respectively. Cooling due to evaporation can add up to another 40 °C cooling to these temperatures. So, the surfaces of the evaporating pellets or droplets are considerably colder than the roughly −40 °C threshold for homogeneous freezing. While the quoted temperatures are found only at the surfaces of the evaporating objects, there will still be a sizeable zone where the

temperature drops to below −40 °C. In that zone, a very large number of ice crystals form. Evidence points to the fact that many water droplets nucleate in the highly supersaturated vapor in the chilled zone, mostly by homogeneous condensation, and those droplets then freeze almost instantaneously. Initially, there is severe competition for available vapor among the ice crystals, so that not all of the crystals survive. Once diffusion and turbulence has spread the crystals to a larger volume, the competition diminishes and the remaining crystals can continue to grow. The overall efficiency of the process, the numbers of ice crystals produced per gram of dry ice or liquid spray, is found to be not very sensitive to environmental temperature, cloud liquid water content and other variables. At temperatures lower than about −3 °C, dry ice pellets initiate on the order of 10^{13} crystals per gram (FUKUTA *et al.*, 1971; HORN *et al.*, 1982). Volatile sprays produce very similar results, 10^{11} to 10^{13} g^{-1} (HICKS and VALI, 1973; KUMAI, 1982), with the higher values derived from field-scale testing where mixing of the seeded plume with the cloud probably reduced the impact of competition.

In order to utilize coolants, the pellets or spray must be introduced directly into a supercooled water cloud, or a supersaturated vapor zone. The ability of the coolants to form ice in a supersaturated vapor leads to the potential for creating ice clouds in previously cloud-free air. There are as yet no reliable aerosol nuclei which can match this capability. For seeding water clouds, introduction of the coolants directly into the cloud poses considerable difficulties, since dispersion either from aircraft, or from balloons is necessary. On the other hand, by carrying the nucleant directly into the cloud, its designated location and dosage rate are well established.

Dry ice is dispersed by mechanical devices which assure that the feed rate is constant and that pellet sizes are maintained uniform. Seeding rates usually employed are about 10–100 gram per second (0.1 to 1 gram per meter of flight path). Pellet sizes are typically about 1 cm; such pellets fall about 1.5 km before evaporating completely. With the continuous release of dry ice pellets, the passage of a seeding aircraft through a cloud produces a "curtain" of ice crystals.

Liquid coolants are dispersed by spraying. The vapor pressure of the liquid is usually sufficient to provide the pressure necessarry to force the liquid through the spray nozzle. The liquid is drawn from the bottom of the tank. If additional pressure is needed, inert nitrogen gas is used to pressurize the vessel. The lifetime (travel distance) of the spray droplets depends on the sizes of the droplets and on wind speed. In any case these distances are limited to a few meters. This is a restriction on the applicability of the method; seeded volumes are even smaller than with dry ice. On the other hand, the method is well suited for ground-based applications, and is in use at several major airports for dispersing supercooled fogs.

In general, the fate of the initial ice plume depends on the vertical and horizontal winds within the cloud or fog. The growth of the ice crystals is in turn determined by those motions and by the conditions they encounter. The detailed

nature of the effect of the seeding on the cloud is, as to be expected, highly dependent on the characteristics of the cloud. High ice concentrations caused by the localized release of coolants can be readily documented with aircraft sampling, and the formation of precipitation and of radar echo can also be clearly observed at times (e.g. ENGLISH and MARWITZ, 1981; MARWITZ and STEWART, 1981). For example, in a stratiform cloud studied by HUGGINS and RODI (1985), ice crystal concentrations of near 10^5 m^{-3} were observed over regions of about 1 km in extent 20 minutes after seeding, and precipitation fell from the seeded clouds about 24 minutes after seeding.

Such field studies provide excellent information on how cloud response varies with conditions, with seeding rates, etc. Numerical simulations of seeding effects (e.g. KOPP *et al.*, 1983; KRASNOVSKAYA *et al.*, 1987) are also helpful in understanding the interactions of the numerous variables involved.

Overall, the use of coolants offers a practical way of initiating ice crystals. The efficacy of the method at temperatures close to 0 °C is a particular advantage. Producing the ice crystals over large volumes of air is a problem, and the coolants have to be delivered directly into the clouds. Application of the method is quite widespread. Research is also continuing, directed mostly toward understanding of cloud responses, and toward optimization of the seeding procedure.

4.6.3 Cloud seeding aerosols

Heterogeneous ice nucleation by particles (aerosols) is the most common method of seeding clouds. The discovery of this possibility followed soon after the observation of cloud glaciation by dry ice. VONNEGUT (1947) reported that silver iodide and lead iodide particles were effective as ice nuclei in supercooled clouds in the laboratory, and in a fog at −4 °C. It is noteworthy, that, forty years later, the two most frequently used cloud seeding materials are still silver iodide and lead iodide.

The factors influencing the ice-nucleating ability of a particle has already been explored in the preceding sections. Those are, of course, the main considerations relevant to the use of cloud seeding aerosols. In fact, a great deal of attention has been given already to silver iodide (AgI) as one of the most active ice nucleating substances known. While the results presented in Sections 4.4 and 4.5 were derived mainly from laboratory and theoretical studies, here the focus will be on the field applications of these nucleating agents, i.e. generation, testing, delivery and cloud effects.

The basic requirements for cloud seeding application of an ice nucleant are that it produce large numbers of ice crystals at temperatures as close to 0 °C as possible, and that its dispersion into clouds be relatively easy and inexpensive. Materials best meeting these requirements are those which have a high inherent efficiency (many possible sites per unit surface area) and which can therefore be utilized as small aerosol particles, yielding many particles per unit mass. Additional requirements are stability, i.e. no loss of activity due to irradiation

or chemical interactions, and lack of undesirable (toxic) effects. Silver iodide (AgI), lead iodide (PbI_2), cupric sulfide (CuS), metaldehyde, 1,5-dihydroxynaphthalene, and a few other substances have been developed and tested for cloud seeding use. It should be added, that in most cases, the aerosol contains other components in addition to the basic substances mentioned, and the actual chemical composition and physical state of the product strongly influences its nucleating ability. These characteristics are, in turn, determined by the method of generation of the aerosol.

To achieve small particle sizes, nucleating aerosols are produced by recondensation from vapors: the substance is vaporized at high temperature, and condensation takes place as the vapor cools due to mixing with environmental air. Vaporization is accomplished in the flame of a liquid or solid fuel. The corresponding devices are referred to as "burners" or "generators" if a gas or liquid fuel is used, and as "pyrotechnics" or "flares" if the seeding material is mixed with a solid combustible material. In a typical silver iodide generator an acetone carrier liquid (in which AgI is solubilized by NaI, NH_4I, or KI) is burned either by itself, or is fed into a propane or gasoline flame. The physical arrangements of such generators are extremely variable, depending on intended use, cost, and on the user's design preferences. Generators have been built for both airborne and ground use. Output rates vary from a low of few grams per hour to kilograms per hour. In some projects, up to hundreds of generators have been deployed, at times with the possibility of remote control to turn the generators on and off. A great deal of effort has been dedicated to the optimization of such generators. The principal design variables are the composition of the mixture, the flow rates applied, the flame temperature obtained in the burner head, and the period of operation. An important environmental variable is wind (or ventilation) speed, determining the quenching rate of the emitted vapors, and the initial coagulation of the condensed particles. The output variables are the composition and the sizes of the particles, and, ultimately, the activity of the particles as ice nuclei.

Pyrotechnic mixtures are formulated to be either slow burning or explosive. Steadily-burning "flares" are used attached to aircraft, or dropped from aircraft, or are fired through the clouds as rockets. Explosive mixtures are used in projectiles fired from cannons, and also in rockets. The mixtures contain, in addition to the nucleant, fuel, oxidant and binder. The composition of the mix is adjusted to produce a uniform controlled burn and a desired particle size distribution for the nucleant. Usually, pyrotechnics have lower output rates than solution burners, partially because of the larger particle sizes that are produced, and partially because of the more complex chemical composition of the particles.

Evaluations of generator outputs is a demanding task in itself. The generators have to be operated in realistic and repeatable conditions, the aerosols have to be diluted to usable levels for the tests, and the nucleation tests have to be performed in some cloud chamber or other type of ice nucleus measuring device. Important major facilities have been constructed for such tests, but the results

still cannot be referred to any kind of standard. Intercomparisons of results from different test facilities are often disappointing; the problems of ice nucleus measurements discussed in Section 4.5 are clearly evident in these attempts. Discrepancies of several orders of magnitude might appear depending on the test conditions used, so that the application of chamber test results to the prediction of ice-forming potential in clouds can only be viewed as rough approximations.

The results of generator tests are usually expressed in terms of the numbers of nuclei per gram of material, often termed "effectiveness", as a function of temperature. The results of a number of such measurements are shown in Fig. 4.16 for different generators and from different testing facilities. The general character of the curves is evident in all results: a very sharp rise (several orders of magnitude within a degree or so of temperature), followed by a broad temperature region of nearly constant values. The initial rise tends to occur near -5 °C for AgI, in reasonable agreement with the threshold values shown in Section 4.4. The maximum yields, at temperatures of -15 °C, or below, may reach 10^{15} to 10^{16} nuclei per gram of silver, and values of 10^{13} to 10^{14} are not uncommon for activity at -10 °C. As shown by curve 6 in Fig. 4.16, even higher yields are possible, at least in the laboratory, by producing small patches of AgI on other particles. It is the high output that makes silver iodide such an attractive material for cloud seeding. If the test results were directly transferable to the atmosphere, 1 g of AgI could yield 10^4 m^{-3} nuclei at -10 °C (roughly ten times the average natural concentration) in nearly 10 km^3 of cloud volume. In fact, practical results are far short of these numbers, as will be discussed later, and there is so much variability in the results that the planning of cloud seeding activities still faces numerous major uncertainties.

Aerosols as cloud seeding nuclei have the advantage that they can travel considerable distances in the atmosphere, thus allowing diffusion into large volumes of air. If the entire volume in which clouds form, or the inflow air into clouds is to be filled with artificial ice nuclei, this can only be accomplished with aerosols. Seeding generators at the ground, or airborne generators, can be operated upwind of the clouds to be influenced. However, the spreading of the aerosol plume in practical circumstances is not easily predicted, leading to considerable uncertainties in the targeting of the seeding material and in the concentrations actually reached in the clouds. Direct introduction of the seeding material into the clouds, by using generators or flares mounted on aircraft, by dropping flares into the cloud from above, or by firing projectiles into the cloud reduces the targeting uncertainty, but leads to relatively small volumes of air being treated. In either case, loss of nucleating aerosol by cloud and precipitation scavenging also has to be considered. Much effort has been expended in the study of diffusion and transport of seeding plumes, since an understanding of these factors is indispensable to successful cloud seeding. In some studies of plume transport, tracer particles or gases were released together with the ice nuclei in order to make detection of the plume and analysis of the results easier. It has been found that specific tests are required for each area and cloud type

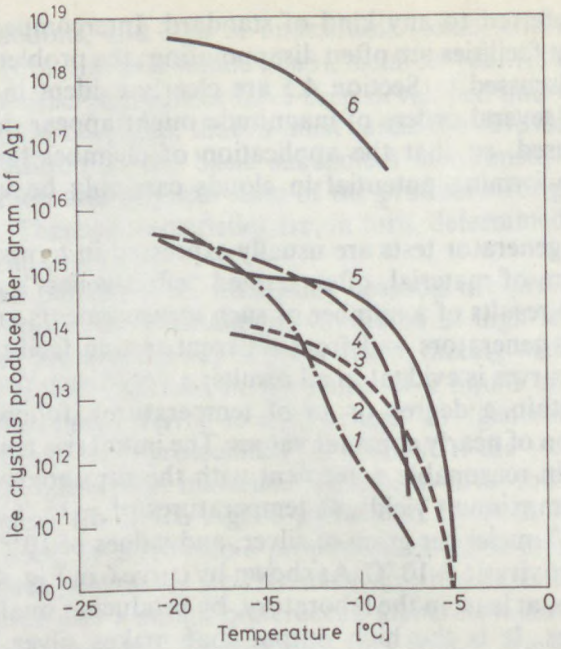

Fig. 4.16

Examples of the cumulative nucleus spectra (numbers of ice crystals per gram of AgI as a function of test temperature) observed in cloud chambers for different AgI aerosols. *1* – GARVEY (1975), for the output of a burner with a solution of AgI and NaI; *2* – FEDERER and SCHNEIDER (1981), for a pyrotechnic mixture used in cloud seeding rockets; *3* – VOLKOVITSKY *et al.* (1987), for a full-scale test of a 2% AgI pyrotechnic mixture; *4* and *5* – DEMOTT (1988), for a AgI–AgCl aerosol produced in a burner, and for a 2AgI. NaI complex which was tested in a chamber undergoing adiabatic expansion; *6* – PLAUDE and SOSNIKOVA (1987), for an aerosol generated by evaporation of a solution containing $1:3\times10^{-5}$ mass ratio of AgI to NH_4I

to be dealt with. This is especially true for generators located on the ground; local terrain conditions exert strong and often unpredictable influences.

In view of the many uncertainties in nucleating efficiency and in transport, it has been found very useful to study the activities of cloud seeding materials directly in natural clouds. Such "seeding trials" involve the generation and delivery of the seeding material by whatever method is chosen, and the effect of the seeding is monitored by an aircraft equipped with appropriate instrumentation. A tracer material may be also used to give independent confirmation that sampling by the aircraft is carried out in the seeding plume (e.g. STITH and BENNER, 1987). The principal parameters of interest are the concentrations of ice crystals, their growth rates, and the rate of spread of the ice crystal plume. The growth of the ice crystals is, of course, accompanied by the liquid water content becoming depleted. Motions within the cloud, and the level of turbulence, define the larger-scale patterns. The evolution of precipitation, as graupel or as aggregates of crystals, is the stage to which the seeding effect is

to be followed, although it is often quite difficult to continue to identify the effects of seeding separately from the natural evolution of the cloud. Determinations of the silver content of precipitation have been utilized as aids to relating precipitation rate, and location, to seeding (e.g. WARBURTON *et al.*, 1985). Radar observations can also be of considerable help in that regard. There is definite merit in performing the seeding trials in a randomized fashion, so that seeded clouds can be rigorously compared with non-seeded clouds. Perhaps the most complete series of such studies were performed over a five-year period with summertime convective clouds of moderate dimensions (COOPER and LAWSON, 1984); the results clearly show the increased ice concentrations and the initial growth of the ice particles to the graupel stage. Other, similar studies were reported by ISAAC *et al.* (1977), BLUMENSTEIN *et al.* (1987), KRAUSS *et al.* (1987), and many others.

The primary effect of cloud seeding with ice nuclei is the creation of additional ice particles. The growth of those particles to precipitation sizes is the goal in what came to be called the "static" seeding method. The preceding discussion was oriented primarily toward the static seeding concept. But, there is another important aspect of seeding with ice nuclei not mentioned up to this point. In some situations (usually with higher dosage rates of seeding material) the release of latent heat accompanying the ice formation has a sizable effect on the dynamics of the cloud. When this is the primary effect sought, the seeding is referred to as "dynamic" seeding. Dynamic seeding, or the stimulation of cloud growth, is thought to bring about an increased flux of water vapor into the cloud and an increase in the efficiency of precipitation formation. Considerable experimental and theoretical work has been dedicated to this concept, but a fully cogent explanation of the process has not yet emerged, and the the field evidence is not certain either. For further details on this concept the reader may consult WOODLEY *et al.* (1982) and ORVILLE (1986). Since the formation of additional ice particles and the release of latent heat are, in reality, inseparable, the distinction between static and dynamic seeding is only one of degree.

Numerical model simulations of seeding effects can provide many additional insights into the parameters influencing the final outcome. Seeding rates, locations and timing can be altered in systematic ways to explore the sensitivity of cloud evolution to these variables. Model calculations of this type range from simple ones, which treat the evolution of droplets and ice particles within a closed parcel, to complex ones, which contain descriptions of the three-dimensional distributions of different hydrometeors and include the flow fields in and around the cloud. Once again, discussion of these models exceeds the scope of this volume; some examples to consult in the literature are: KOPP *et al.* (1983), BUIKOV and DORMAN (1985), COTTON *et at.* (1986), ORVILLE *et al.* (1987).

As mentioned before, cloud seeding is still a rapidly-developing science. Even though established, large-scale field-programs exist, and some of those appear to be producing useful practical results, the scientific bases of many aspects of cloud seeding are poorly understood. Laboratory and field experimentation, as well as theoretical and numerical modeling studies are continuing. From that

perspective, the study of ice nucleation is part of a multi-faceted search for knowledgeable modifications of clouds. Improved understanding of natural ice formation and of the many aspects of artificial ice nucleation are fundamental to progress in that important endeavour.

References

ADMIRAT, P., 1978: Natural and artificial increases of ice forming power of air in the Po Valley. *Riv. Ital. Geofis. Sci. Affini*, **5**, 156–158.

AL-NAIMI, R. and SAUNDERS, C. P. R., 1985: Measurement of natural deposition and condensation-freezing ice nuclei with a continuous-flow chamber. *Atmos. Environ.*, **19**, 1871–1885.

ANDERSON, B. J. and HALLETT, J., 1976: Supersaturation and time dependence of ice nucleation from the vapor on single crystal substrates. *J. Atmos. Sci.*, **33**, 822–832.

ANDERSON, R. C., MILLER, R. C., KASSNER, J. L. Jr. and HAGEN, D. E., 1980: A study of homogeneous condensation-freezing nucleation of small water droplets in an expansion cloud chamber. *J. Atmos. Sci.*, **37**, 2508–2520.

ANGELL, C. A., 1982: Supercooled Water. Chap. 1. In *Water—A Comprehensive Treatise*, (ed. F. Franks), Plenum Press, Vol. 7., pp. 1–81.

ARNY, D. C., LINDOW, S. E. and UPPER, C. D., 1976: Frost sensitivity of Zea mays increased by application of *Pseudomonas syringae*. *Nature*, **262**, 282–284.

BASSET, D. R., BOUCHER, E. A. and ZETTLEMOYER, A. C., 1970: Adsorption studies on ice-nucleating substrates. Hydrophobed silicas and silver iodide. *J. Coll. Int. Sci.*, **34**, 436–446.

BEREZINSKII, N. A. and STEPANOV, G. V., 1986: Dependence of the concentration of natural ice-forming nuclei of different size on the temperature and supersaturation. *Izvestiya, Atmos. Ocean. Phys.*, **22**, 722–727 (English translation).

BEREZINSKII, N. A., STEPANOV, G. V. and KHORGUANI, V. G., 1986: Altitude variation of relative ice-forming activity of natural aerosol. *Meteor. i Gidrol.*, **12**, 102–105 (86–89 Engl. edit.).

BEREZINSKII, N. A., KARPOV, V. G., MYAKON'KII, G. B., SMIRNOV, S. D., STEPANOV, G. V. and KHORGUANI, V. G., 1980: Apparatus, method and results from investigating atmospheric ice nuclei. *Meteor. i Gidrol.*, **8**, 105–110 (89–94 Engl. edit.).

BERTRAND, J., BAUDET, J. and DESSENS, J. 1973: Seasonal variations and frequency distributions of ice nuclei concentrations at Abidjan, West Africa. *J. Appl. Meteor.*, **12**, 1191–1195.

BIGG, E. K., 1953: The supercooling of water. *Proc. Phys. Soc., B.*, **56**, 688–694.

BIGG, E. K., 1971: Report in the ice nucleus workshop—Fort Collins, August 1970. *Second Intern. Workshop Cond. Ice Nucl.* (ed. L. O. Grant.), Colo. St. Univ., Ft. Collins, Colorado, pp. 97–105.

BIGG, E. K., 1973: Ice nucleus measurements in remote areas. *J. Atmos. Sci.*, **30**, 1153–1157

BIGG, E. K., MOSSOP, S. C., MEADE, R. T. and THORNDIKE, N. S. C., 1963: The measurement of ice nucleus concentrations by means of Millipore filters. *J. Appl. Meteor.*, **2**, 266–269.

BIGG, E. K. and STEVENSON, C. M., 1970: Comparison of concentrations of ice nuclei in different parts of the world. *J. Rech. Atmos.*, **6**, 41–58.

BLUMENSTEIN, R. R., RAUBER, R. M., GRANT, L. O. and FINNEGAN, W. G., 1987: Application of ice nucleation kinetics in orographic clouds. *J. Clim. Appl. Meteor.*, **26**, 1363–1376.

BÓNIS, K., 1971: On the thermodynamics of the crystal formation in small solution droplets. *Gerlands Beitr. Geophys.*, Leipzig, **80**, 1–12.

BORYS, R. D. and DUCE, R. A., 1979: Relationship among lead, iodine, trace metals and ice nuclei in a coastal urban atmosphere. *J. Appl. Meteor.*, **18**, 1490–1494.

BOWDLE, D. A., HOBBS, P. V. and RADKE, L. F., 1985: Particles in the lower troposphere over the High Plains of the United States. III: Ice nuclei. *J. Clim. Appl. Meteor.*, **24**, 1370–1376.

BRAHAM, R. R. Jr., (editor), 1986: Precipitation enhancement—A scientific challenge. *Meteor. Monogr.* (Amer. Meteor. Soc.), **21** (43), 171 pp.

BRAHAM, R. R. Jr. and SPYERS—DURAN, P., 1974: Ice nucleus measurements in an urban atmosphere. *J. Appl. Meteor.*, **13**, 940–945.

BRYANT, G. W., HALLETT, J. and MASON, B. J., 1959: The epitaxial growth of ice on single-crystalline substrates. *J. Phys. Chem. Solids*, **12**, 189–195.
BUIKOV, M. V. and DORMAN, B. A., 1985: Numerical simulation of modification of mixed stratiform clouds containing several crystal forms. *Trudy Ukrain. Reg. Res. Inst.*, N 205.
BUTORIN, G. T. and SKRIPOV, V. P., 1972: Crystallization of supercooled water. *Soviet Phys. – Cryst.*, **17**, 322–326.
CLAUSSE, D., BABIN, L., BROTTO, F., AGUERD, M. and CLAUSSE, M., 1983: Kinetics of nucleation in aqueous emulsions. *J. Phys. Chem.*, **87**, 4030–4034.
COOPER, W. A., 1974: A possible mechanism for contact nucleation. *J. Atmos. Sci.*, **31**, 1832–1837.
COOPER, W. A. and KNIGHT, C. A., 1975: Heterogeneous nucleation by small liquid particles. *J. Aerosol Sci.*, **6**, 213–221.
COOPER, W. A. and LAWSON, R. P., 1984: Physical interpretation of the results from the HIPLEX-1 experiment. *J. Clim. Appl. Meteor.*, **23**, 523–540.
COTTON, W. R., TRIPOLI, G. J. RAUBER, R. M. and MULVIHILL, A. E., 1986: Numerical simulation of the effects of varying ice crystal nucleation rates and aggregation processes on orographic snowfall. *J. Clim. Appl. Meteor.*, **22**, 1190–1203.
CWILONG, B. M., 1947: Sublimation in a Wilson chamber. *Proc. Roy. Soc.*, **190**, 137–143.
DEMOTT, P. J., 1988: Comparison of the behavior of AgI-type ice nucleating aerosols in laboratory-simulated clouds. *J. Wea. Modif.*, **20**, 44–50.
DEMOTT, P. J., FINNEGAN, W. G. and GRANT, L. O., 1983: An application of chemical kinetic theory and methodology to characterize the ice nucleating properties of aerosols used in weather modification. *J. Clim. Appl. Meteor.*, **22**, 1190–1203.
DENNIS, A. S., 1980: *Weather Modification by Cloud Seeding*. Academic Press, 267 pp.
DESHLER, T., 1982: Contact ice nucleation by submicron atmospheric aerosols. *Amer. Meteor. Soc., Cloud Phys. Conf.*, Chicago, pp. 111–114.
DETWILER, A. G. and VONNEGUT, B., 1981: Humidity required for ice nucleation from the vapor onto silver iodide and lead iodide aerosols over the temperature range −6 to −67 C. *J. Appl. Meteor.*, **20**, 1006–1012.
DORSEY, N. E., 1948: The freezing of supercooled water. *Trans. Amer. Phil. Soc.*, **38**, 247–328.
DUFOUR, L., 1861: Sur la congelation de l'eau et sur la formation de la grele. *Arch. Sci. Phys. Natur.*, **10**, 346–371.
DYE, J. E. and BREED, D. W., 1979: The microstructure of clouds in the high-frequency hail area of Kenya. *J. Appl. Meteor.*, **18**, 96–99.
EDWARDS, G. R., EVANS, L. F. and ZIPPER, A. F., 1970: Two-dimensional phase changes in water adsorbed on ice-nucleating substrates. *Trans. Faraday Soc.*, **66**, 220–234.
EDWARDS, G. R., EVANS, L. F. and LAMER, V. K., 1962: Ice nucleation by monodisperse silver iodide particles. *J. Coll. Sci.*, **17**, 749–758.
ENGLISH, M. and MARWITZ, J. D., 1981: A comparison of AgI and CO_2 seeding effects in Alberta cumulus clouds. *J. Appl. Meteor.*, **20**, 483–495.
EVANS, L. F., 1965: Requirements for an ice nucleus. *Nature*, **206**, 822.
EVANS, L. F., 1967: Two-dimensional nucleation of ice. *Nature*, **213**, 384–385.
EVANS, L. F. and LANE, J. E., 1973: Line tension and ice nucleation theory. *J. Atmos. Sci.*, **30**, 326–331.
FALL, R. and SCHNELL, R. C., 1985: Association of an ice-nucleating pseudomonad with cultures of the marine dinoflagellate, *Heterocapsa niei*. *J. Marine Res.*, **43**, 257–265.
FEDERER, B., 1968: Über den Einfluss der Oberflacheneigenschaften von Halbleitern auf ihre Eiskeimfahigkeit. *Z. Angew. Math. Phys.*, **19**, 637–664.
FEDERER, B. and SCHNEIDER, A., 1981: Properties of pyrotechnic nucleants used in Grossfersuch IV. *J. Appl. Meteor.*, **20**, 997–1005.
FINDEISEN, V. W. and SCHULTZ, G., 1944: Experimentelle Untersuchungen über die atmospherische Eisteilchenbildung, I. Forsch. u. Erfahrungsber. *Reichswetterd., A.*, **27**, 38–48.
FLETCHER, N. H., 1958: Size effect in heterogeneous nucleation. *J. Chem. Phys.*, **29**, 572–576.
FLETCHER, N. H., 1959: Entropy effect in ice crystal nucleation. *J. Chem. Phys.*, **30**, 1476–1482.
FLETCHER, N. H., 1960: Nucleation and growth of ice crystals upon crystalline substrates. *Austr. J. Phys.*, **13**, 408–418.

FLETCHER, N. H., 1969: Active sites and ice crystal nucleation. *J. Atmos. Sci.*, **26**, 1266–1271.
FLETCHER, N. H., 1970: *The Chemical Physics of Ice*. Cambr. Univ. Press, 271 pp.
FUKUTA, N., 1975: A study of the mechanism of contact ice nucleation. *J. Atmos. Sci.*, **32**, 1597–1603.
FUKUTA, N., 1982: Ice nucleation mechanisms and ice nucleus measurements. *Időjárás*, **86**, 98–103.
FUKUTA, N., 1985: Mechanism of heterogeneous deposition ice nucleation near water saturation. *J. Rech. Atmos.*, **19**, 117–124.
FUKUTA, N., SCHMELING, W. A. and EVANS, L. F., 1971: Experimental determination of ice nucleation by falling dry ice pellets. *J. Appl. Meteor.*, **10**, 1174–1179.
FUKUTA, N. and MASON, B. J., 1963: Epitaxial growth of ice on organic crystals. *J. Phys. Chem. Solids*, **24**, 715–718.
FUKUTA, N. and PAIK, Y., 1973: Water adsorption and ice nucleation on silver iodide surfaces. *J. Appl. Phys.*, **44**, 1092–1100.
FUKUTA, N. and PAIK, Y., 1976: A supersonic expansion method of ice nuclei generation for weather modification. *J. Appl. Meteor.*, **15**, 996–1003.
GAGIN, A., 1975: The ice phase in winter continental clouds. *J. Atmos. Sci.*, **32**, 1604–1614.
GAGIN, A. and NOZYCE, H., 1984: The nucleation of ice crystals during the freezing of large supercooled drops. *J. Rech. Atmos.*, **18**, 119–130.
GARVEY, D. M., 1973: Photolytic activation of ice-nucleating properties of silver iodide hydrosols. *J. Atmos. Sci.*, **30**, 165–167.
GARVEY, D. M., 1975: Testing of cloud seeding materials at the cloud simulation and aerosol laboratory, 1971–1973. *J. Appl. Meteor.*, **14**, 883–890.
GENADIEV, N., 1971: Sur le comportement des noyaux naturels et artificiels lors de congelations reiterees. *J. Rech. Atmos.*, **5**, 137–147.
GEORGII, H.-W., 1963: Investigations on the deactivation of inorganic and organic freezing-nuclei. *Zeitschr. für angew. Math. u. Physik*, **14**, 503–509.
GORBUNOV, B. Z., KAKUTKINA, N. A., KOUTZENOGII, K. P., PASHENKO, A. E. and SAFATOV, A. S., 1987: Kinetics of ice nucleation on aerosol particles in supercooled fog — I. The influence of water vapour depletion. *J. Aerosol Sci.*, **18**, 261–267.
GORBUNOV, B. Z., KAKUTKINA, N. A., KUTSENOGIY, K. P., PASCHENKO, A. E., SAFATOV, A. S. and SUTKIN, Yu. Ye., 1986: Small-volume fog chamber with automatic recording of ice crystals. *Izvestiya, Atmos. Ocean. Phys.*, **22**, 248–249 (English translation).
GREEN, R. L. and WARREN, G. J., 1985: Physical and functional repetition in a bacterial ice nucleation gene. *Nature*, **317**, 645–648.
GUENADIEV, N., 1970: Sur le mecanisme de congelation des guettes d'eau sous l'influence d'un aerosol d'iodure d'argent. *J. Rech. Atmos.*, **3**, 81–91.
HAGEN, D. E., ANDERSON, R. J. and KASSNER, J. L. Jr., 1981: Homogeneous condensation–freezing nucleation rate measurements for small water droplets in an expansion cloud chamber. *J. Atmos. Sci.*, **38**, 1236–1243.
HALLETT, J., 1972: Influence of cloud dynamics on the relationship between ice nucleus measurement and ice crystal concentration. *J. Rech. Atmos.*, **6**, 213–221.
HESS, W. N. (editor), 1974: *Weather and Climate Modification*. John Wiley & Sons Inc., 842 pp.
HICKS, J. R. and VALI, G., 1973: Ice nucleation in clouds by liquefied spray. *J. Appl. Meteor.*, **12**, 1025–1034.
HOBBS, P. V. and LOCATELLI, J. D., 1970: Ice nucleus measurements at three sites in Western Washington. *J. Atmos. Sci.*, **27**, 90–100.
HORN, R. D., FINNEGAN, W. G. and DEMOTT, P. J., 1982: Experimental studies of nucleation by dry ice. *J. Appl. Meteor.*, **21**, 1567–1570.
HUFFMAN, P. J., 1973: Supersaturation spectra of AgI and natural ice nuclei. *J. Appl. Meteor.*, **12**, 1080–1082.
HUGGINS, A. W. and RODI, A. R., 1985: Physical response of convective clouds over the Sierra Nevada to seeding with dry ice. *J. Clim. Appl. Meteor.*, **24**, 1082–1098.
ISAAC, G. A., CROZIER, C. L., CHISHOLM, A. J., MACPHERSON, J. I., BOBBITT, N. R., and MACHATTIE, L. B., 1977: Preliminary tests of a cumulus cloud seeding technique. *J. Appl. Meteor.*, **16**, 949–958.

KACHURIN, L. G., 1978: *Physical Foundations of Atmospheric Processes Modification.* Gidrometeoizdat, Leningrad, 455 pp. (in Russian)

KANNO, H., SPEEDY, R. J. and ANGELL, C. A., 1975: Supercooling of water to −92 C under pressure. *Science,* **189,** 880–881.

KATZ, U. and PILIE, R. J., 1974: An investigation of the relative importance of vapor deposition and contact nucleation in cloud seeding with AgI. *J. Appl. Meteor.,* **13,** 658–665.

KIKUCHI, K., MURAKAMI, M. and SANUKI, Y. 1982: Preliminary measurements of the center nucleus of snow crystals using an energy dispersive X-ray microanalyzer. *Memoirs Nat. Inst. Polar Res., Tokyo,* **24,** 157–174.

KING, W. D., 1978: Vapor depletion in processing membrane filters: the effect of chamber parameters. *J. Appl. Meteor.,* **17,** 1498–1509.

KITIGAWA-KITADE, T. and MARUYAMA, H., 1979: Long term observations of ice nucleus concentrations in Tokyo. *Papers Meteor. Geophys.,* **30,** 133–139.

KNIGHT, C. A., 1973: Two-dimensional phase changes and the heterogeneous nucleation of ice. *J. Atmos. Sci.,* **30,** 324–326.

KNIGHT, C. A., 1976: Homogeneous nucleation of ice in water as a function of pressure: A test of classical nucleation theory. *J. Coll. Int. Sci.,* **111,** 23–39.

KNIGHT, C. A., 1979: Ice nucleation in the atmosphere. *Adv. Coll. Int. Sci.,* **10,** 369–395.

KNIGHT, C. A. and WEINHEIMER, A. J., 1987: Nucleation on cylindrical nuclei. *J. Coll. Int. Sci.,* **119,** 599–601.

KOBAYASHI, T., 1965: The growth of ice crystals on covellite and lead iodide surfaces. *Contr. Inst. Low Temp. Sci., Sapporo, A.,* **20,** 1–22.

KOPP, F. J., ORVILLE, H. D., FARLEY, R. D. and HIRSCH, J. H., 1983: Numerical simulation of dry ice cloud seeding experiments. *J. Clim. Appl. Meteor.,* **22,** 1542–1556.

KRASNOVSKAYA, L. I., SEREGIN, Yu. A. and KHVOROSTIANOV, V. I., 1987: State-of-art in supercooled clouds and fog seeding with cooling agents. In *Some Problems of Clouds Physics,* Gidrometeoizdat, Leningrad, pp. 50–64.

KRAUSS, T. W., BRUINTJES, R. T. and VERLINDE, J., 1987: Microphysical and radar observations of seeded and nonseeded continental cumulus clouds. *J. Clim. Appl. Meteor.,* **26,** 585–606.

KUHNS, I. E. and MASON, B. J., 1968: The supercooling and freezing of small water droplets falling in air and other gases. *Proc. Roy. Soc., A.,* **302,** 437–452.

KUMAI, M., 1976: Identification of nuclei and concentrations of chemical species in snow crystals sampled at the South Pole. *J. Atmos. Sci.,* **33,** 833–841.

KUMAI, M., 1982: Formation of ice crystals and dissipation of supercooled fog by artificial nucleation, and variation of crystal habit at early growth stages. *J. Appl. Meteor.,* **21,** 579–587.

LANGER, G. and RODGERS, J., 1975: An experimental study of the detection of ice nuclei on membrane filters and other substrata. *J. Appl. Meteor.,* **14,** 560–570.

LANGHAM, E. J. and MASON, B. J., 1958: The heterogeneous and homogeneous nucleation of supercooled water. *Proc. Roy. Soc. A,* **247,** 493–505.

LEVKOV, L. and KONSTANTINOV, P., 1975: Effect of adsorbed water molecules on ice-forming activity of PbI_2 aerosol. *Comp. R. Acad. Bulg. Sci.,* **28,** 1489–1491.

LINDEMANN, J., CONSTANTITIDUO, H. A., BARCHET, W. R. and UPPER, C. D., 1982: Plants as sources of airborne bacteria, including ice nucleation-active bacteria. *Appl. Environ. Microbiol.,* **44,** 1059–1063.

LINDEMANN, J. and UPPER, C. D., 1985: Aerial dispersal of epiphytic bacteria over bean plants. *Appl. Environ. Microbiol.,* **50,** 1229–1232.

LINDOW, S. E., ARNY, D. C. and UPPER, C. D., 1978: *Erwinia herbicola:* A bacterial ice nucleus active in increasing frost injury to corn. *Phytopath.,* **68,** 523–527.

MAKI, L. R., GALYAN, E. L., CHANG-CHIEN, M-M. and CALDWELL, D. R., 1974: Ice nucleation induced by *Pseudomonas syringae. Appl. Microbiol.,* **28,** 456–459.

MARWITZ, J. D. and STEWART, R. E., 1981: Some seeding signatures in Sierra storms. *J. Appl. Meteor.,* **20,** 1129–1144.

MASON, B. J., 1958: The supercooling and nucleation of water. *Adv. Phys.,* **7,** 221–234.

MASON, B. J. and MAYBANK, J., 1958: Ice-nucleating properties of some natural mineral dusts. *Quart. J. Roy. Meteor. Soc.,* **84,** 235–241.

MATHIAS, S. F., FRANKS, F. and HATLEY, R. H., 1985: Preservation of viable cells in the undercooled state. *Cryobiol.*, **22**, 537–546.
MCDONALD, J. E., 1964: A thermodynamic relation in the theory of homogeneous nucleation of supercooled droplets. *J. Atmos. Sci.*, **21**, 225–226.
MEYER, J. and PFAFF, W., 1935: Zur Kenntnis der Kristallisation von Schmelzen. III. *Z. anorg. u. allg. Chemie*, **224**, 305–314.
MICHELMORE, R. W. and FRANKS, F., 1982: Nucleation rates of ice in undercooled water and aqueous solutions of polyethylene glycol. *Cryobiol.*, **19**, 163–171.
MONTEFINALE, T. and PAPEE, H. M., 1978: Two-step ice nucleation. *J. Coll. Int. Sci.*, **64**, 385.
MORACHEVSKI, V. G., DUBROVICH, N. A., POPOV, A. G. and POTANIN, A. N., 1972: Some common properties of ice nucleating surfaces. *J. Rech. Atmos.*, **6**, 371–375.
MOSSOP, S. C., 1955: The freezing of supercooled water. *Lon. Phys. Soc.* B, **68**, 193–208.
MOSSOP, S. C., 1963: Atmospheric ice nuclei. *Zeitschr. für angew. Math. u. Physik*, **14**, 456–487.
MOUSSON, A., 1858: Einige Tatsachen betreffend das Schmelzen und Gefrieren des Wassers. *Ann. Phys. Chem.*, **105**, 161–174.
ORSER, C., STASKAWICZ, B. J., PANOPOULOS, N. J., DAHLBECK, D. and LINDOW, S. E., 1985: Cloning and expression of bacterial ice nucleation genes in *Escherichia coli*. *J. Bact.*, **164**, 359–366.
ORVILLE, H. D., 1986: A review of dynamic-mode seeding of summer cumuli. In *Precipitation Enhancement–A Scientific Challenge*. (ed. R. R. Braham Jr.), *Meteor. Monogr. (Amer. Meteor. Soc.)*, **21**(43), pp. 43–63.
ORVILLE, H. D., HIRSCH, J. H. and FARLEY, R. D., 1987: Further results on the numerical cloud seeding of stratiform-type clouds. *J. Wea. Modif.*, **19**, 57–61.
PALANISAMY M., THANGARAJ, K., GOBINATHAN, R. and RAMASAMY, P., 1986: X-ray diffraction and ice nucleation studies of AgI–AgCl solid solutions. *J. Cryst. Growth*, **79**, 1005–1009.
PARUNGO, F. P. and LODGE, J. P. Jr., 1967: Freezing of aqueous solutions of non-polar gases. *J. Atmos. Sci.*, **24**, 439–440.
PASHENKO, A. E. and GORBUNOV, B. Z., 1987: Kinetics of ice nucleation of aerosol particles in supercooled fog—II. Ice crystal growth and precipitations. *J. Aerosol Sci.*, **18**, 269–275.
PASSARELLI, R. E. Jr., CHESSIN, H. and VONNEGUT, B., 1973: Ice nucleation by solid solutions of silver-copper iodide. *Science*, **181**, 549–551.
PASSARELLI, R. E., Jr., CHESSIN, H. and VONNEGUT, B., 1974a: Ice nucleation by miersite. *J. Appl. Meteor.*, **13**, 610–612.
PASSARELLI, R. E., Jr., CHESSIN, H. and VONNEGUT, B., 1974b: Ice nucleation in a supercooled cloud by CuI–3AgI and AgI aerosols. *J. Appl. Meteor.*, **13**, 946–948.
PEREZ, P. J., GARCIA, J. A. and CASANOVA, J., 1985: Ice nuclei concentrations in Valladolid, Spain, and their relation to meteorological parameters. *J. Rech. Atmos.*, **19**, 153–158.
PITTER, R. L. and PRUPPACHER, H. R., 1973: A wind tunnel investigation of small water drops falling at terminal velocity in air. *Quart. J. Roy. Meteor. Soc.*, **99**, 540–550.
PLAUDE, N. O. and SOSNIKOVA, E. V., 1987: Formation of ice crystals on particles of complex chemical composition. In *Some Problems of Cloud Physics*, Gidrometeoizdat, Leningrad, pp. 94–102.
PLUMMER, P. L., 1973: Calculated intermolecular frequencies for clathrate and icelike water clusters. In *Physics and Chemistry of Ice* (eds E. Whaley, S. J. Jones, and L. W. Gold), Roy. Soc Canada, Ottawa, pp. 109–113.
PRUPPACHER, H. R. and PFLAUM, J. C., 1975: Some characteristics of ice-nucleation active sites derived from experiments with a ferroelectric substrate. *J. Coll. Int. Sci.*, **52**, 543–552.
PRUPPACHER, H. R. and KLETT, J. D., 1978: *Microphysics of Clouds and Precipitation*. D. Reidel Publ., Dordrecht, 714 pp.
RASMUSSEN, D. H. and MACKENZIE, A. P., 1972: Effect of solute ice-solution interfacial free energy; calculation from measured homogeneous nucleation temperatures. In *Water Structure at the Water-Polymer Interface* (ed. H. H. G. Jellinek), Plenum Press, pp. 126–145.
RAVDELY, A. A. and KOZLOV, G. A., 1970: Homogeneous nucleation of supercooled water. *Doklady Akad. Nauk, USSR*, **195**, 126–128. (in Russian)
REISCHEL, M. T., 1984: Freezing-nucleation in aqueous solutions of clathrate forming gases. *Tellus*, **36B**, 73–84.

REISCHEL, M. T., 1987: Variation of the activity of ice nuclei upon exposure to ammonium ion and iodine. *Tellus,* **39B,** 363–373.
REISCHEL, M. T. and VALI, G., 1975: Freezing nucleation in aqueous electrolytes. *Tellus,* **27,** 414–427.
ROBERTS, P. and HALLETT, J., 1968: A laboratory study of the ice nucleating properties of some mineral particulates. *Quart. J. Roy. Meteor. Soc.,* **94,** 25–34.
ROGERS, D. C., 1982: Measurements of natural ice nuclei with a continuous flow diffusion chamber. *Amer. Meteor. Soc., Cloud Phys. Conf.,* Chicago, pp. 115–118.
ROSINSKI, J., NAGAMOTO, C. T. and KERRIGAN, T. C., 1975: Heterogeneous nucleation of water and ice in the transient supersaturation field surrounding a freezing drop. *J. Rech. Atmos.,* **9,** 107–117.
ROSINSKI, J., HAAGENSON, P. L., NAGAMOTO, C. T. and PARUNGO, F., 1986: Ice-forming nuclei of maritime origin. *J. Aerosol Sci.,* **17,** 23–46.
ROWLAND, S. C., LAYTON, R. G. and SMITH, D. R., 1964: Photolytic activation of silver iodide in the nucleation of ice. *J. Atmos. Sci.,* **21,** 698–700.
SCHAEFER, V. J., 1946: The production of ice crystals in a cloud of supercooled water droplets. *Science,* **104,** 457–459.
SCHALLER, R. C. and FUKUTA, N., 1979: Ice nucleation by aerosol particles: Experimental studies using a wedge-shaped ice thermal diffusion chamber. *J. Atmos. Sci.,* **36,** 1788–1802.
SCHNELL, R. C. and VALI, G., 1972: Atmospheric ice nuclei from decomposing vegetation. *Nature,* **236,** 163–165.
SCHNELL, R. C. and VALI, G., 1976: Biogenic ice nuclei: Part I. Terrestrial and marine sources. *J. Atmos. Sci.,* **33,** 1554–1564.
STEIN, D. and GEORGII, H. W., 1985: Supersaturation spectra of ice nuclei at different locations in Europe and over the North-Atlantic ocean. *J. Rech. Atmos.,* **19,** 179–184.
STITH, J. L. and BENNER, R. L., 1987: Applications of fast response continuous SF6 analyzers to *in situ* cloud studies. *J. Atmos. Ocean. Techn.,* **5,** 599–612.
TABOREK, P., 1985: Nucleation in emulsified supercooled water. *Phys. Rev.* B, **32,** 5902–5906.
TANAKA, T., 1982: The membrane filter method combined with dialysis to detect ice nuclei; an application to the study of ice nucleation mode of volcanic ash. *Időjárás,* **86,** 110–116.
TOMLISON, E. M., 1980: A new horizontal gradient, continuous flow, ice thermal diffusion chamber and detailed observation of condensation-freezing and deposition nucleations. Ph.D. Dissert., Meteor. Dept., Univ. Utah, Salt Lake City, 108 pp.
TURNBULL, D., 1950: Kinetics of heterogeneous nucleation. *J. Chem. Phys.,* **18,** 198–203.
VALI, G., 1968: *Ice nucleation relevant to hail formation.* Sci. Rep. MW-58, McGill Univ., Montreal, 51 pp.
VALI, G., 1971: Quantitative evaluation of experimental results on the heterogeneous freezing nucleation of supercooled liquids. *J. Atmos. Sci.,* **28,** 402–409.
VALI, G., 1975: Remarks on the mechanisms of atmospheric ice nucleation. *Proc. VIII. Int'l Conf. Nucl.,* (Leningrad), Gidrometeoizdat, Moscow, pp. 265–269.
VALI, G., 1976a: Preface to *Report on Third International Workshop on Ice Nucleus Measurements.* Univ. Wyoming, Laramie, pp. 7–15.
VALI, G., 1976b: Contact-freezing nucleation measured by the DFC instrument. *Third Int. Workshop Ice Nucl. Meas.,* Univ. Wyoming, Laramie, pp. 159–178.
VALI, G., 1985: Atmospheric ice nucleation—a review. *J. Rech. Atmos.,* **19,** 105–115.
VALI, G., ROGERS, D. C. and DYE, J. E., 1982: Aerosols, cloud nuclei and ice nuclei. Ch. 3 In *Hailstorms of the Central High Plains* (eds C. A. Knight, and P. Squires), Colorado Univ. Press, pp. 33–57.
VALI, G., CHRISTENSEN, M., FRESH, R. W., GALYAN, E. L., MAKI, L. R. and SCHNELL, R. C., 1976: Biogenic ice nuclei. Part II: Bacterial sources. *J. Atmos. Sci.,* **33,** 1565–1570.
VALI, G., DESHLER, T. and ROGERS, D. C., 1984: Concentrations of ice nuclei of different modes of activation. *Eleventh Int. Conf. Atm. Aerosols Cond. Ice Nucl.,* Budapest, II., pp. 105–109.
VALI, G. and STANSBURY, E. J., 1966: Time-dependent characteristics of the heterogeneous nucleation of ice. *Can. J. Phys.,* **44,** 477–502.
VOLKOVITSKY, O. A., KIM, N. S. and SHKODKIN, A. V., 1987: On the formation of ice-forming

aerosols with optimum size distribution characteristics. In *Some Problems of Cloud Physics*, Gidrometeoizdat, Leningrad, pp. 103–111.

VONNEGUT, B., 1947: The nucleation of ice formation by silver iodide. *J. Appl. Phys.*, **18**, 593–595.

VONNEGUT, B. and CHESSIN, H., 1971: Ice nucleation by coprecipitated silver iodide and silver bromide. *Science*, **174**, 945–946.

VONNEGUT, B. and BALDWIN, M., 1984: Repeated nucleation of a supercooled water sample that contains silver iodide particles. *J. Clim. Appl. Meteor.*, **23**, 486–490.

VYCHUZHANINA, M. V., MIROSHNICHENKO, V. I., PARSHUTKINA, I. P., SOLOVJEV, A. D. and LESKOV, B. N., 1984: Airborne measurements of atmospheric ice nuclei. *Eleventh Int. Conf. Atm. Aerosols Cond. Ice Nucl.*, Budapest, II, 84–88.

WANG, M. K. and VONNEGUT, B., 1984: Repeated nucleation of supercooled water sample. *J. Rech. Atmos.*, **18**, 23–29.

WARBURTON, J. A., YOUNG, L. G., OWENS, M. S. and STONE, R. H., 1985: The capture of ice nucleating and non ice-nucleating aerosols by ice phase precipitation. *J. Rech. Atmos.*, **19**, 249–255.

WISNIEWSKI, J. and LANGER, G., 1980: Ice nucleus concentrations measured during the 1975 Florida Area Cumulus Experiment (FACE). *J. Appl. Meteor.*, **19**, 676–682.

WOOD, G. R. and WALTON, A. G., 1969: Kinetics of ice nucleation from water and electrolyte solutions. *Res. Dev. Prog. Rep. No. 500.*, U.S. Dept. Int., Off. Saline Wat., 171 pp.

WOOD, G. R. and WALTON, A. G., 1970: Homogeneous nucleation kinetics of ice from water. *J. Appl. Phys.*, **41**, 3027–3036.

WOODLEY, W. L., JORDAN, J., BARNSTON, A., SIMPSON, J., BIONDINI, R. and FLUECK, J., 1982: Rainfall results of the Florida Area Cumulus Experiment, 1970–1976. *J. Appl. Meteor.*, **21**, 139–164.

ZAMURS, J., LALA, G. and JIUSTO, J. E., 1977: Factors affecting ice nucleus concentration measurements with a static vapor-diffusion chamber. *J. Appl. Meteor.*, **16**, 419–424.

ZAMURS, J. and JIUSTO, J. E., 1982: An examination of ice nucleus concentrations in eastern New York State. *J. Appl. Meteor.*, **21**, 431–436.

ZETTLEMOYER, A. C., TCHEUREKDJIAN, N. and CHESSICK, J. J., 1961: Surface properties of silver iodide. *Nature*, **192**, 653.

5. Aerosols and climate

5.1 Statement of the problem

From a theoretical point of view, the atmosphere is a thermally driven geophysical fluid system which acts as a kind of heat engine, continually converting heat from the Sun into mechanical energy; that mechanical energy is in turn converted back to heat by frictional dissipation. These processes lend a transient behavior to the atmosphere, which is manifested in a continuous change of the complete atmospheric state with time, and is identified at a particular place with weather.

The introduction of the concept of climate is aimed at looking for a characteristically more persistent behavior of the atmosphere than that exhibited by weather. Therefore, the climate at a given place is commonly defined as being the average weather there. A broader definition of the climate includes all the statistical properties of an ensemble of many different states of the atmosphere.

The problem of climate has received much attention in the last few years and it can be advanced by adopting two different points of view. The theory of external causation of climatic change follows a basically deterministic approach. Within this concept, the climate is defined in terms of averages over an ensemble of internal states which is in equilibrium with the slowly changing external influences (LEITH, 1978). Climatic variations are therefore explained as being the necessary response of the internal system, say the atmosphere, to changes in external conditions, say the incoming solar radiation at the top of the atmosphere.

The theory of internal causation, by contrast, suggests that, even in the absence of any change in the external forcing, a unique climate may not exist. Climatic variations in this context might just be a natural (essentially stochastic) feature of the atmosphere–land–ocean–ice climate system due to the complex nonlinear interactions among the various internal components of the system (HASSELMANN, 1976; LORENZ, 1979).

When tackling the role of aerosol particles in climate modification we adopt the deterministic point of view by specifying any change in the aerosol content of the atmosphere as an external influence on the climatic state. The simplest possible quantitative approach to the problem in this case is the identification of climate with the internal state in energy equilibrium. As is known, the system's energy budget is dominated by the short-wave radiation coming from the Sun, and the long-wave terrestrial radiation escaping back to space. The

approximate balance between the solar and terrestrial energy fluxes defines the mean temperature of the system, i.e., the variable perceived most widely as characterizing the climatic state.

The particulate matter suspended in the atmosphere is likely to play a significant role in the control of climate because it affects the system's radiative balance directly and indirectly in several ways. The direct radiative effect is due to the fact that aerosol particles scatter and absorb the incoming solar radiation, the solar radiation reflected from the Earth's surface and also the outgoing terrestrial radiation. This process results in a redistribution of energy from solar and terrestrial radiation in the atmosphere, and causes atmospheric heating or cooling depending on the relevant optical properties and spatial distribution of the aerosol particles.

The most important indirect influence of aerosol particles on the radiation balance is through their effect on clouds. The action of aerosol particles as condensation and ice nuclei, and as coalescence centers, strongly affect the formation, lifetime and optical properties of clouds, and thereby the radiative transfer in a cloudy atmosphere at both solar and terrestrial wavelengths. Aerosol particles can also be found within or between cloud hydrometeors, either in solution in the drops or in suspension between them, and can cause changes in cloud albedo. A further effect can be aerosol-induced modifications in hydrostatic stability of the air column which in turn can affect the rate of cloud formation (see Subsection 3.5.4).

Some of the influences mentioned above lead to warming, while others represent cooling effects. Absorption by aerosol particles is always a warming influence, either it occurs at solar wavelengths or at terrestrial wavelengths. Backscattering to space of incoming solar radiation represents a cooling effect for the system, but backscattering of reflected short-wave or emitted long-wave radiation directs the beam back towards the surface and is a warming influence. The presence of clouds increases the reflectance of the Earth–atmosphere system, and in this respect it represents a cooling tendency. But in the infrared spectrum, the surface upon becoming covered by a cloud layer experiences a reduction in radiation loss to space, and so increasing cloud cover represents a warming tendency. The different warming and cooling effects do not take place independently, and the interrelationships between them constitute feedback mechanisms, many details of which are as yet poorly understood.

Airborne particulates will also affect the dynamical processes of the atmosphere. The heat sources and heat sinks due to regions of radiative imbalance are known to be at the origin of the general circulation of the atmosphere, which must be modified by the heating or cooling due to aerosol variations. However, not much is known about the details of this problem so far. Aerosol particles have only recently been introduced into general circulation models which couple the radiative effects of aerosols to atmospheric dynamics. Preliminary results indicate small but significant global as well as zonal and regional climatic modifications due to the presence of aerosol in the atmosphere.

The interpretation of external forcing influences on the climatic state is

especially complicated in the case of climate modification of anthropogenic origin. For example, there is now ample evidence for the presence of large concentrations of combustion-generated graphitic carbon particles (see Chapter 2) throughout the Arctic troposphere (CHYLEK *et al.*, 1984; MACCRACKEN *et al.*, 1986). This suggests that such black particles which are very effective absorbers of solar radiation could produce the Arctic warming which is also a symptom of the carbon dioxide increase. Recent estimates by ROSEN *et al.* (1984) have shown that atmospheric heating due to Arctic aerosol is nearly the same as a doubling of the concentration of CO_2. The individual effects of the various forcing influences on the climatic state can only be clarified by improved verification experiments and with better global data coverage. Our scientific knowledge and aerosol data are, however, sufficient at this time to justify and stimulate continued research interest on the impact of aerosols on climate (DEEPAK and GERBER, 1983).

5.2 Modifications of the radiation budget due to aerosol particles

The potential importance of atmospheric haze, dust and smoke to the climatic state of our planet has been recognized for a long time. The pioneering studies of CHARLSON and PILAT (1969), ATWATER (1970), MITCHELL (1971), and COAKLEY and CHYLEK (1975) concluded that the aerosol particles can either decrease or increase the net radiant energy available for the Earth–atmosphere system, leading to either global cooling or global warming, respectively. The cutoff between these two cases depends upon a series of parameters: the spatial localization and the optical characteristics of the aerosol particles at different wavelengths, the angle of the incidence of solar radiation and the reflectance of the ground surface. The details of the effects of aerosol particles on radiative transfer are discussed in Appendix III.

In a broad sense, atmospheric aerosol particles can be classified as either stratospheric (Subsection 5.2.1) or tropospheric (Subsection 5.2.2), and they may be either naturally occurring constituents of the atmosphere or of anthropogenic origin. The response of the climate system to the radiative forcing due to the presence of an aerosol layer can be investigated by performing simple radiation balance calculations (discussed in the present section), or by introducing aerosol particles into climate models of different sophistication (Section 5.3).

5.2.1 Stratospheric aerosols

As it was discussed in Subsections 2.3.3 and 2.4.3, an aerosol layer can be detected in the stratosphere. The particles in this layer have a residence time on the order of several years. Volcanic activity constitutes a major source of particulate matter at these high altitudes, but it has been suggested that high-

flying aircraft and industrial activity could also lead to an increasing stratospheric aerosol concentration.

Simple radiative transfer calculations show that a stratospheric aerosol layer can modify the global radiative balance in one of two ways. Reflection of solar radiation may enhance the planetary albedo, reducing the global surface temperature, whereas the infrared extinction in the aerosol layer can augment the greenhouse effect in the atmosphere and thereby increase the surface temperature. Some ten years ago, there was considerable debate as to which of these two competing mechanisms dominates. Nowadays, all investigators agree that on a global scale, the albedo modification is most important: with an increase in stratospheric aerosol loading the planetary albedo increases, producing a global cooling trend in the troposphere and at the surface. This fact is a consequence of the size distribution of the stratospheric aerosol: these particles have typical sizes which absorb and scatter the incident solar radiation more strongly than they affect the outgoing terrestrial radiation (COAKLEY and GRAMS, 1976).

The study carried out by HARSHVARDHAN and CESS (1976) was among the first works which emphasized that the increase in reflected sunlight constitutes the dominant contribution by stratospheric aerosols. Their calculated global mean temperature change is shown in Fig. 5.1 as a function of the visible optical thickness τ_{vis}. Also illustrated in this figure is the change in surface temperature if the infrared opacity (greenhouse effect) of the stratospheric aerosol layer is neglected. The comparison clearly indicates that the aerosol infrared absorption plays a small role in compensating for the reduction in surface temperature due to the aerosol solar reflectance. The normal stratospheric aerosol concentration

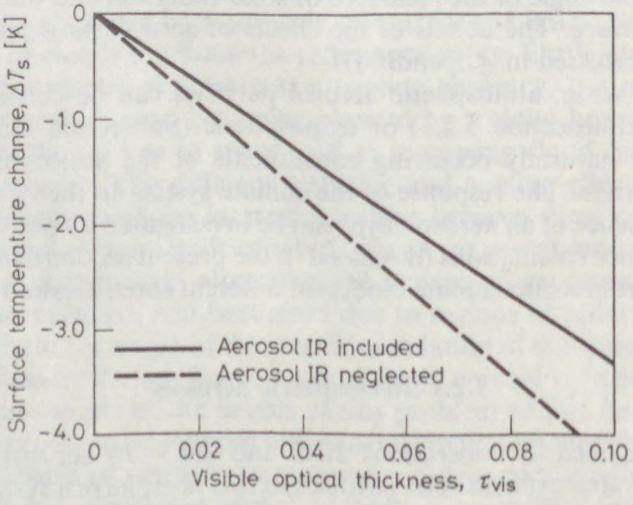

Fig. 5.1

Reduction in global mean surface temperature as a function of the visible optical thickness of stratospheric aerosol (after HARSHVARDHAN and CESS, 1976). (By courtesy of *Tellus*)

($\tau_{vis} = 0.02$) reduces the global mean surface temperature by 0.7 K; a doubling of aerosol concentration would produce a further decrease in surface temperature by the same amount.

LUTHER (1976) compared the solar and terrestrial radiative effects of a stratospheric aerosol layer between 18 and 22 km for a tropical atmosphere. The changes in the short-wave and long-wave fluxes above the aerosol layer were found to be comparable in magnitude. In the troposphere, the reduction in the incoming solar radiation (cooling) turned out to be several times greater than the increase in the downward terrestrial radiation (warming), the difference decreasing with increasing surface albedo.

Changes in the planetary albedo and the average equilibrium temperature of the air column due to perturbations in the solar radiative balance were investigated by HERMAN *et al.* (1976). The perturbations were induced by the introduction of varying amounts of aerosol particles into the stratospheric layer between 15 and 25 km, and results were examined for a wide range of aerosol absorption coefficients. They found that for a mass loading of 0.8 $\mu g\ m^{-3}$ and for non-absorbing aerosols (with a single-scattering albedo $\omega = 1.0$), the air column at all latitudes experiences a cooling during all seasons, with a peak decrease in the average air column temperature of 0.6 $K\ day^{-1}$ in the pole regions. With slightly absorbing ($\omega = 0.9$) and moderately absorbing ($\omega = 0.7$) aerosols, warming of the air column takes place nearly everywhere; for moderate absorption, a peak increase in temperature of 3.5 $K\ day^{-1}$ occurs at high latitudes in summer.

The effect of stratospheric aerosol particles on the Earth's monthly zonal radiation balance, including infrared radiative transfer, was investigated by HARSHVARDHAN (1979). He used a thin stratospheric scattering layer; the aerosols were assumed to be 75% H_2SO_4, non-absorbing droplets. His results also confirmed that the dominant influence of a thin stratospheric aerosol layer ($\tau_{vis} = 0.1$) is an increased reflection of solar energy all over the globe except for the polar-winter region when there is no solar insolation. The reduction in the radiation balance turned out to be nearly uniform and small equatorward of 50° latitude. The largest perturbations in the radiation balance occur at high latitudes in the spring and fall, whereas polar winters show a net gain in the radiation balance due to the increased greenhouse effect. It is interesting to note that the increased sensitivity of polar regions in these studies stems from purely radiative equilibrium considerations, and it appears even if only the visible portion of the wavelength spectrum is taken into account. From both observations and sophisticated modeling work, it is now a well-known fact that polar regions generally undergo larger temperature fluctuations during climatic change periods than do temperate or tropical latitudes.

More recently, LENOBLE *et al.* (1982) developed a simple three-layer model of the Earth–atmosphere system to compute the change in global radiation balance due to a stratospheric aerosol layer. According to their computations, the background stratospheric aerosol on the planetary scale leads to a loss of energy of 27 $W\ m^{-2}$ for an optical thickness of 0.03, including the small infrared

greenhouse effect, i.e., surface cooling occurs. The possibility of surface heating will appear only for much more absorbing aerosols with a single-scattering albedo < 0.9.

Supersonic transport and space shuttle operations have drawn additional attention to the question of the stratospheric aerosol influence. The effects of emissions of sulfur gases and of soot particles by high-flying aircraft were first considered during the Climatic Impact Assessment Program (CIAP) of the US Department of Transportation in the mid-1970's; it was estimated that a fleet of advanced supersonic transports emitting 3×10^7 kg of SO_2 per year between 18 and 21 km might reduce the Earth's surface temperature by roughly 0.05 K. However, the CIAP conclusions were based on a simple residence time model for an aerosol of fixed-size dispersion and, accordingly, were somewhat uncertain.

POLLACK *et al.* (1976b) also investigated the climatic impact of sulfuric acid particles released by supersonic transports and aluminium oxide particles emitted by space shuttle engines. To evaluate the effect of these additional aerosols on the global heat balance, they performed solar and terrestrial radiative transfer calculations. They found that the temperature change obtained by CIAP is an overestimation by about one order of magnitude, and that no significant climate change should result from the aerosols produced by space shuttles, supersonic transports, and other high-flying aircraft, operating at traffic levels projected for the next several decades. Later, this study was further expanded by a more complete treatment of aerosol physics and the incorporation of soot emissions (TURCO *et al.*, 1980). It was concluded that the release of large numbers of small soot or aluminium oxide particles into the stratosphere should not lead to a corresponding significant increase in the concentration of large, optically active aerosols. On the contrary, the increase in large particles is severely limited by the total mass of sulfate available to make large particles *in situ*, and by the rapid loss of small particles via coagulation. TURCO *et al.* (1980) found that a fleet of 300 advanced supersonic aircraft operating daily at 20 km, or the launch of one space shuttle rocket per week, could produce roughly a 20% increase in the large-particle concentration of the stratosphere. Aerosol increases of this magnitude would reduce the global surface temperature by less than 0.01 K, a negligible change.

The studies summarized above were motivated mainly by the growing concern that pollutants produced by our technological civilization may disturb the natural balance of airborne particulates, and thereby may inadvertently change the Earth's radiation budget and climate on a global scale. Recent volcanic eruptions have given a new impulse to these studies.

The earliest well-documented effect on stratospheric temperatures caused by an unusually high aerosol concentration due to a volcanic eruption[1] was analyzed by NEWELL (1970) and MCINTURFF *et al.* (1971). They found a warming at heights above about 15 km in the tropical stratosphere which persisted

[1] Concerning the properties of aerosol particles of volcanic origin see Subsections 2.3.3 and 2.4.2.

for several years after the Mt. Agung eruption on 17 March 1963; the average temperature increase attributed to the eruption was, at most, 2 K everywhere except over Australia, where the volcanic dust caused temperature increases as great as 5 K in the lower stratosphere. Other eruptions which followed that of Agung (including Awu in 1966, Fernandina in 1968, Fuego in 1974 and Mount St. Helens in 1980) were too weak to cause similar excursions of stratospheric temperatures until the event of the volcano El Chichón in southern Mexico which erupted a number of times over the period 28 March through 4 April 1982. Starting with June 1982, an unusual warming of the tropical stratosphere was observed by the Institute for Meteorology, Free University of Berlin (LABITZKE *et al.*, 1983). It quickly spread to northern latitudes and reached a maximum of approximately 5 K during August to November 1982 at the 30 hPa level at 10° N, which is the same magnitude and nearly the same heating pattern as was observed after the Agung eruption. This warming and its northward spread could be correlated closely with direct observations from satellites and lidar of the spreading of dust from the volcano El Chichón. Twenty-two years of statistics now clearly show that the warming induced by the Agung and the El Chichón aerosol is well above the standard deviation of the temperature record.

The generally accepted present view regarding the impact of volcanic eruptions on the radiative balance is basically that which has been developed by POLLACK *et al.* (1976a) and which can be summarized as follows. Silicate dust and concentrated sulfuric acid are the major aerosol components introduced into the stratosphere by a volcanic explosion. The former species is directly injected by the explosion and is the dominant component for the first several months. The latter species results largely from a set of slow photochemical reactions that convert the sulfur-containing gases of the volcanic emission into small particles of sulfuric acid. These particles can be assumed to be 75% aqueous solutions. Radiative transfer calculations at visible and infrared wavelengths have revealed that increases in both silicate and sulfuric acid aerosols due to a volcanic eruption lead to an increase in the global albedo. However, this cooling is offset by the enhanced greenhouse warming due to the aerosol opacity at infrared wavelengths. During the first few months following a volcanic explosion, when the aerosols are mostly dust particles of fairly large diameter, the two effects either cancel out or a small net warming of the surface occurs, accompanied by an increase in stratospheric temperatures. The calculations of POLLACK *et al.* (1976a) indicate that the observed heating of the stratosphere following the eruption of Mt. Agung was due chiefly to the absorption of upwelling terrestrial radiation by the added particles. At later times, and during most of the post-eruption period, smaller-sized dust and sulfuric acid aerosol particles cause a net surface cooling. The integrated effect over all stages following a volcanic eruption is a net cooling of the surface.

Since volcanic aerosols have two competing effects on the Earth's radiation budget—the albedo effect and the greenhouse effect—, it is important to have a correct picture concerning the influence of volcanically induced stratospheric

aerosols upon the planetary albedo of the Earth. Unfortunately, however, considerable differences exist in this respect. For example, HARSHVARDHAN and CESS (1976) suggest that the change of the planetary albedo α_p with the aerosol optical depth τ_{vis} at the wavelength of 0.55 μm is

$$\frac{d\alpha_p}{d\tau_{vis}} \cong 0.2$$

while POLLACK *et al.* (1976a) produce the substantially lower result

$$\frac{d\alpha_p}{d\tau_{vis}} = 0.082.$$

The primary goal of the study of CESS *et al.* (1981) was to explain this large difference by illustrating the importance of performing full-flux calculations, together with incorporating the angular dependence of scattering within the Earth–atmosphere system, when modeling the influence of volcanically induced stratospheric aerosols upon the system albedo. With μ_0 denoting the cosine of the solar zenith angle and α_c the cloud reflectance, CESS *et al.* (1981) have found for clear skies

$$\frac{d\alpha_p}{d\tau_{vis}} = 0.151,$$

for cloudy skies and $d\alpha_c/d\mu_0 = -0.55$

$$\frac{d\alpha_p}{d\tau_{vis}} = 0.033,$$

and for cloudy skies and $d\alpha_c/d\mu_0 = 0$

$$\frac{d\alpha_p}{d\tau_{vis}} = 0.058.$$

Assuming, as did POLLACK *et al.* (1976a), 50% cloud cover, one finds that on a global average $d\alpha_p/d\tau_{vis} = 0.092$. These values illustrate that volcanic aerosols in the stratosphere produce an effect upon clear-sky regions that is five times that produced upon cloudy-sky regions. This result may have important regional consequences.

5.2.2 Tropospheric aerosols

Tropospheric aerosol particles are generally concentrated in the lowest atmospheric layers, and their residence time is usually on the order of days to weeks. Like stratospheric aerosols, the tropospheric aerosol particles modify the Earth's radiation budget through interaction with solar and terrestrial radiation, but their interaction with the long-wave radiation is generally less important, since they are at temperature only slightly lower than that of the ground. They can either increase or reduce the reflection of solar radiation, leading either to a

cooling or a warming of the surface–troposphere system. Results of the calculations carried out by HERMAN and BROWNING (1975), for example, show that, for small values of ground albedo α, the reflected solar flux may either increase or decrease with increasing aerosol loadings, depending upon the imaginary part n_i of the refraction index of the particles. For high ground albedos ($\alpha > 0.4$), an increase in aerosol levels always results in a decrease of reflected flux, i.e., a warming of the system. An extensive review of published observations of aerosol optical properties has been carried out recently by KELLOGG, and his conclusion is that aerosol absorption-to-backscatter ratio is generally so large that when in cloud-free layers over land with an albedo of 0.15 or greater they cause a warming of both the surface and the lower atmosphere (KELLOGG, 1981). Regarding the vertical distribution of the heating rate due to absorption of the solar radiation by aerosols, YAMAMOTO *et al.* (1974) showed that the heating rate is greater in the lower troposphere, especially at low latitudes, and that it increases appreciably with increasing turbidity. The heating rate is very sensitive to the value of n_i; the heating rate for $n_i = 0.03$ is two or more times that for $n_i = 0.01$.

According to the comprehensive evaluation of tropospheric aerosol influence on solar radiation by LIOU and SASAMORI (1975), the solar heating rates may be as much as 5 and 9 K per day near surfaces whose albedos are 0.1 and 0.8, respectively. Their local-albedo calculations for the entire solar spectrum reveal that a surface albedo of about 0.3 to 0.4 is crucial to whether a globally averaged albedo increases or decreases as the result of an additional load of aerosol particles in the atmospheric boundary layer. An increase of aerosol concentration always leads to an increase of the total absorption within the atmosphere. Hence, there should be a warming effect. But an increase of aerosol loading reduces the solar flux available to the surface for absorption. Consequently, the surface should experience a cooling effect. Thus cooling occurs near the surface with warming aloft. The net heating effect for the Earth–atmosphere system, however, depends strongly upon the surface characteristics.

BLANCHET and LEIGHTON (1981) studied the influence of both refractive index and size distribution of aerosol particles on atmospheric heating rates due to solar radiation absorbed by the particles. They found that, for climate studies, the choice of values of the complex refractive index is more crucial than the choice of the shape of the size spectrum. Both the real and the imaginary refractive index can modify the absolute value of the planetary albedo by several percents. However, varying the values of n_i between 0 and 0.1 lead to variations of the heating rate near the ground between 1.5 and 6 K day^{-1}. Using a wide variety of shapes of the aerosol spectrum with the same total volume density of aerosol, they found deviations of about $\pm 27\%$ from the median value in the contribution to the heating rate.

Tropospheric aerosol particles generally have a much higher optical thickness than do stratospheric aerosols, with optical thicknesses typically ranging between 0.1 for the "clear" tropospheric air and 1.0 or even more for very turbid conditions. Due to this large optical thickness, the aerosol influence can be

expected to be large, but because the aerosol particles have a short residence time and they show large temporal and spatial variations, both in quantity and in radiative characteristics, it is more difficult to assess their global climatic impact (LENOBLE, 1984). On a regional scale, strong outbursts of aerosol particles, such as desert dust storms, very likely influence the local climate. For example, JOSEPH and WOLFSON (1975) found for two sites in Israel—one in the coastal plain and one in the Judean hills—that the imaginary part of the refractive index, averaged over the solar spectrum, is considerably smaller during khamsinic conditions—i.e., dry hot weather with desert winds ($n_i = 0.03$) —than for normal days ($n_i = 0.08$). CARLSON and BENJAMIN (1980) investigated the effects of Saharan dust on radiative fluxes. For moderately heavy dust amounts commonly measured over the Sahara and the eastern tropical Atlantic Ocean, typical calculated aerosol heating rates for the combined long-wave and short-wave spectrum were in excess of 1 K day^{-1} for most of the troposphere beneath the top of the dust layer (500 hPa).

In recent years, the number of studies in the area of urban climates and the effect of aerosols on atmospheric variables has grown fairly rapidly. Several of these studies have indicated that strong pollution over large urban and industrial areas is likely to interfere with the local and regional climate. ACKERMAN (1977) developed a one-dimensional, time-dependent heat-transfer model of the boundary layer to study the effects of pollutants on local values of the meteorological variables. The results of his study has led him to conclude that pollutants in general and aerosols in particular have a fairly small effect on urban temperatures because of a strong tendency within the substrate–atmosphere system for self-stabilizing compensation. If the short-wave radiation is absorbed by a layer near the ground, this absorption reduces the transfer of heat from the surface to the atmosphere. This in turn tends to keep the surface and boundary-layer temperatures approximately the same as if no absorption were taking place. The loss of energy due to backscatter may also result in a reduction of the depth of the boundary layer rather than in a reduction in temperature. This reduced depth compensates for reduced heating by spreading the heating over a shallower layer. An additional compensation occurs within the radiative fluxes. The warming of the atmosphere by short-wave radiation is opposed to a lesser degree by an increase in long-wave emission. This also tends to maintain the surface temperature. In addition to this compensation, the results of ACKERMAN's model runs show that the main effect of the aerosols on the urban climate is to increase daytime temperatures. This increase is fairly small and is related to the aerosol concentration. In areas with relatively high background concentrations mixed through the planetary boundary layer, the aerosol heating tends to retard the growth of the mixed layer, but this tendency may be counteracted by an increase in surface temperature.

Observations over the past several years have indicated that a significant component of the aerosol burden of the Arctic troposphere is soot most likely of anthropogenic origin (see in more detail in Subsection 2.4.2). Because soot is a strong absorber of solar radiation, and since the surface albedo at Arctic

latitudes is typically high, the presence of such an aerosol has raised the possibility of an anthropogenically-induced impact upon the Arctic climate through a lowering of the planetary albedo which results in an increased solar absorption by the surface–atmosphere system. Indeed, radiative calculations carried out by CESS (1983) and MACCRACKEN *et al.* (1986) are consistent in suggesting that carbonaceous aerosols should produce surface warming in Arctic regions, but the manner in which this is accomplished is a bit unusual. The direct impact of the aerosol is to reduce absorbed solar radiation at the surface. This effect, however, is minimized by the high surface albedos which in turn, due to the large surface reflection, enhance aerosol solar absorption. This aerosol-induced atmospheric heating then results in increased infrared emission from the atmosphere to the surface that more than compensates for the reduced solar absorption, thus producing surface warming. According to the calculations of MACCRACKEN *et al.* (1986), this surface warming is coupled with an interesting cryospheric feedback process and leads to a springtime Arctic temperature increase that is roughly consistent with observed trends in high latitude temperatures, an effect some have attributed to carbon dioxide-induced changes.

In two interesting papers, SHAW (1983, 1987) drew attention to a curious coincidence involving the mean wavelength of solar radiation and the mean size of tropospheric aerosols. Coarse particles, such as grains of windblown sand, are rapidly removed by impaction and sedimentation, while extremely fine particles, like those detected with condensation nucleus instruments, are quickly removed by diffusion. It follows that particles of some intermediate size remain airborne for longest times, and general considerations indicate that this intermediate size range is between 0.1 and 1.0 μm in diameter, i.e., the very range where particles interact extremely efficiently with solar radiation. Consequently, any mechanism that produces particles of a few tenths of a μm in diameter is a potent candidate for causing the atmospheric radiation balance to change. Now, it is known that a large fraction of the present tropospheric aerosol consists of sulfate particles produced by the atmospheric oxidation of sulfur gases from the biota (see Chapter 2). Therefore, it seems likely that the biologically-produced sulfur that enters the atmosphere is responsible for creating a large fraction of the present optical depth of the background troposphere. In other words, SHAW proposed that sulfur-containing aerosol particles should be looked upon as an efficient regulator of the Earth's radiation budget. This conclusion leads to the problem of biological regulation of the climate system which will be discussed in fuller details in Subsection 5.4.3.

5.3 Modeling the climatic effects of aerosol

Our knowledge of the physical basis of climate and climatic variation is most usefully and comprehensively organized in terms of models, which are mathematical representations of the physical laws which govern the climate system's behavior. From such models, the system's future behavior or a future climatic

state may, in principle, be determined, and in this sense climate models represent the physically most rational basis for studying the climate. Climate models have shown considerable skill in reproducing the present climate of the Earth and that at selected times in the past, and their use in the prediction of future climate is the subject of intensive research (GATES, 1981).

The basic physical laws which govern the behavior of the climate and on which a climate model may therefore be based, are expressed by equations which describe the conservation of momentum, heat and water vapor—the so-called primitive equations. Once all of the numerical approximations, constants and boundary conditions (external forcings) required for a model's solution have been assembled, a time integration can be carried out for an indefinite period starting with arbitrary initial conditions. During the initial period of the calculation, the various large- and small-scale physical processes in the model adjust to each other and to the imposed boundary conditions in accordance with the model's governing equations. After this period (which requires from a few weeks to a few months, depending upon the characteristic time-scale of the physical processes involved), the statistics of the model's solution (i.e., the climate) is assumed to be determined by the model and the boundary conditions only.

If the model is to describe only the climate as averaged, say, over one or two geometric dimensions, the model's governing equations could at least formally be derived by appropriately averaging the primitive equations. In the extreme, such averaging could be performed over all dimensions to yield a zero-dimensional model for the globally-averaged climate, in which case the atmospheric motion becomes implicit; the globally-averaged temperature and water vapor are then the model's dependent variables which are commonly parameterized in terms of the surface temperature and humidity. The model is then developed around the budget equation for the flux of radiation, sensible and latent heat at the surface, of which the prototype model is that of BUDYKO (1969). In another version of such "energy balance models", averaging is performed only in the vertical and longitudinal directions, with each term in the surface heat budget now parameterized in terms of the surface temperature as a function of latitude. Such models, of which that of SELLERS (1969) is the first example, are able to portray the basic latitudinal dependence of the Earth's heat and hydrologic balances when adequate parameterization is made for the meridional transport of heat and moisture. An introductory survey of the global energy balance climate models is presented by NORTH *et al.* (1981).

In other types of these simplified climate models averaging is performed over only one or two geometric dimensions. When both horizontal dimensions (but not the vertical dimension) are suppressed, the resulting column model considers the temperature as a function of pressure (or height) in response to the vertical transfer of heat. When the only heating is by radiation, such a "radiative balance model" is able to portray the overall vertical temperature distribution in the atmosphere. However, when a convective-adjustment parameterization for the vertical flux of heat by convective motions is added, the resulting "radiative–convective model" provides a more realistic tropospheric vertical

temperature structure as first shown by MANABE and STRICKLER (1964). A review of the radiative–convective models that have been used in studies pertaining to the Earth's climate is given by RAMANATHAN and COAKLEY (1978).

At the top of the climate modeling hierarchy are those models in which no explicit restriction regarding the number of geometric degrees of freedom is introduced. Such three-dimensional models undertake a more-or-less straightforward integration of the governing primitive equations over the globe, and with a horizontal resolution of the order of several hundred kilometers they are able to resolve the large-scale transient motion systems that maintain the climate system energetically (SMAGORINSKY, 1974). Such "general circulation models" began in 1955 with the pioneering calculations of PHILLIPS (1960) for a simplified system; the climate simulation capability of such models have recently been reviewed by GATES (1981).

Finally, among the deterministic climate models mention should be made of statistical–dynamical approaches because they also have important applications in studying the climate. A general circulation model generates its own transient motions which transport heat and momentum. Although individual synoptic eddies cannot be predicted on climatic time scales at the right time and the right place, their statistical behavior is almost correct. Now, a statistical–dynamical model is based on the idea that the statistical behavior of the transient eddies can be expressed in terms of the mean flow via parameterization relations (OPSTEEGH, 1981). In that case it is possible to deal with the mean flow directly. A simple procedure is to average the equations for instantaneous flow in time. This leads to a set of equations very similar to the original ones, but with an additional force in the momentum equation and an additional heating term in the thermodynamic equation. These additional terms describe the influence of transient pressure systems on the mean flow. A survey of statistical–dynamical models of the global climate is given by SALTZMAN (1978).

5.3.1 Effects of naturally occurring aerosol and its anthropogenic increase

The hypothetical, naturally occurring background aerosol is capable of depressing the Earth's surface temperature by 2 to 3 K. It therefore rivals the influence of the minor gaseous constituents like nitrous oxide and methane, and its effect is comparable in magnitude but opposite in sign to what might be expected from projected increases in carbon dioxide (UNEP/WMO/ICSU, 1985). In spite of this fact, the influence of aerosol has yet to be investigated with the vigor so far reserved for investigating changes due, for example, to increases in atmospheric carbon dioxide concentration. Although numerous model studies have addressed the impact of aerosol particles upon the Earth's present climate, there remain many unanswered questions.

Simple energy balance climate models are based upon the radiation balance of the Earth–atmosphere system. The early model studies by RASOOL and SCHNEIDER (1971), and YAMAMOTO and TANAKA (1972) can therefore be regarded as a direct extension of the works overviewed in Section 5.2.

In the energy balance model adopted by RASOOL and SCHNEIDER, an aerosol layer was placed just over the surface, and the single-scattering albedo was used to describe the absorption effect of the particles. On the other hand, YAMAMOTO and TANAKA considered both tropospheric and stratospheric aerosols, and they introduced the imaginary part n_i of the refractive index for characterizing the effectiveness of particle absorption. Results of these two approaches are in good agreement. A change of the optical thickness τ_{vis} from 0.1 to 0.3 gave global average surface temperature decrease $\Delta T_s = -3.4$ K in the RASOOL and SCHNEIDER model, and $\Delta T_s = -3.9$ K in the YAMAMOTO and TANAKA model for slightly absorbing aerosols ($\omega = 0.99$ or $n_i = 0.001$); and $\Delta T_s = -2.3$ K and -2.4 K, respectively, for moderately absorbing particles ($\omega = 0.90$ or $n_i = 0.013$).

More recently, COAKLEY *et al.* (1983) employed a one-dimensional (latitudinally dependent) energy balance model for investigating the climatic effects of the naturally occurring aerosols. They varied the optical thickness τ_{vis} for the background aerosol from 0.16 at low latitudes (from the Equator to 25° N latitude) to 0.07 at high latitudes (from 65° N to the Pole), and the surface albedo α from 0.08 at low latitudes to 0.61 at 85° N. Changes in the system albedo were taken to be $\Delta\alpha_p = +0.0094$ at low latitudes and -0.0036 at 85° N due to the presence of an aerosol with real refractive index of $n_r = 1.5$ and imaginary refractive index of $n_i = 0.01$. Model results are summarized in Fig. 5.2. We see that the present background aerosol cools the Earth at all latitudes relative to a hypothetical aerosol-free atmosphere, the decrease in global surface temperature ranging from 2.0 K ($n_i = 0.01$, representative for wind-blown dust particles) to 3.3 K ($n_i = 0$, representative for sea-salt particles). We can also see that although an increased aerosol absorption produces rather significant aerosol heating especially at higher latitudes, this does not imply that such aerosol particles would produce surface warming at the polar region. The near-maximum surface cooling at high latitudes occurs despite a local decrease in the planetary albedo and resulting increse in solar heating caused by the particles at these latitudes. The reason for this surface cooling around latitude 85° is that the individual latitude zones are coupled by advective energy transport, and the high-latitude climatic change illustrated in Fig. 5.2 is controlled, through advection, by aerosol-induced cooling at low and mid-latitudes. In summary, the present naturally occurring background haze exerts a rather substantial influence upon the present climate, particularly at high latitudes; this influence is comparable in magnitude but opposite in sign to what would be expected for a doubling of atmospheric carbon dioxide concentration.

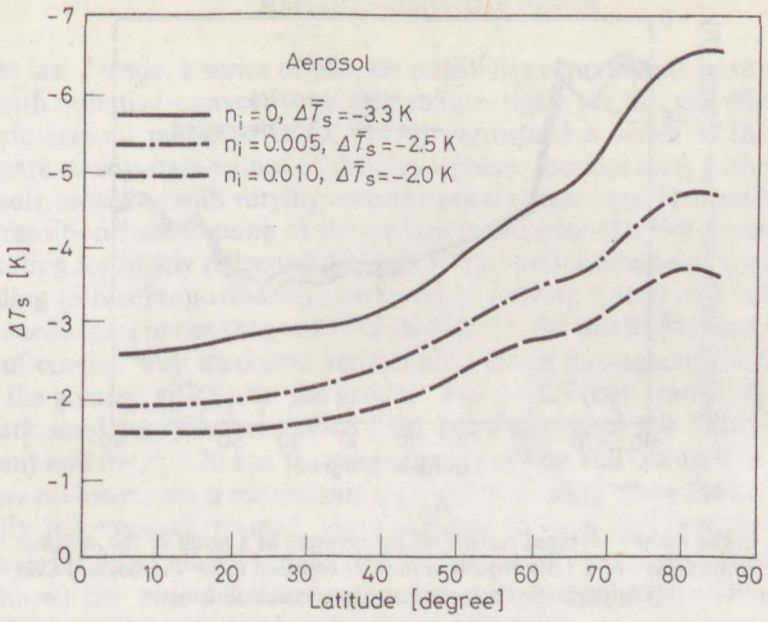

Fig. 5.2

Change in the latitudinal surface air temperature ΔT_s due to an aerosol with a real refractive index of $n_r = 1.5$ (after COAKLEY *et al.*, 1983). (Copyright by the American Meteorological Society)

These conclusions of COAKLEY *et al.* (1983) are consistent with a later study by POTTER and CESS (1984), who employed the annual average version of a two-dimensional (latitude and height dependent), nine-level statistical–dynamical model of the Lawrence Livermore National Laboratory, University of California. The inclusion of background tropospheric aerosol particles within the model was made by using continental-type aerosol over land areas, and maritime aerosol over oceans and sea ice. The results obtained suggest that the naturally occurring aerosol particles reduce the global-mean surface air temperature by 3 to 4 K and that the maximum cooling takes place at high latitudes, despite the fact that aerosols produce a mild increase in solar heating at these latitudes. Changes in zonally averaged surface air temperature and global mean atmospheric temperature as a result of the incorporation of tropospheric aerosols as well as a 1.3% reduction in solar constant are shown in Figs 5.3 and 5.4. We see that these separate climate forcings produce nearly identical climate effects, despite the fact that the two forcings have quite different latitudinal and vertical distributions. This suggests that the climate response to tropospheric aerosol forcing is insensitive to the manner in which the aerosol particles are vertically distributed.

On the other hand, the climate response to aerosol forcing might be substantially amplified by the ice–albedo feedback process. This fact was emphasized by JUNG and BACH (1987) who employed the same aerosol types and the same

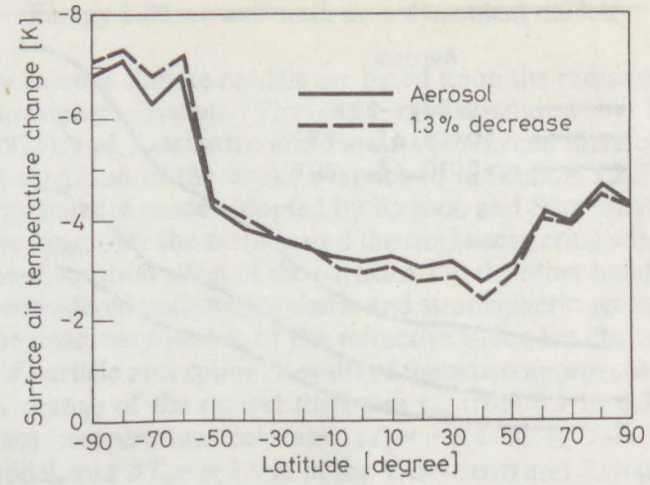

Fig. 5.3

Changes in the zonally averaged surface air temperature as a result of the inclusion of tropospheric aerosols and of a 1.3% reduction in solar constant (after POTTER and CESS, 1984). (Copyright by the American Geophysical Union)

optical thickness distribution given earlier by POTTER and CESS (1984). Their two-dimensional zonally-averaged climate model indicated that due to the presence of the aerosols, the annual temperature change at the surface is -2.1 K with ice–albedo feedback; without ice–albedo feedback the corresponding value is -1.4 K.

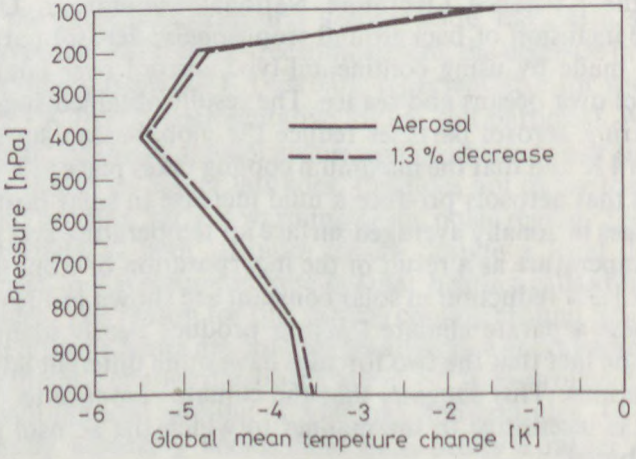

Fig. 5.4

Change in the global mean atmospheric temperature as a result of the inclusion of tropospheric aerosols and of a 1.3% reduction in solar constant (after POTTER and CESS, 1984). (Copyright by the American Geopysical Union)

Radiative–convective models

In the last decade, a series of climate sensitivity experiments have been carried out with radiative–convective models to investigate the thermal effects of atmospheric aerosol particles. RECK (1974) performed a series of calculations to compare steady-state values of the atmospheric thermal state without and with aerosols, as well as with varying aerosol optical parameters. Her results confirmed the transition from cooling of the surface in the case of a low ground reflection to heating for highly reflecting ground. For a surface albedo of $\alpha = 0.07$ (corresponding to blacktop roadway, dark soil or moving water) and volume extinction coefficients in the range of $0 > \beta_e \leq 4\ \mathrm{km}^{-1}$, the model predicts an increased rate of cooling with increased aerosol abundance throughout the troposphere, with the greatest effect near the ground. For $\alpha = 0.3$ (corresponding to light soil or dark sand, and characteristic of the mean albedo of the Earth–atmosphere system) and $0 < \beta_e \lesssim 20\ \mathrm{km}^{-1}$, atmospheric cooling still occurs due to aerosols, but we no longer see a monotonic increase in cooling when the aerosol optical density is increased; instead, there appears to be a decrease in the effect of aerosols for $\beta_e > 3\ \mathrm{km}^{-1}$. Finally, for $\alpha = 0.6$ (i.e., in the range of reflectivity valid for snow) the model indicates at all tropospheric levels a decrease in the radiative cooling with increased aerosol content.

In the subsequent studies of RECK (1975, 1976), and RECK and HUMMEL (1981) the influence of various quantities, such as the height of the aerosol layer, aerosol size distribution, and aerosol absorption (i.e., the imaginary part of the refractive index) is emphasized. It is shown that over a surface having a mean short-wave albedo of $\alpha = 0.3$, the system albedo increases as the optical depth τ increases for both high-level (41.5 hPa) and middle-level (418 hPa) aerosol layers, while for a low-lying aerosol layer (958 hPa) the greatest effect is for $\tau = 0.065$, with a decreasing effect as τ increases. The calculated surface temperatures have turned out to be relatively insensitive to the real part of the refractive index and to the size distribution assumed. The sensitivity to surface albedo is similar for the three main aerosol types characteristic of marine aerosols, continental aerosols and stratospheric aerosols. An increase of 0.1 in the absorptive component of the refractive index n_i increases the calculated surface temperature by 0.4 K for $\alpha = 0.07$ (oceans) and by 1.0 K for $\alpha = 0.60$ (snow and ice). In other words, the heating is increased 2–3 times as the surface albedo is increased by an order of magnitude. A 0.1 increase in n_i corresponds very roughly to a factor of two increase in the percentage of solar absorption by an average particle.

The importance of the combined effects of clouds, aerosols and surface albedo in determining whether heating or cooling of the Earth–atmosphere system occurs is stressed by WANG and DOMOTO (1974). Their model calculations indicate that the increase of atmospheric turbidity due to aerosol alone may decrease the system albedo for the case when the surface albedo is larger than 0.30, i.e., heating of the Earth's atmosphere due to the presence of aerosol is

possible for surface types such as dry grass land, desert or snow-covered ground. For the same reason, the presence of stratospheric aerosol with underlying clouds (high albedo) may also cause heating if higher water vapor concentration is found in the stratosphere.

Heat storage and meridional transport effects have generally not been included in these earlier, steady-state radiative–convective studies of aerosol and climate. In the work of CHARLOCK and SELLERS (1980b), the one-dimensional radiative–convective model structure is retained, but additional sources and sinks of heat, due to surface and atmospheric storage and to oceanic and atmospheric dynamics, are included. These have permitted them the calculation of fairly realistic temperatures in selected latitude belts on a month-by-month (time-marching) basis. The effects of varying aerosol composition throughout the entire column at 40–50° N latitude belt obtained by the annual version of their model are shown in Fig. 5.5. Here, single-scattering albedo ω is varied with a fixed surface albedo of $\alpha = 0.13872$. The strongly absorbing aerosol with $\omega = 0.75$ has $dT_s/d\tau = +4.9$ K, while the non-absorbing aerosol with $\omega = 1.0$ has $dT_s/d\tau = -15.4$ K. It is seen that adding aerosol with $\omega \approx 0.81$ would cause no change in the computed annual mean surface temperature. Figure 5.6 shows

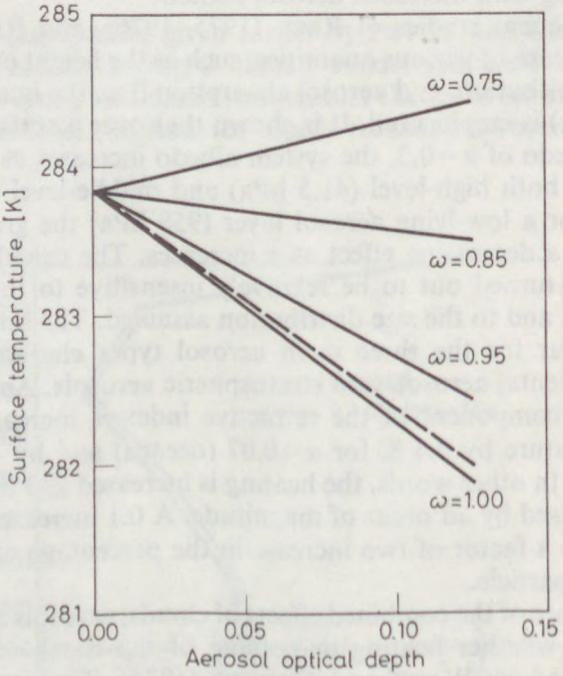

Fig. 5.5

Annual mean surface temperature at the 40–50° N latitude belt as a function of the aerosol optical depth at various single-scattering albedos ω. The dashed line refers to the TOON and POLLACK (1976) aerosol. (After CHARLOCK and SELLERS, 1980b). (Copyright by the American Meteorological Society)

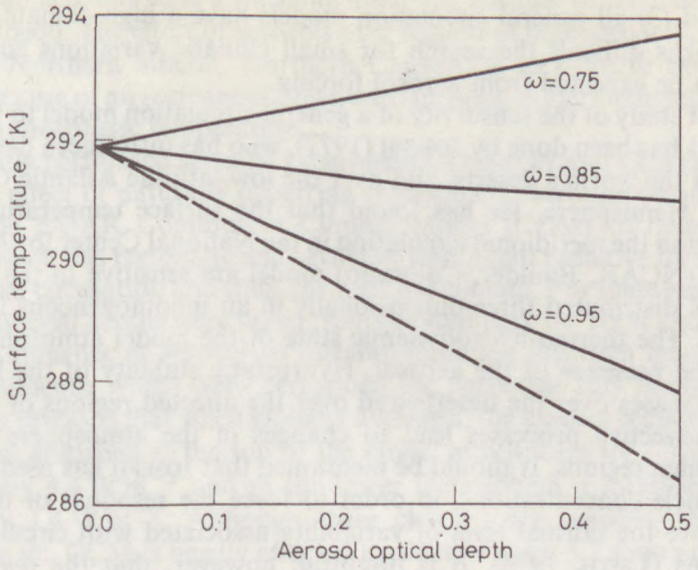

Fig. 5.6

Global surface temperature as a function of the aerosol optical depth for various single-scattering albedos ω. The dashed line refers to the TOON and POLLACK (1976) aerosol. (After CHARLOCK and SELLERS, 1980b). (Copyright by the American Meteorological Society)

aerosol effects on the global version of the model. Aerosol, as with the annual model, has a nearly linear effect on the mean surface temperature. The global surface temperature is less sensitive to the addition of aerosol than the mid-latitude surface temperature. For the addition of aerosol with $\tau = 0.125$, the global surface temperature drops 1.5 K, while the annual surface temperature in the 40–50° N latitude belt decreases by 1.8 K.

General circulation models

Introduction of aerosol particles into a general circulation model is evidently the best way for identifying possible dynamical and hydrological changes in response to the radiative forcing by aerosol which energy balance models or radiative–convective models either ignore or only crudely approximate. However, as it has been stressed by LENOBLE (1984), some important points have to be kept in mind, to avoid exaggerated optimism: (1) radiation codes which are compatible with the available computer time in general circulation models are highly simplified and ignore the diurnal (and sometimes the annual) cycles; (2) all the present general circulation models include simplifications and constraints which, in fact, can hide some aerosol influences or block some feedback processes (e.g., sea-surface temperature is generally fixed according to present climatic values, which may seem at least surprising, when looking for climatic modifica-

tions); and (3) all general circulation models have a high climate noise level, which makes difficult the search for small climatic variations such as those which can be expected from aerosol forcing.

The first study of the sensitivity of a general circulation model to the presence of aerosols has been done by JOSEPH (1977), who has introduced desert aerosols over all of the world's deserts, and over the low-latitude Atlantic Ocean in the Northern Hemisphere. He has found that the surface temperature, air temperature, and the meridional circulation in the National Center for Atmospheric Research (NCAR, Boulder, Colorado) model are sensitive to the presence of an aerosol distributed three-dimensionally in an inhomogeneous fashion over the globe. The thermo-hydrodynamic state of the model atmosphere also adjusts to the presence of the aerosol. Hydrostatic stability of the lower atmosphere increases over the deserts and over the affected regions of the Atlantic Ocean. Advective processes lead to changes in the atmosphere outside the aerosol-laden regions. It should be mentioned that JOSEPH has used abnormally large particle concentrations, in order to force the response of the model to stand above the normal level of variability associated with circulation model simulations (LEITH, 1973). It is doubtful, however, that the results of such studies can be scaled to obtain changes to be expected for concentrations at the background levels.

The trade winds frequently carry Saharan dust out over the tropical Atlantic Ocean during the northern summer (see Subsection 2.2.1). In order to evaluate its effects on the weather and climate of the region, the Goddard Laboratory for Atmospheric Sciences (GLAS, Greenbelt, Maryland) general circulation model has been modified by RANDALL *et al.* (1984) to include the effects of Saharan dust. Their results suggest that heating by absorption can produce a narrowing and intensification of the Intertropical Convergence Zone (and consequently of the tropical rain belt) and a marked weakening of the trade winds. The precipitation effect is systematic and progressive; that is, it is stronger for optically thick dust than for optically thin dust. The result obtained for the wind component is interesting, since in nature it is the easterlies that transport the dust.

TANRE *et al.* (1984), in the framework of a European project at the European Centre for Medium Range Weather Forecasts (ECMWF, Shinfield Park, Reading), have introduced into the Center's low-resolution model five types of aerosol (continental, maritime, urban, volcanic and stratospheric) and their optical properties have been computed in accordance with the International Radiation Commission. The effect of the aerosol particles on the model climate has been found to be just at the limit of the noise level for the dynamic processes but to be significant for the mass field. There is a warming effect of aerosol particles over high latitudes in the lower levels; a cooling effect near the surface over the desert regions and over latitudes without continents; and a warming of the troposphere nearly everywhere, increasing upwards to reach a maximum in the stratosphere (up to 3 K at 30° S). Saharan and continental aerosols have a cooling effect for the surface that reaches a maximum of 4 K over the Sahel

region. Urban aerosols have a warming influence, because of their small single-scattering albedo. The effect of aerosols over regions of high albedo (Greenland, Antarctica, Northern Siberia, Northern Canada) is to increase surface temperature, because of an increase of downward infrared radiation in relation with the higher atmospheric temperature.

In a recently performed series of experiments, COAKLEY and CESS (1985) have inserted the effect of naturally occurring tropospheric aerosols on solar radiation into the NCAR Community Climate Model (CCM) to determine the manner in which this regionally and vertically dependent radiative forcing might affect regional circulation and thus, the regional climate. For these experiments, the aerosol optical depths were taken from the summary by TOON and POLLACK (1976). The influence of aerosol on infrared radiation has been ignored.

The experiments, which were performed for perpetual July boundary conditions, have revealed that when globally averaged, the aerosol reduces the solar radiative flux absorbed at the top of the model atmosphere by 3.0 W m^{-2}, at the surface by 4.4 W m^{-2} and in the lower troposphere it increases the flux absorbed by 1.4 W m^{-2}. Although these changes are sizeable, the climate simulated by the CCM is hardly affected by them. Figure 5.7 shows changes in the zonal average surface temperatures, and the most notable aspect of this figure is the lack of change. In energy balance model calculations for the same perturbation, the changes in the zonal mean temperature range from −2 K at the Equator to almost −6 K at the Pole; the change in the global means with

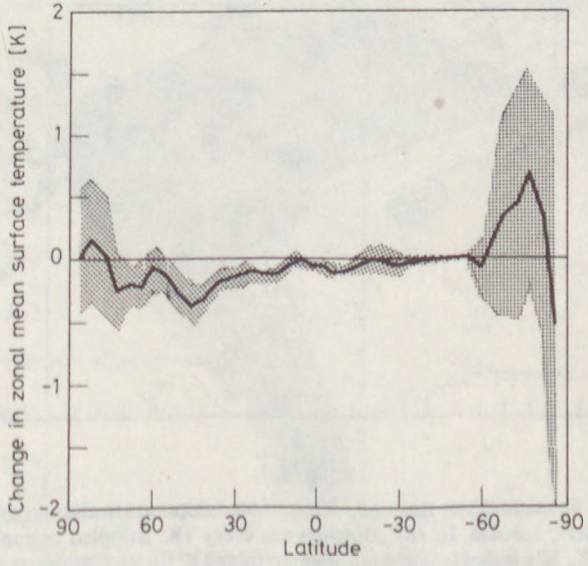

Fig. 5.7

Change in zonal mean surface temperature due to radiative forcing by the naturally occurring tropospheric aerosol. Shaded region indicates level of noise. (After COAKLEY and CESS, 1985). (Copyright by the American Meteorological Society)

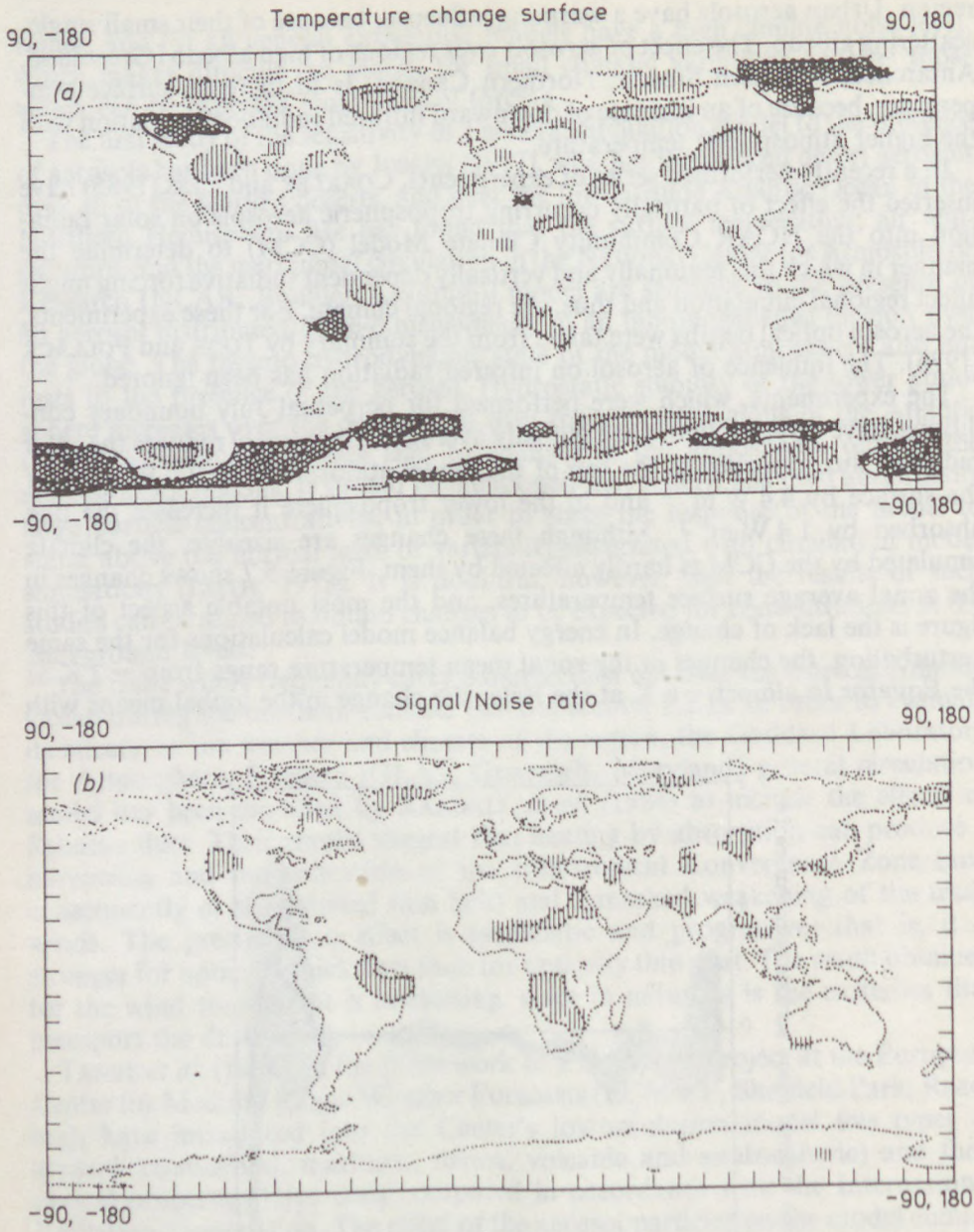

Fig. 5.8

Signal *(a)* and signal-to-noise ratio *(b)* for surface temperature change due to naturally occurring tropospheric aerosol. In *(a)* contours are every 1K. Stippled regions indicate cooling less than −1K, X's indicate warming greater than 1K. In *(b)* contours are 2, 4, etc. Stippled regions indicate signal-to-noise ratio less than −2, o's indicate signal-to-noise ratio greater than 2. Because sea-surface temperature is fixed, the zero contour is removed for both *(a)* and *(b)* in order to draw attention to the significant changes for land areas. (After Coakley and Cess, 1985). (Copyright by the American Meteorological Society)

these simple models is −3 to −4 K. The CCM's global mean temperature change is −0.08 K which is equivalent to −0.27 K for the continents. Figure 5.7 also shows that, unlike the simpler models, heating rather than maximum cooling takes place near the poles.

The lack of response is caused by the fixed sea-surface temperature in the CCM. With fixed surface temperatures the oceans in the model serve as infinite heat reservoirs. Even though temperatures of the land surfaces and in the atmosphere change in response to the radiative forcing, contact between the atmosphere and the ocean heavily regulates the changes that take place. Furthermore, fixed sea-surface temperatures in a model hamper feedback processes that might greatly affect the response to a particular forcing. For example, the thermal inertia of the oceans may inhibit the increase of water vapor in the atmosphere which through the model's radiative energy budget greatly amplifies the temperature changes.

In addition to the large-scale changes being small, the CCM results of COAKLEY and CESS show that the magnitudes of the surface temperature changes for any region are also small, generally less than 1 K (Fig. 5.8). Furthermore, regions for which the changes are significant (i.e., the signal-to-noise ratio exceeds 2) are small in spatial extent and isolated from one another. So, although surface cooling is pervasive, only rarely is the cooling sufficiently large to stand above the normal variability exhibited by the model.

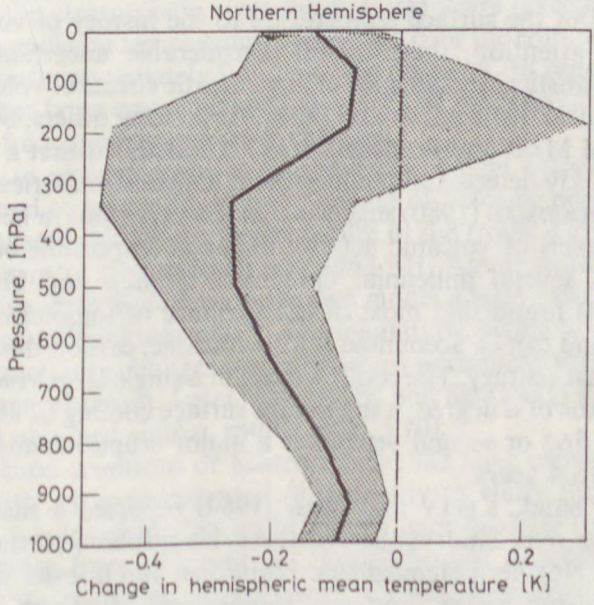

Fig. 5.9

Changes in atmospheric temperatures averaged over the Northern Hemisphere. Shaded area indicates level of noise. (After COAKLEY and CESS, 1985). (Copyright by the American Meteorological Society)

With regard to changes in the vertical temperature profile, the CCM yielded the mean profile for the Northern Hemisphere as shown in Fig. 5.9. We can see that the atmosphere as a whole cools but, at any particular level, the cooling fails to stand significantly above the normal climate variability. Model calculations have also indicated that between 30° S and 60° N the aerosol suppresses convective activity by reducing solar heating for land surfaces. As a result the upper troposphere, which for these regions and time of year (July) is heated largely through moist convective processes, cools more so than the surface and lower troposphere which are directly affected by the interaction of the aerosol with solar radiation.

COAKLEY and CESS (1985) have obtained small but significant changes in climate for isolated portions of the globe. The most notable changes could be observed for a region of Africa just north of the Equator where the background tropospheric aerosol pushed the model towards a drying of the region or "desertification". That is, for this region the radiative forcing due to aerosol gives rise to changes in convection and wind fields which in turn lead to a significant reduction in precipitation.

5.3.2 Effects of volcanic eruptions

Volcanic eruptions have long been suggested as one of the important causes of past climate variations, and there has been no dearth of studies correlating the long-term record of the surface temperature to the history of volcanic events. In spite of this attention, there is still considerable uncertainty about the magnitude and statistical significance of any climatic effects of volcanoes, as well as their geographical distribution and duration. Among others, SCHNEIDER and MASS (1975), and MASS and SCHNEIDER (1977) concluded that a volcanic dust signal can be weakly detected in the long-term temperature series. The analysis of BRYSON and GOODMAN (1980) suggests that the variations in hemispheric and perhaps world levels of volcanic activity might be important on the scale of several years to several millennia. GILLILAND (1982), and GILLILAND and SCHNEIDER (1984) found that most of the variance of long-term surface temperatures over land can be accounted for by volcanic, carbon dioxide and solar forcing for the past century. The cooling effect of a single large volcanic eruption is only a few tenths of a degree; a maximum surface cooling of about 0.5 to 1.0 K occurs in the first or second year after a major eruption; and the recovery time is about 2 to 4 years.

On the other hand, KELLY and SEAR (1984) reported a marked air temperature decrease over land in the Northern Hemisphere in the two months following major Northern Hemispheric eruptions, and a lesser decrease in the 18 months following major Southern Hemisphere eruptions. According to PARKER (1985), the results obtained by KELLY and SEAR are as valid as can be in the present situation, but such results may suffer from slight systematic bias induced by the Southern Oscillation. PARKER's analysis of sea-surface tem-

peratures for the Northern Hemisphere around the times of major volcanic eruptions in the past 100 years has not revealed any consistent tendency to significant post-eruption coolness. His air temperature anomaly maps suggest that volcanic eruptions do not predispose the atmospheric circulation to particular patterns.

A very comprehensive statistical analysis of the effect of volcanic eruptions on continental temperature has quite recently been performed by BRADLEY (1988). In his paper a new, homogeneous set of high-quality gridded temperature data for continental regions of the Northern Hemisphere was examined in relation to the timing of major explosive eruptions. BRADLEY concluded that very large, but historically rare, explosive eruptions—like Krakatoa in 1883, Santa Maria in 1902, and Katmai in 1912—have a very pronounced, short-lived impact on continental surface temperature. The effect is generally maximized in the 2 to 3 months following the eruption, diminishing thereafter for up to 2–3 years. Over Northern Hemisphere land areas as a whole, initial temperature depression averaged about 0.4 K. Summer and autumn months experience the greatest temperature depression whereas winters often show little or no effect. BRADLEY emphasizes the latitude of an eruption as an important factor in determining the extent of its influence on temperature. High-latitude eruptions have their biggest effect at high and mid latitudes whereas low-latitude eruptions mainly affect low and mid latitudes. Consequently, middle latitudes are particularly vulnerable to both low- and high-latitude eruptions. Finally, BRADLEY's results indicate that considering all known eruptions which injected material into the stratosphere over the last 100 years (except the five largest eruptions), a significant temperature depression over the continents is detectable only in the month immediately following the eruption. In other words, there is no evidence that large eruptions over the last 100 years have had a significant effect on low-frequency temperature changes.

In addition to various statistical approaches, model calculations have also widely been used to assess the climatic impact of volcanic aerosols. HANSEN *et al.* (1978) simulated the climate perturbation in the tropical atmosphere due to stratospheric aerosol produced by the 1963 Mt. Agung volcanic eruption by introducing into their radiative–convective model a time variable aerosol layer with a peak optical thickness of 0.2. The magnitude, sign and time delay of the computed temperature changes are in excellent agreement with those observed after the volcanic eruption. Later, CHARLOCK and SELLERS (1980b) repeated the same test and obtained similar results (Fig. 5.10).

The El Chichón eruptions of March/April 1982 have provided the scientific community with an unprecedented opportunity to study the aerosol–climate problem with advanced models and through later analysis to compare model results with those from observations. POLLACK and ACKERMAN (1983) have carried out a series of calculations with a one-dimensional, time-marching, radiative–convective model to assess the impact of the El Chichón volcanic cloud on the radiation budget of the northern tropics during the 6-month period following the injection of volcanic material into the stratosphere. Extensive

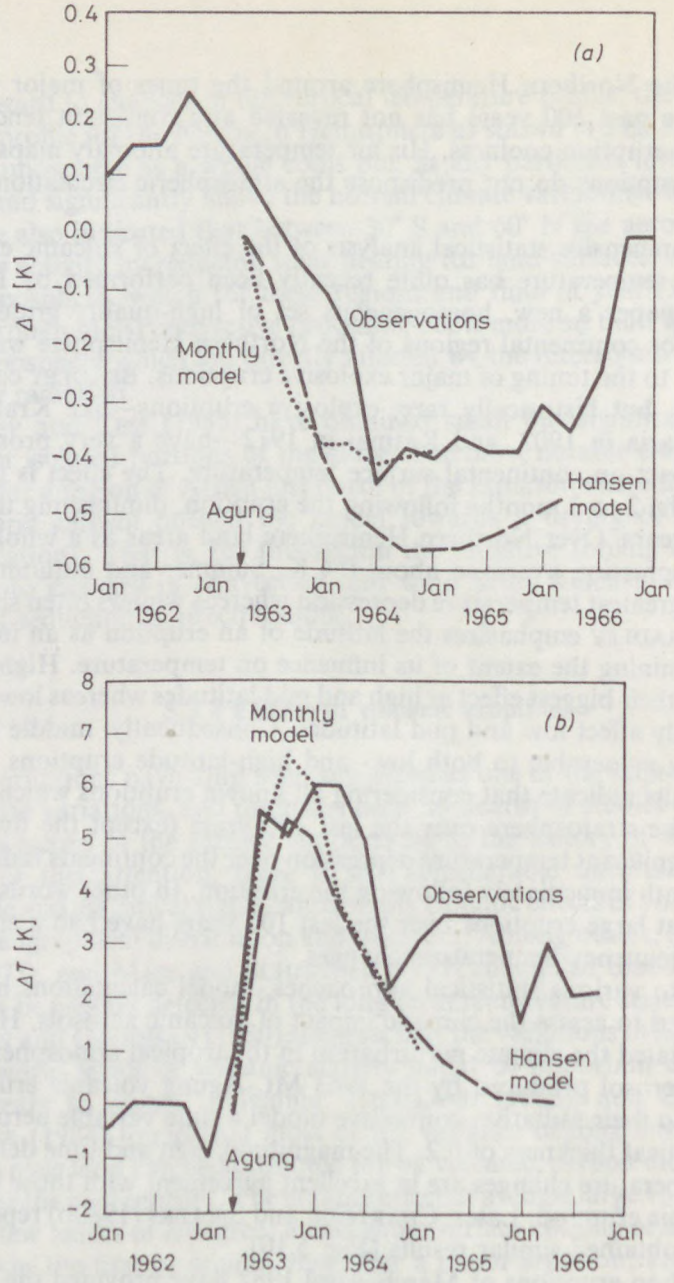

Fig. 5.10.

(a) Departure of tropical surface temperatures from the climatological mean as a function of time. Observations (solid) refer to the area between 30° N and 30° S latitudes. Dashed curve shows the results of the Hansen model, dotted curve shows the results of the monthly model by CHARLOCK and SELLERS. *(b)* Departure of tropical stratospheric temperatures from the climatological mean as a function of time. The observations (solid) are an Australian radiosonde station's reports from the 60 hPa level. The results of the monthly model by CHARLOCK and SELLERS are for 0–100 hPa, and those of the Hansen model (dashed) are for 55 hPa. The time of the Mt. Agung volcanic eruption is marked. (After CHARLOCK and SELLERS, 1980b). (Copyright by the American Meteorological Society)

measurements of the volcanic cloud obtained from airborne, spacecraft and ground platforms were used to define the model parameters and to test the predictions of the model. The El Chichón cloud was predicted to have caused an increase in planetary albedo of 10%, a decrease in total solar radiation of 2 to 3% at the ground on cloudless days, and an increase in temperature of 3.5 K at the 24 km (30 hPa) level. These predictions are compatible with relevant observations. HARSHVARDHAN *et al.* (1984) have used a zonally averaged multilayer energy balance model to investigate the likely impact of the El Chichón induced stratospheric aerosol enhancement on Northern Hemispheric tem-

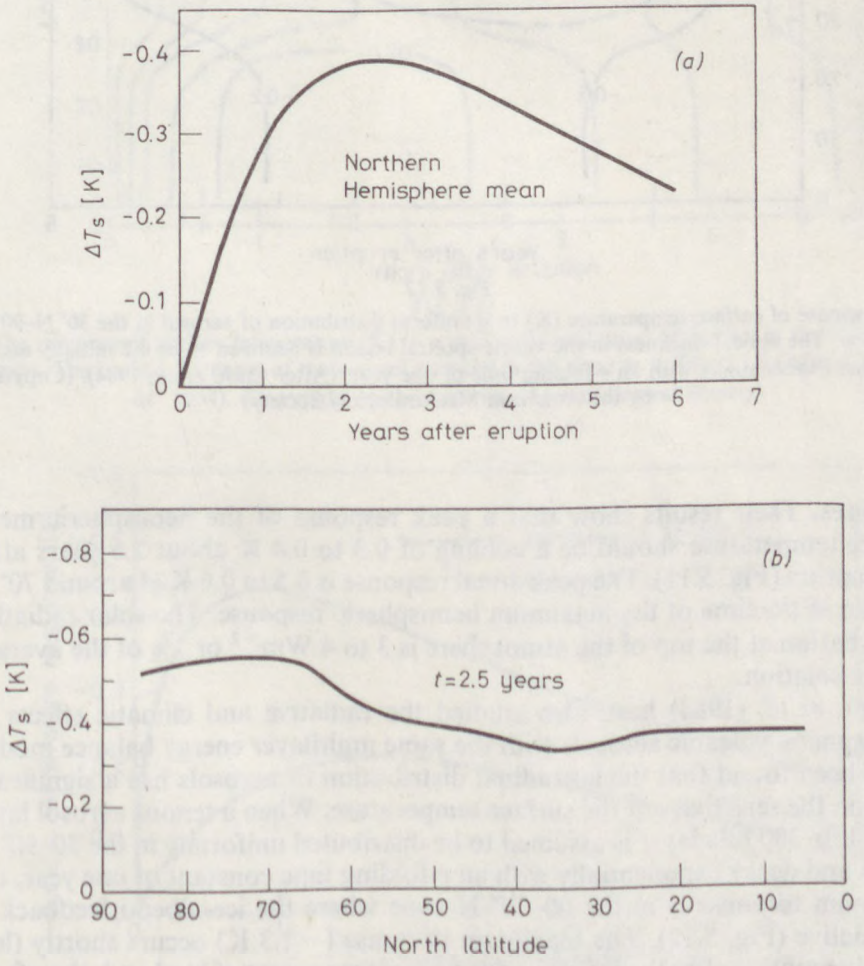

Fig. 5.11

The change in surface air temperature due to the effects of the El Chichón eruption. Upper figure shows mean Northern Hemisphere temperature changes as a function of time. Lower figure shows latitudinal distribution of change 2.5 years after the eruption. (After HARSHVARDHAN *et al.*, 1984). (Copyright by A. Deepak Publishing)

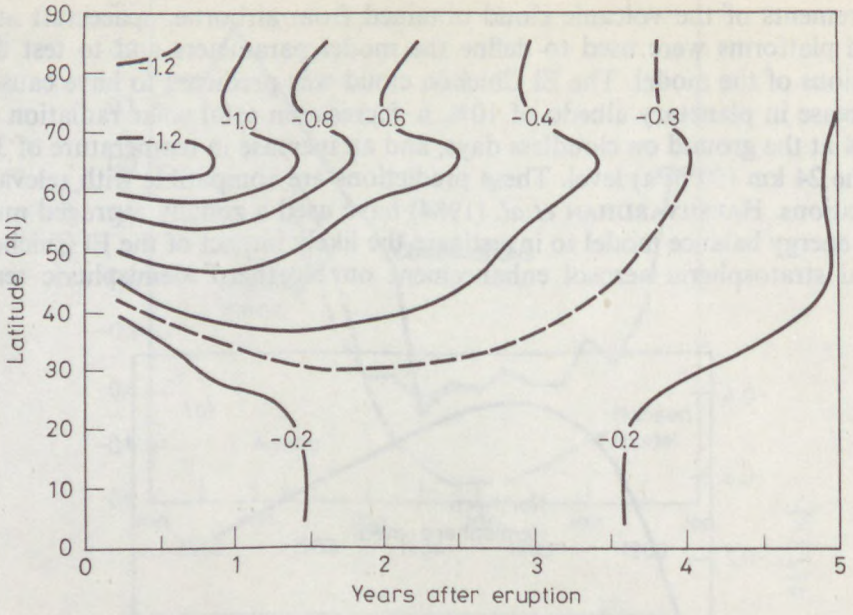

Fig. 5.12

The response of surface temperature (K) to a uniform distribution of aerosol in the 30° N–90° N region. The optical thickness in the visible spectral region is assumed to be 0.2 initially and decreases exponentially with an *e*-folding time of one year. (After CHOU *et al.*, 1984). (Copyright by the American Meteorological Society)

peratures. Their results show that a peak response of the hemispheric mean surface temperature should be a cooling of 0.3 to 0.4 K about 2.5 years after the eruption (Fig. 5.11). The peak zonal response is 0.5 to 0.6 K at around 70° N latitude at the time of the maximum hemispheric response. The solar radiative perturbation at the top of the atmosphere is 3 to 4 Wm^{-2} or 1% of the average solar insolation.

CHOU *et al.* (1984) have also studied the radiative and climatic effects of stratospheric volcanic aerosols with the same multilayer energy balance model. It has been found that the latitudinal distribution of aerosols has a significant effect on the sensitivity of the surface temperature. When a tenous aerosol layer in the 150–200 hPa layer is assumed to be distributed uniformly in the 30–90° N region and decay exponentially with an *e*-folding time constant of one year, the maximum response is in the 60–70° N zone where the ice-albedo feedback is most active (Fig. 5.12). The maximum response (−1.3 K) occurs shortly (less than six months) after the eruption due to the large extent of land and, therefore, the small thermal inertia of the surface in that latitude zone. The *e*-folding time of the response in that latitude zone is 3.5 years. The response gradually propagates to the tropics through dynamic transport of heat where the maximum (−0.24 K) is only ⅕ of that in the 60–70° N zone. When the same amount

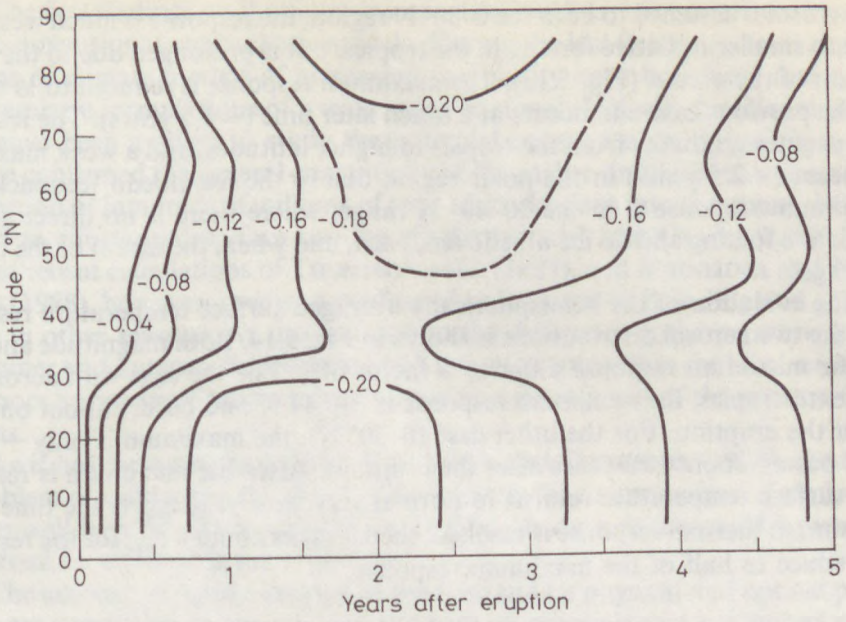

Fig. 5.13

The response of surface temperature (K) to a uniform distribution of aerosol in the 0°–30° N region. The optical thickness of the aerosol particles is the same as in Fig. 5.12. (After CHOU *et al.*, 1984). (Copyright by the American Meteorological Society)

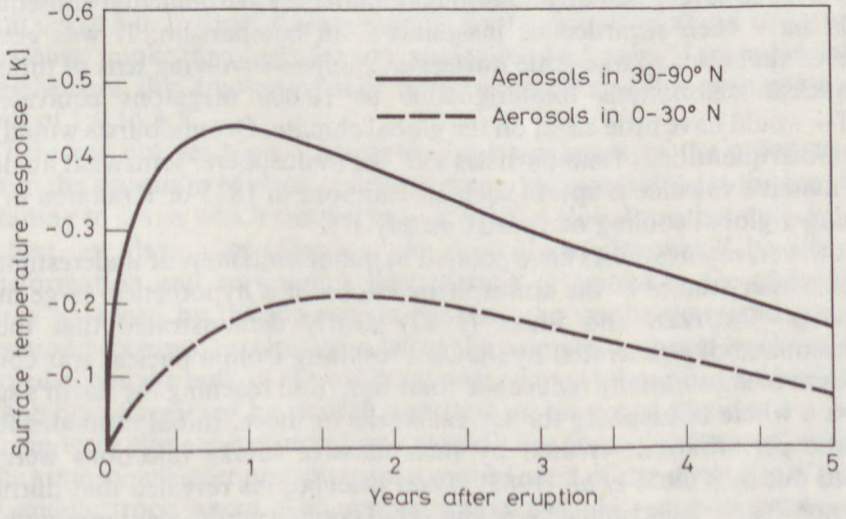

Fig. 5.14

The response of the hemispherically averaged surface temperature to a uniform distribution of aerosol particles in the 30° N–90° N region (solid curve) and in the 0°–30° N region (broken curve). The optical thickness of the aerosols is the same as in Fig. 5.12. (After CHOU *et al.*, 1984). (Copyright by the American Meteorological Society)

of aerosol is assumed to be in the 0–30° N region, the response is much weakened due to smaller radiative forcing in the tropics, but is prolonged due to the larger extent of the oceans (Fig. 5.13). The maximum response is reduced to ⅕ of that of the previous case and occurs at a much later time (~1.5 years). The response propagates gradually from the tropics to higher latitudes, and a weak maximum appears (~2.5 years) in the polar region due to the ice-albedo feedback. The minimum response is in the 30–40° N range, where there is no direct aerosol radiative forcing and no ice-albedo feedback, and where the extent of the oceans is large.

The evolution of the hemispherically averaged surface temperature response for the two aerosol distributions is shown in Fig. 5.14. Both magnitude and time of the maximum response differ by a factor of 2. For the case with aerosols in the extratropics, the maximum response is −0.44 K and occurs about one year after the eruption. For the other case (0–30° N), the maximum is only −0.2 K and occurs about two years after the eruption. After the maximum is reached, the surface temperature returns to normal very slowly. If t_{max} is the time when maximum thermal response is reached, then it takes about 4 t_{max} for the response to reduce to half of the maximum response.

5.3.3 Effects of a large-scale nuclear exchange

The possible climatic (and biological) after-effects of a nuclear war were long neglected under the assumption that its immediate impacts on human populations were so severe that any additional long-term environmental consequences might have been regarded as insignificant in comparison. It was generally believed that even a large-scale nuclear exchange—involving tens of thousands of nuclear detonations totalling 5000 to 10 000 megatons equivalent of TNT—would have little effect on the global climate. Groundbursts would inject enormous quantities of soil particles into the atmosphere, somewhat analogous to a massive volcanic eruption such as Tambora in 1815 or Krakatoa in 1883, causing a global cooling of approximately 1 K.

However, recent studies have pointed to major omissions or underestimations in the earlier studies of the atmospheric effects of a hypothetical large nuclear exchange. CRUTZEN and BIRKS (1982) clearly demonstrated that the carbonaceous smoke generated by the fires resulting from a nuclear war could be sufficient to substantially reduce the solar radiation reaching the Earth's surface across a whole hemisphere for several weeks or more. Initial estimates for the climatic perturbations created by such massive smoke injections were then carried out by TURCO *et al.* (1983). Their calculations revealed that during the first month after injection, a large and rapid cooling could occur especially over central continental areas in the Northern Hemisphere. Because the predicted maximum decrease in surface temperature of about 30 K is the difference in temperature between summer and winter in middle latitudes, TURCO coined the phrase *nuclear winter* to describe the effect.

The first findings on the climatic impacts of nuclear war came from simplified one-dimensional atmospheric models. During the last five years, several generations of climate models of increasing complexity have been used and detailed parametric formulations of a wide range of climatologically significant processes have been applied to study the potential consequences. All of these works have confirmed the general contentions of the earlier simplified calculations that injection of hundreds of millions of tons of smoke deep into the atmosphere may lead to substantial surface cooling (GOLITSYN and MACCRACKEN, 1987). The most recent calculations of THOMPSON *et al.* (1987), and SCHNEIDER and THOMPSON (1988), however, predict a cooling of only about 10 K in July and generally less in other seasons. As this is closer to the difference in temperature between summer and autumn, SCHNEIDER and THOMPSON argue that the label *nuclear fall* is more appropriate than nuclear winter as a description of the current simulations.

As it has been emphasized by SCHNEIDER and THOMPSON (1988), the overall problem of estimating the detailed environmental consequences of nuclear war goes well beyond climate modeling. It depends on a sequence of issues, some marked by untestable uncertainties.

The amount of smoke created in the fires and its physical and optical properties are dependent on the amount and type of materials that are ignited and the conditions under which the burning takes place. Available scientific information shows that the plausible range of smoke production for a large nuclear war lies between 25 and 400 Tg, with the corresponding carbon soot production lying between 10 and 225 Tg (PENNER, 1986). If both wood and petroleum-based fuels are burned, a range for hemispheric average absorption optical depth is from about 0.4 to 3.0. In most climate models, soot amounts of about 50 Tg are used as baseline smoke injections for a large nuclear exchange. If spread evenly over a hemisphere, this amount of soot would produce a visible absorption optical depth of 1.0 to 1.5.

There has not yet been a comprehensive treatment of the processes which govern the transition of smoke particles from their generation in the fires to their spreading to scales which can begin to affect the global weather and climate. In the first few days after injection, the smoke particles would be affected by transformation and scavenging. The lifetime of smoke in the atmosphere is mainly governed by the interaction between the smoke mass and cloud condensation processes, precipitation being the primary means of removal. Smoke injected above the bulk of atmospheric water vapor (above 2–3 km) has a lower probability of removal by rainfall and thus an increased lifetime.

Long-term climatic perturbations would arise from the remnant smoke left in the atmosphere after precipitation removed most of the smoke from the lower and middle troposphere. This remnant smoke could range in amounts from virtually nothing for small smoke injections in winter wars, to 50% or more of the injected smoke from large summer wars involving many urban targets, which would correspond to a global average absorption optical depth of a few tenths. The residence time of the smoke particles in the stably-stratified strato-

spheric layers would be controlled mainly by circulation patterns and would likely be six months or more, with the lowering and strengthening of the inversion at the tropopause. Chemical scavenging mechanisms, as well as the enhanced radiative cooling and vertical overturning in the stratosphere would tend to limit the smoke lifetime.

Most of the simulations of the climate effects of nuclear war have focused on the short-term "acute" changes in the first month following the injection of smoke into the atmosphere. Figure 5.15 shows the temperature effect during the first month of the classical baseline simulation of a 5000-Mt nuclear exchange by TURCO *et al.* (1983). The maximum temperature decrease of 35 K in this case occurs three to four weeks after the nuclear attack and should be viewed as representative of a value averaged over a hemisphere for a completely land-covered planet. The authors suggested that, for the Earth, the large heat capacity of the oceans, which was necessarily neglected in their one-dimensional model, would probably reduce the magnitude of this temperature change by about a factor of two.

The one-dimensional calculations by TURCO *et al.* (1983) were followed very quickly by climate perturbation studies based on models with two- and three-dimensional resolution (e.g. COVEY *et al.*, 1984, 1985; THOMPSON, 1985; MALONE *et al.*, 1986). These models suggested that the moderating influence of the ocean was indeed about a factor of two. Refinements in more physically realistic models have combined to reduce further the average land surface temperature perturbations in the Northern Hemisphere compared to the one-dimensional models. This is primarily a result of two additional processes which have been taken into account: infrared opacity of the smoke providing some greenhouse

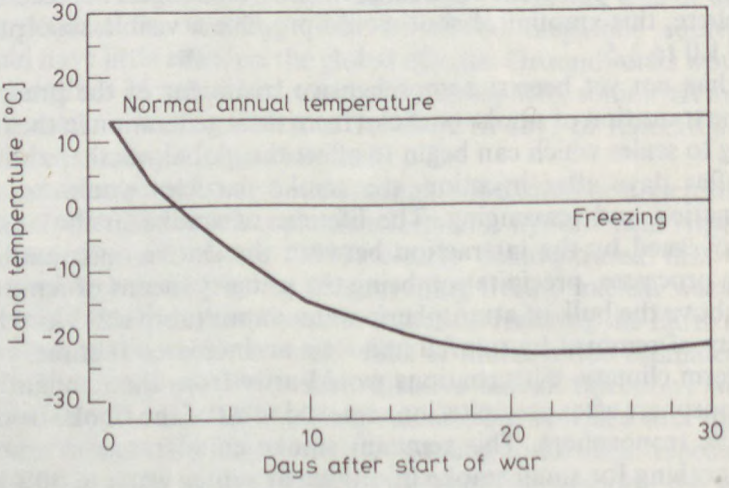

Fig. 5.15

Hemispherically averaged surface temperature variations after a 5000-Mt nuclear exchange. (After TURCO *et al.*, 1983). (Reprinted by permission from the authors. Copyright by Macmillan Magazines Ltd.)

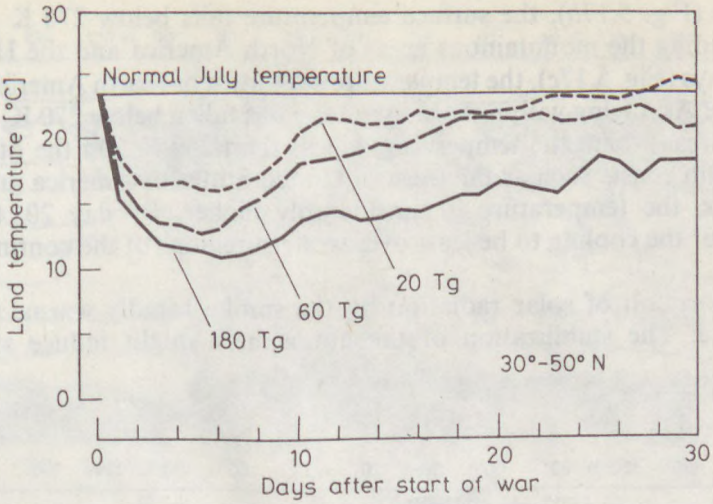

Fig. 5.16

Sensitivity of mid-latitude average land surface temperatures to three smoke injection amounts as indicated. (After SCHNEIDER and THOMPSON, 1988). (Reprinted by permission from the authors. Copyright by Macmillan Magazines Ltd.)

effect compensatory warming and patchy distribution of smoke, allowing some solar heating in relatively clear periods. For illustration, Fig. 5.16 shows the results obtained by SCHNEIDER and THOMPSON (1988) for the sensitivity of middle latitude average land surface temperatures to three smoke injection amounts; the 180 Tg case is equivalent to an injection of 50 Tg of carbon soot.

The global circulation model simulations performed by THOMPSON (1985) suggest that a substantial fraction of smoke generated by a large nuclear war in summer over NATO and Warsaw Pact territories will rise in altitude because of the heating of smoke which produces a self-lofting effect—and a smaller fraction of smoke will spread to non-combatant areas in the tropics and cross the Equator in less than two weeks. The upwards and southwards dispersal of smoke in winter is much smaller than in summer because of weaker solar heating. In July, widespread large temperature decreases can occur over Northern Hemisphere land areas, and some environmental effects could extend to the mid-latitudes of the Southern Hemisphere a few weeks after a large nuclear exchange in which Northern Hemisphere cities were targeted. Surface temperature effects in January are less pronounced, but biologically harmful temperature decreases could occur in Northern Hemisphere subtropics.

MITCHELL and SLINGO (1988) supposed that 180 Tg of smoke were distributed evenly between 0 and 9 km and between 30° and 60° N on the 1st of July. Their 11-layer atmospheric general circulation model also indicated that the geographical distribution of the changes in surface temperature might be far from uniform. Before the smoke was introduced, the temperature over land (30 to 60° N) generally exceeded 280 K (Fig. 5.17*a*). Two days after the introduction of

the smoke (Fig. 5.17*b*), the surface temperature falls below 270 K in limited areas including the mountainous areas of North America and the Himalayas. After 10 days (Fig. 5.17*c*), the temperature over most of North America, Europe and eastern Asia lying within the smoke zone has fallen below 270 K, and there are large areas where the temperature is less than 260 K. On the other hand, along certain coasts such as the western United States of America and around inland seas, the temperature is considerably higher. By day 20, there is a tendency for the cooling to be least over western regions of the continents (Fig. 5.17*d*).

The absorption of solar radiation by the smoke rapidly warms the upper troposphere. The stabilization of the atmosphere might induce substantial

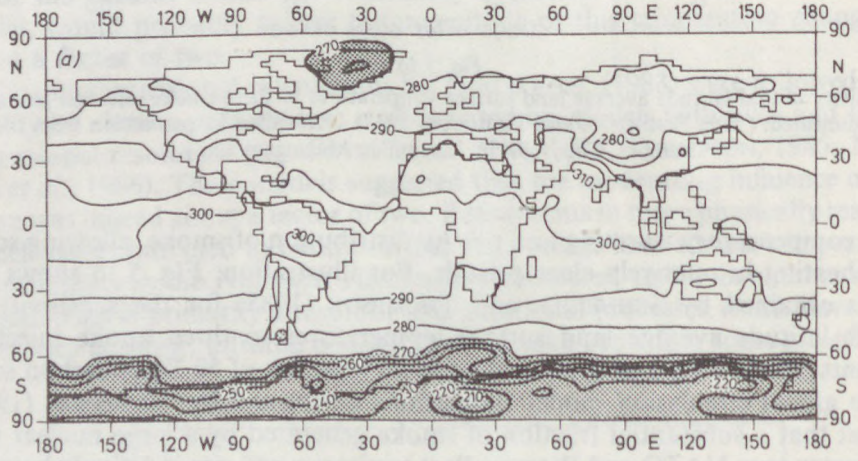

Fig. 5.17a

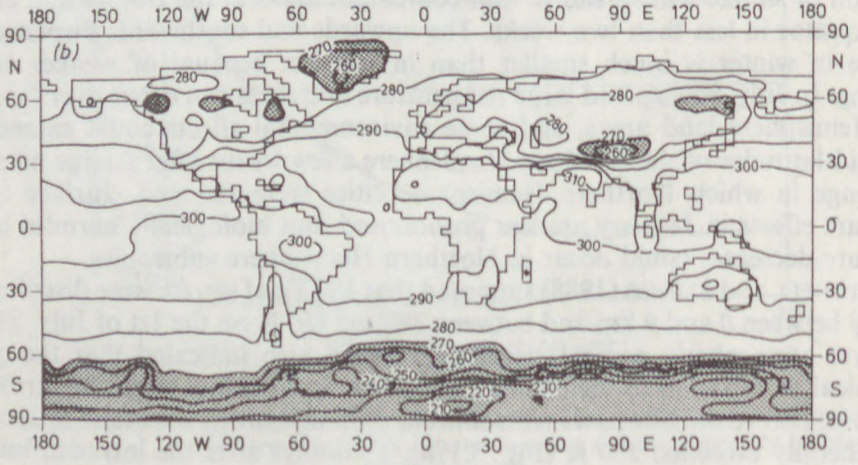

Fig. 5.17b

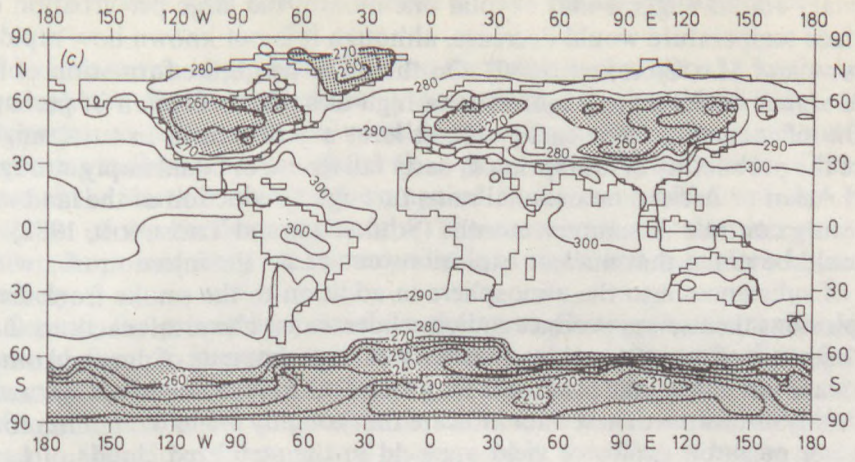

Fig. 5.17c

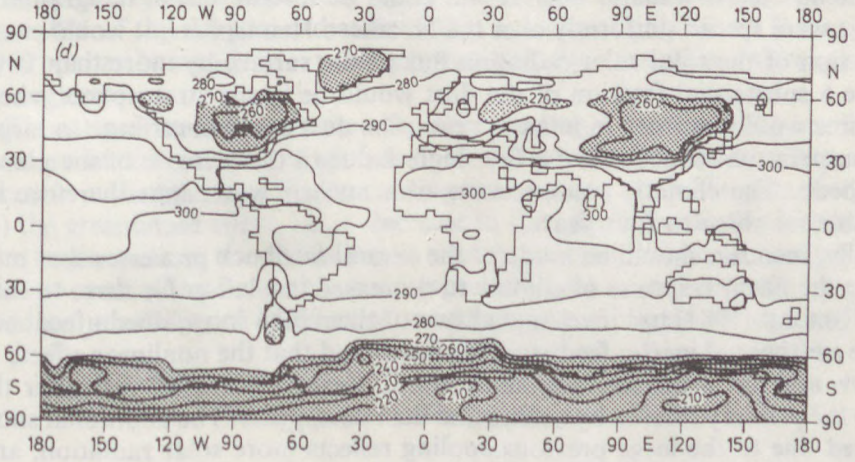

Fig. 5.17

Geographical distribution of the changes in daily mean surface temperature due to the injection of 180 Tg of smoke between 0 and 9 km and between 30° and 60° N. Contours every 10 K, regions with temperature below 270 K are stippled. *(a)* July mean. *(b)* Day 2 of the simulation. *(c)* Day 10 of the simulation. *(d)* Day 20 of the simulation. (After MITCHELL and SLINGO, 1988). (Copyright by the American Geophysical Union)

reductions in simulated precipitation. In the first 30 days of the simulation carried out by SCHNEIDER and THOMPSON (1988), average rainfall reductions of 20 to 50% were observed in the Northern Hemisphere mid-latitudes. Even larger percentage reductions can occur over land areas because these areas are more strongly stabilized than ocean owing to low-altitude cooling.

Longer-term "chronic" effects of a major nuclear war have also been investigated by extending climate calculations over time spans of the order of a year.

Preliminary results suggest that beyond one month, the large perturbation of the surface temperature would decrease, although it is not known how rapidly (GOLITSYN and MACCRACKEN, 1987). On the other hand, the formation of an elevated stable smoke layer might cause a high-altitude absorption of perhaps 5 to 40% of incoming solar energy for at least a year which, in turn, might enhance the probability of late spring or early fall frosts, or could imply strongly reduced Asian or African monsoonal rains through a reduction of the land-sea temperature contrast in summer months (SCHNEIDER and THOMPSON, 1988).

It should be noted that nuclear explosions can cause the injection of a wide variety of substances into the atmosphere in addition to the smoke from fires. The explosions themselves produce radionuclides, cause chemical reactions that lead to injection of nitrogen oxides, and can loft large amounts of dust and other surface materials if they take place near the ground (GOLITSYN and MACCRACKEN, 1987). Analysis of nuclear test data indicate that roughly 0.1 to 0.6 million tons of dust per megaton explosive yield are held in the stabilized clouds of land surface detonations. Therefore, the amount of submicron dust particles that could be injected in a major nuclear war could be several tens of teragrams. If this dust were spread uniformly over the Northern Hemisphere, it would cause a reduction of the total solar radiation flux at the surface by more than 10%. Because a substantial fraction of the dust would be in the stratosphere where its lifetime would be from months to years, the dust could contribute to large-scale temperature reductions of a few degrees due to the increase of the planetary albedo. The climatic consequences of a nuclear war might therefore be detectable for three to four years.

Finally, mention should be made of the several feedback processes that may prolong the linear response of climate to decreased insolation for three to four years. ROBOCK (1984) has investigated two of them: the snow/albedo feedback and the ice/thermal inertia feedback. He has found that the nonlinear effects of the snow and ice feedbacks become apparent during the second year after the war, as the primary forcing by smoke and dust disappears. The additional snow produced due to the large previous cooling reflects more solar radiation, and therefore large areas of cooling more than 5 K can be found in the middle and high latitudes over land in the second summer after the war. Over the ocean, the largest cooling in the second year is at the poles in the winter. This pattern is caused by the enhanced amplitude of the seasonal cycle of temperature: cooling produces more sea ice which lowers the thermal inertia of the ocean. On the other hand, VOGELMANN *et al.* (1988) argue that the smoke injected into the atmosphere could fall out onto snow and ice, and would lower cryospheric albedos by as much as 50%. They show that dirty snow, in general, would have a small temperature effect at mid- and low latitudes but could have a large temperature effect at polar latitudes, particularly if the soot is able to reappear significantly in later summers.

5.4 The role of clouds in the radiation balance

Clouds have two important effects on the radiation budget of a vertical column through the Earth–atmosphere system. First, as a result of their scattering properties at solar radiation wavelengths, they reflect a large amount of the incoming radiation back to space. On a global average, the albedo of the cloudy part of the Earth is about 0.5, compared to the mean albedo of the cloudless fraction of the Earth of about 0.14. The absorption of solar energy by liquid water drops and ice particles are relatively small and can often be neglected entirely.

Second, the presence of clouds in the atmosphere results in a change in the upward flux of infrared radiation. For these wavelengths, the situation is virtually the reverse: since most clouds are effectively black to the planetary infrared radiation and cooler than the surface, both an increase in the horizontal extent of the cloud coverage and an increase in the effective height of the cloud tops reduce the upward flux of the infrared radiation escaping from the Earth–atmosphere system to space. A dense low-level water cloud may absorb more than 90% of the infrared radiation within a depth of only 50 m. The scattering by drops can be large, but is usually outweighed by absorption and can therefore be neglected.

Thus, there are two opposite effects on the global radiation balance from an increase in the amount of global cloud cover: (1) the albedo effect, i.e., an increase in the planetary albedo causing a decrease in available solar energy, and (2) the greenhouse effect, i.e., a decrease in the infrared radiative loss to space. The importance of understanding in what ways cloudiness eventually acts as a climate-controlling factor has been especially accentuated recently by concern over the possibility of inadvertent modifications of clouds by man's activities.

5.4.1 The net radiative effect of clouds

In order to achieve global radiative equilibrium, the total infrared flux F_{ir} emitted to space by the Earth–atmosphere system must be equal to the solar energy absorbed in the system, F_A. The total infrared flux consists of the amount of surface radiation that escapes through the atmosphere directly to space and the atmospheric emission to space; the latter being the sum of the amount of cloud-top radiation that escapes to space plus the atmospheric emission of infrared radiation to space that originates in the fraction of the atmosphere lying above the clouds. The downward solar flux available for the system depends upon the solar constant σ_0 and the planetary albedo of the system α_p:

$$F_A = \frac{\sigma_0}{4}(1-\alpha_p), \tag{5.1}$$

where

$$\alpha_p = \alpha_c A_c + \alpha_s(1-A_c), \tag{5.2}$$

with α_c denoting the albedo of the cloudy fraction of the Earth and α_s the albedo of the clear-sky fraction of the globe as seen from space, and A_c the cloud-cover fraction. Now, the albedo and infrared opacity modifications, resulting from a change in cloud cover, produce competitive feedback mechanisms, and a convenient cloud sensitivity parameter for determining the predominant mechanism may be defined as

$$\delta = \frac{\partial F_A}{\partial A_c} - \frac{\partial F_{ir}}{\partial A_c}, \tag{5.3}$$

where δ is the change in net radiation due to a change in the amount of clouds A_c. For $\delta < 0$ the albedo modification dominates, whereas if $\delta = 0$ the albedo and greenhouse effects compensate, such that there is no net cloud-amount feedback irrespective of any change in global cloud cover with changing global climate.

Assuming that α_c and α_s are not functions of cloud amount, one can obtain

$$\frac{\partial \alpha_p}{\partial A_c} = \alpha_c - \alpha_s \tag{5.4}$$

and therefore

$$\delta = -Q(\alpha_c - \alpha_s) - \frac{\partial F_{ir}}{\partial A_c}, \tag{5.5}$$

where $Q = \sigma_0/4$. The magnitude of the albedo effect depends on Q which for regional or zonal conditions depends on latitude and time of year, and on the difference between the cloud albedo and the clear-sky albedo. This latter difference is greatest over low-latitude oceanic areas, where α_s is small and smallest over high-latitude snow- and ice-covered regions, where α_s is large. The magnitude of the greenhouse effect, $\partial F_{ir}/\partial A_c$, depends mainly on the height of the cloud top and the tropospheric lapse rate. The greater the height of the cloud and the greater the lapse rate, the greater the magnitude of $\partial F_{ir}/\partial A_c$, other things being equal.

Choosing $\alpha_c = 0.50$, $\alpha_s = 0.12$ and $\partial F_{ir}/\partial A_c = -75$ Wm^{-2}, SCHNEIDER (1972) gives $\delta = -58$ Wm^{-2} as the yearly-average and global-average value of the net flux difference, the minus sign indicating that on a global scale the albedo modification dominates. In other words, the effect of an increase in the global-average cloud-cover amount (but not necessarily of an increase in the amount of thin cirrus clouds by themselves) is a decrease in the global average surface temperature, provided that all other factors remain unchanged. This result does not apply in high latitudes, especially in the winter months, but, rather, the opposite effect has been computed for polar regions.

Following the work of SCHNEIDER (1972), many other investigators have suggested a confusing variety of values for $\partial F_{ir}/\partial A_c$. The range of values in the literature, based on model calculations, is from -33 Wm^{-2} (OHRING and ADLER, 1978) to -91 Wm^{-2} (CESS, 1976). Most of this range is probably

attributable to different assumptions on cloud-amount and cloud-height distributions, and temperature and water vapor profiles, although some variability is also introduced as a result of different radiation codes and differences in the way the average value of $\partial F_{ir}/\partial A_c$ is computed. Even though the range of estimates of $\partial F_{ir}/\partial A_c$ is quite large, when combined with reasonable estimates of the value of $(\alpha_c - \alpha_s)$, they all yield negative values for δ, except that suggested by CESS (1976).

With regard to the choices for α_c and α_s, CESS (1976) remarks that SCHNEIDER's value of $\alpha_c = 0.50$ appears to be a bit high; moreover, $\alpha_s = 0.12$, as employed by SCHNEIDER, is a surface rather than a clear-sky albedo. CESS has determined $\partial F_{ir}/\partial A_c$ from a regression relationship between zonal, annual averages of outgoing infrared radiation based on satellite observations, and zonal, annual averages of cloudiness and surface temperature based on conventional climatological data. For the Northern Hemisphere, he has obtained that $\partial F_{ir}/\partial A_c = = -91\ \mathrm{Wm}^{-2}$. When combined with his estimate of $\alpha_c = 0.44$ and $\alpha_s = 0.18$, this value of $\partial F_{ir}/\partial A_c$ leads to $\delta = +2.6\ \mathrm{Wm}^{-2}$. Using similar analysis techniques for the Southern Hemisphere, $\delta = -0.6\ \mathrm{Wm}^{-2}$ has been found. These results imply an almost complete cancellation of the albedo effect of clouds by their greenhouse effect, i.e., that cloud cover is not a significant climate feedback mechanism.

To explain why the infrared component of cloud-amount feedback, as represented by $\partial F_{ir}/\partial A_c$, deduced from the satellite observations is so much larger than that obtained in model calculations, CESS and RAMANATHAN (1978) have suggested that with an increase in total cloud amount, there is typically an increase in the high-cloud fraction and a decrease in the low-cloud fraction visible from space. Since higher clouds have a greater greenhouse effect, the value of $\partial F_{ir}/\partial A_c$ for the real atmosphere is larger than is obtained in model calculations, in which it is generally assumed that changes in cloud amounts of individual cloud layers are the same as the change in total cloud cover. CESS and RAMANATHAN (1978) have indeed found that with an increase in total cloud amount the high-cloud fraction decreases, and their results tend to confirm the original conclusion of CESS (1976) that $\delta \approx 0$.

CESS and RAMANATHAN (1978) have also pointed to the desirability of arriving at estimates of δ, and particularly $\partial F_{ir}/\partial A_c$, from observations. Along this line, OHRING and CLAPP (1980) have examined the problem with the use of data on the components of the radiation budget at the top of the atmosphere obtained from the processing of 45 months of scanning radiometer measurements of the polar orbiting NOAA satellites. They have used a regression approach to obtain values of $\partial F_{ir}/\partial A_c$ and δ; their estimates have led to the global values of $\partial F_{ir}/\partial A_c = -65\ \mathrm{Wm}^{-2}$ and $\delta = -40\ \mathrm{Wm}^{-2}$. These values indicate that the estimated albedo effect of cloudiness is nearly twice as large as the infrared effect of the clouds. A similar work, carried out by HARTMANN and SHORT (1980), using daily observations of albedo and outgoing terrestrial radiation derived from NOAA scanning radiometer measurements has confirmed this conclusion.

The results obtained from this method suggest that globally the effect on the radiation balance of the high albedo of clouds is two or more times greater than the effect of cloudiness in reducing the long-wave radiation loss to space, so that an increase in the fractional area of the current distribution of cloud would tend to cool the Earth. They found very large geographical variations in the radiative effects of clouds related to circulation features.

5.4.2 Climatic impacts of anthropogenically altered cloud characteristics

In the previous section we have discussed the two opposing effects of cloud amount. However, there are additional effects of anthropogenic origin as well, which modify cloud optical thickness, and hence planetary albedo, at solar wavelengths, and these have no compensatory effect at longer wavelengths, since to a good approximation clouds are effectively black there. The SMIC report (1971) pointed to the possibility that pollution increases the concentration of cloud droplets, via increased nucleus concentration, an effect which, of itself, would lead to optically denser and hence more reflective, brighter clouds. At the same time, a different and opposite effect of the aerosol was also adverted, namely that clouds might become darker ("dirty clouds" with lower albedo would form) with increasing emissions of dark (i.e. carbon) particles. The relative magnitude of these opposing influences on cloud albedo was later thoroughly discussed by TWOMEY (1974, 1977a,b) and TWOMEY *et al.* (1984).

The liquid water content ϱ in clouds and the cloud-column liquid water content $\int_0^h \varrho \mathrm{d}z$ (h being the geometric thickness of the cloud) are determined by thermodynamic and large-scale environmental factors, whereas the droplet concentration N in clouds is determined primarily by the aerosol particles (see Chapter 3). Thus, the atmospheric motion pattern decides where clouds will develop, how thick they will be and what their water content will be, but it is primarily the aerosol that decides how many droplets there will be within a unit volume. For arbitrary drop-size distribution $\mathrm{d}N(r)/\mathrm{d}r$ one cannot relate the cloud optical thickness τ to ϱ and N in any simple way, although it is clear that any change in $N = \int [\mathrm{d}N(\mathrm{r})/\mathrm{d}r]\mathrm{d}r$ will alter τ even if ϱ is held constant. Nevertheless, by assuming narrow size distribution and an extinction efficiency of the cloud which differs only little from the asymptotic value 2 at visible wavelengths, TWOMEY (1977a) could show that

$$\tau \propto h N^{1/3} \varrho. \tag{5.6}$$

This relationship has the consequence that an increase in the cloud nucleus concentration produces an increase in optical thickness.

As is discussed in Appendix III, only a few parameters are needed to give the reflectance and absorptance of an attenuating layer quite precisely. These parameters are the optical thickness τ, the single-scattering albedo ω and the

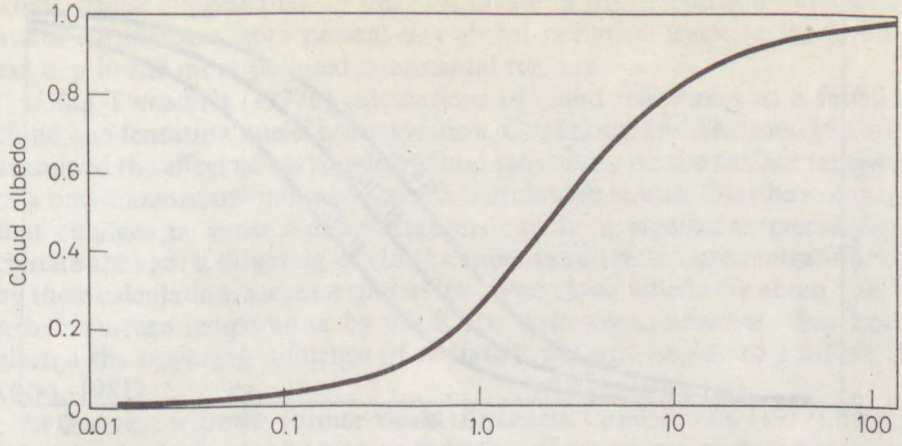

Fig. 5.18

The dependence of cloud albedo on scaled optical thickness τ' (after TWOMEY, 1977a). (Reprinted by permission from the author. Copyright by Elsevier Science Publishers)

asymmetry factor g. In clouds and fogs (in which the absorption of solar energy is relatively small), the "scaled optical thickness" $\tau' = (1-g)\tau$ is a better measure of the scattering power of a thick layer than τ (TWOMEY, 1977a). For optically thick clouds, one can therefore consider reflectance Re (and other optical properties) of the layer to be functions of τ' and ω only. For fixed ω, Re increases monotonically with τ', but the rate of increase decreases monotonically with increase in τ'; for fixed τ', Re evidently decreases with decrease in ω (i.e., with increasing absorption).

In Fig. 5.18 the dependence of cloud albedo has been plotted against the scaled optical thickness τ'; this figure can be applied quite accurately to any cloud layer, provided it is optically thick. Figure 5.18 was converted to cloud geometric thickness to obtain Fig. 5.19. The central curve in this figure applies to a cloud with volume-mean radius of the cloud drops $\bar{r}=8$ μm, $g=0.858$, $\varrho=0.3$ g m^{-3}, $N=140$ cm^{-3}; these values represent a typical maritime cloud situation. The extinction coefficient of such a cloud would be 0.00078 cm^{-1}, so a 1 km geometric path in the cloud corresponds to an optical path of 78.

Since a higher drop concentration leads to a larger optical thickness, an increase in N (while holding ϱ constant) is equivalent to a displacement of the central curve to the left, while a reduction in N is accounted for by a displacement to the right. Figure 5.19 shows the effect of an eightfold increase in N and a reduction in N to one-eighth of the value applying to the central ($N=140$) curve. The effect of changes of this order are seen to be appreciable. For $h \approx 0.1$ km (a thin cloud layer), the albedo is increased from 0.25 to 0.43 for an eightfold increase in drop concentration; for a cloud layer which is 1 km deep, the albedo is increased from 0.82 to 0.90.

Now, observations have clearly confirmed that increased pollution leads to increasing atmospheric concentration of cloud-nucleating particles (see Subsec-

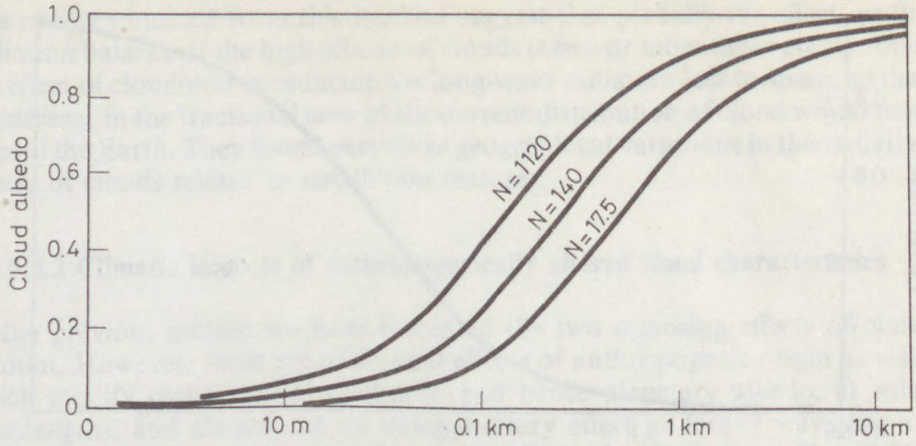

The data of Fig. 5.18 converted to geometric thickness of cloud. The central solid curve relates to fairly clean maritime conditions in which the cloud nucleus concentration and ensuing cloud drop concentration are 140 cm^{-3}. The effect of an eightfold increase in the concentration is the curve to the left, while the curve to the right applies to case of a concentration of one-eight of the first value. (After TWOMEY, 1977a). (Reprinted by permission from the author. Copyright by Elsevier Science Publishers)

tion 3.3.4); the nuclei which influence droplet number are predominantly sulfate particles even in oceanic regions (see Section 3.4). Consequently, addition of man-made cloud nuclei can lead to an increase in the solar radiation reflected by clouds. On the other hand, recent observations have verified the earlier expectation that pollution increases the number of dark light-absorbing particles in the atmosphere, i.e. anthropogenic aerosol particles imbedded in cloud droplets may tend to lower the reflectance of clouds. Based upon his considerations, TWOMEY (1977a) reached the conclusion, later confirmed by more accurate calculations of GRASSL (1982), that the optical thickness effect—brightening of clouds with increasing drop concentrations—must be more influential for optically thin clouds, whereas optically thick clouds, which are already very bright, are more susceptible to increased absorption, while insensitive to optical thickness. In other words, an increase in global pollution could, at the same time, make thin clouds brighter and thick clouds darker, the crossover in behavior occurring at a cloud thickness which depends on the ratio of absorption to the cube root of the drop concentration. The sign of the net global effect, warming or cooling, therefore involves both the distribution of the cloud thickness and the relative magnitude of the rate of increase of cloud-nucleating particles *vis-à-vis* particulate absorption.

By introducing the distribution of cloud optical thickness into the discussion of the problem and using experimental data from concurrent measurements of particulate short-wave absorption and nucleus concentration, TWOMEY *et al.* (1984) concluded that the brightening effect is the predominant one for global climate mainly because of the prevalence of quite thin clouds in the atmosphere.

Their results suggest that an increase of about 0.1 in planetary albedo could attend an increase from present-day global pollution levels to the levels now existing in the more polluted continental regions.

Using TWOMEY's (1977b) calculations of cloud reflectance as a function of cloud condensation nuclei concentration, CHARLOCK and SELLERS (1980a) have examined the effect of varying low-cloud reflectivity on the surface temperature of a one-dimensional radiative–convective climate model. They have concluded that changes in aerosol concentrations can be a significant mechanism for climate change: a doubling of cloud condensation nuclei concentration would, by their calculation, increase global low-level cloud albedo by about 0.045 and reduce surface temperature by 0.9 K. In their work, however, they have neglected the opposing influence of radiation absorption due to aerosols (KELLOGG, 1981).

In contrast with the former work, ACKERMAN and BAKER (1977) have considered only the direct short-wave radiative effects of unactivated aerosol particles in and below stratus clouds. They found that the effect of adding absorbing aerosol particles into clouds can be the increase of the system albedo for thin clouds as a result of increased backscatter by the particles, or the decrease of the albedo at larger optical thicknesses where absorption becomes important. For a given surface albedo, non-absorbing unactivated particles increase the system albedo at all thicknesses. According to their calculations, the effect of surface albedo on energy absorbed by particles within the cloud is slight. About 5 to 10% of the incident solar energy at $\lambda = 0.5$ μm is absorbed by unactivated particles in thick clouds. This corresponds to an average heating rate of about 0.2 to 0.5 K per hour, i.e. this excess heating is comparable to the latent heat released during the formation of clouds, and thus absorbing particles may have a significant effect on the energetics of stratus clouds.

NEWIGER and BÄHNKE (1981) have also found that aerosol particles are the main absorbers of solar radiation in clouds in the visible spectrum. The possible contribution of rain drops to cloud absorption is, under favorable conditions, equivalent to a weakly absorbing aerosol.

5.4.3 Climatic impacts of biologically altered cloud characteristics

In Subsection 5.2.2 we have already mentioned the possibility that the climate system is biologically regulated by sulfur-containing aerosol particles. This problem is strongly related to the nowadays very popular and attractive hypothesis that the Earth is a single huge organism which intentionally creates an optimum environment for itself. The idea stems from a geological evidence which is not obvious at all: during the time, 3.2×10^9 years, that life has been present on Earth, the physical and chemical conditions of most of the planetary surface have never varied from those most favorable for life. "For this to have happened by chance is as unlikely as to survive unscathed a drive blindfold through rush-hour traffic", LOVELOCK (1979) claimed. He offered an alternative

explanation that, early after life began it acquired control of the planetary environment and that this homeostasis by and for the biosphere has persisted ever since. Historic and contemporary evidence and arguments for this explanation led him and MARGULIS to introduce the Gaia hypothesis in the early 1970's (LOVELOCK and MARGULIS, 1974). It postulated the Earth to be a self-regulating system comprising the biota and their environment, with the capacity to maintain the climate and the chemical composition at a steady state optimal for life.

Since that time, the debate on the Gaia hypothesis has never ceased. To some the idea of planetary-scale homeostasis is more like religion than science. Others acknowledge its depth and beauty but, as a science, they find the hypothesis in need of more explicit formulation, so that empirical testing can be designed (SCHNEIDER, 1986). Today, nobody denies that life may control climate, for example, intentionally or by chance; e.g., as suggested by SHAW (1987), it surely participates in the regulation of the climate system.

On the basis of our present knowledge, however, it is very probable that the role of biospheric aerosol particles in the atmosphere is even more important than SHAW postulated. There is a considerable body of evidence suggesting that sulfate particles, constituting the essential part of fine aerosols under remote and unpolluted marine tropospheric conditions, give the majority of cloud condensation nuclei (see Chapter 3). Consequently, biogenic sulfate particles not only themselves opalize the atmosphere, but they have an important indirect effect on climate since cloud elements, which would have not formed without the presence of these particles, influence the transfer of solar radiation in a significant way. MÉSZÁROS (1988) who emphasized this additional role of sulfate aerosol, went further by noting that the biosphere might regulate the global water cycle, because the condition for the formation of precipitation would be certainly very different from the present one if there were no biogenic sulfate particles in the air.

The major source of sulfate aerosol in the marine atmosphere appears to be dimethylsulfide (DMS; see Chapter 2) which is produced by planktonic algae in sea water, and oxidizes in the air to form these particles. CHARLSON *et al.* (1987) proposed that the rate of DMS emission from the oceans is determined by the climatic conditions which have a regulating effect on phytoplankton population. In this case, a Gaia-like feedback loop can be assumed between plant and climate. During a glacial period, the areas covered by ice on the continents and oceans increase, and there is some exposure of continental shelf now under water. The decrease in ocean area during a cold spell could therefore lead to a drop in the global flux of DMS to the atmosphere. The largest flux of DMS comes from the tropical and equatorial oceans. This suggests that the most important climatic role of DMS is to modify the amount of cloudiness and reflected solar energy back to space over the warmest ocean regions. A cooling of the climate and a reduction in area of the tropical seas could thus lead to a smaller DMS flux, and a decrease of cloud cover and planetary albedo, providing a stabilizing negative feedback.

It is well known that the predominant effect of future human activities on

global climate is likely to be one of warming, mainly due to the increasing concentrations of greenhouse gases. According to the calculations of CHARLSON *et al.* (1987), an approximate doubling of the number concentration of cloud condensation nuclei would be needed to counteract the warming caused by a doubling of atmospheric carbon dioxide. Would Gaia really help us to avoid an unintended global warming through more aerosol production? The most uncertain link in the feedback loop is the effect of cloud albedo on DMS emission: its sign would have to be positive (i.e. DMS-producing planktonic algae should flourish when the temperature is higher) in order to regulate the climate. A most recent analysis of Vostok (Antarctica) ice-core sulfate data by LEGRAND *et al.* (1988) failed to prove this assumption. They deduced a 20 to 45% increase in non-seasalt sulfate content in the Antarctic atmosphere during full glacial (compared with interglacial) conditions, which opposes the idea of a Gaia-like feedback.

The climatic impact of biologically altered cloud characteristics is no more than one aspect of the whole Gaia story. The questions whether Gaia exists or not, or whether she is purposeful or just powerful are connected with problems including the issue of a better understanding of the global influence of life on its environment.

References

ACKERMAN, T. P., 1977: A model of the effect of aerosols on urban climates with particular applications to the Los Angeles Basin. *J. Atmos. Sci.*, **34**, 531–547.

ACKERMAN, T. and BAKER, M. B., 1977: Shortwave radiative effects of unactivated aerosol particles in clouds. *J. Appl. Meteor.*, **16**, 63–69.

ATWATER, M. A., 1970: Planetary albedo changes due to aerosols. *Science*, **170**, 64–66.

BLANCHET, J. P. and LEIGHTON, H. G., 1981: The influence of the refractive index and size spectrum on atmospheric heating due to aerosols. *Beitr. Phys. Atmos.*, **54**, 143–158.

BRADLEY, R. S., 1988: The explosive volcanic eruption signal in Northern Hemisphere continental temperature records. *Climatic Change*, **12**, 221–243.

BRYSON, R. A. and GOODMAN, B. M., 1980: Volcanic activity and climatic changes. *Science*, **207**, 1041–1044.

BUDYKO, M. I., 1969: The effect of solar radiation variations on the climate of the earth. *Tellus*, **21**, 611–619.

CARLSON, T. N. and BENJAMIN, S. G., 1980: Radiative heating rates for Saharan dust. *J. Atmos. Sci.*, **37**, 193–213.

CESS, R. D., 1976: Climate change: An appraisal of atmospheric feedback mechanisms employing zonal climatology. *J. Atmos. Sci.*, **33**, 1831–1843.

CESS, R. D., 1983: Arctic aerosols: Model estimates of interactive influences upon the surface–atmosphere clear-sky radiation budget. *Atmos. Environ.*, **17**, 2555–2564.

CESS, R. D., COAKLEY, J. A. and KOLESNIKOV, P. M., 1981: Stratospheric volcanic aerosols: A model study of interactive influences upon solar radiation. *Tellus*, **33**, 444–452.

CESS, R. D. and RAMANATHAN, V., 1978: Averaging of infrared cloud opacities for climate modeling. *J. Atmos. Sci.*, **35**, 919–922.

CHARLOCK, T. P. and SELLERS, W. D., 1980a: Aerosols, cloud reflectivity and climate. *J. Atmos. Sci.*, **37**, 1136–1137.

CHARLOCK, T. P. and SELLERS, W. D., 1980b: Aerosol effects on climate: Calculations with time-dependent and steady-state radiative–convective models. *J. Atmos. Sci.*, **37**, 1327–1341.

CHARLSON, R. J., LOVELOCK, J. E., ANDREAE, M. O. and WARREN, S. G., 1987: Oceanic phytoplankton, atmospheric sulphur, cloud albedo and climate. *Nature*, **326**, 655–661.

CHARLSON, R. J. and PILAT, M. J., 1969: Climate: The influence of aerosols. *J. Appl. Meteor.*, **8**, 1001–1002.

CHOU, M.-D., PENG, L. and ARKING, A., 1984: Climate studies with a multilayer energy balance model. Part III: Climatic impact of stratospheric volcanic aerosols. *J. Atmos. Sci.*, **41**, 759–767.

CHYLEK, P., RAMASWAMY, V. and SRIVASTAVA, V., 1984: Graphitic carbon content of aerosols, clouds and snow, and its climatic implications. *Sci. Total Environ.*, **36**, 117–120.

COAKLEY, J. A. and CESS, R. D., 1985: Response of the NCAR Community Climate Model to radiative forcing by the naturally occurring tropospheric aerosol. *J. Atmos. Sci.*, **42**, 1677–1692.

COAKLEY, J. A., CESS, R. D. and YUREVICH, F. B., 1983: The effect of tropospheric aerosols on the earth's radiation budget: A parameterization for climate models. *J. Atmos. Sci.*, **40**, 116–138.

COAKLEY, J. A. and CHYLEK, P., 1975: The two-stream approximation in radiative transfer: Including the angle of the incident radiation. *J. Atmos. Sci.*, **32**, 409–418.

COAKLEY, J. A. and GRAMS, G. W., 1976: Relative influence of visible and infrared optical properties of a stratospheric aerosol layer on the global climate. *J. Appl. Meteor.*, **15**, 679–691.

COVEY, C., SCHNEIDER, S. H. and THOMPSON, S. L., 1984: Global atmospheric effects of massive smoke injections from a nuclear war: Results from general circulation model simulations. *Nature*, **308**, 21–25.

COVEY, C., THOMPSON, S. L. and SCHNEIDER, S. H., 1985: "Nuclear winter": A diagnosis of atmospheric general circulation simulations. *J. Geophys. Res.*, **90**, 5615–5628.

CRUTZEN, P. J. and BIRKS, J. W., 1982: The atmosphere after a nuclear war: Twilight at noon. *Ambio*, **11**, 114–125.

DEEPAK, A. and GERBER, H. E. (Eds). 1983: *Report of the Experts Meeting on Aerosols and Their Climatic Effects* (Williamsburg, Virginia, 28–30 March 1983). WCP–55.

GATES, W. L., 1981: The climate system and its portrayal by climate models: A review of basic principles. II: Modeling of climate and climate change. In *Climatic Variations and Variability: Facts and Theories* (Ed.: A. Berger.) NATO Advanced Study Institutes Series C, Vol. 72, A. Reidel Publ. Co., Dordrecht. 435–459.

GILLILAND, R. L., 1982: Solar, volcanic, and CO_2 forcing of recent climatic changes. *Climatic Change*, **4**, 111–131.

GILLILAND, R. L. and SCHNEIDER, S. H., 1984: Volcanic, CO_2 and solar forcing of Northern and Southern Hemisphere surface air temperatures. *Nature*, **310**, 38–41.

GOLITSYN, G. S. and MACCRACKEN, M. C., 1987: *Possible Climatic Consequences of a Major Nuclear War*. WCP–142 (WMO/TD-No. 201)

GRASSL, H., 1982: The influence of aerosol particles on radiation parameters of clouds. *Időjárás*, **86**, 60–75.

HANSEN, J. E., WANG, W.-C. and LACIS, A. A., 1978: Mount Agung eruption provides test of a global climatic perturbation. *Science*, **199**, 1065–1068.

HARSHVARDHAN, 1979: Perturbations of the zonal radiation balance by a stratospheric aerosol layer. *J. Atmos. Sci.*, **36**, 1274–1285.

HARSHVARDHAN, ARKING, A., KING, M. D. and CHOU, M.-D., 1984: Impact of the El Chichón stratospheric aerosol layer on Northern Hemisphere temperatures. In *Aerosols and Their Climatic Effects* (Eds: H. E. Gerber and A. Deepak). A. Deepak Publishing, Hampton, Virginia, USA. 261–273.

HARSHVARDHAN and CESS, R. D., 1976: Stratospheric aerosols: Effect upon atmospheric temperature and global climate. *Tellus*, **28**, 1–10.

HARTMANN, D. L. and SHORT, D. A., 1980: On the use of earth radiation budget statistics for studies of clouds and climate. *J. Atmos. Sci.*, **37**, 1233–1250.

HASSELMANN, K., 1976: Stochastic climate models, Part I: Theory. *Tellus*, **28**, 473–485.

HERMAN, B. M. and BROWNING, S. R., 1975: The effect of aerosols on the earth–atmosphere albedo. *J. Atmos. Sci.*, **32**, 1430–1445.

HERMAN, B. M., BROWNING, S. R. and RABINOFF, R., 1976: The change in earth–atmosphere albedo and radiational equilibrium temperatures due to stratospheric pollution. *J. Appl. Meteor.*, **15**, 1057–1067.

JOSEPH, J. H., 1977: The effect of a desert aerosol on a model of the general circulation. *Proc. Symp. Radiation in the Atmosphere,* Garmisch-Partenkirchen, FRG, 19–28 August 1976. (Ed.: H.-J. Bolle) Science Press, Princeton, USA. 487–492.

JOSEPH, J. H. and WOLFSON, N. 1975: The ratio of absorption to backscatter of solar radiation by aerosols during Khamsin conditions and effects on the radiation balance. *J. Appl. Meteor.*, **14,** 1389–1396.

JUNG, H. J. and BACH, W. 1987: The effects of aerosols on the response of a two-dimensional zonally-averaged climate model. *Theor. Appl. Climatol.*, **38,** 222–233.

KELLOGG, W. W., 1981: Comments on "Aerosol, cloud reflectivity and climate". *J. Atmos. Sci.*, **38,** 664–665.

KELLY, P. M. and SEAR, C. B., 1984: Climatic impact of explosive volcanic eruptions. *Nature,* **311,** 740–743.

LABITZKE, K., NAUJOKAT, B. and MCCORMICK, M. P., 1983: Temperature effects on the stratosphere of the April 4, 1982 eruption of El Chichón, Mexico. *Geophys. Res. Lett.*, **10,** 24–26.

LEGRAND, M. R., DELMAS, R. J. and CHARLSON, R. J., 1988: Climate forcing implications from Vostok ice-core sulphate data. *Nature,* **334,** 418–420.

LEITH, C. E., 1973: The standard error of time-average estimates of climatic means. *J. Appl. Meteor.*, **12,** 1066–1069.

LEITH, C. E., 1978: Predictability of climate. *Nature,* **276,** 352–355.

LENOBLE, J., 1984: A general survey of the problem of aerosol climatic impact. In *Aerosols and Their Climatic Effects* (Eds: H. E. Gerber and A. Deepak). A. Deepak Publishing, Hampton, Virginia, USA. 279–294.

LENOBLE, J., TANRE, D., DESCAMPS, P. Y. and HERMAN, M., 1982: A simple method to compute the change in earth–atmosphere radiative balance to a stratospheric aerosol layer. *J. Atmos. Sci.*, **39,** 2565–2576.

LIOU, K.-N. and SASAMORI, T., 1975: On the transfer of solar radiation in aerosol atmospheres. *J. Atmos. Sci.*, **32,** 2166–2177.

LORENZ, E. N., 1979: Forced and free variations of weather and climate. *J. Atmos. Sci.*, **36,** 1367–1376.

LOVELOCK, J. E., 1979: *Gaia—A New Look at Life on Earth.* Oxford Univ. Press, Oxford, 157 pp.

LOVELOCK, J. E. and MARGULIS, L., 1974: Atmospheric homeostasis by and for the biosphere: The Gaia hypothesis. *Tellus,* **26,** 2–10.

LUTHER, F. M., 1976: Relative influence of stratospheric aerosols on solar and longwave radiative fluxes for a tropical atmosphere. *J. Appl. Meteor.*, **15,** 951–955.

MACCRACKEN, M. C., CESS, R. D. and POTTER, G. L., 1986: Climatic effects of anthropogenic Arctic aerosols: An illustration of climate feedback mechanisms with one- and two-dimensional climate models. *J. Geophys. Res.*, **91,** 14 445–14 450.

MALONE, R. C., AUER, L. H. GLATZMAIER, G. A. and WOOD, M. C., 1986: Nuclear winter: Three-dimensional simulations including interactive transport, scavenging, and solar heating of smoke. *J. Geophys. Rev.*, **91,** 1039–1053.

MANABE, S. and STRICKLER, R. F., 1964: Thermal equilibrium of the atmosphere with a convective adjustment. *J. Atmos. Sci.*, **21,** 361–385.

MASS, C. and SCHNEIDER, S. H., 1977: Statistical evidence on the influence of sunspots and volcanic dust on long-term temperature records. *J. Atmos. Sci.*, **34,** 1995–2004.

MCINTURFF, R. M., MILLER, A. J., ANGELL, J. K. and KORSHOVER, J., 1971: Possible effects on the stratosphere of the 1963 Mt. Agung volcanic eruption. *J. Atmos. Sci.*, **28,** 1304–1307.

MÉSZÁROS, E., 1988: On the possible role of the biosphere in the control of atmospheric clouds and precipitation. *Atmos. Environ.*, **22,** 423–424.

MITCHELL, J. F. B. and SLINGO, A., 1988: Climatic effects of nuclear war: The role of atmospheric stability and ground heat fluxes. *J. Geophys. Res.*, **93,** 7037–7045.

MITCHELL, J. M., 1971: The effect of atmospheric aerosols on climate with special reference to temperature near the earth's surface. *J. Appl. Meteor.*, **10,** 703–714.

NEWELL, R. E., 1970: Stratospheric temperature change from the Mt. Agung volcanic eruption of 1963. *J. Atmos. Sci.*, **27,** 977–978.

NEWIGER, M. and BÄHNKE, K., 1981: Influence of cloud composition and cloud geometry on the absorption of solar radiation. *Beitr. Phys. Atmos.*, **54,** 370–382.

NORTH, G. R., CAHALAN, R. F. and COAKLEY, J. A., 1981: Energy balance climate models. *Rev. Geophys. Space Phys.*, **19,** 91–121.

OHRING, G. and ADLER, S., 1978: Some experiments with a zonally averaged climate model. *J. Atmos. Sci.*, **35,** 186–205.

OHRING, G. and CLAPP, P., 1980: The effect of changes in cloud amount on the net radiation at the top of the atmosphere. *J. Atmos. Sci.*, **37,** 447–454.

OPSTEEGH, J. D., 1981: Climate modelling. In *Climatic Variations and Variability: Facts and Theories* (Ed.: A. Berger). NATO Advanced Study Institutes Series C, Vol. 72, A. Reidel Publ. Co., Dordrecht. 751–758.

PARKER, D. E., 1985: Climatic impact of explosive volcanic eruptions. *Meteor. Mag.*, **114,** 149–161.

PENNER, J. E., 1986: Uncertainties in the smoke source term for nuclear winter studies. *Nature*, **324,** 222–226.

PHILLIPS, N. A., 1960: The general circulation of the atmosphere: A numerical experiment. In *Dynamics of Climate* (Ed.: R. L. Pfeffer). Pergamon Press, Oxford. 18–25.

POLLACK, J. B. and ACKERMAN, T. P., 1983: Possible effects of the El Chichon volcanic cloud on the radiation budget of the northern tropics. *Geophys. Res. Lett.*, **10,** 1057–1060.

POLLACK, J. B., TOON, O. B., SAGAN, C., SUMMERS, A., BALDWIN, B. and VAN CAMP, W., 1976a: Volcanic explosions and climatic change: A theoretical assessment. *J. Geophys. Res.*, **81,** 1071–1083.

POLLACK, J. B., TOON, O. B., SUMMERS, A., VAN CAMP, W. and BALDWIN, B., 1976b: Estimates of the climatic impact of aerosols produced by space shuttles, SST's, and other high-flying aircraft. *J. Appl. Meteor.*, **15,** 247–258.

POTTER, G. L. and CESS, R. D., 1984: Background tropospheric aerosols: Incorporation within a statistical–dynamical model. *J. Geophys. Res.*, **89,** 9521–9526.

RAMANATHAN, V. and COAKLEY, J. A., 1978: Climate modeling through radiative–convective models. *Rev. Geophys. Space Phys.*, **16,** 465–489.

RANDALL, D., CARLSON, T. and MINTZ, Y., 1984: The sensitivity of a general circulation model to Saharan dust heating. In *Aerosols and Their Climatic Effects* (Eds: H. E. Gerber and A. Deepak) A. Deepak Publishing, Hampton, Virginia, USA. 123–132.

RASOOL, S. I. and SCHNEIDER, S. H., 1971: Atmospheric carbon dioxide and aerosols: Effects of large increases on global climate. *Science*, **173,** 138–141.

RECK, R. A., 1974: Influence of surface albedo on the change in the atmospheric radiation balance due to aerosols. *Atmos. Environ.*, **8,** 823–833.

RECK, R. A., 1975: Influence of aerosol cloud height on the change in the atmospheric radiation balance due to aerosols. *Atmos. Environ.*, **9,** 89–99.

RECK, R. A., 1976: Thermal and radiative effects of atmospheric aerosols in the Northern Hemisphere calculated using a radiative–convective model. *Atmos. Environ.*, **10,** 611–617.

RECK, R. A. and HUMMEL, J. R., 1981: Influence of aerosol optical properties on surface temperatures computed with a radiative–convective model. *Atmos. Environ.*, **15,** 1727–1731.

ROBOCK, A., 1984: Snow and ice feedbacks prolong effects of nuclear winter. *Nature*, **310,** 667–670.

ROSEN, H., HANSEN, A. D. A. and NOVAKOV, T., 1984: Role of graphitic carbon particles in radiative transfer in the Arctic haze. *Sci. Total Environ.*, **36,** 103–110.

SALTZMAN, B., 1978: A survey of statistical–dynamical models of the terrestrial climate. *Adv. Geophys.*, **20,** 183–303.

SCHNEIDER, S. H., 1972: Cloudiness as a global climatic feedback mechanism: The effects on the radiation balance and surface temperature of variations in cloudiness. *J. Atmos. Sci.*, **29,** 1413–1422.

SCHNEIDER, S. H., 1986: A goddess of the Earth?: The debate on the Gaia hypothesis—An editorial. *Climatic Change*, **8,** 1–4.

SCHNEIDER, S. H. and MASS, C., 1975: Volcanic dust, sunspots, and temperature trends. *Science*, **190,** 741–746.

SCHNEIDER, S. H. and THOMPSON, S. L. 1988: Simulating the climatic effects of nuclear war. *Nature*, **333,** 221–227.

SELLERS, W. D., 1969: A global climatic model based on the energy balance of the earth–atmosphere system. *J. Appl. Meteor.*, **8,** 392–400.
SHAW, G. E., 1983: Bio-controlled thermostasis involving the sulfur cycle. *Climatic Change,* **5,** 297–303.
SHAW, G. E., 1987: Aerosols as climate regulators: A climate–biosphere linkage? *Atmos. Environ.*, **21,** 985–986.
SMAGORINSKY, J., 1974: Global atmospheric modeling and the numerical simulation of climate. In *Weather and Climate Modification* (Ed.: W. N. Hess). John Wiley and Sons, Inc., New York. 633–686.
SMIC, 1971: *Inadvertent Climate Modification. Report of the Study of Man's Impact on Climate.* MIT Press, Cambridge, Massachusetts, 308 p.
TANRE, D., GELEYN, J. F. and SLINGO, J., 1984: First results of the introduction of an advanced aerosol–radiation interaction in the ECMWF low resolution global model. In *Aerosols and Their Climatic Effects* (Eds: H. E. Gerber and A. Deepak). A. Deepak Publishing, Hampton, Virginia, USA. 133–177.
THOMPSON, S. L., 1985: Global interactive transport simulations of nuclear war smoke. *Nature,* **317,** 35–39.
THOMPSON, S. L., RAMASWAMY, V. and COVEY, C., 1987: Atmospheric effects of nuclear war aerosols in general circulation model simulations: Influence of smoke optical properties. *J. Geophys. Res.*, **92,** 10 942–10 960.
TOON, O. B. and POLLACK, J. B., 1976: A global average model of atmospheric aerosols for radiative transfer calculations. *J. Appl. Meteor.*, **15,** 225–246.
TURCO, R. P., TOON, O. B., ACKERMAN, T. P., POLLACK, J. B. and SAGAN, C., 1983: Nuclear winter: Global consequences of multiple nuclear explosions. *Science,* **222,** 1283–1292.
TURCO, R. P., TOON, O. B., POLLACK, J. B., WHITTEN, R. C., POPPOFF, I. G. and HAMIL, P., 1980: Stratospheric aerosol modification by supersonic transport and space shuttle operations—Climate implications. *J. Appl. Meteor.*, **19,** 78–89.
TWOMEY, S., 1974: Pollution and the planetary albedo. *Atmos. Environ.*, **8,** 1251–1256.
TWOMEY, S., 1977a: *Atmospheric Aerosols.* Elsevier Sci. Publ. Co., Amsterdam, 302 p.
TWOMEY, S., 1977b: The influence of pollution on the shortwave albedo of clouds. *J. Atmos. Sci.*, **34,** 1149–1152.
TWOMEY, S., PIEPGRASS, M. and WOLFE, T. L., 1984: An assessment of the impact of pollution on global cloud albedo. *Tellus,* **36B,** 356–366.
UNEP/WMO/ICSU, 1985: *Assessment Conference on the Role of Carbon Dioxide and of Other Radiatively Active Constituents in Climate Variations and Associated Impacts.* Villach, Austria, 9–15 October 1985.
VOGELMANN, A. M., ROBOCK, A. and ELLINGSON, R. G., 1988: Effects of dirty snow in nuclear winter simulations. *J. Geophys. Res.*, **93,** 5319–5332.
WANG, W.-C. and DOMOTO, G. A., 1974: The radiative effect of aerosols in the earth's atmosphere. *J. Appl. Meteor.*, **13,** 521–534.
YAMAMOTO, G. and TANAKA, M., 1972: Increase of global albedo due to air pollution. *J. Atmos. Sci.*, **29,** 1405–1412.
YAMAMOTO, G., TANAKA, M. and OHTA, S., 1974: Heating of the lower troposphere due to absorption of the visible solar radiation by aerosols. *J. Meteor. Soc. Japan,* **52,** 61–68.

Appendix I

Basic concepts of nucleation

(Thermodynamic/kinetic approach[1,2])

Phase changes are accompanied by changes in the internal energy of the substance. This can be readily appreciated from the fact that phase changes are associated with the release, or uptake, of heat—the latent heats of phase changes. When two phases are in equilibrium, which is only possible at the melting, sublimation and vaporization points along the lines of the phase diagram, addition or removal of latent heat shifts the balance between the relative amounts of the two phases: more solid melts and becomes liquid, etc. Equilibrium between any two phases is expressed by equality of the chemical potentials of the two phases. Removal or addition of latent heat constitutes an energy exchange with the environment (nonclosed system).

At conditions away from equilibrium (supercooling, superheating, supersaturation, etc.) the chemical potentials of the two phases are no longer equal. The stable phase is that which has the lower internal energy—the more ordered phase from the point of view of statistical thermodynamics. The metastable phase has a higher internal energy and it is the difference between the energies of the stable and metastable phases which provides the driving energy for the phase change. However, the formation of a small volume of the new phase within the old one involves the formation of an interphase surface (or interface). The creation of that surface involves an investment of energy which thus opposes the driving energy. Nucleation is the phenomenon of initiation of the new, stable phase within the metastable phase.

In terms of chemical potentials per molecule, μ_i and μ_j for the metastable and stable phases respectively, and with subscripts i and j standing for labels s, l and v of the solid, liquid and vapor phases, the free energy difference for n molecules is just

$$\Delta F_n = n(\mu_j - \mu_i) \tag{I.1}$$

which will be a negative quantity for cases of interest here. The quantities in (I.1)

[1] Key developments of the theory were provided by J. W. Gibbs, M. Volmer, R. Becker and W. Doring, L. Szilard, J. B. Zeldovich, and L. Farkas over the first third of this century.

[2] For more rigorous derivations of the results quoted here, the reader is referred to the many excellent descriptions of basic and advanced topics in nucleation theory. Some examples are: Zettlemoyer (1969), Abraham (1974), Krastanov and Miloshev (1980), Mutaftschiev (1982).

are, of course, functions of temperature or saturation ratio, so that ΔF_n increases for conditions further and further removed from equilibrium.

For a cluster of n molecules of the new phase (the embryo), the surface energy of the interface can be expressed as

$$\Delta F_s = \beta n^{2/3} \sigma_{ij} \tag{I.2}$$

where β is a constant whose value depends on the shape and density of the cluster, σ_{ij} is the interfacial energy per unit surface area, and $n^{2/3}$ is proportional to the surface area of the interface.

The net free energy change associated with the formation of the embryo is $\Delta F = \Delta F_s + \Delta F_n$. This sum of the two terms is illustrated, for a given condition (fixed temperature, etc.), in Fig. I.1 as a function of cluster size. It is evident from the figure, and from the fact that one of the terms varies with n to the ⅔ power while the other term of opposite sign varies linearly with n, that ΔF has a maximum, ΔF^*, at some cluster size n^*, called the critical embryo size. This maximum, or critical point, separates the region of small clusters, where growth

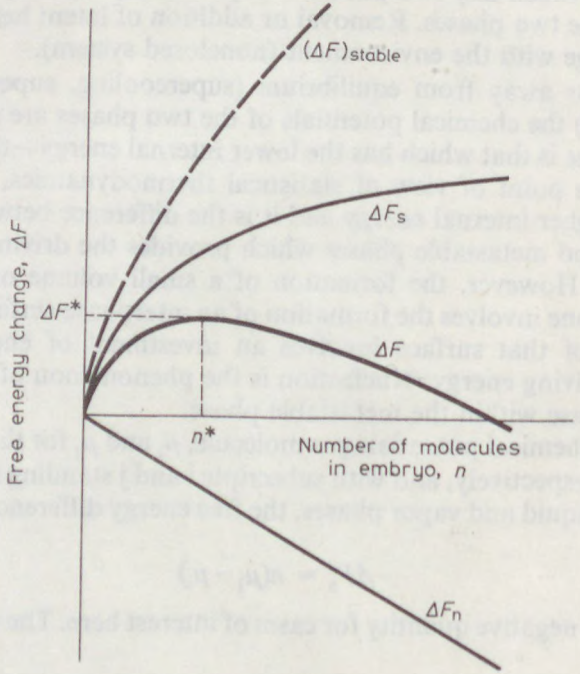

Fig. I.1

The free energy of formation of clusters of the condensed phase, as a function of cluster size (heavy line), and the surface and volume components of the total change. The broken line indicates the free energy change of clusters when the less-ordered phase is the thermodynamically stable one (subsaturation for vapor, or above the melting temperature of a solid)

of the cluster involves a net increase in free energy, from the region where growth involves a decrease in energy. Growth at sizes exceeding n^* can proceed spontaneously, while at smaller sizes it cannot. Nucleation is the formation of an embryo of critical size n^*.

The equations given above can be readily solved for ΔF^* and n^*. From an examination of Fig. I.1 it can be seen that if ΔF_n increases in magnitude for given n, i.e. the state of the system is moved further from equilibrium (greater supercooling, for example), the critical free energy decreases, and the critical point is reached with smaller and smaller embryos. This point is further illustrated by the family of curves shown in Fig. I.2: ΔF is plotted as a function of n (just as in Fig. I.1) for a set of different conditions, such as increasing supercooling, or increasing supersaturation.

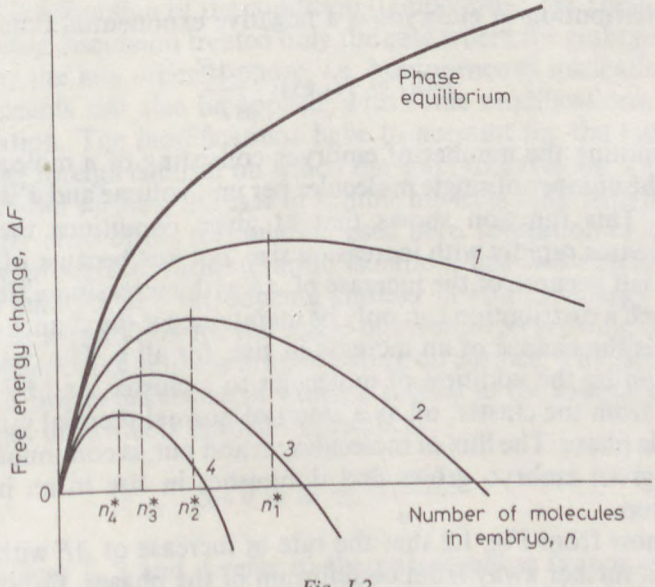

Fig. I.2

The free energy of cluster formation for different conditions. At phase equilibrium, the free energy increases monotonically with increasing cluster size. In metastable conditions (supersaturation or supercooling), the free energy change is a maximum at some critical cluster (embryo) size n^*. The sequence of curves 1 to 4 correspond to increasing supersaturations or increasing supercoolings

Without supersaturation, or supercooling, both the volume and surface terms (given by equations I.1 and I.2, respectively) would be positive, so that the total free energy change would increase monotonically and rapidly with size, without a maximum, as indicated in Fig. I.1 by the curve labeled $(\Delta F)_{\text{stable}}$. Hence, there is no possibility for nucleation in a thermodynamically stable system, only in a metastable one.

The question remains: how can clusters grow to the critical size? To answer that question, it is necessary to look at the molecular state of a generally disordered phase, vapor or liquid. While most of the molecules are independent, and move about as such, clusters of molecules are also always present: dimers, trimers, and so on. These clusters are bonded in a way that is close to the bonding of the molecules in the more ordered phase. In fact, clusters form even in normally stable phases—few molecules of a liquid-like cluster within the vapor, or solid-like clusters of a few molecules within liquid. Such clusters have very short lifetimes, and have a greater probability of breaking apart than of growing, in accordance with the monotonic increase of ΔF with cluster size. However, in the metastable state the clusters have a finite chance of reaching the critical size corresponding to ΔF^*, as will be shown below. Appropriately, clusters of the more ordered phase within the metastable parent phase are called embryos.

The size distribution of embryos is a negative exponential function:

$$N(n) = N_0 \exp \frac{-\Delta F}{kT} \qquad \text{(I. 3)}$$

with $N(n)$ denoting the number of embryos consisting of n molecules per unit volume, N_0 the number of single molecules per unit volume and T is the absolute temperature. This function shows that at given conditions the number of embryos decreases rapidly with increasing size, not just because of the negative exponential, but because of the increase of ΔF with increasing n (for subcritical embryos). Such a distribution can only be maintained if the chance of a decrease in size exceeds the chance of an increase in size, for all n. The changes in sizes are brought on by the addition of molecules to a cluster, and by the removal of molecules from the cluster, all as a result of normal thermal motions within the metastable phase. The flux of molecules, in and out, is continuous and rapid, so that any given embryo grows and diminishes in size in an irregular and "noisy" fashion.

Recalling now from Fig. I.2 that the rate of increase of ΔF with n decreases for conditions further away from equilibrium of the phases, Eq. (I.3) indicates that the distribution becomes broader, i.e. the average size increases. Hence, with increasing supercooling, or increasing supersaturation, the critical embryo size becomes smaller, while the average embryo size increases. It is easy to see, that this leads to an increased probability of nucleation. The simple definition given above was that the formation of an embryo of critical size constituted nucleation of the stable phase; a more precise view is that even embryos of critical size, or larger, have a finite probability of decaying back to subcritical size, and that probability is lower than the probability of growth. Conversely, for a subcritical embryo the probability of decay exceeds the probability of growth.

Analytically, the probability of nucleation is usually expressed as the nucleation rate, J, or the number of critical embryos forming per unit time and per unit volume. A nucleation event is then defined as $JVt = 1$ with V as the volume

of the sample, and t as time. Among a large number N of identical volumes V, one can also define the probability of nucleation over time δt as

$$-\frac{\delta N}{N} = JV\delta t \tag{I.4}$$

The right-hand size stands for the fraction of the sample in which nucleation can be expected over the interval δt. The value of J can be calculated from the number of critical size embryos $N(n^*)$ and the rate at which those embryos are expected to grow by the addition of yet another molecule to the embryo. A somewhat simplified form of the expression for J is

$$J = A \exp \frac{-\Delta F^*}{kT} \tag{I.5}$$

with A a near-constant factor. In examining this expression, one has to remember that ΔF^* is a function of the condition (temperature, etc.) being considered.

The foregoing discussion treated only the case where the embryo is surrounded entirely by the less ordered phase, i.e. homogeneous nucleation. However, the same concepts can also be applied, with some modifications, to heterogeneous nucleation. The modifications have to account for the influence of the substrate—the foreign catalyst on which the embryo develops. The substrate is considered a solid surface; the case of soluble nuclei is dealt with differently (cf. Chapter 3). In terms of the formulation used here, formation of an embryo on top of a foreign surface, rather than in isolation, has two effects: altering the shape of the embryo, and introducing another interfacial energy term.

The simplest assumption for the shape of an embryo growing on a substrate is that of a spherical cap, like a droplet sitting on surface. That shape is defined by the contact angle, the cosine of which is related to the interfacial energies of the three types of contacts between substances:

$$\cos\theta \equiv m = \frac{\sigma_{13} - \sigma_{23}}{\sigma_{12}} \tag{I.6}$$

where the indices 1, 2 and 3 refer to the parent phase (vapor or liquid), the embryo (liquid or solid) and the substrate, respectively. Using this model, and assuming a plane substrate surface, the free energy change associated with the formation of the embryo is

$$\Delta F_h = \Delta F_n + \Delta F_s + \Delta F_c \tag{I.7}$$

where the first two terms are similar to those given by Eqs (I.1) and (I.2), with appropriate allowance for the shape change, and ΔF_c is the interfacial energy between the embryo and the substrate. The subscript h is introduced to refer to heterogeneous nucleation. It can be shown that the critical free energy change, $\Delta F_h{}^*$, differs only in a factor $f(m)$ from that obtained for the homogeneous case, that $f(m)$ is always less than unity, and its value is smaller, the smaller the contact angle is. The reduced free energy change is what allows

heterogeneous nucleation to proceed at smaller supercoolings, or supersaturations, than are required for homogeneous nucleation.

The rate of nucleation is still obtained by an equation of the form (I.5), with a different value for the constant A, and with ΔF_h^* substituted instead of ΔF^*.

The foregoing picture can be further elaborated by taking into account the curvature of the substrate surface, to make it applicable to nucleation on aerosol particles which are comparable in size to the critical embryo size. Instead of the factor $f(m)$ one then obtains a factor $f(m,R)$ where R is the radius of the particle. Yet other elaborations of the theory account for different embryo shapes—prisms, cyliners, and so on. Such treatments can be readily formulated within the general framework of the theory outlined above.

The approach here presented, and its extensions, have a number of fundamental limitations, so the value of refined details is often questionable. Perhaps the most important limitation arises from the impossibility to determine interfacial energies on the scale of the embryos, and there are good reasons to question the applicability of macroscopic determinations to the scale of few molecules. Allowing the interfacial energies to be adjustable parameters, and attempting to match some predictions to observations, often leaves the theory with so many degrees of freedom that no useful results are obtained at all in the end. The problem seems especially severe for heterogeneous ice nucleation and for condensation on insoluble surfaces; for these processes the experimental difficulties are also formidable, so that the true qualities of the nucleating surface are not readily defined. For homogeneous condensation and homogeneous freezing, the approximations appear to be less debilitating, as reasonable agreement with observations can be achieved. Heterogeneous condensation on soluble nuclei is actually best described by the Köhler theory of vapor pressure change with solute concentration and curvature. That formulation predicts only the activity, but not the rate, of condensation nucleation; the rate is controlled in practice by the rate of change of supersaturation.

Another major difficulty facing theoretical descriptions of nucleation lies in the formation of embryos at preferential sites on the substrate surface. Again, this problem is most severe for ice nucleation, but is likely to be also a factor in condensation on mixed and non-uniform particles. How to characterize such surface sites? In a way, this is an even more severe manifestation of the problem of proper description of the interface between embryo and substrate. So far, there are not many lines along which the problem can be approached; some are discussed in the main body of this volume.

In summary, the simple theory here presented, and more detailed versions of it, can provide important guidance to concepts of nucleation, and can be used to make some testable qualitative predictions. Strict quantitative agreement with observations can hardly be expected because of limitations built into the theory with its basic assumptions. And, of course, the observations have their own limitations. The observational problems of characterizing surfaces on the scale of few atoms, plus the rapidly expanding complexities which theories face when attempting to treat molecule-to-molecule and molecule-to-substrate in-

teractions on more rigorous bases, indicate that the simple thermodynamic/kinetic theory will not be readily replaced. It may be anticipated that efforts will continue toward improvements of the thermodynamic/kinetic theory, in spite of its insurmountable limitations, in parallel with developments of more advanced treatments.

References

ABRAHAM, F. F., 1974: *Homogeneous Nucleation Theory*. Academic Press, New York.

KRASTANOV, L. and MILOSHEV, G., 1980: *Theoretical Bases of the Phase Transitions of Water in the Atmosphere*. Meteor. Serv. Hungarian Peopl. Repl., Budapest.

MUTAFTSCHIEV, B., 1982: *Interfacial Aspects of Phase Transformations*. D. Reidel Publ. Co., Dordrecht.

ZETTLEMOYER, A. C. (ed.), 1969: *Nucleation*. M. Dekker, New York.

Appendix II

Growth of cloud droplets

Part A: Droplet growth by condensation

Let us consider a solution droplet whose vapor pressure ϱ_r is lower than that of its surroundings and which consequently grows by vapor diffusion. The volume of the vapor phase is very large relative to that of the droplet. If the temperature (T) and vapor density (ϱ) far from the droplet are constant, a steady state diffusion field is built up. The flux of vapor molecules crossing any spherical surface with a radius R (the droplet is in the center of the sphere) will be constant and independent of time. The constant vapor flux controls the growth of the droplet since vapor molecules diffusing in the direction of the droplet condense on the droplet surface[1]. In this way the droplet growth is given by

$$\frac{dm}{dt} = 4\pi R^2 D \frac{d\varrho}{dR} \tag{II.1}$$

where m is the mass of the droplet with radius r, D is the diffusion coefficient of water vapor (see Table II.1) and t is the time.

The integration of Eq. (II.1) from ϱ_r (the vapor density at the droplet surface) to ϱ_1 at infinite distance from the droplet yields

$$4\pi D \int_{\varrho_1}^{\varrho_r} d\varrho = \int_{\infty}^{r} \frac{dm}{dt} \frac{dR}{R^2}$$

which can be written in the form of

$$\frac{dm}{dt} = 4\pi r D(\varrho_1 - \varrho_r)$$

By noting that

$$m = \frac{4}{3}\pi r^3 \varrho_2$$

[1] This in not always the case (e.g. SEDUNOV, 1972). The condensation coefficient defined as the ratio of condensing and colliding molecules can be lower than 1.

the growth equation will be

$$r\frac{dr}{dt} = D\frac{\varrho_1 - \varrho_r}{\varrho_2} \tag{II.2}$$

where ϱ_2 is the density of the droplet.

In addition to vapor diffusion the heat conduction must also be calculated since during condensation latent heat is released. Considering that the direction of heat conduction is opposite to the direction of vapor diffusion we can write that

$$L\frac{dm}{dt} = -4\pi R^2 K\frac{dT}{dR} \tag{II.3}$$

where L is the latent heat of condensation, while K is the thermal conductivity of air (their numerical values are given in Table II.1).

Taking into account the equation of ideal gases and the Clausius-Clapeyron equation[1], after some algebraic calculation (see FLETCHER, 1962; MASON, 1971) the rate of increase of the droplet mass will be

$$r\frac{dr}{dt} = G(S - S') \tag{II.4}$$

where S and S' are the supersaturation in the environment and the equilibrium supersaturation for the droplet, respectively. The coefficient G in this equation

Table II.1

Diffusion coefficient and coefficient of thermal conductivity of water vapor as well as the latent heat of condensation as a function of temperature (MASON, 1971)

	40 °C	20 °C	10 °C	0 °C	−10 °C	−20 °C	−40 °C
Diffusion coefficient $[m^2 s^{-1}] \cdot 10^5$	2.84	2.53	2.39	2.25	2.11	1.98	1.72
Coefficient of thermal conductivity $[J\ m^{-1} s^{-1} K^{-1}] \cdot 10^2$	2.71	2.55	2.48	2.40	2.32	2.23	2.07
Latent heat (condensation) $[J\ kg^{-1}] \cdot 10^{-6}$	2.406	2.454	2.477	2.500	2.525	2.549	2.603

[1] As it is known this equation gives the saturation vapor pressure ($p_{2\infty}$) as a function of the temperature

$$\frac{dp_{2\infty}}{p_{2\infty}} = \frac{L}{R_w}\frac{dT}{T}$$

where R_w is the gas constant referring to 1 g of water.

is given by

$$G = \frac{D\varrho_1}{\varrho_2}\left(1 + \frac{DL^2\varrho_1 M_w}{RT^2K}\right),$$

where R is the gas constant ($=8.314$ J mol^{-1} K^{-1}), and M_w the molecular weight of water (18.016).

Considering now a parcel of air which is undergoing adiabatic lifting, the supersaturation in the cooling air varies as

$$\frac{dS}{dt} = Q_1 v - Q_2 \frac{dw}{dt} \tag{II.5}$$

where v is the updraft speed, w is the liquid water content, while Q_1 and Q_2 are physical parameters which can be calculated by using the relationships:

$$Q_1 = \frac{LM_w g}{RT^2 c_p} - \frac{M_a g}{RT}$$

and

$$Q_2 = \frac{L^2 M_w}{TPM_a c_p} + \frac{RT}{p_{2\infty} M_w}$$

In these formulae g is the gravitation constant (9.80665 m s^{-2}), c_p is the specific heat of the air at constant pressure (1.005 J kg^{-1} K^{-1}), P is the atmospheric pressure, while M_a is molecular weight of dry air (28.964). Finally, we note that formula (II.4) is strictly valid only for droplets which do not move. For moving droplets a so-called ventilation factor must be applied. However, in the size range of cloud droplets ($r < 30$ μm) this effect can practically be neglected (FLETCHER, 1962).

Part B: Drop growth by coalescence

Let us consider a cloud consisting of small drops with radius r. In the cloud one large drop falls. The radius of the large drop is R, while its falling speed is denoted by V. During unit time the large drop sweeps through a volume of $R^2\pi(V-v)$, where v is the falling speed of smaller drops[1]. Thus, the mass increase of the large drop during unit time will be

$$\frac{dM}{dt} = R^2\pi(V-v)wE \tag{II.6}$$

where M is the mass of the drop with radius R, w is the liquid water content, and E is the so-called collection efficiency.

Taking into account that

[1] The falling speed can be calculated by Eq. (2.1).

$$M = \frac{4}{3} R^3 \pi \varrho_2$$

the rate of increase of the radius of large drop will be

$$\frac{dR}{dt} = \frac{E(V-v)}{4\varrho_2} w \tag{II.7}$$

which is equivalent to Eq. (3.11).

The collection efficiency is defined as follows (LANGMUIR, 1948). During its fall in the cloud, the large drop does not capture all the small drops in the volume of $R^2\pi(V-v)$. It collects droplets which are apparently in a smaller volume: $x^2\pi(V-v)$ where $x<R$ is a hypothetical radius. This is due to the fact that only those small drops are collected, the inertia of which is higher than a certain critical value (inertial deposition, see Subsection 2.1.2). Accordingly, the collection efficiency is defined by

$$E = \frac{x^2}{R^2} \tag{II.8}$$

Results of experimental works and numerical calculations show that in the size range of cloud drops ($R<100$ μm) the collection efficiency increases with increasing R. This involves that if large cloud drops form by condensation, the initiation of the coalescence is more probable.

It should be mentioned that this discussion is valid only if each collision is accompanied by the coalescence of the two colliding drops. Thus, the collection efficiency defined above is more correctly termed as collision efficiency. However, as a first approximation we can assume that the collection efficiency is equal to the collision efficiency.

Further, it should also be noted that the above concept is a continuous model for collection growth. This means that all large drops of the same radius collect smaller drops at an equal rate. However, in the reality collection is not continuous as first proposed by TELFORD (1955). By chance a small fraction of large drops collect droplets at a higher rate than average collection efficiencies indicate. This process can be simulated by the so-called stochastic growth models. The readers interested in such kind of models are referred to the book of PRUPPACHER and KLETT (1980).

References

FLETCHER, N. H., 1962: *The Physics of Rainclouds*. University Press, Cambridge.

LANGMUIR, I., 1948: The production of rain by chain reaction in cumulus clouds at temperatures above freezing. *J. Meteor.*, **5**, 175–192.

MASON, B. J., 1971: *The Physics of Clouds*. Clarendon Press, Oxford.

PRUPPACHER, H. R. and KLETT, J. D., 1980: *Microphysics of Clouds and Precipitation*. D. Reidel Publ. Co., Dordrecht.

SEDUNOV, Y. S., 1972: *Physics of the Formation of Liquid Phase in the Atmosphere* (in Russian). Gidromet. Izdat., Leningrad.

TELFORD, J., 1955: A new aspect of coalescence theory. *J. Meteor.*, **12**, 436–444.

Appendix III

Radiative transfer calculations

Aerosol particles are radiatively active components of the atmosphere. They affect the energy balance of the Earth–atmosphere system in a direct way by absorbing and scattering the incident radiation, and an indirect way as condensation nuclei, which increase the cloud particle concentration and thus the optical thickness of clouds.

Absorption is the process whereby some or all of the radiant energy is transferred to the substance or medium on which it is incident or through which it traverses, and is associated with the resultant change in internal energy (or temperature) of the medium. Scattering, on the other hand, is a process by which a particle continuously abstracts energy from the incident radiation, without any change in the physical state of the particle. Since at present there is no simple procedure for computing the scattering of radiation by a collection of particles of irregular shape, the Mie theory for the scattering by spherical particles is used to approximate the actual interaction between aerosol particles and radiation field.

The optical properties of any aerosol depend on the index of refraction n of the material composing the particle. Physically the index of refraction is the ratio of the velocity of light in vacuum and the velocity of light in the medium. Normally, n is a function of the radiation wavelength, and it consists of a real part n_r and an imaginary part n_i; i.e. it can be expressed as

$$n = n_r - in_i. \tag{III.1}$$

In general, the reflection and refraction processes (including scattering) are due to n_r, while n_i determines the effectiveness of absorption for a given material.

The angular and spatial redistribution of the incident radiation by scattering and reflection depends strongly on the ratio of particle size to wavelength of the radiation. This ratio is the so-called size parameter of a spherical particle

$$x = \frac{2\pi r}{\lambda}, \tag{III.2}$$

where r is the radius of the particle and λ the wavelength of the incident radiation. When particles are much smaller than the incident wavelength ($x \lessapprox 1$), the scattering is called Rayleigh scattering. In this case, particles tend to scatter light equally into the forward and rear directions. For particles whose sizes are

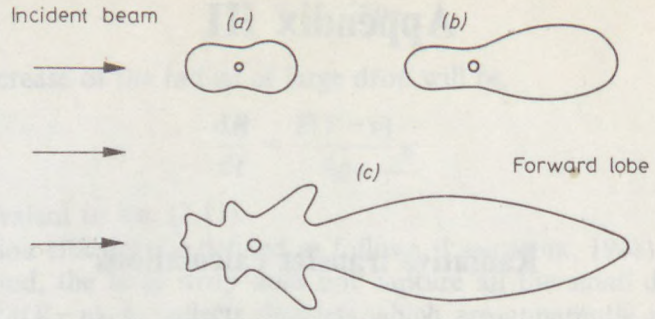

Fig. III.1

Demonstrative angular patterns of the scattered intensity from particles of three sizes: *(a)* small particles, *(b)* large particles, and *(c)* larger particles (after LIOU, 1980). (Reprinted by permission from the author. Copyright by Academic Press, New York)

comparable to or larger than the wavelength ($x \lesssim 1$), the scattering is referred to as Mie scattering, and the scattered energy is increasingly concentrated in the forward directions with greater complexities as shown in Fig. III.1.

Extinction is the attenuation ("damping") of the radiant flux owing to absorption and scattering. The extinction efficiency Q_e of a single particle is defined as the extinction cross section σ_e over the cross-sectional area of the particle:

$$Q_e = \frac{\sigma_e}{\pi r^2}. \tag{III.3}$$

The extinction cross section (or optically effective cross section for extinction) of a single particle is given by

$$\sigma_e = \frac{\beta_e}{N}, \tag{III.4}$$

with N as the total number of particles per unit volume and β_e defined as

$$\beta_e = \frac{1}{L}\frac{dL}{ds}. \tag{III.5}$$

In (III.5), L is the radiance (W $m^{-2}sr^{-1}$) and ds an element of distance along the path of radiation. Therefore, β_e describes the fractional change of radiance after penetrating unit depth of the attenuating medium, and is called the volume extinction coefficient of the medium. Consequently, the extinction efficiency Q_e is a function of both the refractive index n and the size parameter x of the particle. Its values for typical smoke and dust aerosols at wavelengths 0.5 and 11 μm are shown in Fig. III.2 as a function of the radius of single spherical particles.

With Eqs (III.3) and (III.4), the volume extinction coefficient $\beta_e(r_1, r_2)$ attributable to particles with radii between r_1 (smallest particles) and r_2 (largest

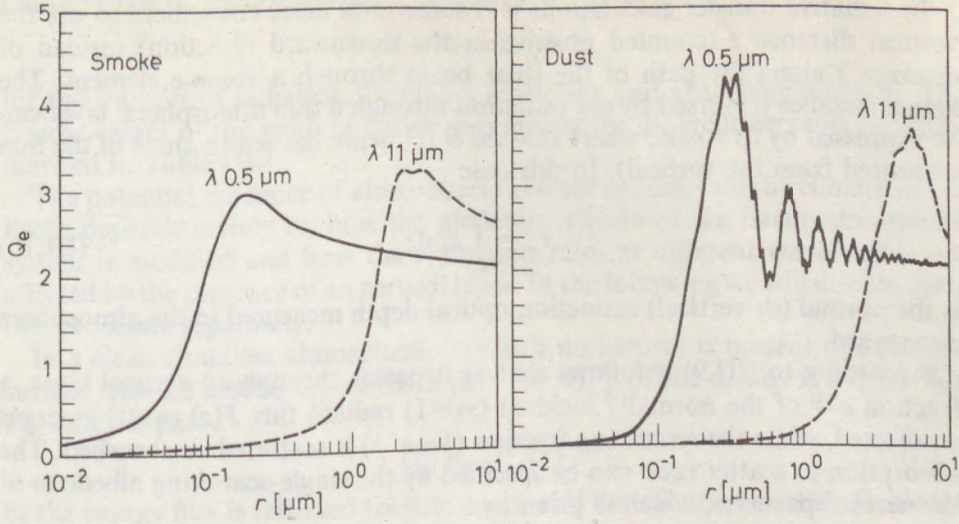

Fig. III.2

Extinction efficiency of *(a)* smoke and *(b)* dust aerosol particles at wavelengths of 0.5 and 11 μm, as a function of particle radius r (after RAMASWAMY and KIEHL, 1985). (Copyright by the American Geophysical Union)

particles in a volume element) is

$$\beta_e(r_1, r_2) = \pi \int_{r_1}^{r_2} Q_e(n, x) r^2 \frac{dN(r)}{dr} dr, \tag{III.6}$$

where $dN(r)/dr$ specifies the size distribution of the particles relevant to the volume element. Similar definitions can be written for scattering and absorption with subscripts s and a, respectively. These quantities are related by

$$\beta_e = \beta_s + \beta_a. \tag{III.7}$$

The integration of (III.6) between the points s_1 and s_2 along the path of radiation leads to the extinction optical thickness

$$\tau_e = \int_{s_1}^{s_2} \beta_e ds. \tag{III.8}$$

With Eqs (III.8) and (III.5), the incident radiance $L(s_1)$ and the transmitted radiance $L(s_2)$ are related by

$$L(s_2) = L(s_1) e^{-\tau_e}. \tag{III.9}$$

Therefore, the significance of optical thickness is that when $\tau_e = 1$, the radiance of the direct (unaffected) beam has been reduced by the factor $1/e$.

In radiative transfer calculations it is sometimes more convenient to use the vertical distance z (counted positive in the downward direction) instead of distance s along the path of the solar beam through a volume element. The actual distance traversed by the radiation through a thin atmospheric layer can be expressed by $ds = m dz$, where $m = \sec \Theta$ (Θ being the zenith angle of the Sun measured from the vertical). In this case

$$\tau_e = \int_{z_1}^{z_2} \beta_e \, dz \tag{III.10}$$

is the normal (or vertical) extinction optical depth measured in the atmosphere downward.

According to (III.9) it follows that as it passes through an aerosol layer, a fraction $e^{-\tau_e}$ of the normally incident ($m = 1$) radiant flux $F(z)$ (watt) emerges unaffected, while the remaining fraction $(1 - e^{-\tau_e})$ is scattered or absorbed. The absorption to scatter ratio can be specified by the single-scattering albedo ω of the aerosol particles, which is given by

$$\omega = \frac{\beta_s}{\beta_e} = 1 - \frac{\beta_a}{\beta_e} \tag{III.11}$$

and represents that fraction of the total extinction of the radiant flux which reappears as scattered radiation due to a single-scattering event within a volume element: if $\omega = 1$, there is no absorption; if $\omega = 0$, only absorption occurs. Thus, $(1 - \omega)$ is the fraction of radiant flux which is absorbed by the aerosol.

In the context of radiative flux arguments, forward scattering only redistributes intensities, but backward scattering is equivalent to reflection. The fraction g of the incident radiation scattered forward in a volume element is called the asymmetry factor of the scattering diagram schematically illustrated in Fig. III.1. For 100% forward scattering, $g = 1$; and for symmetric (isotropic) scattering (50% backscatter), $g = 0$. Therefore, $(1 - g)$ represents the backscattering factor of the aerosol particle.

With the radiative characteristics defined above, the various properties of an aerosol layer can be described in the following way. The absorptance A of the medium, defined as the ratio of the absorbed radiant flux to the incident radiant flux is given by

$$A = (1 - \omega)(1 - e^{-\tau_e}). \tag{III.12}$$

The reflectance Re of the medium, i.e. the ratio of the reflected radiant flux to the incident flux is

$$Re = \omega(1 - g)(1 - e^{-\tau_e}). \tag{III.13}$$

Finally, the transmittance Tr of the medium, defined as the ratio of the radiant flux transmitted through the layer to the incident flux is

$$Tr = e^{-\tau_e} + \omega g(1 - e^{-\tau_e}). \tag{III.14}$$

On the basis of the conservation of energy we have

$$A + Re + Tr = 1$$

for the transfer of radiation through a scattering and absorbing medium. The typical values of the main radiative parameters for different aerosols are summarized in Table III.1.

The potential influence of atmospheric aerosol particles on the climate of the Earth depends mainly on how the planetary albedo of the Earth–atmosphere system is modified and how the extinction rates at different wavelenghts are affected by the presence of an aerosol layer. In the following we will discuss these two processes separately.

In a clean cloudless atmosphere, in which no aerosol is present, the Earth's surface with an albedo α absorbs a part $(1-\alpha)F\downarrow$ of the downward solar flux $F\downarrow$, and the part

$$(F\uparrow)_{\text{clean}} = \alpha F\downarrow \tag{III.15}$$

of the energy flux is reflected back to space and therefore it is not available for heating the Earth–atmosphere system.

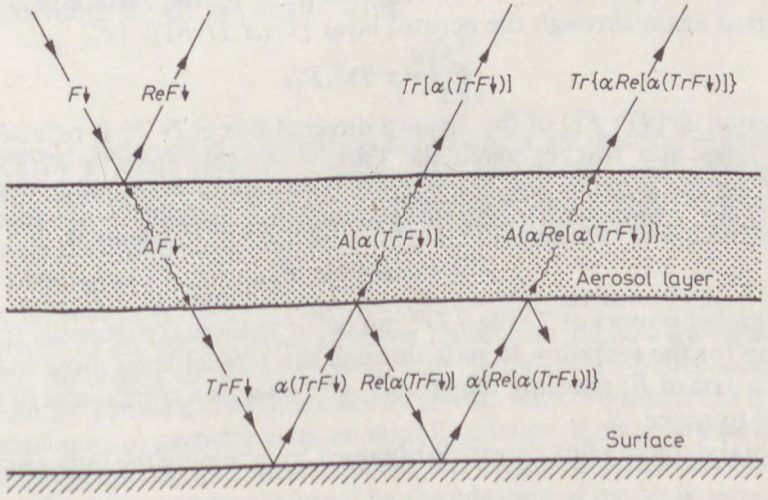

Fig. III.3

Schematic diagram of solar flux densities in a reflecting and absorbing aerosol layer above a surface of albedo α

Let us consider now a simple two-layered system which consists of the clean atmosphere and of a single homogeneous aerosol layer just above the Earth's surface, as shown in Fig. III.3 (PALTRIDGE and PLATT, 1976; TWOMEY, 1977). In this case, $(F\uparrow)_{\text{aerosol}}$ first consists of the incident radiation which is reflected by the aerosol layer and never reaches the Earth's surface:

$$F_1\uparrow = Re\ F\downarrow.$$

Table III.1

Range of the main radiative characteristics for the basic aerosol types (after Standard Radiation Atmosphere in WMO/ICSU, 1983)

Aerosol type	Radiative characteristics			
	ω at 0.55 μm	$1-g$	ω at 10 μm	$\frac{\beta_e \text{ at } 10\ \mu m}{\beta_e \text{ at } 0.55\ \mu m}$
Soot	0.209	0.66	0	0.038
Oceanic	1	0.22	0.692	0.250
Dustlike	0.653	0.12	0.558	1.08
Water-soluble	0.957	0.37	0.209	0.019
Maritime	0.989	0.26	0.680	0.19
Continental	0.891	0.36	0.486	0.097
Urban	0.647	0.41	0.173	0.033
H_2SO_4 (75%)	1	0.27	0.010	0.050
Volcanic	0.947	0.30	0.130	0.035

Its second component is the downward flux reaching the Earth's surface through the aerosol layer ($Tr\,F\downarrow$), reflected there by the surface ($\alpha Tr\,F\downarrow$) and transmitted again through the aerosol layer [$Tr(\alpha\ Tr\,F\downarrow)$], i.e.,

$$F_2\uparrow = \alpha\ Tr^2\ F\downarrow.$$

The fraction $Re(\alpha Tr\,F\downarrow)$ of the upward directed flux $\alpha\ Tr\,F\downarrow$ is reflected by the aerosol layer and reaches again the Earth's surface. Here, $\alpha\ Re(\alpha Tr\ F\downarrow)$ is reflected by the ground, and the fraction $Tr[\alpha Re(\alpha Tr\ F\downarrow)]$ passes through the aerosol layer. Consequently, the third component of $(F\uparrow)_{\text{aerosol}}$ is

$$F_3\uparrow = \alpha^2 Tr^2\ Re\ F\downarrow,$$

etc. No higher powers of Tr than Tr^2 can occur in these components since there is no way for the radiation to pass through the aerosol layer more than twice: once as a part of $F\downarrow$ reaching the ground, and once as a component of $(F\uparrow)_{\text{aerosol}}$ escaping to space.

The total outgoing flux density is obtained by summing the individual contributions:

$$\begin{aligned}(F\uparrow)_{\text{aerosol}} &= ReF\downarrow + \alpha Tr^2(1+\alpha Re+\alpha^2 Re^2+\ldots)F\downarrow \\ &= \left(Re+\frac{\alpha Tr^2}{1-\alpha Re}\right)F\downarrow. \qquad \text{(III.16)}\end{aligned}$$

Solar energy not reflected back to space is necessarily absorbed either by the Earth's surface or by the atmosphere. Therefore, the addition of an aerosol layer to the atmosphere (or an increase of the particle concentration in an existing aerosol layer) will cause a net warming of the Earth–atmosphere system if

$$(F\uparrow)_{\text{clean}} > (F\uparrow)_{\text{aerosol}},$$

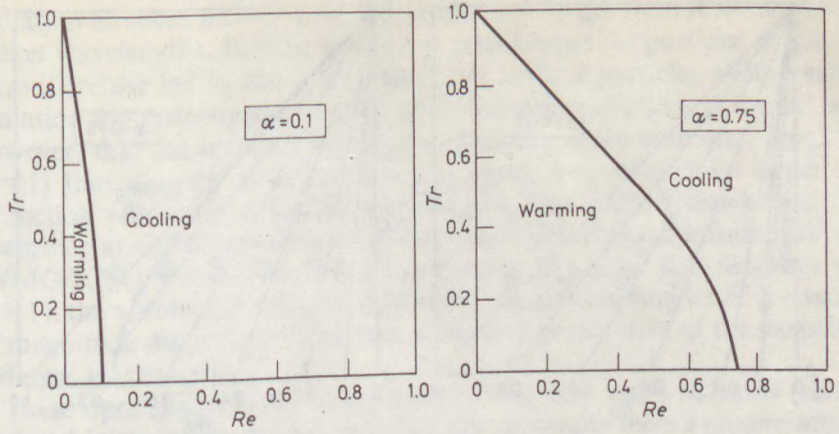

Fig. III.4

Effect of an aerosol layer on the net warming or cooling (after TWOMEY, 1977). (Reprinted by permission from the author. Copyright by Elsevier Science Publishers)

i.e. if, according to (III.15) and (III.16),

$$\alpha > Re + \frac{\alpha Tr^2}{1 - \alpha Re}. \tag{III.17}$$

Consequently, the necessary condition for having a net increase in temperature of the system due to the insertion of aerosol is that the effective reflection factor (system albedo or planetary albedo) of the combined surface–aerosol system standing on the right side of the inequality (III.17) becomes less than the surface albedo α owing to the presence of aerosol.

Using the inequality (III.17), one can calculate the surface albedo α for which the insertion of an aerosol layer of given reflectance Re and transmittance Tr makes no difference to the surface albedo. The results of such calculations, carried out by TWOMEY (1977), are shown in Fig. III.4. To the left of the curves, insertion of aerosol particles gives an initial tendency of planetary warming. To the right of the curves, the initial tendency is a net cooling. In other words, both heating and cooling can be produced by the addition of aerosols, depending on the numerical values of the surface albedo α and of the radiative properties Re and Tr of the aerosol layer (i.e. its extinction optical depth τ_e, single-scattering albedo ω and asymmetry factor g).

When the aerosol optical depth is small ($\tau_e \to 0$), as it is at least in the case of a dry atmospheric aerosol layer, Eq. (III.13) can be simplified to

$$Re = \omega\tau_e - \omega g\tau_e, \tag{III.18}$$

and Eq. (III.14) reduces to

$$Tr = 1 - \tau_e + \omega g\tau_e. \tag{III.19}$$

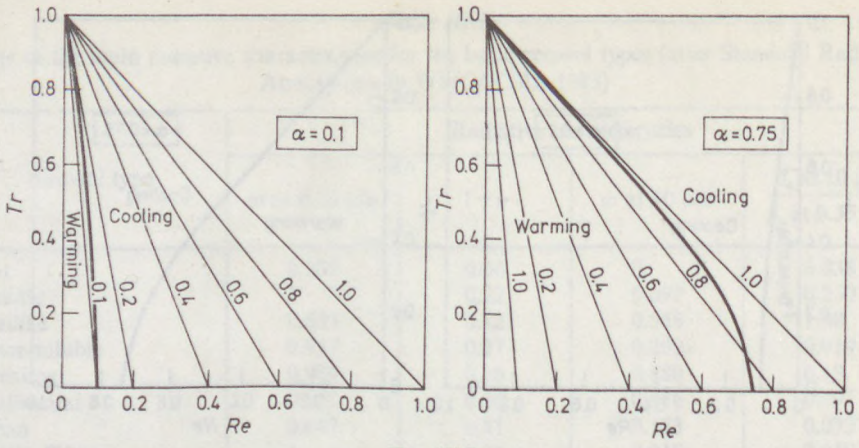

Fig. III.5

The diagram shown in Fig. III.4 with lines superimposed each of which refers to a different value for the parameter $Re/(1-Tr)$ and with separate regions of heating from regions of cooling for that value. (After TWOMEY, 1977). (Reprinted by permission from the author. Copyright by Elsevier Science Publishers)

These equations show that in this "thin-atmosphere approximation" the reflectance and transmittance of an aerosol layer are linear functions of the layer optical depth, and

$$\frac{Re}{1-Tr} = \frac{\omega(1-g)}{1-\omega g}. \tag{III.20}$$

For a given value of the fraction of forward scattering g, the ratio $Re/(1-Tr)$ yields a unique description for the single-scattering albedo ω of the aerosol particles. Curves $Re/(1-Tr) = \text{const}$ have been drawn on a reproduction of Fig. III.4 in Fig. III.5.

For the case $\alpha = 0.1$, corresponding to a dark ocean surface, a necessary condition for warming to occur is that $Re/(1-Tr) < 0.15$. Mie scattering theory gives $g \sim 0.8$ for a Junge size distribution of aerosol particles. Hence, the condition for warming with $\alpha = 0.1$ can be derived as $\omega \lesssim 0.15$ which is possible, although improbable. For $\alpha = 0.75$ (a value typical of snow with some vegetation, fog and moderately thick cloud, etc.), on the other hand, an approximate condition for warming to take place is $Re/(1-Tr) < 0.93$ or $\omega < 0.98$ for all but the larger values of Re. However, since forward scattering is dominant in the atmosphere, larger values of Re in combination with small values of Tr are only of academic interest.

Let us now summarize the relative influence of visible and infrared optical properties of an aerosol layer on the climate.

If we compare the extinction efficiency of a particle having a radius of about 0.2 μm at a wavelength of 0.5 μm with its efficiency at a wavelength of 11 μm, we find (as shown in Fig. III.2) that the extinction efficiency of the particle for

radiation at short wavelengths is considerably larger than it is for radiation at longer wavelengths. Radiative transfer calculations for particles of similar sizes have therefore led to the assumption that aerosol particles affect visible solar radiation more strongly than they affect infrared radiation. It should be noted, however, that the infrared extinction efficiency of an extremely small particle ($x \ll 1$) that absorbs at infrared wavelengths may in fact be larger than its extinction efficiency at visible wavelengths, especially if the particle is non-absorbing at visible wavelengths and strongly absorbing at infrared wavelengths (WMO/ICSU, 1983). Further, we can see in Fig. III.2 that for large particles ($x \gg 1$), the visible and infrared extinction efficiencies may be of the same order of magnitude despite the difference in the size parameters of the particles at the different wavelengths.

These optical properties indicate that both very small particles (radii < 0.05 μm) and fairly large particles (radii > 1 μm) generally have a greater attenuation influence on terrestrial infrared radiation than on incident solar radiation. The absorption and scattering of the terrestrial radiation by an aerosol layer causes an increase in the downward flux of infrared radiation below the layer and a decrease in the net infrared flux at the top of the atmosphere. Thus, this type of aerosol-induced changes to the terrestrial radiative fluxes contributes to a net warming at the surface. On the other hand, particles of intermediate sizes absorb and scatter the incident solar radiation more strongly than they affect the terrestrial radiation. Consequently, in this case the aerosol layer causes a reduction of the radiant energy available at the surface, and thus may lead to a net cooling of the lower layers. In the case of a low-level aerosol layer, however, the absorption of the solar radiation is likely to contribute to the warming of the surface when dynamical processes ensure intense heat exchange between the aerosol layer and the underlying layer.

Finally it should be noted that as far as the aerosol layer itself is concerned, the radiative cooling of the layer is considerably (about an order of magnitude) less than its heating due to absorption of solar radiation. The aerosol contribution to the outgoing terrestrial radiation may become important in the 8 to 12 μm atmospheric window region of the infrared spectrum in cases when heavy concentrations of aerosol particles develop. In such cases the radiative cooling at the top of the aerosol layer may be as large as cooling by the presence of water vapor, i.e. about 2 K/day (GRASSL, 1973; WANG and DOMOTO, 1974; ACKERMAN *et al.*, 1976, 1977).

References

ACKERMAN, T. P., LIOU, K.-N. and LEOVY, C. B., 1976: Infrared radiative transfer in polluted atmospheres. *J. Appl. Meteor.*, **15**, 28–35.

ACKERMAN, T. P., LIOU, K.-N. and LEOVY, C. B., 1977: Corrections to "Infrared radiative transfer in polluted atmospheres". *J. Appl. Meteor.*, **16**, 1372–1373.

GRASSL, H., 1973: Aerosol influence on radiative cooling. *Tellus*, **25**, 386–395.

LIOU, K.-N., 1980: *An Introduction to Atmospheric Radiation*. Academic Press, New York, 392 p.

PALTRIDGE, G. W. and PLATT, C. M. R., 1976: *Radiative Processes in Meteorology and Climatology*. Elsevier Sci. Publ. Co., Amsterdam, 318 p.

RAMASWAMY, V. and KIEHL, J. T., 1985: Sensitivities of the radiative forcing due to large loadings of smoke and dust aerosols. *J. Geophys. Res.*, **90**, 5597–5613.

TWOMEY, S., 1977: *Atmospheric Aerosols*. Elsevier Sci. Publ. Co., Amsterdam, 302 p.

WANG, W.-C. and DOMOTO, G. A., 1974: The radiative effect of aerosols in the earth's atmosphere. *J. Appl. Meteor.*, **13**, 521–534.

WMO/ICSU, 1983: A preliminary cloudless standard atmosphere for radiation calculations. In *Report of the Experts Meeting on Aerosols and Their Climatic Effects* (Eds: A. Deepak and H. E. Gerber). WCP–55.

Appendix IV

Terminology used

To all extents possible the terminology used in this book follows the recommendations of the Committee on Nucleation and Atmospheric Aerosols of the International Association of Meteorology and Atmospheric Physics. To make the survey of this book easier this terminology is presented in this appendix.

A.

1. *Aerosol particle* – Solid or liquid particle mostly consisting of some substance(s) other than water, and without the stable bulk liquid or solid phases of water on it.

2. *Haze particle* – Partly or wholly water-soluble aerosol particle at humidities *exceeding that necessary for* deliquescence and in stable equilibrium with respect to changes in humidity.

3. *Cloud droplet* – Bulk (thermodynamically stable) liquid water droplet, usually formed on a cloud condensation nucleus, and growing to a size (mass) determined by the available supply of vapor.

4. *Ice crystal* – Bulk (thermodynamically stable) solid water, initially formed by the freezing of a cloud droplet or haze particle, or by deposition nucleation, and growing to a size (mass) determined by the available supply of water vapor.

B.

1. *Condensation Nuclei* (CN) – Those particles which will grow to visible size when any liquid condenses on them at supersaturations just below that necessary to activate small ions.

2. *Aitken Nuclei* (AN) – Those particles that grow to visible size when water condenses on them at supersaturations just below those that will activate small ions.

Both of these definitions refer to methods of detection and counting of aerosol

by making them "visible" to an instrument by the condensation of some liquid (CN) or of water specifically (AN) on them.

C.

1. *Cloud Condensation Nuclei* (CCN) – Particles which can serve as nuclei of atmospheric cloud droplets, i.e. particles on which water condenses at supersaturations typical of atmospheric cloud formation (fraction of a % to a few percent, depending on cloud type). Concentrations of CCN need to be given in terms of a supersaturation spectrum covering the range of interest or at some specified supersaturation value.

D.

1. *Primary processes (mechanisms) of ice formation* – Nucleation of ice from the liquid or vapor phases of water, either homogeneously or heterogeneously. The purpose of this terminology is to emphasize the distinction from secondary processes.

2. *Secondary processes (mechanisms) of ice formations* – Creation of ice particles by processes which require prior existence of some other macroscopic (thermodynamically stable) ice particles; examples are splintering of freezing drops, crystal fragmentation, etc.

E.

1. *Ice Nuclei* (IN) – Generic name for substances, usually in the form of aerosol particles, which under suitable conditions of supersaturation or supercooling nucleate ice. This term is to be used if no distinction is intended or is possible as to the specific nucleation mechanism involved.

2. *Ice nucleation modes* – Names or short phrases are needed to refer to particular nucleation modes. Since the details of the molecular embryo formation are difficult to ascertain, it is of great importance that references to nucleation modes be made with the utmost care for clarity of usage, relying, if needed, on more complete descriptions of the phenomenon in question.

The basic distinction that has to be made is whether nucleation is from the vapor or from the liquid phase. There may be some ambiguity when the metastable phase is the vapor, since the formation of liquid-like, or liquid layers might actually be involved in the creation of ice embryos, but unless there is definite evidence for this, the pragmatic view is to consider the bulk vapor as the initial phase.

2.1 *Deposition nucleation* – The formation of ice in a (supersaturated) vapor environment.

2.2 *Freezing nucleation* – The formation of ice in a (supercooled) liquid environment.

2.2.1 *Condensation freezing* – The sequence of events whereby a cloud condensation nucleus (CCN) initiates freezing of the condensate.

2.2.2 *Contact freezing* – Nucleation of a supercooled droplet subsequent to an aerosol particle's coming into contact with it. (This name is preferable to "contact nucleation" as it focuses attention on the fact that the basic process is freezing.)

2.2.3 *Immersion-freezing* – Nucleation of supercooled water by a nucleus suspended in the body of water.

Index

absorptance 258
absorption
– in an aerosol layer 14, 68, 194, 196–203, 206, 235, 259–262
–, definition of 255
– in a cloud layer 14, 194, 229–234
absorption to scatter ratio 201, 258
accumulation mode 37–40, 46
acidification 74
aerocolloidal system, *see* aerosol
aerosol
–, Brownian motion of 17, 18, 20, 22, 70, 71, 168
–, chemical composition of 45–63
–, classification of 19
– collection procedures 20–22
–, concentration of 19, 20, 26, 32–35, 42–44
–, definition of 17, 265
–, diffusion coefficient of 18
–, formation of 23–30
–, growth of 64–68
–, inertial sampling of 21
–, radiative characteristics of 194, 255, 260
–, removal of 68–74
–, residence time of 17, 29, 74, 75
–, Reynolds number of 17
–, sedimentation velocity of 17
–, size of 18, 35–44, 64–68
–, source strengths fo 29, 31
aerosol chamber 26, 27
Aitken particles
–, characterization of 20, 26, 32–35, 46
–, definition of 19, 265
–, formation of 25, 29, 32
albedo effect 196, 199, 200, 229–232
anthropogenic influence
– on aerosol formation 24, 27, 29, 31–33, 40, 123, 195, 196, 198, 223
– on CCN production 96, 102, 103, 108, 124, 232, 233
– on the chemical composition of aerosol 55, 57, 63
– on climate 13, 195, 198, 202, 203, 222–228
– on cloud characteristics 120, 122–124, 233–235
– on composition of the atmosphere 13, 236, 237
– on ice nuclei production 177
anvil clouds 144
Arctic haze 33, 40, 52, 55, 57, 58, 107, 195, 202, 203
ash particles 30, 62
asymmetry factor 68, 233, 258, 260, 261
atmosphere 13
atmospheric window 263

backscattering factor 68, 258
bacteria 30, 145, 176, 177
biogeochemical cycle 14
biological control of climate 203, 235–237
biological source
– of aerosols 15, 28, 30, 31, 55, 203
– of CCN 97, 103, 108, 236, 237
– of DMS 28, 236, 237
– of ice nuclei 175–177
Boltzmann constant 18, 88
bubble formation 23
bulk analysis method 44, 46, 51
bulk deposition 73

carbonaceous particles 55, 57, 73, 74, 195, 203, 222, 223, 225, 232
carbon dioxide 13, 14, 179, 180, 195, 203, 205, 206, 216, 237
cascade impactor 22, 44, 46, 53, 59, 66
chemical diffusion chamber 93
chemical potential 243
cirrus clouds 144, 230
Clausius–Clapeyron equation 252
clear-sky albedo 230, 231
climate models 203–205
climate noise 212–215
climate system 193, 203–205
climatic change
–, anthropogenic origin of 13, 195, 198
–, external and internal causation of 193–195, 204
cloud albedo 14, 194, 200, 210, 229–236
cloud-amount feedback 230, 231
cloud chamber experiments 136–138, 143, 151, 159, 165, 166, 182–184
cloud condensation nuclei (CCN)
– artificial 106, 120–124
–, chemical nature of 15, 104–106
–, concentration of 86, 95–101
–, definition of 14, 85, 266
–, generation of 102, 103
– interstitial 101
–, size of 103–105
cloud droplet
–, concentration of 116, 232–235
–, definition of 265
–, falling speed of 17, 253
–, growth of 109–111, 117, 251–254
–, size distribution of 112–116, 232
–, stochastic growth models of 254
cloud seeding
– in supercooled clouds 178–186
– in warm clouds 120–122
cloud sensitivity parameter 230, 231
coagulation
–, definiton of 18
– efficiency 19
– equation 18, 19
– gravitational 72
– thermal 18, 19, 20, 26, 34, 35, 37, 44, 45, 71, 74, 198
coalescence
– of aerosol particles 18
– of cloud elements 14, 72, 116, 119, 123, 253, 254
coarse particle mode 37–39
coarse particles 37, 38, 53, 203
collection efficiency 21, 22, 61, 72, 73, 117, 168, 253, 254
collision efficiency 254
collision of particles 18
condensation
–, definition of 86
condensation coefficient 251
condensation-freezing 163, 164, 169, 267
condensation nuclei
–, definition of 265
contact angle parameter 146–148, 247
contact freezing 164, 165, 168, 267
continental aerosol
–, chemical composition of 24, 56, 57
–, optical properties of 260
–, size distribution of 39, 40, 66, 67
continental clouds 97, 118
critical point 244, 245
critical sedimentation velocity 18
critical supersaturation 85–93, 95, 100, 101, 106, 147
cumulonimbus clouds 144
cumulus clouds 101, 104, 112, 123

deliquescence 87
deposition, *see* dry and wet deposition
deposition nucleation 134, 146, 147, 149, 150, 159
– in the atmosphere 162–165, 167
–, definition of 266
deposition nuclei 131, 170
deposition threshold 150
deposition velocity 69–71, 73
desert aerosols 25, 55, 57, 58, 202, 212
diffusion battery 20
diffusion chamber 40, 66, 93–95, 105–108, 169–171
diffusion coefficient
– of aerosol particles 18, 20, 106, 252
– of water vapor 252
diffusiophoresis 72
dimethyl sulfide (DMS) 28, 108, 236, 237
dispersal of materials
– from sea surface 23, 24
– from solid surface 15, 24, 25, 37

dispersed system 17
distribution functions 35, 36
dry deposition 15, 68–71
dry ice 179–181
dynamic flow chamber 94, 95
eddy correlation method 69
electrical mobility
– of aerosol particles 20
– of the air 15, 33
electrical mobility analyzer 20, 26, 36
electron microprobe analysis 44, 60
elemental composition 56–58
embryo
–, critical size of 86, 133, 135, 136, 139, 146, 147, 244, 245, 246, 248
–, definition of 244, 246
–, formation of 132, 134, 146, 153, 155, 244, 246, 247
–, shape of 133, 146, 147, 247
–, size distribution of 246
energy balance 30, 68, 193–204, 229–237
energy balance models 204, 206–208, 213, 219, 220, 223, 224
enrichment factor 24, 57
entrainment 111, 113, 114
entropy relation 135
epitaxial growth 153–156
eutrofication 74
expansion chamber 19, 20, 26, 32, 36, 93, 134, 136–138, 165, 170
extinction 22, 43, 68, 196, 233, 256, 258
extinction cross section 256
extinction efficiency 232, 256, 262, 263

falling speed of drops 71, 116, 117
falling velocity, *see* sedimentation velocity
filter methods 61, 62, 167, 170, 171
fine particles 38, 53, 203
flares 182, 183
fog dispersion 180
forward scattering 255, 256, 258, 262
free energy 87–89, 91, 134, 135, 146, 155, 156, 243–245, 247
free path 17, 18
freezing experiments 167
freezing nucleation 134, 146–150, 159
– in the atmosphere 162–165
–, definition of 266
freezing nuclei 131, 146, 147, 152
freezing threshold 150
frost prevention 176

Gaia hypothesis 236, 237
gas constants 252, 253
gas-to-particle conversion 15, 25–31, 55, 62, 103
general circulation models 194, 205, 211–216, 224–227
generators
– of ice nuclei 182, 183
germ formation 86, 87, 91
see also embryo formation
giant particles
– and CCN formation 104, 105, 123
–, characterization of 20, 23, 30, 36, 38–44, 46, 50, 67
–, definition of 19
gradient method 69
gravitation constant 17, 253
greenhouse effect 196–199, 224, 225, 229–232, 237
ground albedo, *see* surface albedo

haze particle 64, 87, 145, 163, 168, 195, 265
heterogeneous condensation 63, 86, 180, 248
heterogeneous nucleation 133, 145–160, 181, 247, 248
homeostasis 236
homogeneous condensation 63, 86, 248
homogeneous nucleation 133–145, 179, 180, 247, 248
human effects, *see* anthropogenic influence
hydrological cycle 13–15, 204, 236
hygroscopic particles 85, 95, 103, 104, 111, 114, 117, 120, 121
hysteresis phenomenon 65

ice albedo feedback 203, 207, 208, 220, 222, 228
ice crystal
–, definition of 265
ice formation
–, primary processes of 132, 266
–, secondary processes of 132, 266
ice nuclei
–, characteristics of 148–160
–, concentration of 169–175

–, definition of 14, 131
–, formation of 30, 131, 175–177
–, size of 174, 175
ice nucleus spectrum 150–152, 166
immersion freezing 164–166, 267
impaction efficiency, *see* collection efficiency
impactor 21, 22, 36, 40, 42, 55, 61, 66, 168
in-cloud scavenging 71, 73
inertial deposition 20, 254
infrared opacity, *see* greenhouse effect
integrating nephelometer 21
interfacial energy 132, 134, 135, 143–147, 244, 248
Intertropical Convergence Zone 212
irradiation chamber experiments 26
isopiestic method 66

Junge size distribution 36, 38, 115, 262

Köhler's formula 88
Köhler theory 248

La Porte anomaly 122
large particles
– and CCN formation 104, 105
–, characterization of 20, 36, 38–44, 46, 50, 67
–, definition of 19
latent heat of phase change 121, 135, 141–143, 185, 204, 235, 243, 252
lidar technique 22, 43, 199
lightning 28
light scattering counters 43
liquid water content 110, 117, 118, 232–234

maritime aerosol
–, chemical composition of 55–57
–, optical properties of 260
–, size distribution of 40, 50, 51, 76
maritime clouds 97, 118, 233
mass concentration 19, 57
mean free path of gas molecules 18
membrane filter 22, 38, 44, 47–49, 66, 167
memory effect 156, 158, 159
metastable phase 131, 243
meteoritic particles 23, 30, 61, 62, 76, 175
methane 13
Mie scattering 256
Mie theory 255, 262
mineral particles, *see* soil particles
mixed clouds 72
mixing chamber 165
modeling
– of atmospheric particles 75–77
– of climatic effects of particles 203–229
molecular weight
– of dry air 253
– of water 253
monodisperse system 18, 19
morphological methods 45, 49

neutron activation analysis 45, 53, 57, 58
nimbostratus clouds 144
nitrate particles
–, production of 27, 28, 31
–, residence time of 74
nitrogen oxides 26–28, 31, 46, 228
noctilucent clouds 30
nuclear war and climate 222–228
nuclear winter 222, 223
nucleation
–, definition of 132, 243, 245
–, probability of 165, 246, 247
nucleation event 156, 246
nucleation rate 136, 138–144, 161, 246–248
nucleation site 156–159
nuclei mode distribution 37, 38, 40
Nuclepore filter 22, 106
number concentration 19, 20, 25, 26, 32–35, 66
number size distribution 35–41

optical counter 20–21, 36, 66
optical depth (thickness)
– cloud layer 232–234
–, definition of 257, 258
– increase in a nuclear war 223
– scaled 233, 234
– stratospheric aerosol layer 196–198, 200, 206, 209–211, 217, 220, 221
– tropospheric aerosol layer 201–203, 206, 208–212
optically effective cross section 256
osmotic coefficient 88, 89
Ostwald phase rule 134
oxidation of gases 27–29, 73
ozone 14, 29

parametrization 204, 205, 223
particle generator 120
phase change of water soluble aerosol 64, 65
phoretic forces 72, 164
photochemical reactions 25–27, 199
pH value of cloud water 29
planetary albedo 196, 197, 199–201, 203, 206, 209, 210, 219, 228, 229, 232, 235, 259, 261
pollens 23, 30
polydisperse system 19
precipitation formation
– artificial 14, 120–124, 154, 178
– natural 14, 109, 116–119
primitive equations 204, 205
productive rate of particles 29, 31
proton-induced X-ray emission (PIXE) method 45, 57
pyrotechnics 182

radar echo 121
radiance 256, 257
radiation transfer
– in aerosol layer 14, 19, 45, 68, 194–200
–, basic elements of 255–263
– in clouds 14, 194, 195, 229–232
radiative balance, *see* energy balance
radiative balance models 204
radiative–convective models 204, 205, 209–211, 217, 235
radioactive isotopes 15
Raoult's law 65
Rayleight scattering 255
reflectance 258
refractive index 201, 202, 206, 207, 209, 255, 256
residence time
–, definition of 74
– of CCN 102
– of stratospheric aerosols 30, 195
– of tropospheric aerosol 29, 74, 75, 200, 202

Saharan dust 25, 55, 202, 212
scattering
– by aerosol particles 14, 194, 196–198
– by cloud particles 194, 229
–, definition of 255
– isotropic 258
sea salt particles
– and cloud formation 104, 109
–, concentration and size distribution of 24, 49–51, 53
–, formation of 23, 24
– and precipitation formation 117–124
sedimentation 15, 17, 18, 20, 60, 61, 203
sedimentation velocity 17, 18, 69, 70
seeding trials 184, 185
single particle method 44, 52
single-scattering albedo 197, 198, 206, 210, 211, 213, 232, 258
size distribution function 35, 36, 38, 257
size parameter 255, 256
soil particles
–, formation of 24, 25
– injection into the atmosphere 199, 222, 228
solar constant 207, 208, 229, 230
soot particles 28, 55, 195, 198, 202, 223, 225
Southern Oscillation 216
specific heat 253
spores 30
stable phase 131, 243
stable system 18
statistical–dynamical models 205–208
Stokes–Cunningham correction 18
Stokes equation 17
stratocumulus clouds 121
stratospheric aerosol
–, chemical composition of 60–63, 197
–, concentration of 28, 30, 34, 35, 42–44
–, radiative characteristics of 43, 195–200
– residence time 195, 228
–, size distribution of 40, 41, 198
stratus clouds 101, 108, 123, 181, 235
sub-cloud scavenging 71–74
sulfate particles
–, concentration and size distribution of 46, 49–52, 66
– and condensation of water vapor 15, 65, 66, 88–91, 105–109, 124, 234, 236
–, deposition of 73
– in ice cores 237
–, production of 15, 23, 27–31, 203
–, residence time of 74, 75
– in the stratosphere 28, 30, 42, 60–63, 197, 198

– in the troposphere 46, 49, 58, 59, 203
sulfur dioxide 26–29, 31, 63, 73
supercooled clouds 14, 120, 131, 145, 167, 174, 178–186
supersaturation spectrum 86, 90, 95–101, 103–105, 110, 152
surface albedo 195, 197, 201–203, 206, 209, 210, 213, 228, 235, 259, 261, 262
surface radius 36
symmetric scattering 258
system albedo, *see* planetary albedo

thermal conductivity
– of air 252
– of water vapor 252
thermal diffusion chamber 93, 94, 106
thermal precipitator 20
thermal reactions 26, 27
thin atmosphere approximation 262
threshold temperature 148, 149, 154, 155, 163, 179
trace components 13
transmittance 258
tropospheric background aerosol
–, chemical composition of 45–60
–, climatic impact of 205–216
–, concentration of 32–34, 42–43
–, definition of 34
– radiative characteristics of 68, 200–203
– residence time 200
–, size distribution of 38–41, 203

urban aerosol
–, chemical composition of 28, 45, 55–57, 116
–, climatic impact of 202, 213
–, optical properties of 260
–, radiation transfer modification by 202
–, size distribution of 37, 39

ventilation factor 253
viruses 30
viscosity
– dynamic gas 17
volatile nuclei 106
volcanic activity
– and aerosol formation 28, 30, 31, 41
– and atmospheric ice nuclei 175
– and atmospheric optical properties 43, 198–200
– and climate variations 216–222
– and size distribution of particles 41
– and stratospheric sulfate particles 61–63, 195, 199
volume distribution 38
volume effect 167
volume extinction coefficient 209, 256

warm clouds 117, 119, 120–123, 180
water-insoluble particles 24, 87, 91–93, 114, 119, 153
water-soluble particles 45–60, 71, 87–92, 103, 105, 109, 145, 260
wet deposition 15, 40, 68, 71–74, 132, 183, 223
wettable particles 91, 92
wind tunnel 69, 70

X-ray fluorescence analysis 44, 59, 60

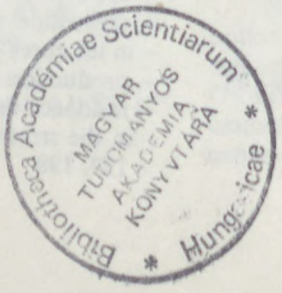

The myriad tiny solid and liquid aerosol particles in the atmosphere of our planet continuously influence man's everyday life through modifying, directly or indirectly, the processes of weather and climate. These particles control visibility in the air, the intensity of the solar radiation reaching the Earth's surface and of the terrestrial radiation escaping to space, as well as the electric and radioactive properties of the atmospheric environment. Specific fractions of these particles, the nuclei, can initiate water droplet and ice crystal formation, and therefore play an important role in the regulation of the planetary water cycle. Introduction of suitable nuclei in clouds may stimulate precipitation artificially, while inadvertent emission of different pollutants into the atmosphere by human activities may have an impact on the future of our climate.

This book contains a concise presentation of the physical and chemical properties of aerosol particles and nuclei, as well as a coherent description of their role in cloud and precipitation formation and climate regulation. The subject is treated at a level appropriate for introductory graduate courses and for beginners in the field, but researchers in areas related to atmospheric sciences will also find the volume useful.

ISBN 963 05 5682 0

ATMOSPHERIC PARTICLES AND NUCLEI